1985

Granitoids and rare-element pegmatites of the Georgia Lake area, northwestern Ontario

Zayachkivsky, Borys

GRANITOIDS AND RARE-ELEMENT PEGMATITES OF THE GEORGIA LAKE AREA, NORTHWESTERN ONTARIO

by

Borys Zayachkivsky

A Thesis submitted in partial fulfillment
of the requirements for the Degree of
Master of Science

Faculty of Science
Lakehead University
Thunder Bay, Ontario
Canada

ABSTRACT

The Georgia Lake pegmatite field is located in the Quetico Gneiss Belt of the Superior Province. Spodumene-bearing and subordinate beryl-bearing pegmatites of the Georgia Lake area are flanked to the south and east by an extensive granitoid terrain, which previously has not been subdivided. Granitoids of the immediate Georgia Lake area were investigated in conjunction with rare-element pegmatites to determine the character of the granitoids as parental intrusions to rare-element pegmatites. The granitoids include two-mica leucogranites occurring as a large plutonic mass south of the pegmatite field and as smaller satellitic intrusions, the Kilgour Lake Group granitoids centered on a small gabbroic-metagabbroic unit near Kilgour Lake and tonalitic sills dispersed throughout the pegmatite field. The distinction of the three types of granitoids was made on the basis of field observations, petrography and analytical geochemistry. Two-mica leucogranites and tonalitic sills were derived as partial melts of pelitic metasediments and metagreywacke, respectively. The Kilgour Lake Group granitoids were presumed to be the products of fractional crystallization of a mafic melt generated in the upper mantle or lower crust.

Mineralogical studies were carried out on perthitic microcline, tantalite-columbite and Sn oxide minerals from

rare-element pegmatites. Results indicate that perthitic microcline in all pegmatites is of the maximum microcline structural state, tantalite-columbite minerals occur in a partly to completely disordered structural state and the dominant Sn oxide mineral is staringite.

Division of spodumene-bearing rare-element pegmatites into Southern, Central and Northern Groups was made on the basis of internal textural variations, mineralogy and differences in geochemistry of perthitic microcline and muscovite. The Southern Group consists of one pegmatite which is unique to the Georgia Lake pegmatite field with respect to development of mineralogical zones and strong internal fractionation of Rb and Cs. Central Group pegmatites are linked by a fractionation trend, with respect to Rb and Cs, across the group. A similar fractionation trend is not observed across the Northern Group pegmatites. The pegmatite groupings reflect different modes of source fluid derivation, although all pegmatites of the Georgia Lake area originated as the result of a common anatectic event responsible for the intrusion of two-mica leucogranites. Central and Southern Group pegmatites were derived from low viscosity fluids differentiated from granitic melts, while Northern Group pegmatites are presumed to be the products of fluids generated by direct anatexis of metasediments.

ACKNOWLEDGEMENTS

I would like to thank Dr. S. A. Kissin for supervision of this thesis and for valuable advice rendered during all stages of the project. I am also grateful to Dr. R. H. Mitchell for teaching me the methods of analytical geochemistry. Laboratory assistance was provided by Dr. T. J. Griffith, A. Mackenzie, K. Pringnitz and M. Artist-Downey. Drs. M. P. Gorton and C. Cermignani assisted me with electron microprobe analysis at the University of Toronto. The study of tantalite-columbite minerals from the Georgia Lake rare-element pegmatites was originally suggested by F. W. Breaks, Ontario Geological Survey. Analyses of tantalite-columbite and Sn oxide minerals were performed by R. Chapman and obtained through Dr. P. Černý, University of Manitoba. Backscattered electron images of tantalite grains were produced by D. R. Owens, CANMET, Ottawa. Some chemical analyses were performed by the Geoscience Laboratories, Ontario Geological Survey and obtained through Dr. G. C. Patterson, Resident Geologist, Thunder Bay. Assistance with field work and sample preparation was provided by A. Butler. Thin and polished sections for this project were, in part, prepared by R. Bennett and D. Crothers. Some of the figures in this thesis were drafted by S. Spivak. Finally I would like to thank L. MacGillivray for typing the manuscript. Financial assistance for this project was provided through Ontario Geoscience Research Grant number 225 to S. A. Kissin.

TABLE OF CONTENTS

TABLE OF CONTENTS
Continued

LIST OF TABLES

LIST OF TABLES
Continued

LIST OF FIGURES

LIST OF FIGURES
Continued

LIST OF FIGURES
Continued

LIST OF FIGURES
Continued

LIST OF FIGURES
Continued

LIST OF FIGURES
Continued

LIST OF FIGURES
Continued

PART ONE INTRODUCTION

General Statement

The Georgia Lake rare-element pegmatite field came into prominence in the 1950s following the discovery of a spodumene-bearing pegmatite on Georgia Lake (Pye, 1965). All other known occurrences, mainly of the lithium-bearing type, were located soon after the initial discovery. The Georgia Lake area comprises the largest concentration of known rare-element pegmatites in Ontario (Breaks, 1980). Up to 40 lithium and beryllium pegmatites are exposed in outcrop over an area of approximately 600 km^2.

The Georgia Lake area is located about 140 km northeast of Thunder Bay near the southeast corner of Lake Nipigon (Fig. 1-1). The major access road to the area is Highway 11, which passes north-south along the western portion of the pegmatite field. The Camp 75 Road of Domtar Forest Products branches from Highway 11 south of Orient Bay near Keemle Lake and provides accessibility to northern and northwestern parts of the study area. This is the only secondary road in the area that is maintained at present. The abandoned Camp 95 Road traverses the central portion of the pegmatite field but is presently in a state of deterioration, although the entire length of this road is still passable with a four-wheel drive vehicle. An alternative access route to eastern portions of the Georgia Lake pegmatite field is via the Little Bear Quarry Road,

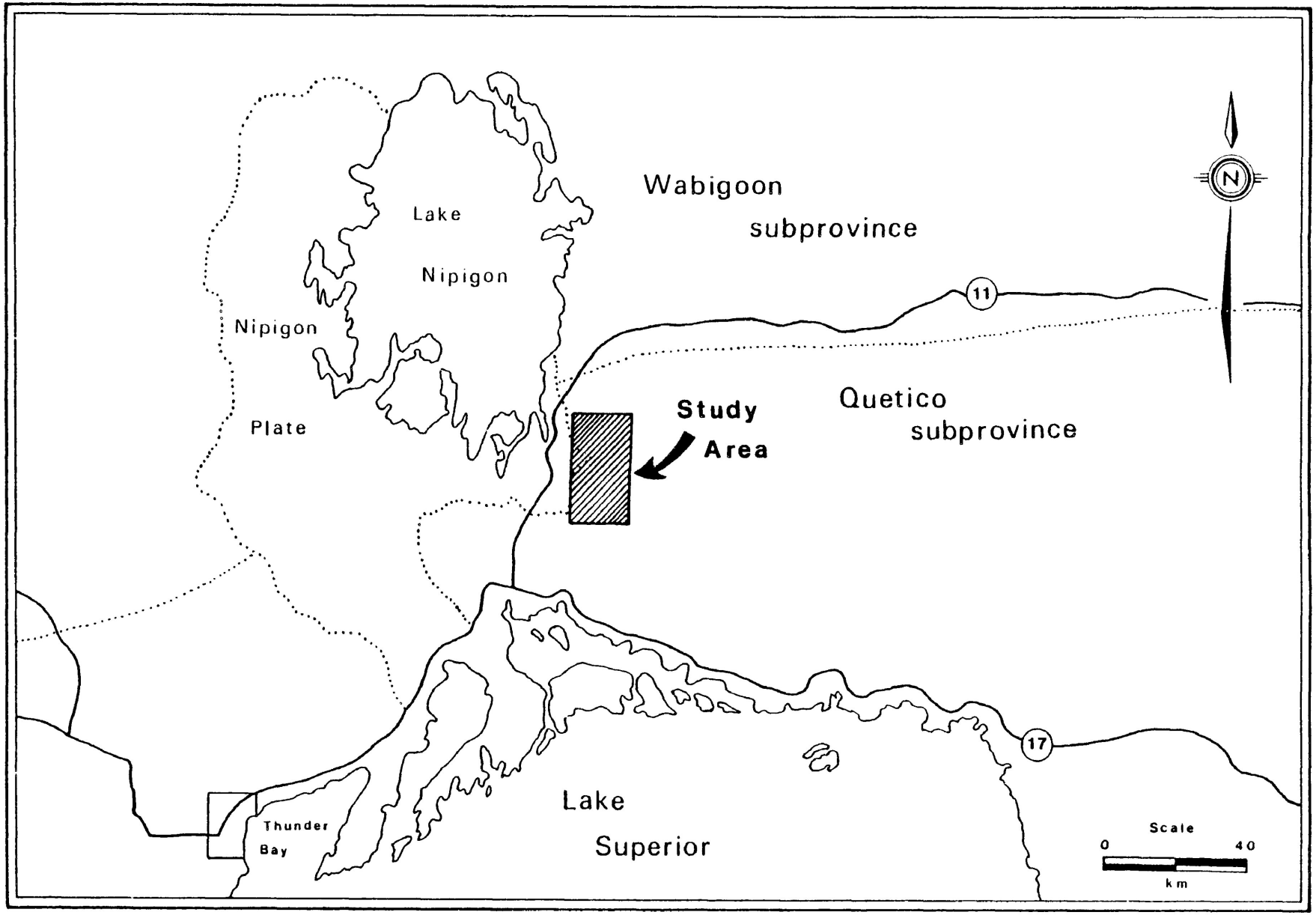

Fig. 1-1. Location of the Georgia Lake pegmatite field, northwestern Ontario.

which branches from Highway 17 at the Kama Hills just east of Ozone Creek and continues north to Central Lake, where the road forks. The western fork passes through the eastern part of the pegmatite field and also provides accessibility to Cosgrave, Barbara, Georgia and Jean Lakes.

Aims Of The Thesis

The Georgia Lake rare-element pegmatite field has not been investigated to the same extent as other more prominent pegmatite fields in Canada, such as the Winnipeg River district of Manitoba and the Preissac-Lacorne district of Quebec, as a result of the subeconomic rare-element pegmatite potential of the Georgia Lake area. Thus, little new geological and geochemical information on the area has been produced. Most available information on the area is over 20 years old and produced within a limited period of time. There is a lack of geochemical data for rocks of the Georgia Lake area, and the nature of the granitoids of the area as possible parental material to the rare-element pegmatites is not known.

The general purpose of this study is to provide new information concerning the rare-element pegmatites and granitoids of the area and to assess the economic potential of other rare-element minerals in the pegmatites exclusive of spodumene. In summary, the aims of the thesis are:

(1) To provide some geochemical data for the granitoids and rare-element pegmatites of the Georgia Lake area on a reconnaissance scale;

(2) Study the nature of the granitoids of the area;

(3) Observe fractionation trends across the pegmatite field and within individual pegmatites as indicators of petrogenesis;

(4) Provide data for Ta-Nb-Sn minerals in rare-element pegmatites and assess their economic potential.

Previous Geological Work

The Ontario Department of Mines mapped the Georgia Lake area in the late 1950s over a period of several years after the staking rush prompted by the discovery of spodumene in this area. The objectives of the survey were to study the nature, distribution and genesis of area pegmatites and to produce a geological map of the Georgia Lake area. The results are summarized by Pye (1965). A Ph.D. thesis (Milne, 1962) details the mineralogy of the more prominent pegmatites and provides maps of some pegmatites. General descriptions of the pegmatite occurrences are also summarized by Mulligan (1965). Interest in the lithium pegmatites of the Georgia Lake area subsided soon after 1960 as a result of a 50% drop in the price of lithium hydroxide and a decrease in the consumption of lithium (Lasmanis, 1978). The area has since remained idle except for sporadic

staking activity and a brief examination of several pegmatites by the Ontario Geological Survey in 1980 (Breaks, 1980).

Present Field Work

Field work for this project was carried out in May, 1984. During this period 15 rare-element pegmatite occurrences were visited. The main purpose of the field work was to collect an array of samples from pegmatites for subsequent geochemical analysis. Samples were not obtained from two of the rare-element pegmatites visited (Dunning and Foster occurrences) because of the poor quality of sample material available. Traverses were also made across many of the granitic bodies outcropping within and along the flanks of the pegmatite field.

General Geology

The Georgia Lake area is located within the Quetico Gneiss Belt of the Superior Province. Major Archean lithologies include metasedimentary schists and gneisses of amphibolite grade, granitoids rarely grading into more mafic phases, and granitic pegmatites. Diabase sills of Proterozoic age occur as intrusions into earlier lithologies and obscure the entire western portion of the Georgia Lake pegmatite field. The distribution of the major lithologies

in the Georgia Lake area is summarized in Fig. 1-2. Other subordinate geological units of the Georgia Lake area include Archean amphibolite dykes, Proterozoic diabase dykes and Sibley dolostones, which are occasionally baked white by overlying diabase sills.

Granitoids flank the southern and eastern portions of the pegmatite field and occur as small satellitic and isolated bodies throughout the pegmatite field. Granitoids range in size from batholiths to small stocks and sills. Compositionally, granitoids range from granites, granodiorites, tonalites to monzodiorites. Mafic granitoids locally grade into gabbro and metagabbro. Simple granitic pegmatites occur as irregular masses and dykes cross-cutting pre-existing lithologies and concentrate in granitoids along the southern and eastern limits of the pegmatite field. Rare-element pegmatites of the spodumene- and beryl-bearing type occur as discontinuous shallow to steeply dipping dykes and sills irregularly distributed throughout the pegmatite field.

Supracrustal metasediments are the oldest rocks of the Georgia Lake area and range from paragneisses to schists. The supracrustal rocks represent recrystallized wackes and pelitic sediments. Compositionally, the supracrustal rocks are most commonly biotite-quartz-feldspar gneisses. Schistose textures occur sporadically and were observed

Fig. 1-2. General geology of the Georgia Lake area. Granitoid sampling locations are identified with small squares.

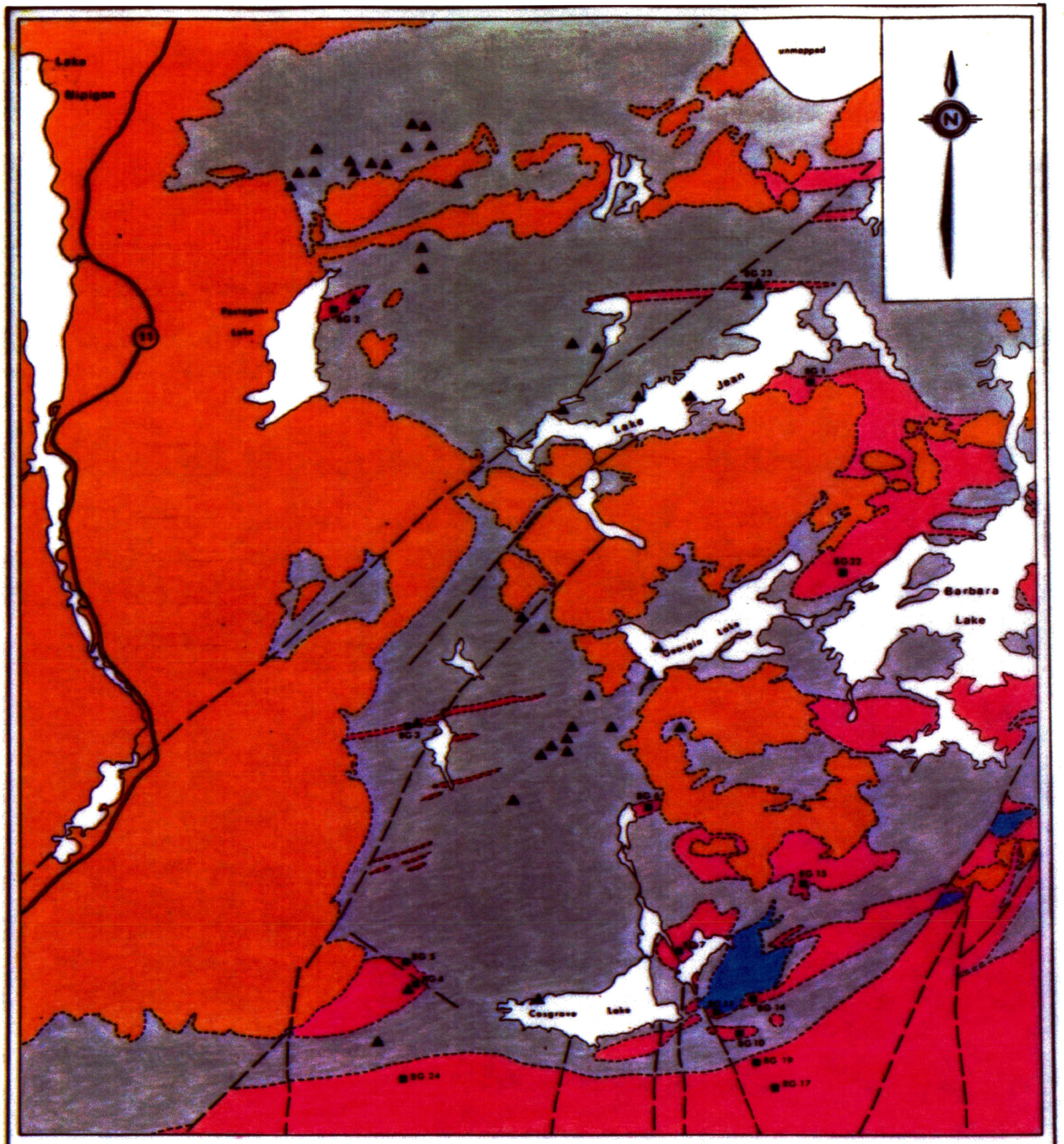

LEGEND

Proterozoic

- Diabase

Archean

- Felsic igneous rocks
- Mafic meta-igneous rocks
- Metasediments

Scale

0 2 4 6 8

Kilometres

SYMBOLS

- Rare-element pegmatite occurrence (Archean)
- Location of granitoid rock sample
- Lineament
- Geological contact
- Highway

Geology from ODM Map 2056 by E.G. Pye

to be common in the vicinity of Postagoni Lake. Porphyroblasts of garnet, cordierite and staurolite occur commonly in gneisses from central and southern portions of the pegmatite field. Garnet crystals were observed in several outcrops as porphyroblasts up to 1 mm in diameter. Cordierite occurs as light semicircular knots up to several centimetres in diameter. Staurolite occurs as dark brown to black, euhedral crystals up to 1 cm in length. Both cordierite and staurolite stand in relief above the metasediments and are confined to thin aluminous metapelitic units, which are well exposed in outcrops along the Camp 95 Road between Blay Lake to an area south of Georgia Lake. Other subordinate minerals of the metasediments include amphiboles and chlorite.

Relict bedding features are scattered throughout the metasediments in the central to southern parts of the pegmatite field. Graded and cross-beds were observed in metasediments north of Blay Lake. In outcrop, relict bedding commonly strikes east-west to northeast-southwest and dips steeply to the north although reversals in dip were noted by Pye (1965). Foliation in metasediments is expressed by an alignment of biotite grains, which commonly parallel the strike of the relict bedding. Occasionally, the foliation deviates by as much as 20° from the strike of the bedding such as in metasediments south of Rim Lake. These observations suggest a deformation history in the

area that is more complex than is presently understood.

PART TWO GRANITOIDS

Lithology And Geological Setting

The Georgia Lake pegmatite field occurs along the southern margin of a supracrustal metasedimentary belt. To the south and east, an extensive terrain of migmatitic rocks with dispersed granitic plutons forms a belt that characterizes the southern portion of the Quetico Subprovince east of Lake Nipigon (Stockwell et al., 1970). Thus, the area under study occupies a portion of the Quetico Subprovince where two contrasting geological domains are in contact. Granitoid lithologies in this area are similar to those described by Breaks and Bond (1977) and Breaks et al. (1978) of the English River Subprovince. Although granitoids comprise only a small portion of the bedrocks of the study area, they represent northernmost exposures of the migmatitic-plutonic belt. Subdivision of granitoids of the Georgia Lake area can be made into three separate suites; a potassic suite, a sodi-potassic suite and a sodic suite. Even though the later two suites are insignificant in extent relative to the potassic suite, their presence as distinct geological entities has previously been unnoticed. In the Georgia Lake area, the potassic suite is represented by two-mica leucogranites occupying the southern and eastern flanks of the pegmatite field. The sodi-potassic suite is composed of granodiorites and tonalites that grade into mafic lithologies and are

collectively refered to as the Kilgour Lake Group. The sodic suite of granitoids is represented by tonalitic sills, dispersed throughout the pegmatite field. The distribution of these units is summarized in Fig. 2-1. Twenty-four representative samples were obtained in the course of field work characterizing the granitoid lithologies of the Georgia Lake area. Locations of studied samples are shown on the generalized geological map of the Georgia Lake area (Fig. 1-2) and descriptively summarized (Table 2-1).

Two-Mica Leucogranites

Within the study area, two-mica leucogranites occur as the Glacier Lake Pluton and several smaller satellitic stocks. The Glacier Lake Pluton is part of an extensive granitic mass of batholithic proportions (McCrank et al., 1981). Only the northern contact is exposed in the study area. The eastern, southern and western contacts are unmapped. The northern contact of the Glacier Lake Pluton with metasediments is represented by a contact zone approximately 100 m wide characterized by lit-par-lit interlayering of metasedimentary supracrustals and leucocratic pegmatitic granite to gneissic sills paralleling the general strike of the pluton contact. The leucocratic sills display a pronounced foliation and commonly pinch-and-swell structures. These sills become progressively wider and eventually merge into each other forming the

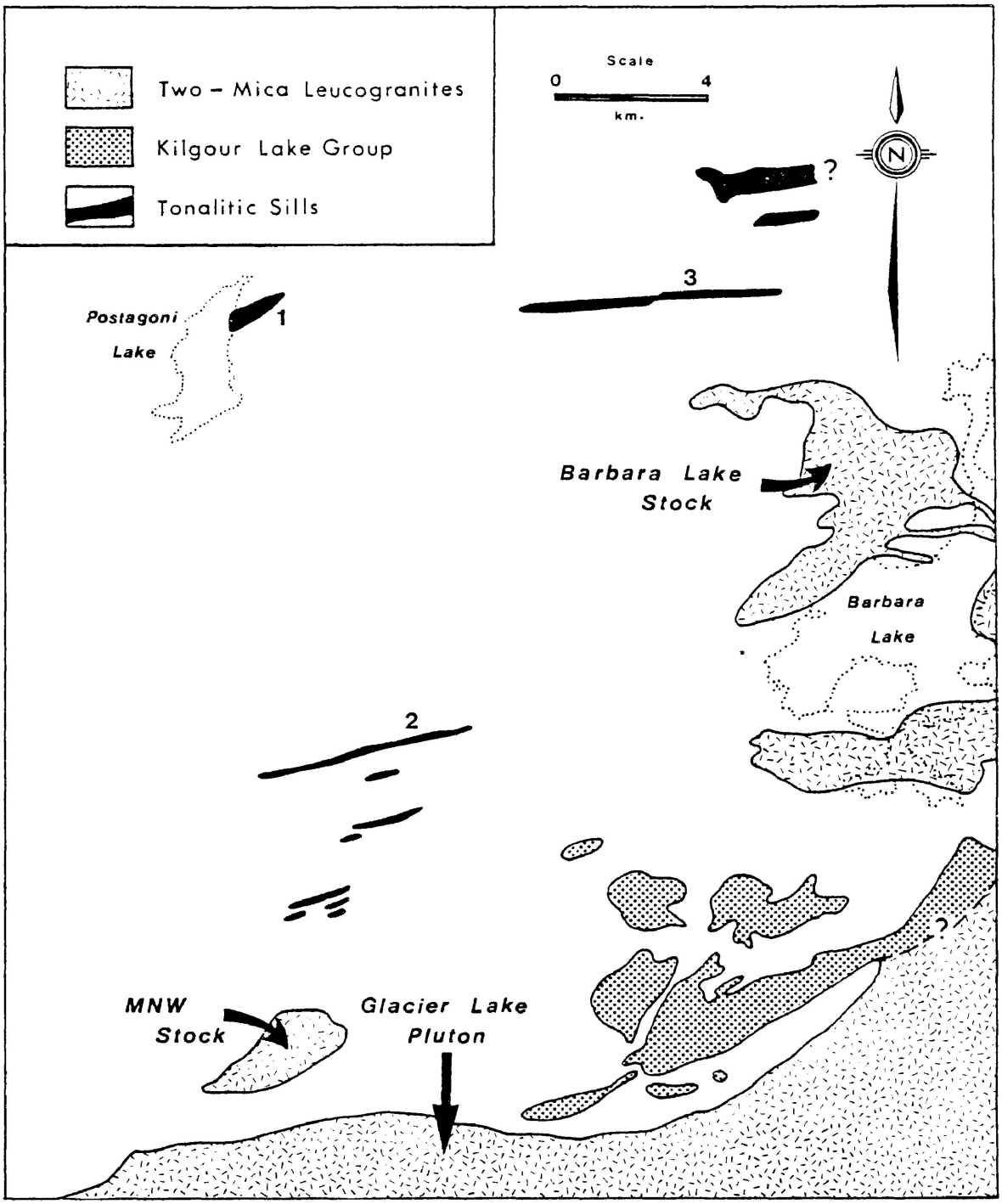

Fig. 2-1. Distribution of major granitoid lithologies of the Georgia Lake area.
1 - Postagoni Lake leucotonalite; 2 - Blay Lake leucotonalite; 3 - Parole Lake tonalite.

Table 2-1: Locations of studied granitoid samples of the Georgia Lake Area.

Two-mica leucogranites

BG1	Barbara Lake Stock; on motor road 2 km east of Lake Jean
BG22	Barbara Lake Stock; on motor road 1 km west of North Channel, Barbara Lake
BG4	MNW Stock; 2 m east of MNW rare-element pegmatite
BG5	MNW Stock; 75 m south of north contact along the Jackfish River
BG17	Glacier Lake Pluton; 1 km southwest of sample BG19
BG19	Glacier Lake Pluton; pegmatitic leucogranite, 0.5 km west of motor road at contact with metasediments
BG24	Glacier Lake Pluton; 4 km southwest of Cosgrave Lake

Kilgour Lake Group

BG6	East of Connor Lake
BG7	On motor road west of Kilgour Lake
BG10	1.5 km southwest of Stein Lake
BG11	1 km southeast of the southern end of Kilgour Lake
BG14	0.5 km west of Stein Lake
BG15	1.5 km southeast of Rim Lake

Tonalitic Sills

BG2	100 m north of Dive Lake in the vicinity of Postagoni Lake
BG3	50 m west of Brink rare-element pegmatite, north end of Blay Lake
BG23	500 m south of "Camp 75", north of Lake Jean

gradational contact of the Glacier Lake Pluton. The pluton contact is a foliated pegmatitic granite with the presence of ubiquitous muscovite and biotite. The muscovite to biotite proportion appears to be at a maximum in the region to the southeast of Cosgrave Lake and decreases easterly along the pluton contact and southerly toward the centre of the pluton. The leucocratic pegmatitic granite along the northern contact of the Glacier Lake Pluton is generally fine-grained with abundant quartz and white microcline. Porphyritic phases occur with thin microcline grains up to 1 cm in length aligned parallel to foliation defined by micas. Red garnet crystals are common only along the northern contact of the pluton and are largest (up to 2 mm) and most abundant southwest of Cosgrave Lake. Garnet is not present 0.5 km south of the contact zone. Also, at progressively greater distances from the contact and southerly toward the pluton centre, foliation in granite becomes weaker, and the proportion of pegmatitic granite steadily decreases.

Two other bodies in the study area identified as two-mica leucogranite include the MNW Stock (Breaks, 1980) and another unit here named the Barbara Lake Stock (Fig. 2-1). The MNW Stock occurs about 3 km west of Cosgrave Lake and is an elliptically shaped body elongated roughly northeast-southwest. The western portion of the MNW Stock is obscured by an overlying diabase sill. The longest

surficial dimension of this body is approximately 4 km. The MNW Stock displays a relative mineralogical and textural homogeneity with respect to the Glacier Lake Pluton. Grain size of feldspar is in the range 2 to 3 mm with no porphyritic phases observed. The muscovite to biotite ratio remains constant with an intermediate relative proportion of the two minerals, where observed. Foliation in the MNW Stock is not pronounced, even near the contacts, although a distinct flow banding imparted by trains of elongate quartz grains striking N 55° E and dipping 85° S occurs in the central part of the stock. The MNW Stock hosts several north-striking, steep-dipping, tourmaline-bearing pegmatite dykes, one of which is the MNW zoned rare-element pegmatite. A series of small irregular pegmatites near the north contact of the MNW Stock display a graphic intergrowth of quartz and feldspar. The north contact of the MNW Stock with biotite-quartz-feldspar schist is knife sharp and well exposed at the rapids on the Jackfish River where the orientation is strike N 90° W and dip 55° N. This orientation parallels the foliation at metasediments of the contact. Outcrop exposure along the eastern and southern limits of the MNW Stock is poor and contacts were not observed.

The Barbara Lake Stock is the northernmost exposure of two-mica leucogranite in the Georgia Lake area. It is an arcuate body lying between Barbara and Jean Lakes.

A western portion of the stock is obscured by overlying diabase. The Barbara Lake Stock is in sharp contact with metasediments, where observed. The body is homogeneous with respect to texture and mineralogy, but a slight increase in grain size of feldspar and quartz occurs toward the northern contact. The proportion of muscovite to biotite in rock specimens is intermediate and increases slightly toward the northern contact. The mica that is present does not impart a distinct foliation. Simple granitic pegmatite dykes that cross-cut the granite are numerous and variably oriented.

Kilgour Lake Group

The Kilgour Lake Group of granitoids and related rocks occurs east and southeast of Cosgrave Lake and is centered on a small, inhomogeneous, gabbroic to metagabbroic body refered to as the Kilgour Lake-Stein Lake Metagabbro by McCrank et al. (1981). Area covered by the group is about 70 km^2. Lithologies from the northern segment of the Kilgour Lake Group are unfoliated, nonporphyritic granodiorites to tonalites. The appearance of these granitoids is similar to that of the two-mica leucogranites to the south except for the lack of muscovite and higher mafic content in the former. The tonalites from the northeastern portion of the Kilgour Lake Group are heavily cross-cut by granitic pegmatite. Outcrops southeast of Rim Lake are dominated

by pegmatite which commonly displays a layered structure. The percentage of cross-cutting granitic pegmatite decreases in a southwesterly direction across the Kilgour Lake Group and is presumed to have a source in the vicinity of the pegmatite injection zone on Barbara Lake described by Pye (1965). The southern portion of the Kilgour Lake Group is dominated by granodioritic lithologies. A band of porphyritic granodiorite passes east-west, southeast of Cosgrave Lake and marks the southern boundary of the Kilgour Lake Group. The rock is brick-red with stubby, subhedral phenocrysts of potassium feldspar, as determined from a feldspar staining test, that range up to 2 cm in length. The feldspar phenocrysts do not, in general display preferential alignment although an occasional east-west flow fabric is observed. The central portion of the Kilgour Lake Group is dominated by the more mafic lithologies where, in places, hornblende and biotite form up to 50% of the rock. Pye (1965) reported mafic mineral content in rocks from this area to be as high as 60-70% and with occasional irregular patches of 100% coarse-grained hornblende. A feldspar staining test on a sample containing about 30% mafic minerals showed that about 30% of the felsic component to be potassium feldspar, which is erradically distributed through the rock. The mafic lithologies of the central portion of the Kilgour Lake Group occasionally grade internally into granodiorites and porphyritic granodiorites similar to the type flanking the southern rim of the Kilgour

Lake Group. The Kilgour Lake Group granitoids have intrusive relationships into hosting metasediments. Apophyses on a metre scale are seen penetrating hosting metasediments along the motor road which crosses these granitoids.

Tonalitic Sills

Numerous sodic granitoids with a general east-west elongation occur throughout the pegmatite field. These granitoids are presumed to be sills since they are steeply dipping and roughly strike in the same direction as the fabric of the hosting metasediments. They range in width from a few tens of centimetres up to 3/4 of a km. Three of the largest were examined in the course of field work. The sills at Postagoni and Blay Lakes are leucotonalites (trondhjemites), while the sill extending east from Parole Lake is a tonalite (Fig. 2-1). It is a coincidence that each of these widely separated bodies are cross-cut by rare-element pegmatites.

The Postagoni Lake leucotonalite is a coarse-grained granitoid with closely packed crystals of plagioclase up to 1.5 cm in length, imparting a porphyritic texture. The texture is uniform throughout the body except near the contact with biotite-quartz-feldspar schist, where there is a chill margin of several metres in width. The chill margin texture is very similar to the texture of the feldspar

porphyry dykes described by Pye (1965).

The Blay Lake leucotonalite, about 10 km south of the Postagoni Lake leucotonalite is very similar to the latter intrusive except for a slightly higher mafic content and smaller plagioclase grain size.

The Parole Lake tonalite is very similar texturally to tonalites of the Kilgour Lake Group. It is more mafic and finer-grained than the two leucotonalitic bodies described above.

The tonalitic sills are, in all cases, in sharp contact with hosting metasediments and display no foliation, primary flow fabric or significant internal variation. Feldspar staining tests show these granitoids to be deficient in potassium feldspar.

Modal Analysis

Modal analysis of the granitoid rocks is based on 1000 point counts for each sample determined on microscope thin sections and recorded with a manual point counter. Results are recalculated to 100% and presented in Table 2-2. The analysis of 16 samples comprises seven examples of two-mica leucogranites, six from the Kilgour Lake Group and three from the tonalitic sills.

Table 2-2: Modal Analysis of the Georgia Lake granitoids

	Two-mica leucogranites							Kilgour Lake Group						Tonalites		
	BG1	BG22	BG4	BG5	BG17	BG19	BG24	BG6	BG7	BG10	BG11	BG14	BG15	BG2	BG3	BG23
Plagioclase	40.3	39.7	32.0	36.5	29.8	34.8	36.8	53.6	62.0	46.3	47.8	54.5	58.7	66.6	64.7	62.7
K-feldspar	26.4	19.5	23.0	23.2	24.1	24.3	27.4	14.7	2.5	13.2	10.1	6.3	4.3	5.6	0.2	
Quartz	28.4	33.6	34.9	31.4	33.2	31.6	31.8	18.9	22.1	18.1	2.1	25.4	23.3	25.7	28.5	19.6
Muscovite	1.9	2.2	5.7	5.3	9.3	7.8	0.6							0.4	0.2	tr
Biotite	3.0	5.0	4.5	3.4	3.6	1.2	3.1	8.4	12.1	12.7	4.0	12.9	7.6	1.6	6.0	17.6
Hornblende								2.7	0.5	6.4	25.1	0.2	4.8			
Clinopyroxene											8.1					
Sphene								1.0	0.4	0.5	1.0	0.5	0.8			
Opaque	tr			tr			tr	0.2	0.2	0.5	1.1	tr	0.2			tr
Epidote		tr		0.1				0.4	0.3	0.7	0.2	0.1	0.1	0.1	0.3	tr
Apatite	tr	tr	tr	0.1	tr		tr	0.1	tr	0.2	0.4	tr	tr			tr
Zircon					tr				tr	0.2	0.1	0.1	0.3	tr		tr
Allanite								tr		0.3		tr	tr			0.1
Carbonate								tr							tr	
Garnet						0.3	0.4									

tr = trace (less than 0.1 modal %)

Ubiquitous accessory mineral phases of the two-mica leucogranites include muscovite and biotite while biotite, hornblende and sphene are characteristic accessory minerals of the Kilgour Lake Group. Modal % muscovite in leucogranites is highly variable and ranges up to 10%. Muscovite is not present in the Kilgour Lake Group and is only a trace constituent of the tonalitic sills. Biotite is most abundant in granitoids of the Kilgour Lake Group, although sample BG23 from a tonalitic sill contains the largest amount of biotite. Biotite is the only significant mafic mineral phase of the tonalitic sills and two-mica leucogranites. A small amount of chlorite, included in % biotite, is present in some sections and occasionally difficult to distinguish from biotite. Hornblende and sphene are present only in granitoids of the Kilgour Lake Group. While hornblende increases in content in mafic granitoids, sphene shows an even distribution throughout the group ranging from 0.4 to 1.0 modal %. Clinopyroxene is associated only with mafic granitoids with low quartz contents (2% or less). Garnet is a rare granitoid mineral phase and is present only near the north contact of the Glacier Lake Pluton of the two-mica leucogranites. Other sporadically distributed, rare minerals associated with the Georgia Lake granitoids include epidote, apatite, zircon, allanite, carbonate and opaques all of which show a slight relative enrichment in the Kilgour Lake Group.

Modal analyses of samples are plotted on a Q-A-P diagram (Fig. 2-2) for the classification of granitoid rocks according to Streckeisen (1976) and summarized in Table 2-3. Most of the two-mica leucogranites plot in the granite field near the granite-granodiorite boundary and show a tight clustering. Only sample BG22 from the Barbara Lake Stock falls within the granodiorite field near the granite-granodiorite boundary. Samples from the Kilgour Lake Group are trimodally distributed. Felsic granitoids occurring in close proximity to centrally located mafic phases plot in the field of tonalites or straddle the tonalite-granodiorite boundary. Samples from the northern and southern limits of the Kilgour Lake Group are granodiorites and are closely spaced on the Q-A-P diagram near the boundary with the quartz monzodiorite field. The most mafic sample (BG11) analyzed from the Kilgour Lake Group is quartz deficient and plots in the field of monzodiorite. Samples from the tonalitic sills all plot in the tonalite field.

Petrography

Two-Mica Leucogranites

Petrographic thin sections from the two-mica leucogranites show that an equigranular texture, with grain size ranging from fine to coarse, is characteristic of this group of granitoids. The petrographic grain size

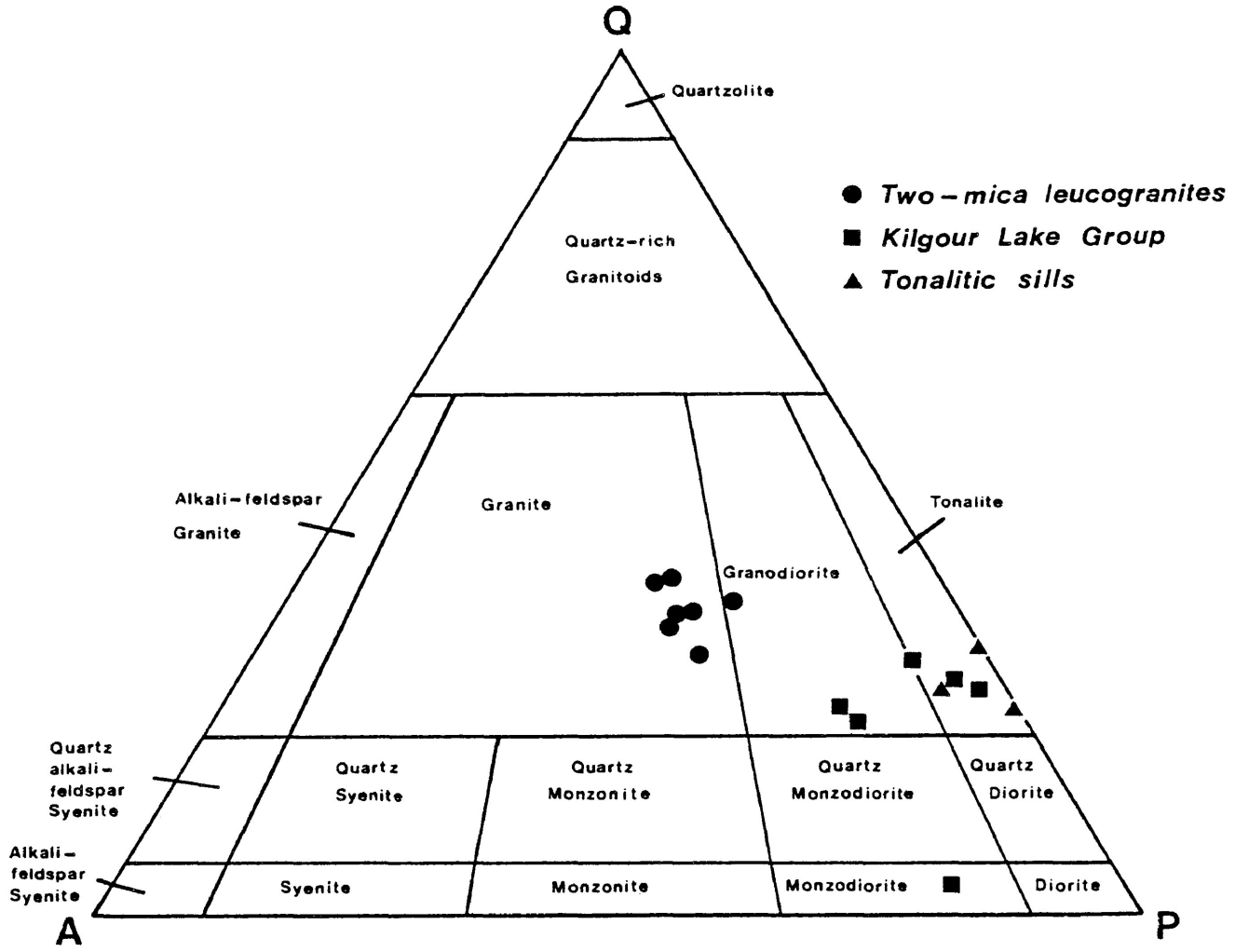

Fig. 2-2. Distribution of granitoids of the Georgia Lake area based on modal Q-A-P. Fields are after Streckeisen (1976).

Table 2-3: Classification of granitoid samples according to Streckeisen (1976).

Sample Number	Rock Classification	Colour Index	Felsic-Mafic Class
BG1	Granite	3	holo-leucocratic
BG22	Granodiorite	5	holo-leucocratic
BG4	Granite	5	holo-leucocratic
BG5	Granite	3	holo-leucocratic
BG17	Granite	4	holo-leucocratic
BG19	Granite	2	holo-leucocratic
BG24	Granite	4	holo-leucocratic
BG6	Granodiorite	12	leucocratic
BG10	Granodiorite	21	leucocratic
BG14	Granodiorite	14	leucocratic
BG7	Tonalite	13	leucocratic
BG15	Tonalite	14	leucocratic
BG11	Monzodiorite	39	mesocratic
BG2	Leucotonalite	2	holo-leucocratic
BG3	Leucotonalite	6	leucocratic
BG23	Tonalite	18	leucocratic

designation used is as follows: coarse-grained (> 5mm), medium-grained (1-5 mm) and fine-grained (< 1 mm). Most samples are medium- to coarse-grained. Sample BG22 from the southern part of the Barbara Lake Stock and BG24 from the western portion of the Glacier Lake Pluton are fine-grained. The samples obtained are fresh with only minor alteration of plagioclase to white mica. In addition, sample BG1 also displays slight chloritization of biotite. Potassium feldspar exhibits characteristic cross-hatch twinning of microcline. String perthite is common in the MNW Stock and in sample BG17 from the Glacier Lake Pluton. Microperthitic textures are less common toward the contact of the Glacier Lake Pluton and rare in samples from the Barbara Lake Stock. Plagioclase grains display fine polysynthetic twinning and slight alteration to white mica. Zoning of plagioclase is observed only in one grain of sample BG17. An insufficient population of oriented plagioclase occurs in all thin sections for quantitative optical determination of anorthite content although, where observed, extinction angles on the (010) plane are small indicating that the plagioclase is sodic (albite-oligoclase). Quartz grains show the greatest diversity in size among the sectioned specimens and always display characteristic undulatory extinction. Myrmekitic texture between quartz and plagioclase, where quartz occurs as tiny circular blebs and vermicular intergrowths in plagioclase, occur in samples from the MNW Stock and sample BG17 from the Glacier Lake

Pluton. There appears to be a correlation between the presence of microperthitic textures in feldspars and the occurrence of myrmekite in the same sections. Biotite generally does not exceed 1 mm in length and is brown-green in all samples. In two samples from the Glacier Lake Pluton (BG19, BG24), biotite along with muscovite shows one preferred orientation. This preferred orientation is not observed in thin sections from either the MNW or Barbara Lake Stocks. Subhedral garnet crystals up to 1.5 mm in diameter (Fig. 2-3) occur only in sections from the northern contact of the Glacier Lake Pluton (BG19, BG24) and are not present in either of the two satellitic bodies.

Kilgour Lake Group

Texturally, samples from the Kilgour Lake Group are equigranular to porphyritic, medium- to coarse-grained. Samples from the Kilgour Lake Group are distinguished in thin section from the two-mica leucogranites by the total lack of muscovite and presence of hornblende, sphene (Fig. 2-4) rare allanite and lower content of potassium feldspar in the Kilgour Lake Group granitoids. Potassium feldspar is fresh and shows the characteristic cross-hatch twinning of microcline in all sections. In sample BG10, microcline occurs as phenocrysts and a subordinate constituent of the groundmass with respect to plagioclase. The phenocrysts are microperthitic and contain poikilitic inclusions of

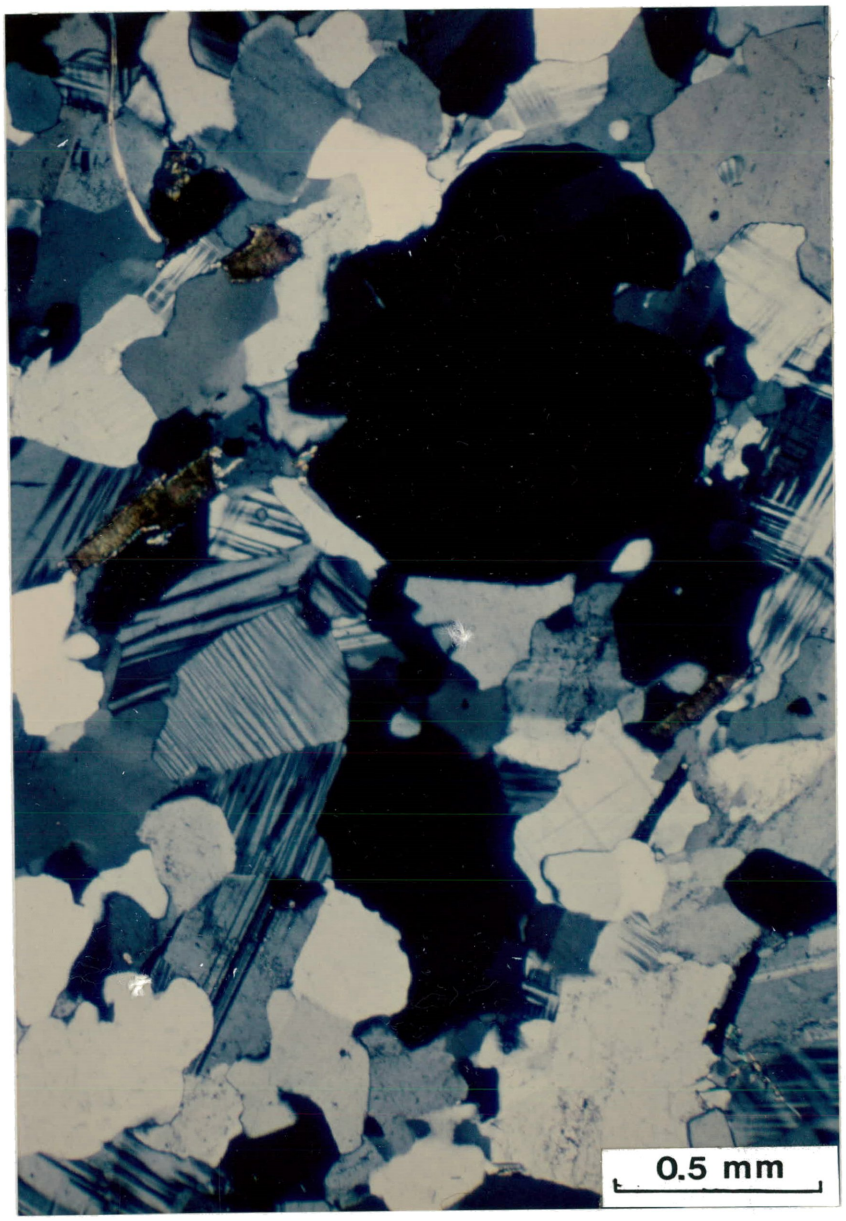

Fig. 2-3. Photomicrograph of sample BG24 displaying characteristic garnet (dark mineral, above centre) from the northern contact of the Glacier Lake Pluton. Other minerals shown include quartz, microcline, sodic plagioclase and biotite (cross-polarized light).

corroded plagioclase up to 0.5 mm in diameter. Microcline in other samples is generally free of microperthite. Quartz displays undulatory extinction in all sections, similar to that in the two-mica leucogranites. Plagioclase commonly shows oscillatory zoning with selective sericitization of the more calcium-rich core. Appearance of biotite is similar to that observed in the two-mica leucogranites. It occurs in pleochroic shades of dull green and brown and is, in general, free of selective chloritization except in sample BG6, where chloritization is pronounced. Biotite shows greater enrichment in the more felsic members of the Kilgour Lake Group. In sample BG11, hornblende is dominant over biotite as the mafic phase. Sphene occurs as a common groundmass phase as subhedral to euhedral diamond-shaped crystals up to 1 mm in length. The distribution of sphene is random and shows slight relative enrichment in sample BG6 from the northwest portion of the Kilgour Lake Group. Allanite is a rare mineral and occurs as subhedral to euhedral, elongate tabular crystals up to 2 mm in length. Colour zoning in shades of yellow-brown and Carlsbad twinning parallel to the long-axis of the crystal are characteristic of allanite. Mafic phases of the Kilgour Lake Group vary from felsic phases by the enrichment in hornblende and apatite, decrease of quartz and appearance of clinopyroxene in the mafic phases. Clinopyroxene in sample BG11 occurs as anhedral light green grains up to 1 mm in diameter but more commonly as much

smaller rounded to subrounded, disseminated grains (Fig. 2-5) commonly intergrown with and mantled by hornblende.

Tonalitic Sills

Constituents of the tonalitic sills are equigranular to porphyritic and medium- to coarse — grained. The coarse-grained and porphyritic character of this group is especially prominent in the leucotonalites (BG2, BG3) from the western portion of the study area. Closely spaced phenocrysts occasionally exceeding 5 mm in length, are separated by a groundmass composed of plagioclase, quartz, biotite and rare microcline which exhibits cross-hatch twinning. The plagioclase phenocrysts are mildly to heavily corroded to white mica with increased alteration toward crystal cores. Groundmass plagioclase also rarely displays antiperthitic textures. Oscillatory zoning in plagioclase is prominent in the non-porphyritic medium-grained tonalite (BG23) where myrmekitic intergrowths are also common in the more sodic outer portions of zoned crystals. Quartz crystals from the tonalitic sills display less strain then in the previously described two granitoid groups. Biotite from the tonalitic sills shows pleochroic colours in shades of yellow-brown and red-brown except in sample BG2 where the biotite has been completely chloritized.

Fig. 2-4. Photomicrograph of sample BG7 displaying characteristic hornblende (green and yellow minerals near centre of photograph) and sphene (euhedral crystal, right of centre of photograph) of the Kilgour Lake Group granitoids. Also visible are quartz, plagioclase, biotite and epidote (cross-polarized light).

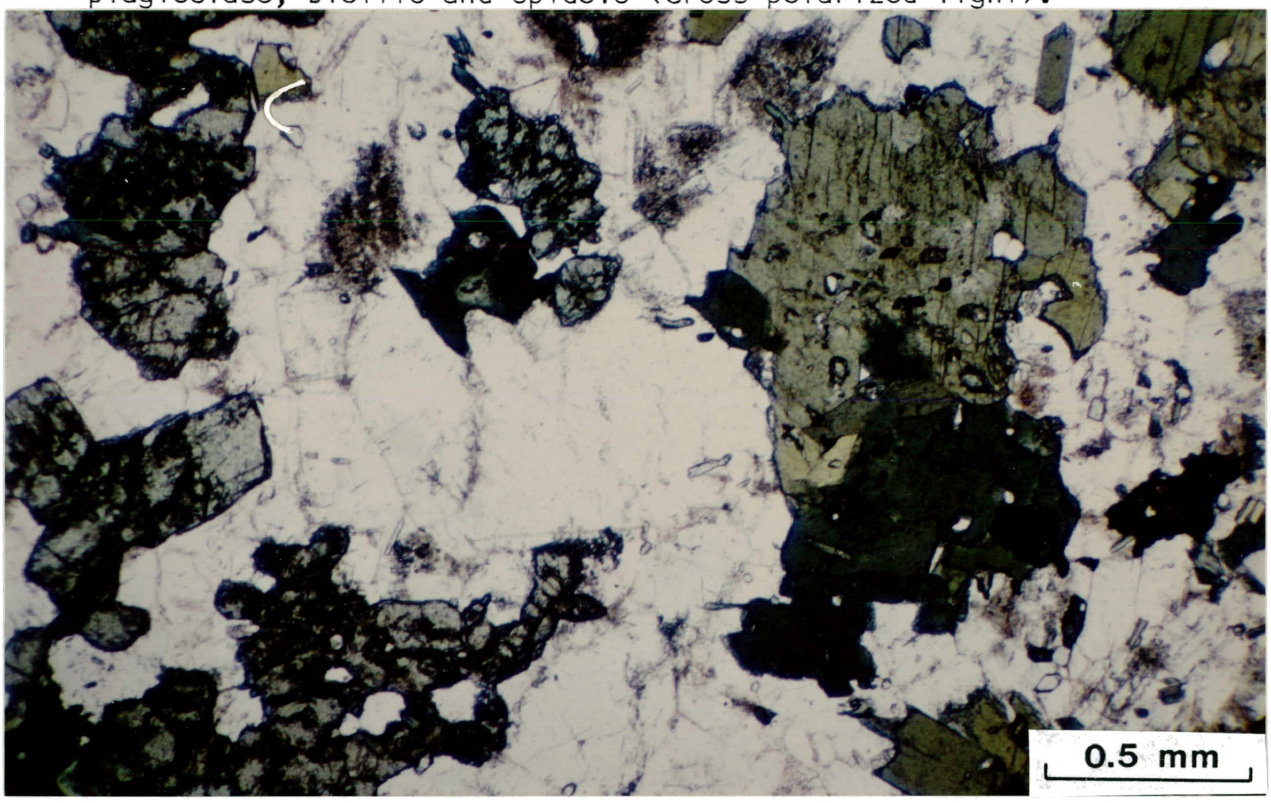

Fig. 2-5. Clinopyroxene (light blue-green, left side of photograph) and hornblende (green mineral, right side of photograph) in sample BG11, monzodiorite from the Kilgour Lake Group. Also distinguished are small apatite crystals and plagioclase (plane-polarized light).

Geochemistry

General Statement

Sixteen samples of granitoids from the Georgia Lake area were geochemically analyzed. SiO_2, TiO_2, Al_2O_3, total iron, MnO, MgO, CaO, Na_2O, K_2O, P_2O_5, Rb, Sr, Ba, Zn, Zr and Nb were determined by X-ray fluorescence spectrometry, FeO by titration and CO_2 and H_2O on a Carbon-hydrogen-nitrogen analyzer. Analyses for Li, Be and Sn were performed by the Geoscience Laboratories of the Ontario Geological Survey by atomic absorption spectrophotometry.

Sample Preparation

Rock samples were sawn into thick slabs and mechanically crushed to small chips less than 1 cm in diameter. Homogenization of the rock chips to a very fine powder was accomplished by grinding in an agate mortar mill. After this, powders retaining a gritty feel were hand finished by mortar and pestle. About 20 to 30 g of powder were produced for each of the 16 samples. Analyses of SiO_2, TiO_2, Al_2O_3, total iron, CaO and K_2O were determined on glass discs by the X-ray fluorescence method. The procedure for producing the glass discs is that of Norrish and Hutton (1969) as modified by Harvey *et al*. (1973). The fusion of rock powders into a glass disc eliminates grain size and mineralogical effects and minimizes matrix effects

resulting from the bulk chemistry of the rock by incorporation of a heavy absorber (lanthanum oxide) and moderate dilution with lithium tetraborate and lithium carbonate. Elemental determination by X-ray fluorescence, other than those listed above, required analysis on pressed powder pellets. The method of powder pellet preparation is described by Norrish and Chappell (1967) and requires the binding of 2 g of fine rock powder into a boric acid shell by the application of ten tons pressure.

Methodology

X-ray Fluorescence Spectrometry - The X-ray fluorescence spectrometer in use in the Instrumentation Lab at Lakehead University is a Philips Model PW 1540. Generator operation for all analyses was set at 50 kv and 50 mA. All elements determined used a chromium anode X-ray tube and a vacuum path for optimum count rates. Flow counter was used in all analyses except for the low energy peaks (Rb, Sr, Zr, Nb, Zn) which required a scintillation counter. Pulse height discrimination required adjustment for each element and occasionally, slight adjustments were necessary for individual elements as a result of drift. Pulse height was set with a (Z) attenuator switch and two potentiometers (window and lower limit). All radiation was unfiltered except for Mn which required a titanium filter to block out interference from the Cr X-ray tube. Analyzing crystals

used include LiF(200), PET, ADP and RbAP. All analyses employed $K\alpha$ radiation peaks except for Ba which employed $L\alpha$. International standards used for calibration include SY-2, MRG-1, GSP-1, G-2, W-1, BCR-1, AGV-1, PCC-1, DTS-1 and T-1. Analytical parameters used for the analysis of each element are summarized in Appendix 1.

All X-ray fluorescence analysis was by a manual method whereby peak and background count rates were recorded and samples rotated by hand. The determination of elemental concentrations was achieved by setting up linear calibration curves with standards based on peak and background count rates. Raw peak and background data were processed by one of three data reduction programs summarized by Mitchell et al (1980). All X-ray fluorescence data processing is on the DEC 2020 computer in the APL language. The program XRF implemented by the APL function PROCESS was used for determination of apparent fluorescent values for all elements as oxides except Zn, for which true concentrations were calculated. Further data reduction of apparent fluorescent values of oxides for matrix absorption effects was performed through the APL function MABSCO. Program XRF2 was used for data reduction of Ba implemented by APL function TIBAV. This program also requests absorption coefficients for each standard and corrects for interference for the $K\alpha$ energy peak of Ti. Program XRF3, implemented by the APL function RBNB, was used for the data reduction of Rb, Sr, Zr and

Nb. This program also requests count data for Y and makes mass absorption corrections and corrects Zr and Nb for interference from secondary energy peaks of Sr and Y, respectively.

Carbon-Hydrogen-Nitrogen Analyzer - H_2O and CO_2 were determined on a Perkin-Elmer 240 CHN analyzer. The method relies on the weight of liberated volatiles adsorbed onto specific compounds after combustion at 1200° C.

Titration - The experiment for determination of wt % FeO is summarized by Mitchell et al. (1980). Briefly, the method involves the dissolution of 0.5 g of rock powder of each sample and titration with a dichromate solution. The volume of dichromate used is directly proportional to wt % FeO.

Error Analysis

Accuracy estimates are presented for all data obtained by X-ray fluorescence spectrometry (Table 2-4) as % error between the obtained value for a calibration standard and its true value. The obtained value was derived by plotting the count rate data of a standard, for which the true concentration or apparent fluorescent value (Mitchell et al., 1980) of an element or oxide are known, on a calibration

Table 2-4: Accuracy estimates for XRF data based on % error from accepted values.

Element/ Oxide	Standard	True Value+	Obtained Value	% Error	Best Obtained Correlation Coefficient Of Calibration Line
		wt. %	wt. %		
SiO_2	G-2	69.78-	69.01	-1.10	0.9986
TiO_2	BCR-1	2.24-	2.24	0.00	0.9996
Al_2O_3	AGV-1	17.05-	17.39	+1.96	0.9981
Fe_2O_3*	BCR-1	13.46-	13.42	-0.30	0.9988
MnO	SY-2	0.32	0.32	0.00	0.9991
MgO	SY-2	2.70	2.46	-8.89	0.9703
CaO	BCR-1	7.04-	7.00	-0.57	0.9999
Na_2O	T-1	4.39	4.44	+1.13	0.9984
K_2O	GSP-1	5.51-	5.24	-4.90	0.9906
P_2O_5	SY-2	0.43	0.43	0.00	0.9760
		PPM	PPM		
Rb	G-2	170	180.2	+5.66	0.9999
Sr	G-2	480	493	+2.64	0.9995
Ba	GSP-1	1300	1282	-1.38	0.9997
Zn	AGV-1	86	74	-13.95	0.9963
Zr	G-2	300	297	-1.00	0.9992
Nb	G-2	13?	17.2	+24.42	0.9873

+ Values from Abbey (1983)

- Apparent fluorescent values from Mitchell *et al.* (1980)

* Total iron as Fe_2O_3

curve from which data was obtained. It is assumed that compositions of calibration standards to be without error except for Nb where the concentration of Nb in standard G-2 is approximate (Abbey, 1983). A larger % error of an obtained value from its true concentration or apparent fluoresent value is directly proportional to a decrease in quality of data. Table 2-4 also summarizes the best obtained correlation coefficients, which reflect the linearity of the used calibration curves. In most cases, accuracy is diminished considerably as a result of a small digression of the calibration curve from a straight line.

The least accurate results of the oxides are for MgO. Weight % MgO was determined on pressed powder pellets which is an unconventional method to derive MgO values. The decrease in accuracy can be attributed to the introduction of matrix and grain size effects. All standards used for MgO determination were of granitoid composition. Similarly, Na_2O determinations with granitoid standards on pressed powder pellets are of greater accuracy than for MgO. MgO determination on glass discs was not possible because of the very poor peak to background count ratio on standards with about 2 wt % MgO or less. Standardization with low MgO concentration standards was necessary because of low sample concentrations, in general. Even so, some sample data fell below the statistically calculated lower limit of detection at the 2σ level of confidence (Jenkins and

DeVries, 1970) of 0.30 wt % MgO on a pressed powder pellet. Data for Zn and Nb are of poor accuracy with respect to the other elements. Data for Zn was uncorrected for matrix effects. All standards used for Zn determination are of granitoid composition. The low accuracy of Nb is attributable to the uncertainty of the true concentration of Nb in standards and the low peak to background count ratio reflecting the close proximity of data to the derived lower limit of detection for Nb of 2 ppm.

Precision estimates of X-ray fluorescence data are presented in Table 2-5. The method takes into consideration the counting statistics as the only significant factor influencing the precision of data. In this sense, the precision estimate is a standard counting error. Precision estimates are determined at the 2σ level of confidence by the method of Bertin (1967) which takes into account the peak and corresponding background counts for each determination. Homogeneity of the sample and perfect stability of the X-ray generator tube are assumed.

The precision estimates correlate directly with accuracy of data and linearity of calibration curves. Poor peak to background ratios of Zn and Nb are reflected in the poor reproducibility of these two elements.

Accuracy and precision of H_2O and CO_2 are considered

Table 2-5: Precision estimates of XRF data at the 2σ level of confidence based on counting statistics

Element/Oxide	Maximum % 2σ	Minimum % 2σ	Average % 2σ
SiO_2	0.32	0.27	0.29
TiO_2	3.28	0.63	1.44
Al_2O_3	1.16	0.90	1.05
Fe_2O_3*	1.34	0.41	0.85
MnO	7.38	1.95	4.04
MgO	12.71	2.19	5.44
CaO	1.27	0.38	0.79
Na_2O	4.89	3.39	4.12
K_2O	0.75	0.39	0.49
P_2O_5	5.18	0.89	2.75
Rb	13.71	1.78	4.19
Sr	13.86	0.64	3.74
Ba	5.67	1.05	2.02
Zn	47.97	8.65	25.60
Zr	14.09	1.85	4.31
Nb	60.06	18.60	37.78

* total iron as Fe_2O_3

to be low because obtained values are below or at the detection limits of H_2O and CO_2 for the CHN analyzer.

Data quality checks for FeO were not performed and not obtained for Li, Be and Sn.

Results

Geochemical data along with CIPW norms for granitoids of the Georgia Lake area are presented in Tables 2-6 to 2-8. There is a distinct bimodal distribution of major, minor and trace element data between the two-mica leucogranites and Kilgour Lake Group granitoids. The affinities of the tonalitic sills are more problematic and show considerable chemical variation from the more felsic to the more mafic phases. On all geochemical plots, two-mica leucogranites, Kilgour lake Group granitoids and tonalitic sills are identified with circles, squares and triangles, respectively (Table 2-9).

Oxide Data - The two-mica leucogranites display an enrichment in SiO_2 and K_2O relative to the Kilgour Lake Group while the Kilgour Lake Group granitoids are enriched in all other oxides relative to the two-mica leucogranites except for Na_2O, which does not show a distinct variation between the two granitoid groups. CO_2 and H_2O reflect greater

Table 2-6: Chemical analysis of two-mica leucogranites

	Barbara Lake Stock		MNW Stock		Glacier Lake Pluton		
Sample	BG1	BG22	BG4	BG5	BG17	BG19	BG24
SiO_2(wt%)	74.19	74.24	73.44	73.76	74.68	77.17	74.05
TiO_2	0.22	0.17	0.27	0.22	0.09	0.04	0.15
Al_2O_3	13.58	13.89	13.64	14.20	14.05	13.07	14.61
Fe_2O_3	0.78	1.49	1.62	1.01	0.74	0.76	0.75
FeO	0.71	0.33	0.53	0.50	0.29	0.19	0.37
MnO	0.02	0.02	0.03	0.03	0.01	0.02	0.02
MgO	0.37	≤0.30	0.32	≤0.30	≤0.30	≤0.30	≤0.30
CaO	0.10	0.42	0.18	0.24	0.40	0.04	0.35
Na_2O	3.55	3.59	3.51	3.53	3.95	4.24	4.60
K_2O	5.68	5.34	5.47	5.29	4.66	4.07	4.50
P_2O_5	0.10	0.13	0.21	0.20	0.12	0.11	0.12
CO_2	≤0.15	≤0.15	≤0.15	≤0.15	0.40	≤0.15	≤0.15
H_2O	0.63	≤0.36	0.54	0.63	0.63	≤0.36	≤0.36
Total	99.93	99.62	99.76	99.61	100.02	99.71	99.52
FeO/Fe_2O_3	0.91	0.22	0.33	0.50	0.39	0.25	0.49
A/(CNK)*	1.12	1.12	1.14	1.19	1.15	1.14	1.12
Li (ppm)	26	107	176	104	28	66	112
Rb	357	303	377	377	168	351	332
Be	5	4	5	6	3	4	6
Sr	104	114	97	97	118	44	99
Ba	756	686	598	600	553	408	559
Zn	≤18	20	24	29	≤18	27	27
Zr	145	138	139	138	81	40	99
Nb	18	9	17	19	8	12	11
Sn	4	5	5	6	4	10	6
K/Rb	132.2	146.2	120.4	116.5	230.4	96.3	112.7
K/Ba	62.43	64.58	75.92	73.17	69.98	82.84	66.91
K/Sr	453.9	388.6	468.0	452.6	328.0	768.2	377.8
Ba/Rb	2.12	2.26	1.59	1.59	3.29	1.16	1.68
Ba/Sr	7.27	6.02	6.16	6.19	4.69	9.27	5.65
Rb/Sr	3.43	2.66	3.89	3.89	1.42	7.98	3.35
Mg/Li	84.62	--	10.80	--	--	--	--
Zr/Sn	36.25	27.60	27.80	23.00	20.25	4.00	16.50
CIPW Norms							
Q	31.10	32.36	31.61	32.56	33.78	36.91	29.64
C	1.59	1.74	1.95	2.67	2.51	1.69	1.82
Or	33.56	31.55	32.32	31.26	27.54	24.05	26.59
Ab	30.04	30.38	29.70	29.87	33.42	35.88	38.92
An	0.00	1.26	0.00	0.00	0.00	0.00	0.97
Di	0.00	0.00	0.00	0.00	0.00	0.00	0.00
Hy	1.25	0.02	0.80	0.70	0.15	0.02	0.02
Ol	0.00	0.00	0.00	0.00	0.00	0.00	0.00
He	0.00	1.05	0.91	0.27	0.25	0.37	0.18
Mt	1.13	0.64	1.02	1.07	0.71	0.56	0.82
Il	0.42	0.32	0.51	0.42	0.17	0.08	0.28
Ap	0.55	0.28	1.00	0.44	0.26	0.22	0.26
Cc	0.00	0.00	0.00	0.00	0.46	0.00	0.00

*A/(CNK)=Molecular proportions of $Al_2O_3/(CaO+Na_2O+K_2O)$

Table 2-7: Chemical analysis of Kilgour Lake Group granitoids

	Grano-diorite	Tona-lite	Porphyritic Granodiorite	Monzo-diorite	Grano-diorite	Tona-lite
Sample	BG6	BG7	BG10	BG11	BG14	BG15
SiO_2(wt%)	64.18	65.17	62.66	56.12	66.76	67.40
TiO_2	1.47	0.40	0.42	0.70	0.53	0.36
Al_2O_3	16.37	16.97	17.77	14.39	16.96	16.31
Fe_2O_3	1.49	2.06	2.84	1.27	1.66	1.46
FeO	1.62	1.41	1.89	6.29	0.98	1.36
MnO	0.05	0.04	0.12	0.14	0.03	0.04
MgO	2.12	2.01	2.67	4.58	1.75	1.46
CaO	2.42	3.10	2.53	6.86	2.14	2.75
Na_2O	4.64	4.65	3.99	3.89	4.77	4.74
K_2O	3.16	3.03	4.61	4.05	3.15	3.31
P_2O_5	0.30	0.30	0.47	0.93	0.20	0.25
CO_2	0.22	$\leq$0.15	0.22	$\leq$0.15	$\leq$0.15	$\leq$0.15
H_2O	1.70	0.71	$\leq$0.36	0.89	0.63	0.54
Total	99.74	99.85	100.19	100.11	99.56	99.98
FeO/Fe_2O_3	1.09	0.68	0.67	4.95	0.59	0.93
A/(CNK)*	1.06	1.03	1.10	0.62	1.12	1.00
Li (ppm)	30	36	27	14	51	150
Rb	109	103	160	97	101	122
Be	2	2	4	4	2	3
Sr	674	792	807	1158	562	686
Ba	1088	1141	1145	1590	976	991
Zn	66	59	76	72	56	50
Zr	152	128	218	219	110	133
Nb	10	9	14	14	7	10
Sn	1	2	2	1	2	2
K/Rb	240.4	244.7	239.4	346.4	258.4	225.4
K/Ba	24.08	22.09	33.45	21.13	26.74	27.75
K/Sr	38.87	31.82	47.46	29.02	46.44	40.09
Ba/Rb	9.98	11.08	7.16	16.39	9.66	8.12
Ba/Sr	1.61	1.44	1.42	1.37	1.74	1.44
Rb/Sr	0.162	0.130	0.198	0.084	0.180	0.178
Mg/Li	426.7	336.1	596.1	1971.4	207.8	58.67
Zr/Sn	152.0	64.0	109.0	219.0	55.0	66.5
CIPW Norms						
Q	18.11	17.54	13.90	0.00	20.38	19.37
C	2.07	1.07	3.14	0.00	2.34	0.47
Or	18.67	17.90	27.24	23.93	18.61	19.56
Ab	39.26	39.34	33.76	32.91	40.36	40.11
An	8.85	13.55	8.40	9.84	9.19	12.17
Di	0.00	0.00	0.00	15.04	0.00	0.00
Hy	5.28	5.31	7.30	8.32	4.36	4.41
Ol	0.00	0.00	0.00	3.88	0.00	0.00
He	0.71	0.00	0.00	0.00	0.47	0.00
Mt	1.12	2.99	4.12	1.84	1.72	2.12
Il	2.79	0.76	0.80	1.33	1.01	0.68
Ap	0.66	0.66	1.03	2.03	0.44	0.55
Cc	0.50	0.00	0.50	0.00	0.00	0.00

*A/(CNK)=Molecular proportions of $Al_2O_3/(CaO+Na_2O+K_2O)$

Table 2-8: Chemical analysis of tonalitic sills

	Postagoni Lake leucotonalite	Blay Lake leucotonalite	Parole Lake tonalite
Sample	BG2	BG3	BG23
SiO_2(wt%)	73.99	68.87	63.46
TiO_2	0.24	0.14	0.93
Al_2O_3	13.66	17.45	18.47
Fe_2O_3	0.91	0.94	1.27
FeO	0.59	0.38	1.58
MnO	0.03	0.02	0.04
MgO	1.07	1.20	2.82
CaO	1.60	2.97	2.88
Na_2O	4.99	5.67	4.91
K_2O	1.49	1.27	1.62
P_2O_5	0.11	0.13	0.21
CO_2	0.22	0.18	$\leq$0.15
H_2O	0.98	0.71	0.80
Total	99.88	99.93	98.99
FeO/Fe_2O_3	0.65	0.40	1.24
A/(CNK)*	1.06	1.09	1.23
Li (ppm)	42	280	900
Rb	30	85	414
Be	1	2	3
Sr	360	458	635
Ba	663	685	944
Zn	41	$\leq$18	73
Zr	96	58	116
Nb	8	6	7
Sn	1	3	4
K/Rb	413.3	123.5	32.37
K/Ba	18.70	15.33	14.19
K/Sr	34.44	22.93	21.10
Ba/Rb	22.10	8.06	2.28
Ba/Sr	1.84	1.50	1.49
Rb/Sr	0.083	0.186	0.652
Mg/Li	154.8	25.71	18.89
Zr/Sn	96.00	19.33	29.00
CIPW Norms			
Q	35.12	23.70	18.68
C	1.68	2.05	3.86
Or	8.80	7.50	9.57
Ab	42.22	47.97	41.54
An	5.90	12.83	13.05
Di	0.00	0.00	0.00
Hy	2.66	2.99	7.41
Ol	0.00	0.00	0.00
He	0.01	0.33	0.00
Mt	1.30	0.88	1.84
Il	0.46	0.27	1.77
Ap	0.24	0.28	0.46
Cc	0.50	0.41	0.00

*A/(CNK)-Molecular proportions of $Al_2O_3/(CaO+Na_2O+K_2O)$

degrees of alteration by the presence of carbonate and secondary micaceous minerals and are generally insignificant in granitoids.

SiO_2 is tightly clustered around 74 wt % in all the two-mica leucogranites except for sample BG19 in which SiO_2 is relatively enriched. The same tight clustering of SiO_2 is not evident in either the Kilgour Lake Group granitoids or the tonalitic intrusions in which the SiO_2 spread in values is over 20% in the former and 10% in the later. These intergranitic variations are illustrated in Harker diagrams (Figs. 2-6 to 2-17). Weight % SiO_2 reflects felsic mineral content which is greatest in the two-mica leucogranites; leucotonalite sample BG2 is an exception. K_2O progressively decrease from a maximum of over 5 wt % in the Barbara Lake and MNW Stocks to over 4 wt % in the Glacier Lake Pluton. In the Kilgour Lake Group, K_2O appears to have greater affinity for the more mafic members of the group (samples BG10, BG11). The tonalitic sills show pronounced depletion and the smallest spread in K_2O values relative to the other granitoid groups (Fig. 2-6). Na_2O does not vary as greatly as K_2O between granitoid groups although the tonalitic sills show slight relative enrichment in Na_2O. A positive correlation is evident between Na_2O and SiO_2 (Fig. 2-7) in granitoids of the Kilgour Lake Group. CaO shows a similar trend to MgO with respect to SiO_2 (Figs. 2-8, 2-9). Two-mica

Table 2-9: List of symbols identifying granitoid groups on all geochemical plots - Figs. 2-6 to 2-42.

Symbol	Granitoid Group	Rock Types
●	Two-Mica Leucogranites	leucogranites
■	Kilgour Lake Group	granodiorites tonalites
■ M	Kilgour Lake Group	monzodiorite
▲	Tonalitic Sills	leucotonalites tonalites

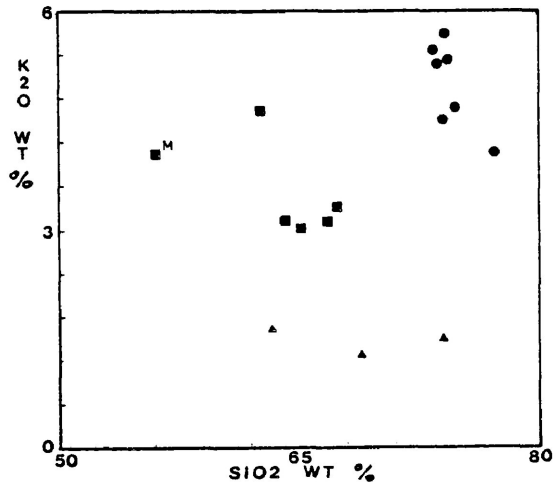

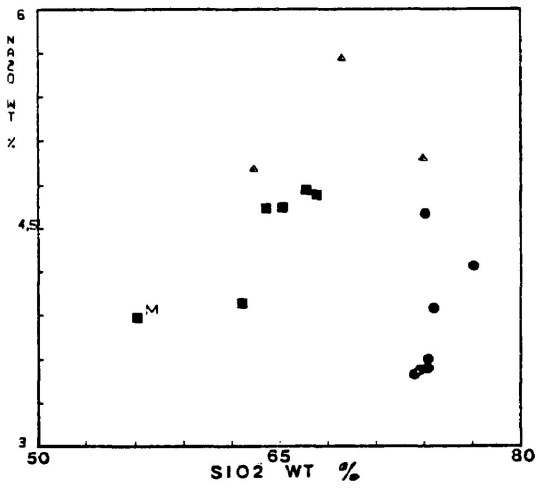

Fig. 2-6 (left). K_2O versus SiO_2 for granitoids.

Fig. 2-7 (right). Na_2O versus SiO_2 for granitoids.

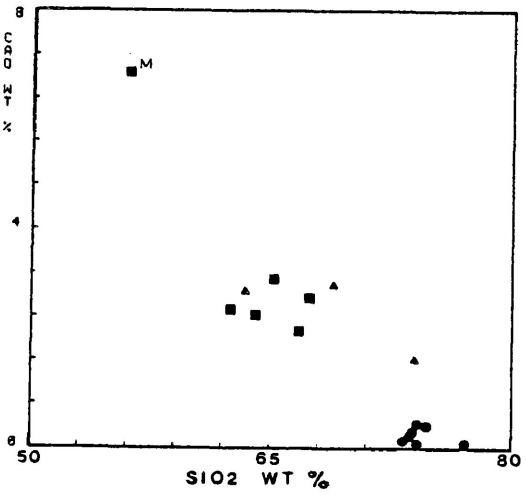

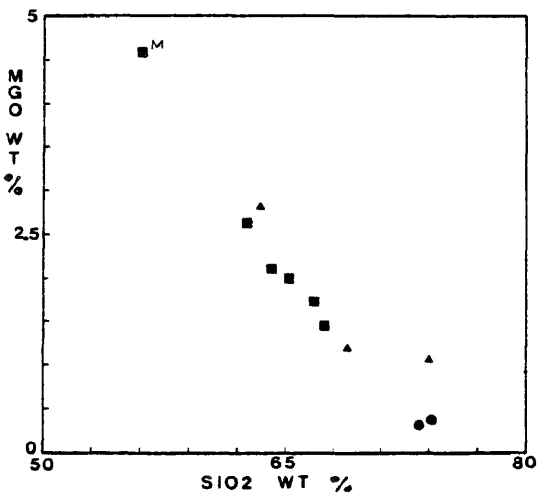

Fig. 2-8 (left). CaO versus SiO_2 for granitoids.

Fig. 2-9 (right). MgO versus SiO_2 for granitoids.

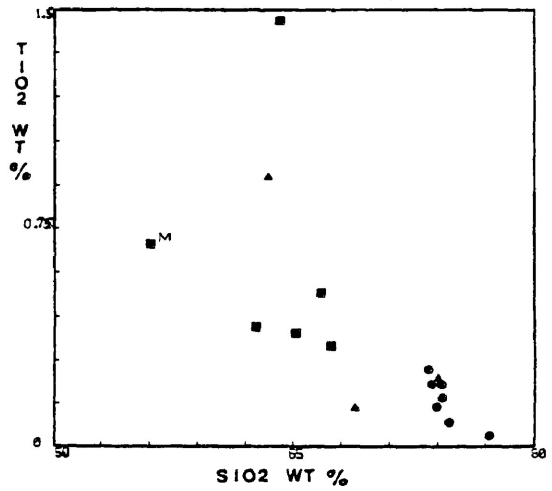

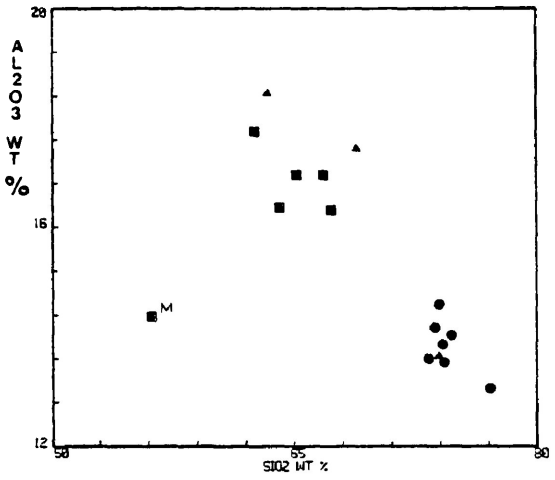

Fig. 2-10 (left). TiO_2 versus SiO_2 for granitoids.

Fig. 2-11 (right). Al_2O_3 versus SiO_2 for granitoids.

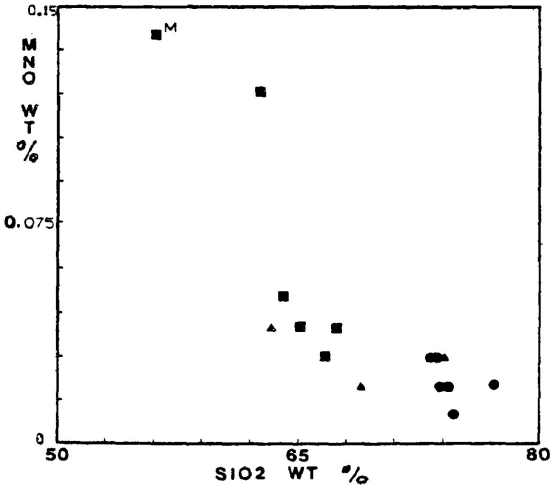

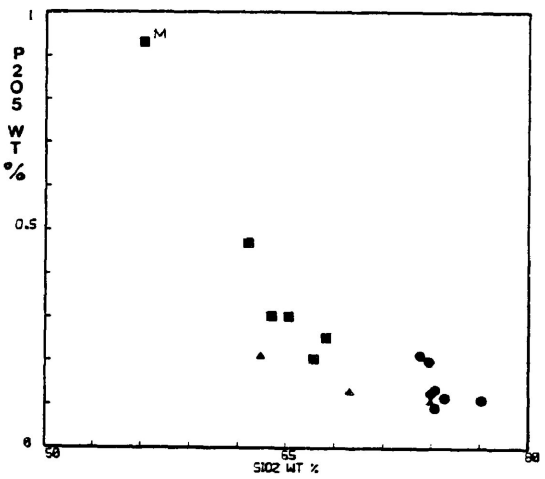

Fig. 2-12 (left). MnO versus SiO_2 for granitoids.

Fig. 2-13 (right). P_2O_5 versus SiO_2 for granitoids.

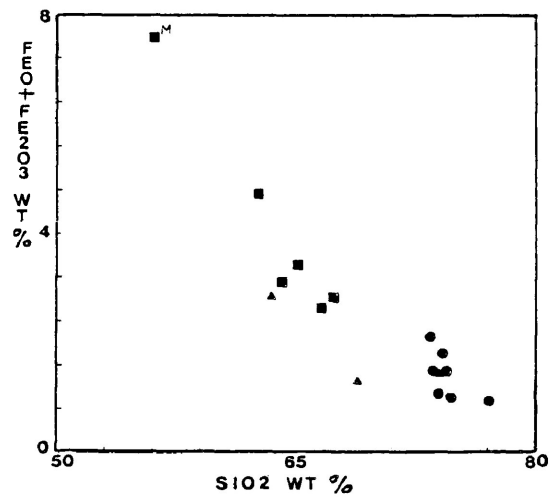

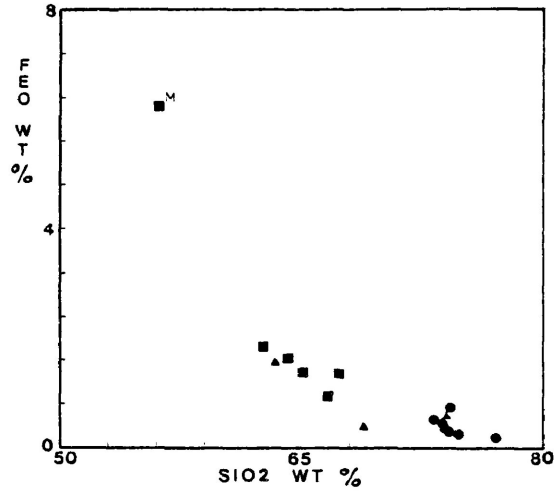

Fig. 2-14 (left). Total iron versus SiO_2 for granitoids.

Fig. 2-15 (right). FeO versus SiO_2 for granitoids.

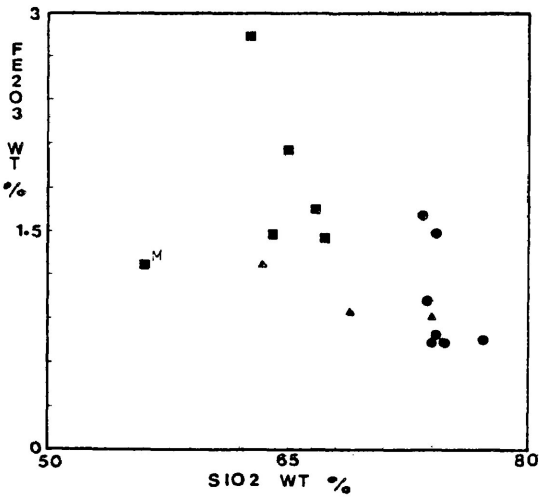

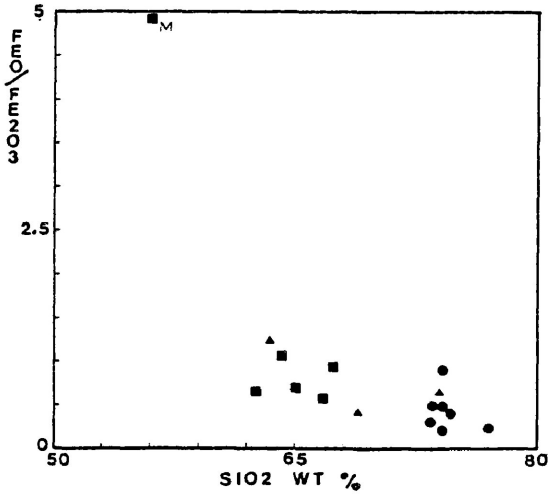

Fig. 2-16 (left). Fe_2O_3 versus SiO_2 for granitoids.

Fig. 2-17 (right). FeO/Fe_2O_3 versus SiO_2 for granitoids.

leucogranites are extremely depleated in CaO and MgO reflecting high degrees of fractionation. A similar negative correlation is observed with TiO_2 against SiO_2 (Fig. 2-10) except for samples BG6 and BG23. The distribution of Al_2O_3 is independent of granitoid group and appears to cluster with respect to SiO_2 content (Fig. 2-11) where granitoids with an SiO_2 range of 60 to 70 wt % contain the greatest % Al_2O_3. MnO and P_2O_5 (Figs. 2-12, 2-13) display very similar negative correlation against SiO_2. Behaviour of iron in the granitoids is similar to CaO and MgO in relation to SiO_2. The distinct negative correlation of total iron to SiO2 (Fig. 2-14) and ferrous iron to SiO_2 (Fig. 2-15) is especially evident in granitoids of the Kilgour Lake Group. This same trend is not followed through by ferric iron (Fig. 2-16) suggesting that the behaviour of total iron is dependent on the ferrous ion. Ferrous to ferric iron ratio is highly variable in each group of granitoids although the average of the two-mica leucogranites (0.441) is less than the felsic granitoids of the Kilgour Lake Group (0.792) and the tonalitic sills (0.765) suggesting that two-mica leucogranites have greater affinity for ferric iron than tonalites or the Kilgour Lake Group granitoids. The distribution of iron oxidation states is summarized in Fig. 2-17. The trends of MgO (Fig. 2-18) and TiO_2 (Fig. 2-19) against total iron are mirror images of TiO_2 and MgO against SiO_2. Distribution of selected alkalis and alkaline earths against each other (Figs. 2-20 to 2-22)

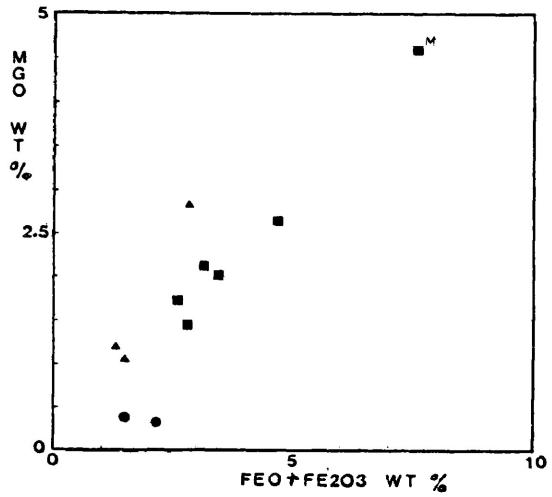

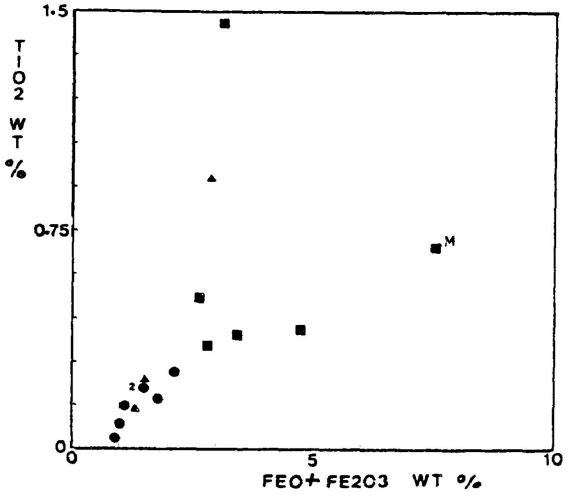

Fig. 2-18 (left). MgO versus Total iron for granitoids.

Fig. 2-19 (right). TiO_2 versus Total iron for granitoids.

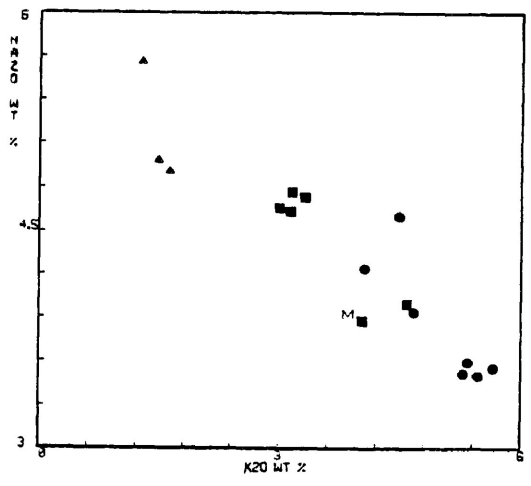

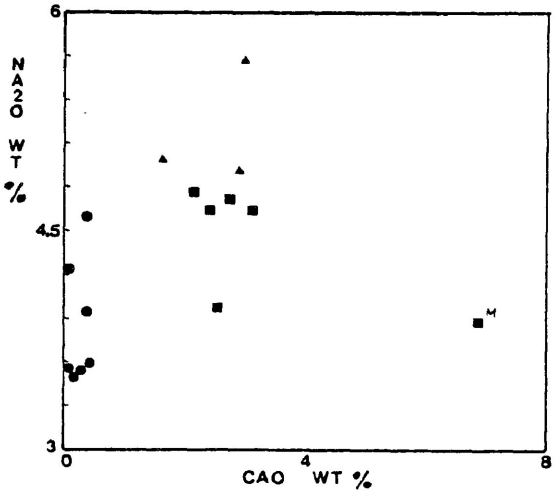

Fig. 2-20 (left). Na_2O versus K_2O for granitoids.

Fig. 2-21 (right). Na_2O versus CaO for granitoids.

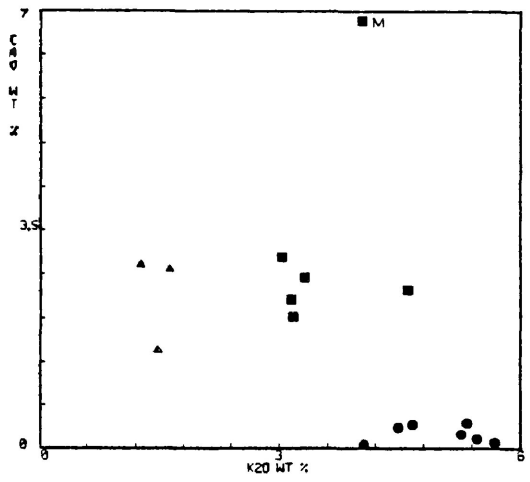

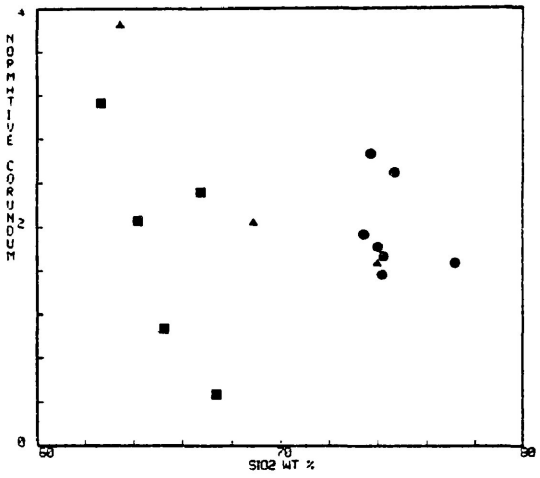

Fig. 2-22 (left). CaO versus K_2O for granitoids.

Fig. 2-23 (right). Normative corundum versus SiO_2 for granitoids.

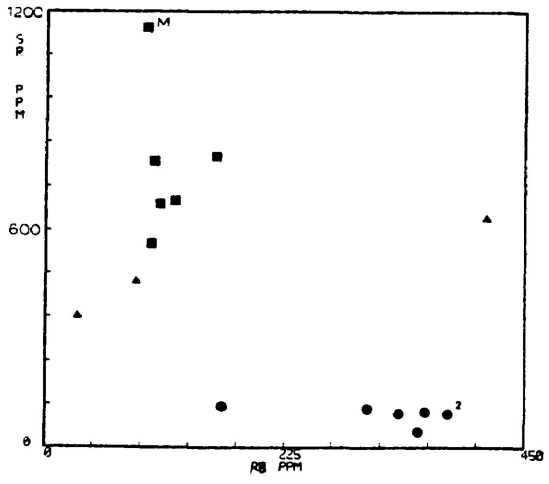

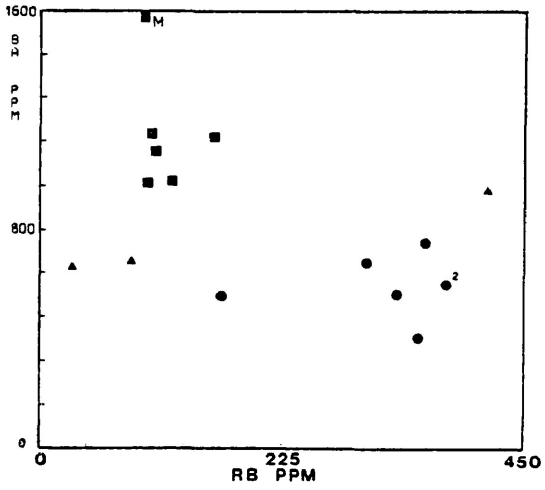

Fig. 2-24 (left). Sr versus Rb for granitoids.

Fig. 2-25 (right). Ba versus Rb for granitoids.

shows that only Na_2O against K_2O is linearly correlatable where the Kilgour Lake Group also partially overlaps with the two-mica leucogranites.

The geochemical distinction of the three suites of Georgia Lake granitoids is readily discernable on ternary chemical plots. A Ca-Na-K molecular proportion diagram (Fig. 2-26) shows that two-mica leucogranites have a considerably greater affinity for Na and K in relation to Ca than the two other granitoid groups. The smaller satellitic stocks of the two-mica leucogranites are slightly skewed toward the K component with respect to the Glacier Lake Pluton. Progressive depletion in Ca is also evident toward the more felsic phases of the Kilgour Lake Group. A similar trimodal distribution of granitoid groups is observable on an AFM plot (Fig. 2-27).

CIPW Norms - All analyzed granitoid samples are corundum normative (Fig. 2-23) except for sample BG11, which is diopside normative and shows olivine in the norm as well. A normative Ab-Or-Qz diagram (Fig. 2-28) with isobaric cotectics of 1 to 5 kbars pressure shows a tight clustering of the most felsic members of the Kilgour Lake Group near the cotectic minimum of granite at 5 kbars. The tonalites are skewed along the Ab-Qz cotectics whereas the two-mica leucogranites deviate from the ternary minimum of 5 kbars pressure along the Or-Qz cotectic with possible lower

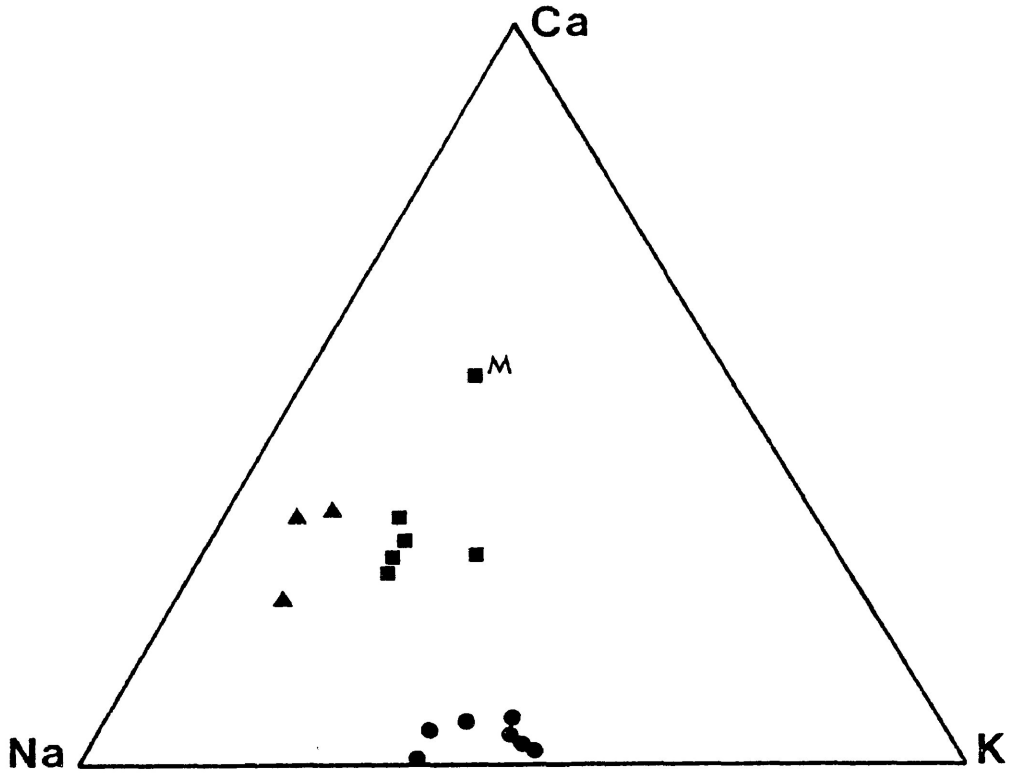

Fig. 2-26. Diagram of molecular proportions Ca-Na-K for granitoids.

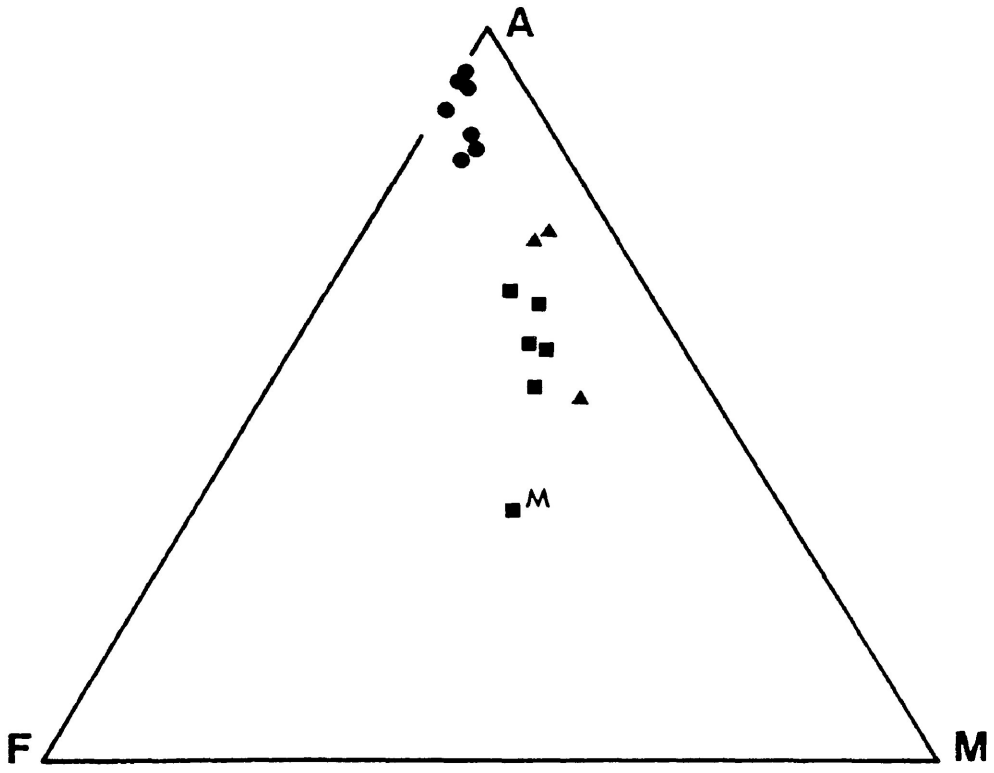

Fig. 2-27. AFM diagram for granitoids.

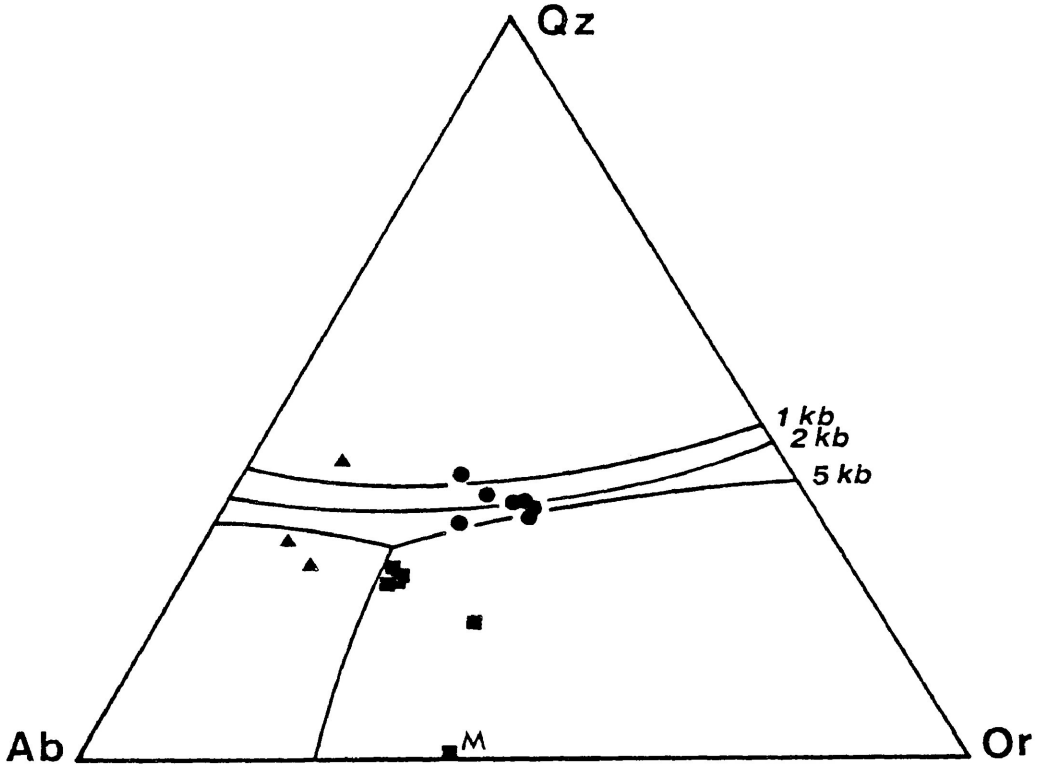

Fig. 2-28. Normative Ab-Or-Qz diagram for granitoids. Isobaric contours are after Tuttle and Bowen (1958) and Luth et al. (1964).

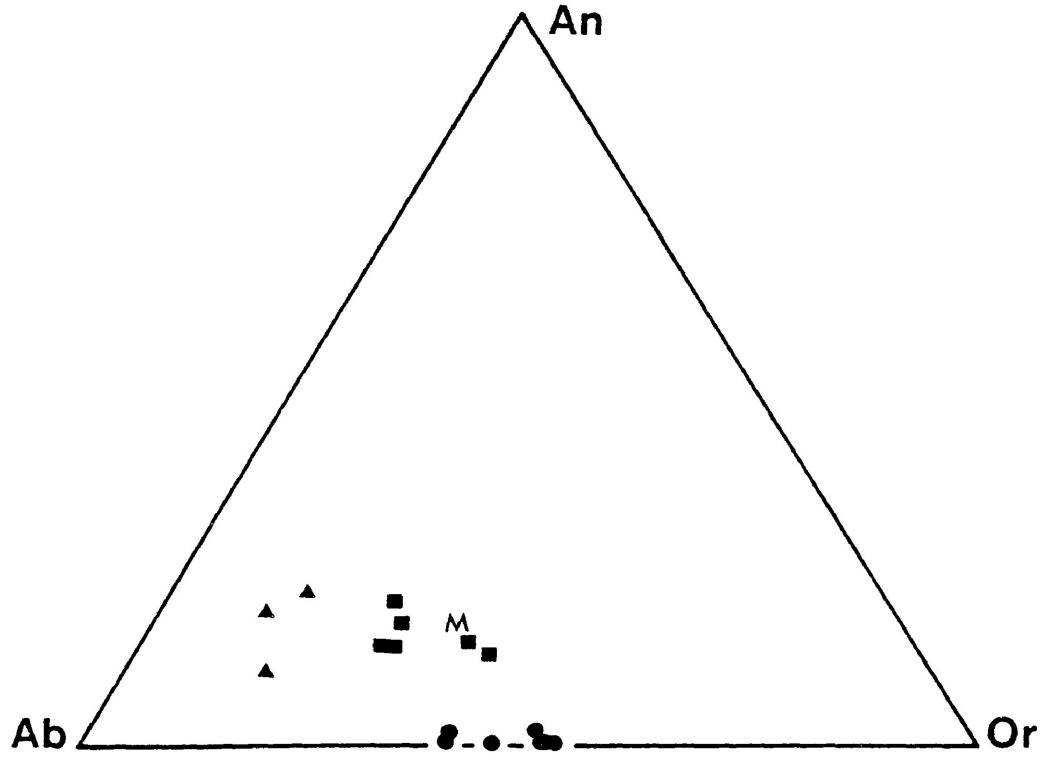

Fig. 2-29. Normative An-Ab-Or diagram for granitoids.

pressure affinities in relation to Kilgour Lake Group granitoids. The normative An-Ab-Or plot (Fig. 2-29) is similar to the Ca-Na-K diagram (Fig. 2-26) except that tonalites and Kilgour Lake Group granitoids are depressed towards the Ab-Or sideline in the former.

Trace Elements - Rb is enriched and Li is slightly enriched in the two-mica leucogranites relative to the other granitoid groups. The anomalously high Li content, for granitoids, of samples BG3 and BG23, representing the tonalitic sills, is most likely the result of rare-element wall rock enrichment from lithium pegmatites because of the close proximity of sampling locations to such pegmatites. Sample BG23 also has high Rb concentration. Sr and Ba are depleated in the two-mica leucogranites relative to the other two granitoid groups. The behaviour of the rare transition metals is variable in granitoids of the Georgia Lake area. Figs. 2-24, 2-25, 2-31 and 2-32 exhibit a selection of rare alkali and alkaline earth, minor and trace element plots, the most significant feature being the bimodal distribution between two-mica leucogranites and the Kilgour Lake Group. Only Fig. 2-40 of Sr against Ba shows a strong positive correlation between rare elements and the trend roughly corresponds to increasing mafic content of the granitoids. Fig. 2-30 adapted from El Bouseily and El Sokkary (1975) displays a distinct clustering of the Kilgour Lake Group granitoids and two-mica leucogranites. On this

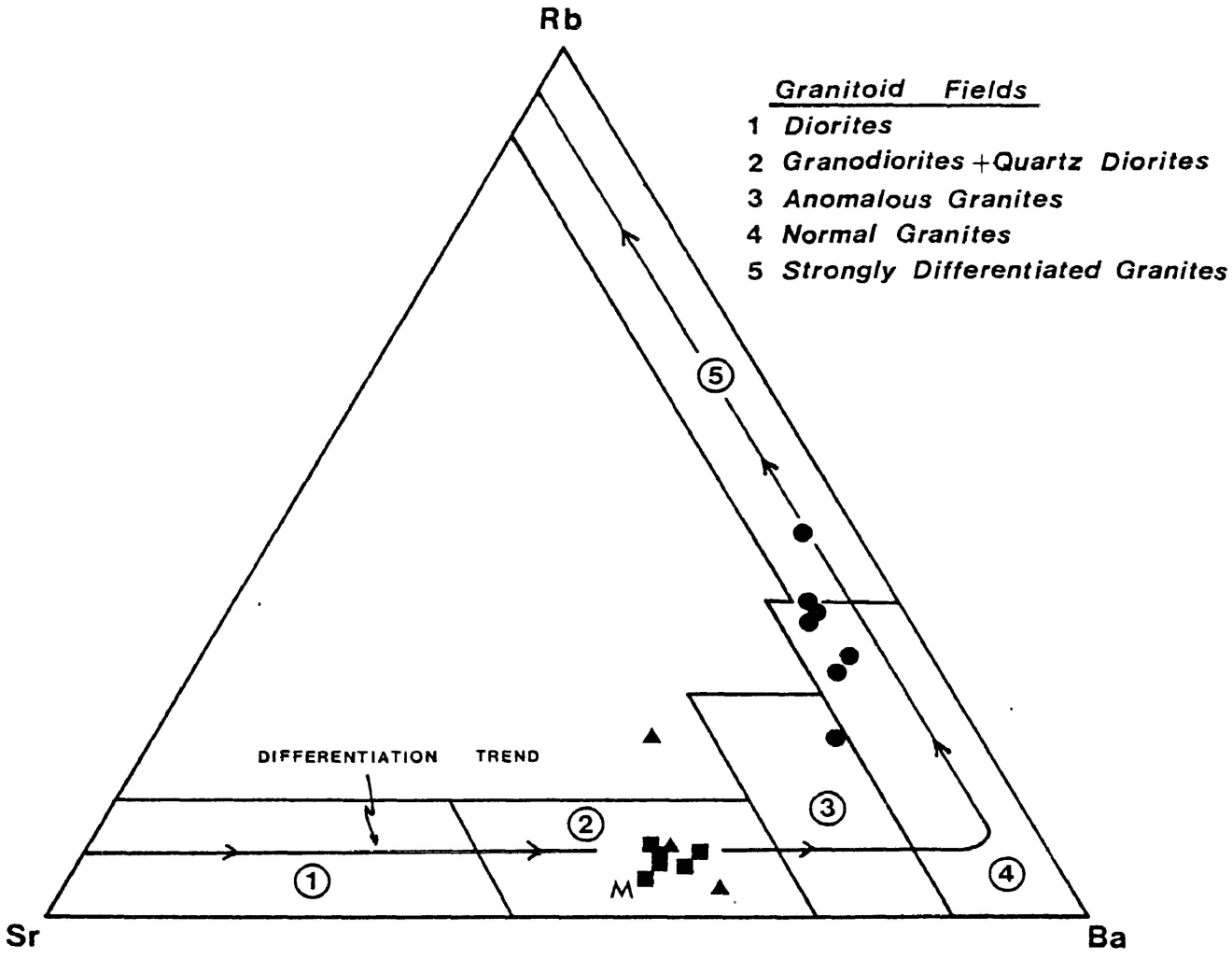

Fig. 2-30. Rb-Sr-Ba diagram for granitoids (from El Bouseily and El Sokkary, 1975).

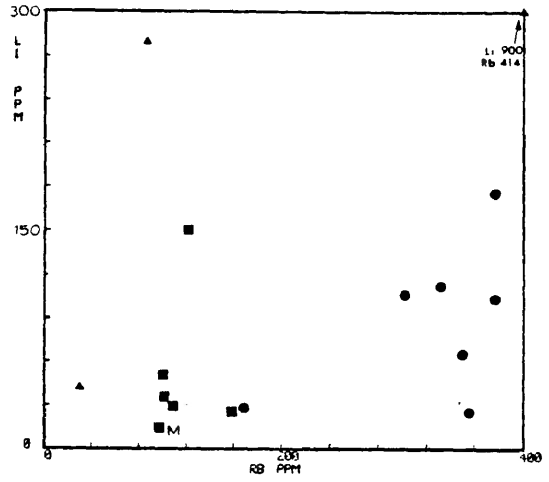

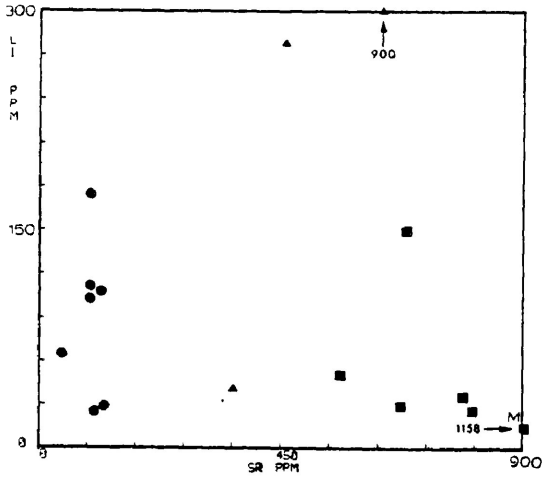

Fig. 2-31 (left). Li versus Rb for granitoids.

Fig. 2-32 (right). Li versus Sr for granitoids.

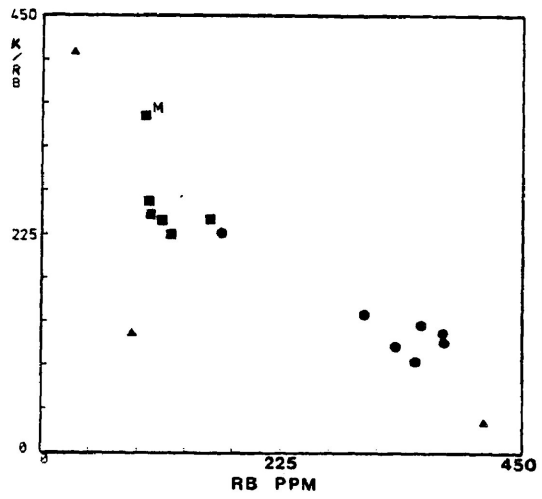

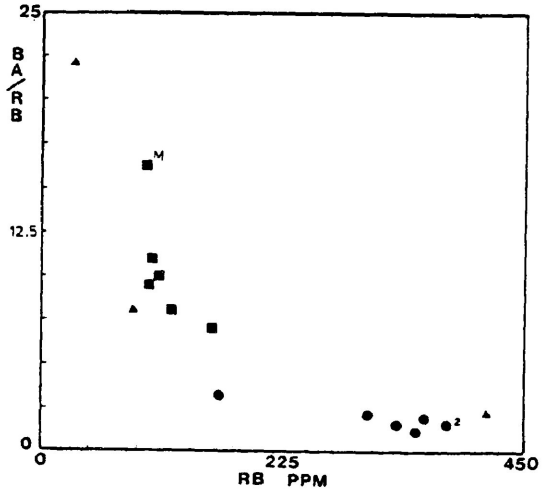

Fig. 2-33 (left). K/Rb versus Rb for granitoids.

Fig. 2-34 (right). Ba/Rb versus Rb for granitoids.

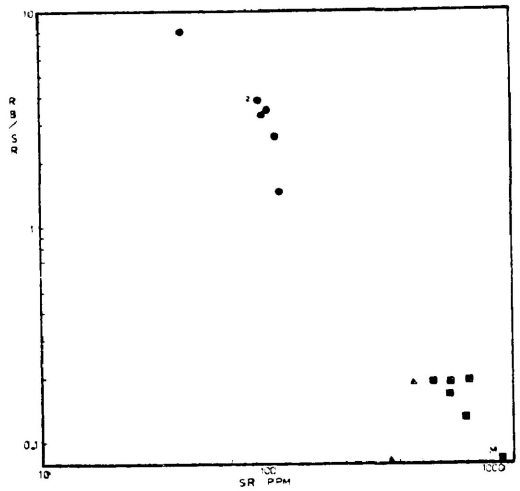

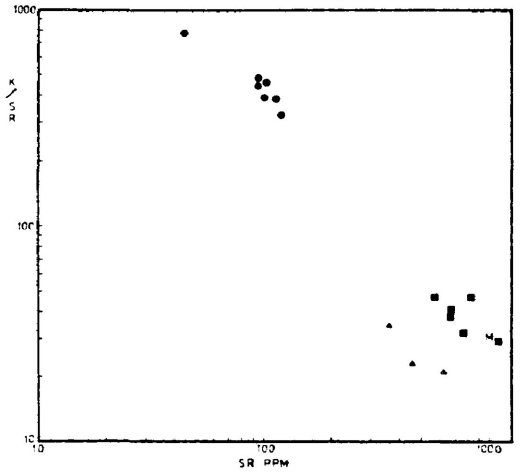

Fig. 2-35 (left). Rb/Sr versus Sr for granitoids.

Fig. 2-36 (right). K/Sr versus Sr for granitoids.

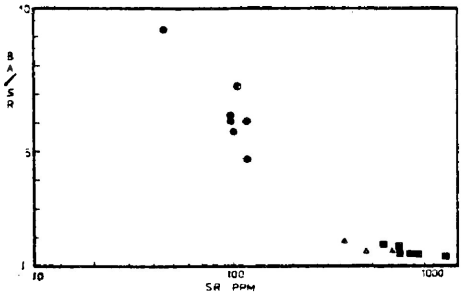

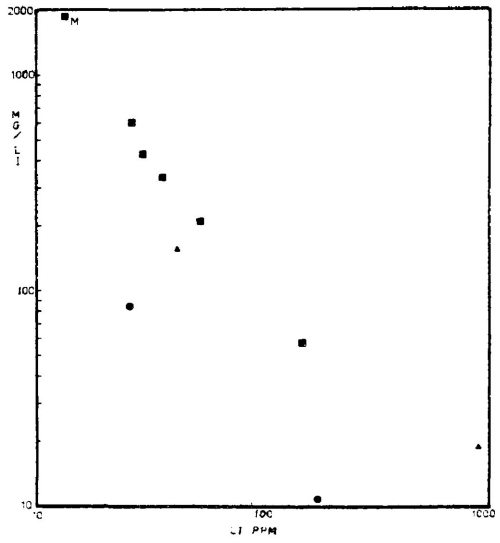

Fig. 2-37 (left). Ba/Sr versus Sr for granitoids.

Fig. 2-38 (right). Mg/Li versus Li for granitoids.

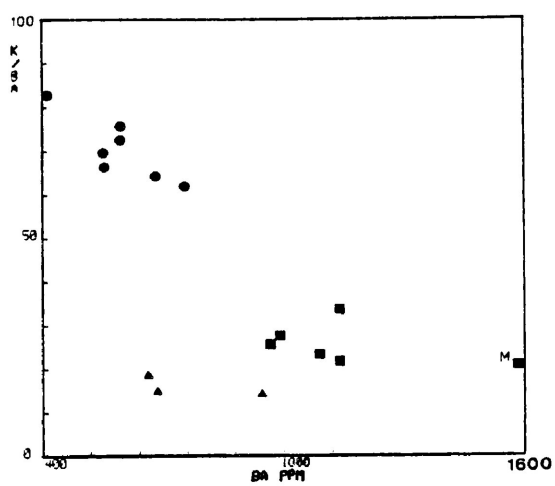

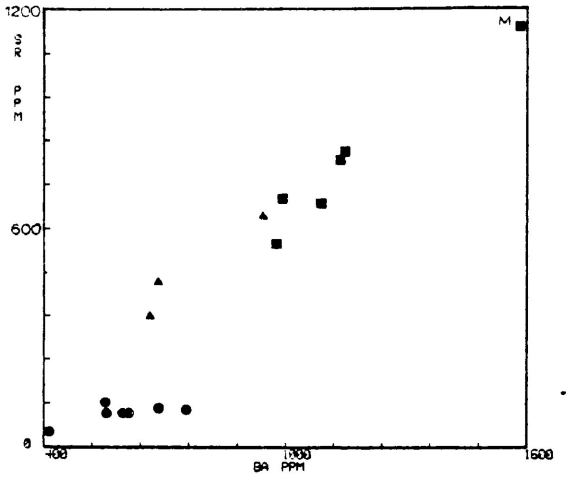

Fig. 2-39 (left). K/Ba versus Ba for granitoids.

Fig. 2-40 (right). Sr versus Ba for granitoids.

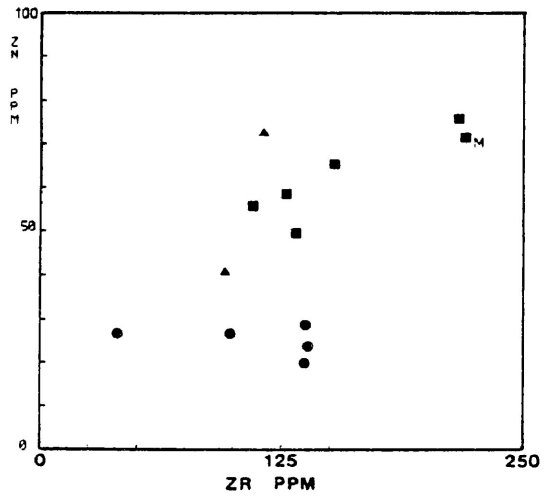

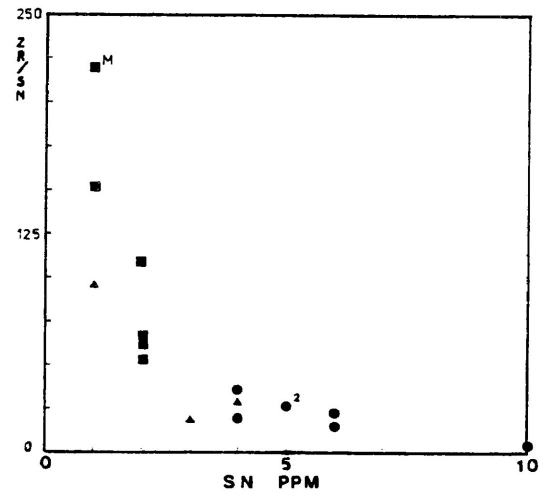

Fig. 2-41 (left). Zn versus Zr for granitoids.

Fig. 2-42 (right). Zr/Sn versus Sn for granitoids.

diagram, tonalitic sills plot together with the Kilgour Lake Group granitoids, except for sample BG23 which has anomalously high Rb, in the field of granodiorites and quartz diorites. Two-mica leucogranites plot as normal to strongly differentiated granites.

Negative linear correlations are observed in all diagrams representing elemental ratios against alkali or alkaline earth elements (Figs. 2-33 to 2-39) for the Kilgour Lake Group and two-mica leucogranites. The elemental distributions in the tonalites is somewhat erratic in relation to the other granitoid groups.

Figs. 2-41 and 2-42 summarize interrelationships between Zn, Zr and Sn in granitoids of the Georgia Lake area.

Discussion

An understanding of the nature of granitoids within and flanking the Georgia Lake pegmatite field is essential to examine the hypothesis of provenance and mechanism of emplacement of rare-element pegmatitic source fluids originating from parental granitic melts. Ayres and Černý (1982) identify four main characteristics of granitoids

presumed to be parental to rare-element pegmatites:

(1) Mineralogy of parental granitoids is characterized by the presence of biotite, biotite and muscovite or muscovite and garnet. The rocks are leucocratic.

(2) Geochemistry of parental granitoids is characterized by high SiO_2, low CaO, 0-5% CIPW normative corundum, enrichment of Li, Rb, Cs, Be, Sn, Ga, Nb and Ta and depletion of Ba, Sr, Ti, Zr, LREE and Eu.

(3) They are generally small stocks occurring as satellites to larger plutons, although genetic relation is not a necessity.

(4) Emplacement of parental granitoids is during late- to post-tectonic stages.

By the criteria of Ayres and Černý (1982), possible parental granitoids to Li-rich, rare-element pegmatites of the Georgia Lake area, based on results obtained in this study, include the MNW and Barbara Lake Stocks. Other granitoids in the vicinity of Barbara Lake may also fit the criteria. It is notable that the concentration of Li in possible parental granites of Li-rich pegmatites does not substantially exceed the Li concentration in other granitoids (Tables 2-6 to 2-8). Mulligan (1973, 1980) observed no relation between Li concentration in granitoids to the presence or absence of lithium pegmatites. It is possible that partitioning of Li into the melt phase occurs to the extent that most Li is removed from a crystallizing granitic melt.

All granitoids of the Georgia Lake area have calc-

alkaline affinities and are peraluminous and CIPW corundum normative, except for the mesocratic granitoids of the Kilgour Lake Group. Based on major, minor and trace element data presented, the geochemical signature of the two-mica leucogranites is clearly distinguishable from the Kilgour Lake Group granitoids. In summary, with respect to granitoids of the Kilgour Lake Group, two-mica leucogranites are enriched in SiO_2, K_2O, Rb and Sn and depleted in TiO_2 FeO, total Fe, MgO, CaO, Sr, Ba and Zn. Geochemical ratios K/Ba, Ba/Sr, Rb/Sr and K/Sr are high and K/Rb, Ba/Rb, Mg/Li and Zr/Sn are low in the two-mica leucogranites in relation to granitoids of the Kilgour Lake Group. Li and Be are somewhat enriched in two-mica leucogranites.

From mineralogy of granitoids and geochemical results, it is clear that several mechanisms of granitoid emplacement were operative during the tectonic history of the Georgia Lake area. Two-mica leucogranites are volumetrically the most significant granitoids of the Georgia Lake area and extend well beyond the immediate study area.

Affinity of the tonalitic sills is more enigmatic than the other granitoids and assignment as a separate intrusive phase is necessitated by distinct mineralogy and variable geochemistry. With respect to the other two groups of granitoids, tonalitic sills are enriched in Na_2O.

In relation to two-mica leucogranites, tonalites are geochemically unfractionated. Similarity in the differentiation sequence of the tonalitic sills to Kilgour Lake Group granitoids is illustrated in Fig. 2-30 although the distinction of the two groups of granitoids is observed (Fig. 2-28) where tonalitic sills deviate to the left of the thermal minimum at pressures below 1 kbar to greater than 5 kbars.

Classification of orogenic granitoids of any age is commonly made on the basis of S- and I-type granitoids (Chappell and White, 1974). This classification has genetic implications and reflects variation in source material. S-type granitoids are presumed to be derived from a metasedimentary source whereas I-type granitoids are derived from an igneous source (Chappell and White, 1974). Most of the basic characteristics of S- and I-type granitoids stem from investigations of Paleozoic granitoids of eastern Australia (Chappell, 1978; Hine et al., 1978). Although the distinguishing characteristics of S- and I-type granitoids are numerous, some of these have been investigated during the present study. S-type granitoids contain greater than 1% CIPW normative corundum, high SiO_2 with a restricted range, less than 3.2% Na_2O in rocks where K_2O is greater than 5.0% and molar $Al_2O_3/(CaO+Na_2O+K_2O)$ or A/(CNK) greater than 1.1. Field criteria of S-type granitoids includes the common presence of muscovite, garnet and ilmenite.

I-type granitoids contain either CIPW normative diopside or less than 1% normative corundum, variable SiO_2, high Na_2O and A/(CNK) less than 1.1. Field criteria of I-type granitoids include the common presence of hornblende, sphene and magnetite (Chappell and White, 1974; Pitcher, 1979b). Anorogenic or A-type granitoids have recently been described (Collins et al,. 1982; Loiselle and Wones, 1979), but a commital of any Georgia Lake area granitoids, based on obtained geochemical data and published A-type characteristics to this group is difficult to establish.

In relation to granitoids of the Superior Province, Smith and Williams (1980) observed compositional distinctions with respect to spatial distribution of granitoids within subprovinces. They distinguished diorite-granodiorite with a predominantly I-type origin to be characteristic of metavolcanic-metasedimentary terrains, while leucogranites, tonalites and trondhjemites with a predominantly S-type origin are characteristic of gneissic terrains, i.e. English River and Quetico Gneiss Belts. The characteristics of granitoids in the Georgia Lake area are in keeping with Smith and Williams observations.

Based on results presented in this study, the two-mica leucogranites can be allied clearly to the S-type granitoids, while the Kilgour Lake Group is a minor representative of I-type granitoid emplacement within the

study area. The distinction of these two groups of granitoids is observed on an A/(CNK) versus SiO_2 diagram (Fig. 2-44), where I-type granitoids are characterized, in general, by lower SiO_2 and A/(CNK) than S-type granitoids. The frequency distribution of peraluminous granitoids of the Georgia Lake area (Fig. 2-43) is not as clear in distinguishing the two types of orogenic granitoids although two-mica leucogranites all plot within the field of S-type granitoids and are somewhat more peraluminous than the felsic Kilgour Lake Group granitoids. Clarke (1981) has argued against the use of the A/(CNK) ratio to distinguish S- from I-type granitoids pointing out several possible situations in which the A/(CNK) ratio may exceed 1.1 in granitoids with a non-S-type origin. This circumstance is observed in the Georgia Lake area granitoids, where the A/(CNK) ratio of some peraluminous granitoids of the Kilgour Lake Group overlaps with S-type leucogranites (Figs. 2-43, 2-44).

The tonalites are marked by variable rock textures and geochemistry, although all are peraluminous with CIPW normative corundum. Based on the A/(CNK) ratio, the more mafic sample (BG23) of the tonalitic group has greater affinity for S-type granitoids then the more leucocratic samples (BG2, BG3; Figs. 2-43, 2-44).

Derivation of granitic rocks in an orogenic setting

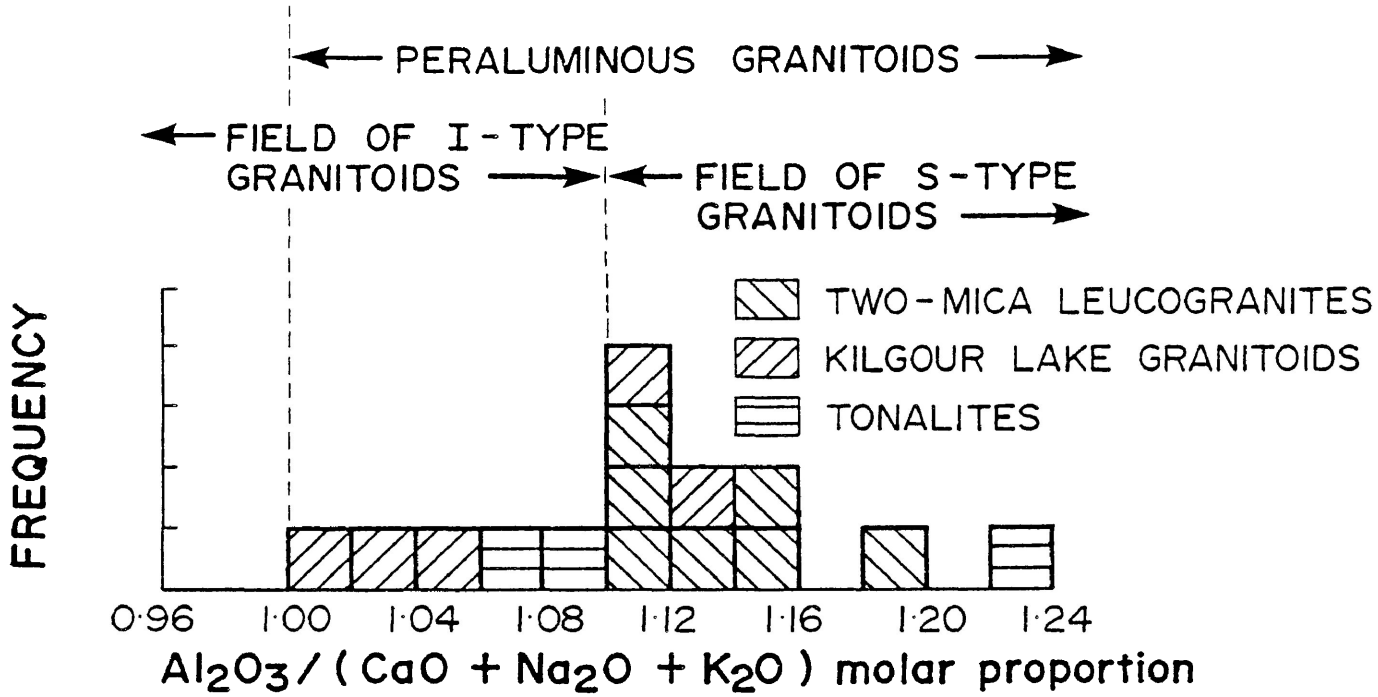

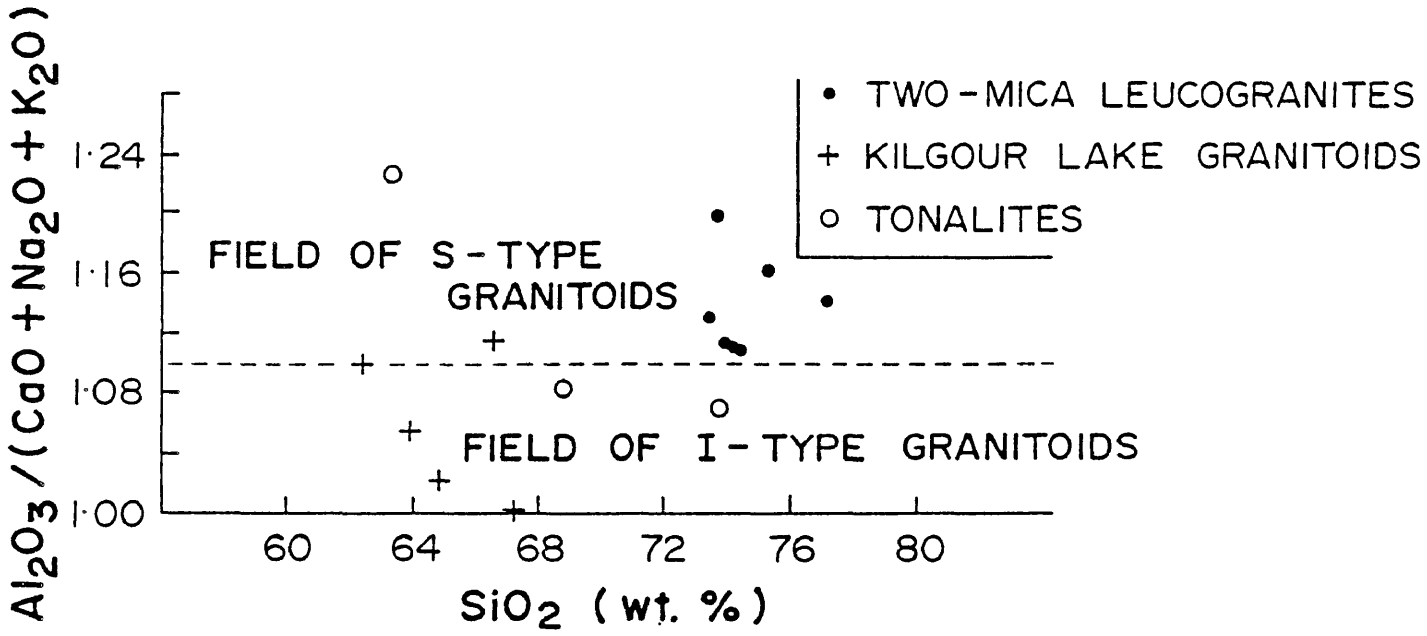

Fig. 2-43 (top). Frequency distribution of the A/(CNK) ratio for peraluminous granitoids.

Fig. 2-44 (bottom). A/(CNK) ratio versus SiO_2 for peraluminous granitoids.

is from either a crustal, mantle or a mixed mantle and crustal source (Didier et al., 1982) where S-type granitoids represent the partial melts of crustal material, and I-type magmas are derived by fractional crystallization of a melt from the mantle or lower crust (Kleeman, 1965) followed by possible contamination by pelitic country rocks (Clarke, 1981). The mechanics of the fractional crystallization process are not clearly understood (Cawthorn et al., 1976).

The data collected during this study suggest that the mechanism of partial melting of deep-seated pelitic metasediments gave rise to the emplacement of the two-mica leucogranites in the Georgia Lake area. This mechanism is suggested by the high K content and the highly peraluminous (White and Chappell, 1977) nature of the two-mica leucogranites and the common presence of metasedimentary xenoliths in the Glacier Lake Pluton. In the sense of Mehnert (1971), the two-mica leucogranites of the Georgia Lake area are diatexites occurring as stocks and plutons of variable size and shape in a defined migmatitic terrain clearly suggestive of an anatectic origin.

The Kilgour Lake Group represents fractionally crystallized granitoids differentiated from a deep-seated mafic source. Indications of this process include the localized nature of the granitoids and the span from centrally located mafic compositions to peripherally

distributed felsic granitoids of granodioritic to tonalitic compositions. In the porphyritic granodiorite that marks the southern limit of the Kilgour Lake Group, mafic, schistose enclaves aligned parallel to foliation are common. Altered mafic clots are also common in monzodiorite. The Kilgour Lake Group granitoids are fractionated from mafic to felsic granitoids, although the most felsic compositions do not achieve the degree of fractionation of two-mica leucogranites. The Kilgour Lake Group represents a minor episode of granitoid emplacement in the Georgia Lake area that preceded the emplacement of two-mica leucogranites. Examination of the compositional distribution of granitoids on an Ab-Or-Qz diagram (Fig. 2-28) reveals that the Kilgour Lake Group granitoids crystallized at a pressure of greater than 5 kbars whereas the two-mica leucogranites crystallized at a pressure of about 1 to 5 kbars. Assuming a constant geothermal gradient and similar viscosities of source melts of the two granitoid groups, the Kilgour Lake Group granitoids are of a deeper lithospheric derivation than two-mica leucogranites. These observations are consistent with the suggestion by White (1979) that I-type granitoids are derived from deeper crustal levels than S-type granitoids.

Tonalitic sills are presumed to be derived by partial melting of metagreywackes in the Georgia Lake area. Derivation of tonalitic, trondhjemitic melts from a basaltic source (Arth, 1979) does not seem likely, since basalts

are not exposed at present levels of erosion. Ermanovics et al. (1979) suggest the bulk of the sodic and potassic magmas of the English River Gneiss Belt were derived as partial melts of supracrustal rocks. A similar mode of origin was suggested by De Albuquerque (1977) for granitoids ranging from tonalites to granites of the southern plutons of Nova Scotia. Kilinc (1972) has shown experimentally that partial melting of greywacke results in the formation of Na-rich, trondhjemitic melts while partial melting of shales results in the formation of K-rich, granitic to quartz monzonitic melts. These observations suggest that tonalitic sills of the Georgia Lake area are possibly consanguineous with the two-mica leucogranites. The partial melting of metagreywacke resulting in the intrusion of tonalites as sill-like bodies was a tectonically insignificant event in proportion to partial melting of metapelites from which the two-mica leucogranites are presumed to be derived.

The tectonic framework of the Georgia Lake area or the Quetico Gneiss Belt, in general, into which the granitoids were emplaced, can be compared to the Hercynotype orogeny model of Zwart (1967) as summarized by Pitcher (1979a, b). The Hercynotype orogen is that of an intercontinental back arc basin in which sediments are continentally derived and volcanism is generally not present. Granitoids in this type of orogen are S-type or mixed S-

and I-type. The suggestion by Ayres (1978) that the Quetico Gneiss Belt represents a deformed linear turbidite basin formed adjacent to volcanic island arc chains may represent the Hercynotype model in an Archean environment. The difficulty in applying the model arises from the significance of plate tectonics in an Archean setting. This topic is especially controversial in relation to medium- to high-grade gneiss belts although more recently the mechanism of Archean plate tectonics has become increasingly popular (Windley, 1976, 1977). Windley's views are based on the principle of uniformitarianism. Contrary to the plate tectonic view, Glikson (1971) suggested the development of high-grade gneiss belts at shield-ocean transition zones resulting from basinal subsidence.

PART THREE RARE-ELEMENT PEGMATITES

Distribution And Structural Setting

In the Georgia Lake area, rare-element pegmatites are hosted by supracrustal metasediments and occasionally cross-cut tonalitic sills. An exception is the MNW pegmatite, which is hosted entirely by two-mica leucogranite. All rare-element pegmatites, except the MNW pegmatite and a series of beryl-bearing pegmatites in the vicinity of Cosgrave Lake, occur at distances generally greater than 2 km from exposures of two-mica leucogranite. The distribution of rare-element pegmatites is irregular, and an apparent concentration in areas of greater outcrop exposure is evident. Rare-element pegmatite occurrences of the Georgia Lake area are identified with triangles in Fig. 3-1. Pegmatite localities that have been examined in detail and sampled during the course of field work are further identified by solid triangles and by their respective property names, as recorded by Pye (1965).

Subdivision of the rare-element pegmatites, exclusive of the simple beryl-bearing variety, is into three groups, the Southern, Central and Northern Groups. These groupings, based on spatial position in the pegmatite field, mineralogy and large scale pegmatite textures, correspond to Milne's (1962) Groups One, Two and Four, respectively. Group Three pegmatites near Parole Lake were not visited but according

Fig. 3-1. Locations of sampled rare-element pegmatites, identified by solid triangles, on a general geology map of the Georgia Lake area.

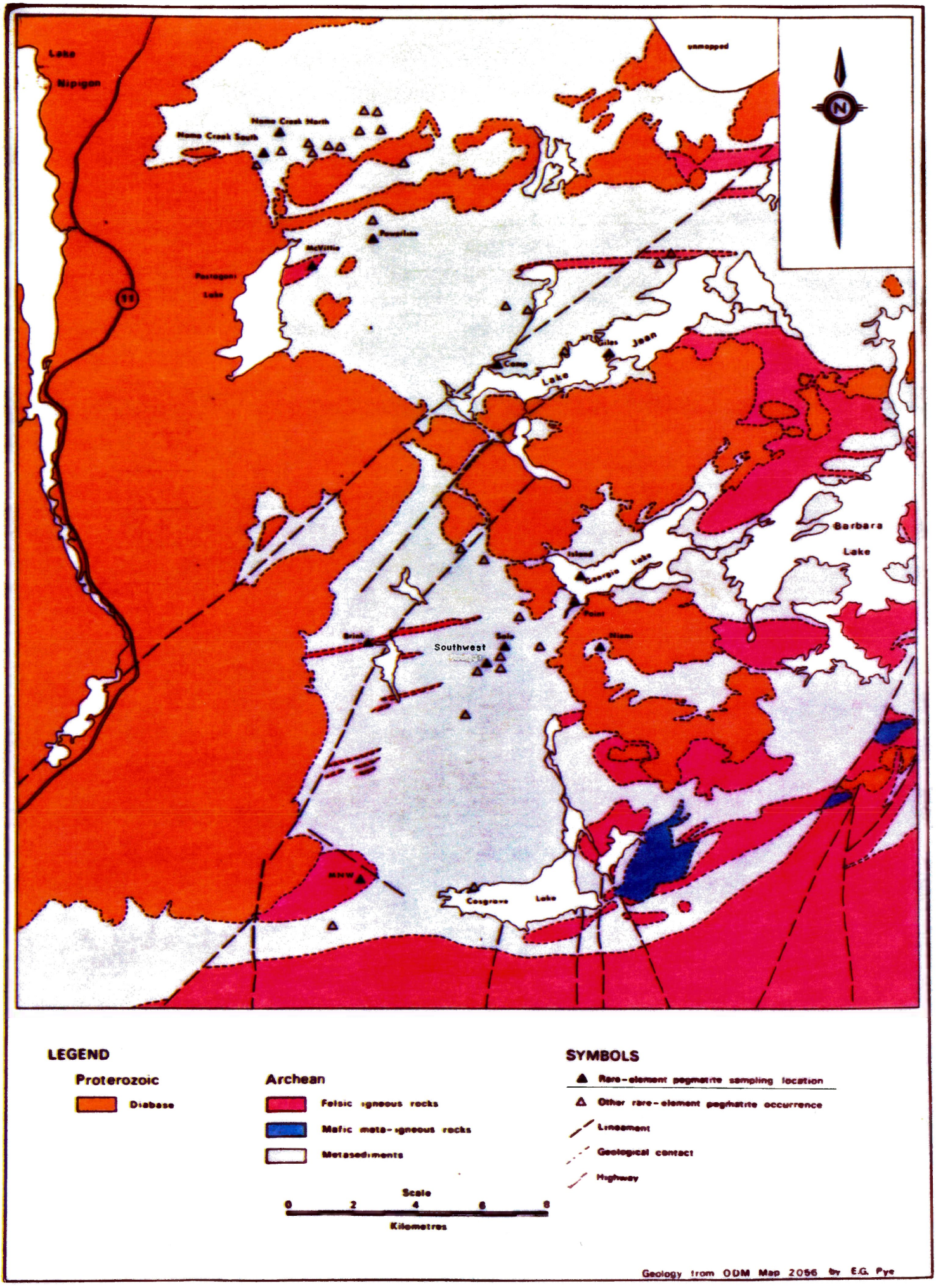
Lake
Nipigon
unmapped
Name Creek North
Name Creek South
Pewabic
McVittie
Penagami
Lake
11
Giles
Joan
Lake
Barbara
Lake
Southwest
Cosgrove
Lake
NNW
LEGEND
Proterozoic
Diabase
Archean
Felsic igneous rocks
Mafic meta-igneous rocks
Metasediments
SYMBOLS
Rare-element pegmatite sampling location
Other rare-element pegmatite occurrence
Lineament
Geological contact
Highway
Scale
0 2 4 6 8
Kilometres
Geology from ODM Map 2056 by E.G. Pye

to Milne (1962) are essentially similar to Group Four pegmatites and will be included with the Northern Group pegmatites.

The MNW pegmatite was the only member of the Southern Group studied in the present work. It outcrops along a height of land east of the Jackfish River. The MNW pegmatite is a north-south-striking, steep-dipping dyke with a maximum width of about 10 m near the southern limit of exposure. The zonal distribution of minerals in this pegmatite is unique in the Georgia Lake pegmatite field and was previously noted by Milne (1962), Mulligan (1965), Pye (1965) and Breaks (1980).

Central Group pegmatites outcrop between Georgia Lake on the east and Blay Lake on the west. Area covered by the Central Group is approximately 50 km^2. Sampled occurrences in this group include the Island, Point, Niemi, Salo, Southwest and Brink deposits. Other pegmatites of the Central Group include the Jackpot and Vegan deposits. Central Group pegmatites are variably orientated, flat to steep dipping dykes which crudely strike in an east, northeast to north direction (Pye, 1965).

The Northern Group of rare-element pegmatites outcrop in a northwest direction from Lake Jean and are exposed over an area of roughly 100 km^2. Sampled occurrences include

the Giles, Camp, McVittie, Powerline and Nama Creek North and South deposits. Pegmatites of the Northern Group occur as dykes of variable orientation although occurrences in the Postagoni Lake to Downey Lake (Nama Creek deposits) location appear to strike roughly in a north to northeast direction. Rare-element pegmatites of the Northern Group cluster in three separate locations from southeast to northwest; the Parole-Jean Lakes area, east of Postagoni Lake and northeast of Downey Lake.

Descriptive Mineralogy

General Overview

Since mineralogical aspects of the rare-element pegmatites form the basis of a thesis (Milne, 1962), only a brief synopsis including modifications based on present observations is presented.

Pegmatites of the Southern, Central and Northern Groups are identified by ubiquitous spodumene with characteristic perthitic microcline and quartz with variable abundance of albite, muscovite and other accessory minerals. Distinction of the Northern and Central Groups is on the basis of groundmass grain size which is fine-grained in the former and commonly medium-grained in the latter. Size classification of pegmatitic minerals is modified from

Cameron et al. (1949):

Fine	less than 2.5 cm
Medium	2.5 to 10.0 cm
Coarse	10.0 to 30.5 cm
Very Coarse	Greater than 30.5 cm

Northern Group pegmatites are also commonly interbanded with fine-grained aplitic material which is absent in Central Group pegmatites. The MNW pegmatite of the Southern Group is distinguishable from other pegmatites by the well defined zonal structure, heavily modified by replacement units, and the distinctive occurrence of spodumene in the Georgia Lake area as a low-temperature pseudomorph after petalite intergrown with quartz (Černý and Trueman, 1978).

Southern Group

The MNW pegmatite is characterized by the segregation of minerals with corresponding textural variations into at least three main zones; wall, intermediate and core zones. Zonal classification is after Cameron et al. (1949) as modified by Norton (1983) and represents successive shells of different mineral assemblages from the contact to the centre of a pegmatite. The three zones of the MNW pegmatite are exposed in outcrop in the southern segment of the pegmatite (Figs. 3-2, 3-3). Zoning in the MNW

Fig. 3-2. Mineral zones in the MNW pegmatite.
Bottom right hand corner-core zone; quartz and SQUI *reddish due to hematite staining).
Bottom left hand corner to hammer-intermediate zone; cleavelandite (white), muscovite (brown) and disseminated tourmaline (black).
From hammer to pegmatite contact-wall zone; quartz and cleavelandite (white, grey) and muscovite (brown).
At the pegmatite contact, a thin border unit of tourmaline (black) and bleached wall rock are visible.
Top of photograph-two-mica leucogranite.

* Spodumene-quartz intergrowth

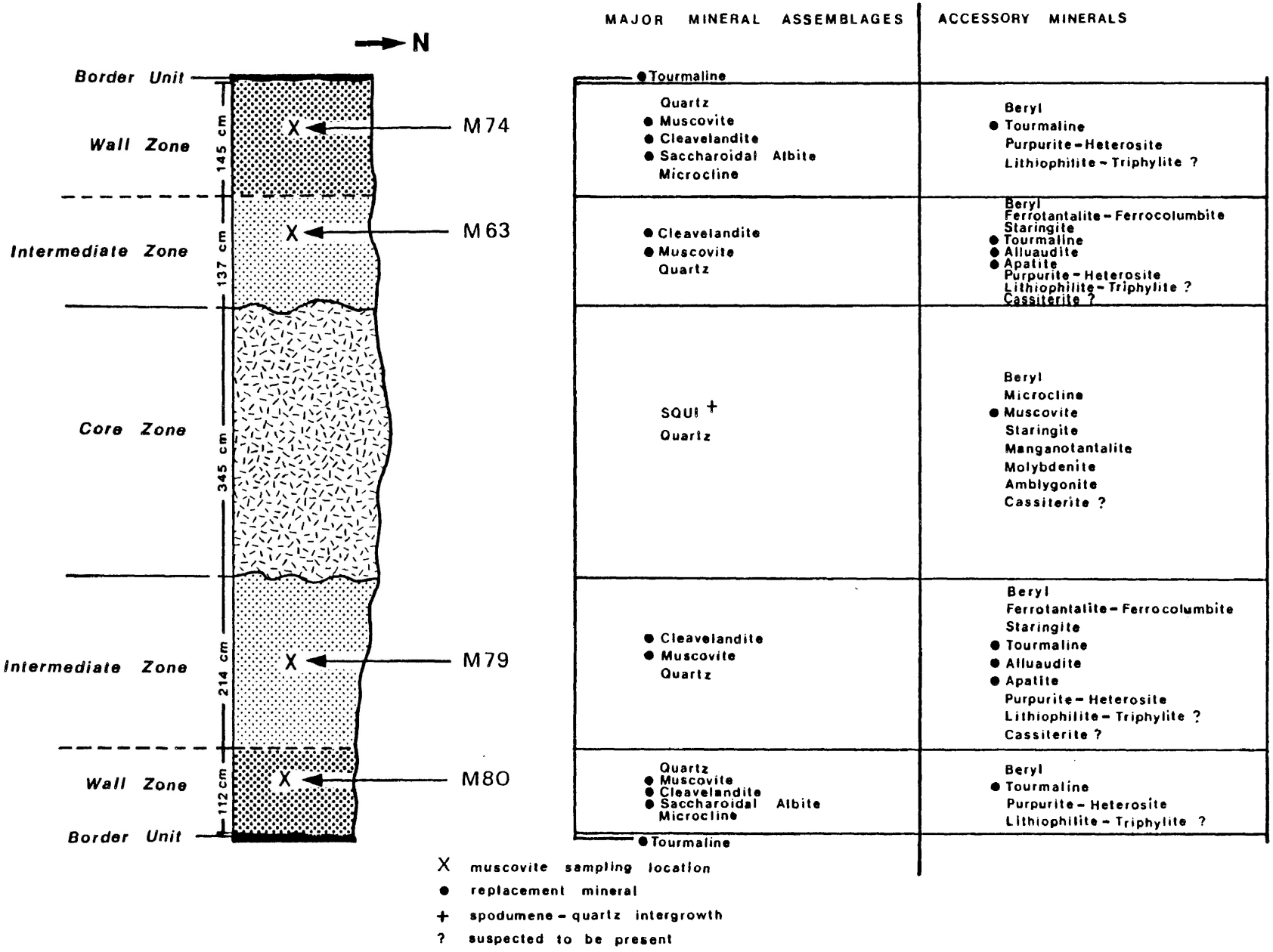

Fig. 3-3. Cross-section of the southern segment of the MNW pegmatite including mineralogy of each zone.

pegmatite is symmetrical with wall and intermediate zones distributed on either side of the core zone in roughly equal proportions on each side. Along the southern segment of the pegmatite, a thin border unit composed almost entirely of black tourmaline crystals separates the wall rock two-mica leucogranite from the wall zone of the MNW pegmatite. Crystals of tourmaline up to 2 cm in diameter grow inward toward the pegmatite, while a very fine dissemination of tourmaline separates the border unit from the bleached wall rock. Bleached wall rock, characterized by a deficiency of mica or other mafic constituents, is widest (up to 4 cm) where the border unit is best developed. The border unit and corresponding bleached wall rock become progressively more diffuse toward the northern end of the pegmatite.

The wall zone forms the bulk of the pegmatite, as observed on surface exposure, and progressively increases in proportion toward the northern end of the pegmatite where the entire pegmatite is composed of the wall zone. Primary minerals in the wall zone are dominated by massive quartz, with subordinate blocky perthitic microcline and white to light yellow beryl. Perthitic microcline increases in abundance toward the northern end of the pegmatite, where it occurs as very coarse, white to light pink subhedral crystals with subordinate quartz, muscovite and cleavelandite. Milne (1962) separated these microcline

units into an outer intermediate zone although geochemical evidence obtained during the present study does not support the existence of distinctive zonal subdivision.

Secondary units of white to light pink cleavelandite occur sporadically throughout the wall zone, although they are somewhat enriched toward the southern end of the pegmatite. Medium-grained, silvery-yellow muscovite books, commonly with tourmaline inclusions, occur in association with cleavelandite. The wall zone is invaded by microcrystalline masses, irregular patches and stringers of white to pink, saccharodial albite with disseminated fine-grained crystals of black tourmaline. Occasionally, the tourmaline disseminations are segregated within the albite masses imparting a layered structure (Fig. 3-4). The albite masses increase in proportion toward the northern end of the pegmatite.

The contact between the wall and intermediate zones is diffuse (Fig. 3-2) and is distinguished by the decrease of quartz and increase in cleavelandite in the later. Volumetrically, the intermediate zone is the smallest of the zones in the MNW pegmatite but is significant in the enrichment of rare minerals associated with cleavelandite. It occurs along the flanks of the core zone in the southern segment of the exposed portion of the pegmatite and as a small segregation in the wall zone toward the northern

end of the pegmatite. Cleavelandite of the intermediate zone occurs as coarse platey pink, white to grey fans which appear to have developed at the expense of core zone quartz and spodumene-quartz intergrowth (Fig. 3-5). Hematitic staining is common along boundaries between individual plates of cleavelandite. Sn oxide minerals with ferrocolumbite-ferrotantalite inclusions occurs as black, irregular masses up to 7 cm and are hosted entirely by cleavelandite (Fig. 3-6). The amount of ferrotantalite-ferrocolumbite inclusions in Sn oxide minerals was observed to be less than 10% and these occur as tiny euhedral to anhedral irregularly distributed highly reflective grains in polished sections. Tabular crystals of ferrocolumbite up to 2 cm in length are associated with and commonly penetrate Sn oxide minerals (Fig. 3-7). Sn oxide minerals are erratically distributed but appears to be slightly enriched toward the southern end of the pegmatite.

Muscovite is the second most abundant mineral of the intermediate zone and occurs as loose, silvery-yellow books up to 10 cm in diameter.

Secondary phosphates are common in the intermediate zone, and to a lesser extent, in the wall zone. Purpurite-heterosite is the most abundant secondary phosphate and occurs as a supergene oxidation product of lithiophilite-triphylite (Moore, 1973). On surface exposure,

Fig. 3-4. Layering in fine-grained saccharoidal albite imparted by fine-grained tourmaline (small black grains $\leq$1 mm in diameter); wall zone, MNW pegmatite.

Fig. 3-5. Cleavelandite fans (right side of photograph) indicating an albitization front advancing on core zone quartz (left side of photograph) and SQUI (below centre); MNW pegmatite.

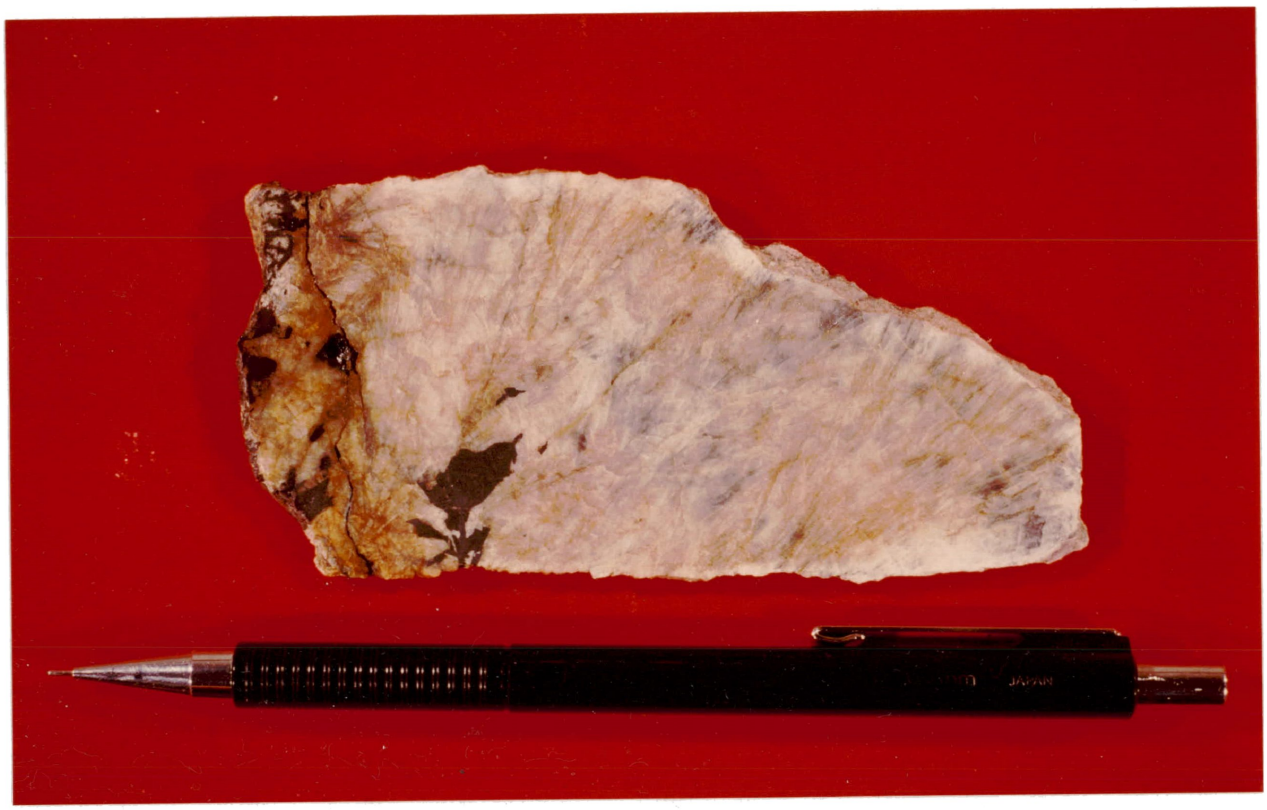

Fig. 3-6. Sn oxide minerals with ferrocolumbite-ferrotantalite inclusions (black) in cleavelandite; intermediate zone, MNW pegmatite.

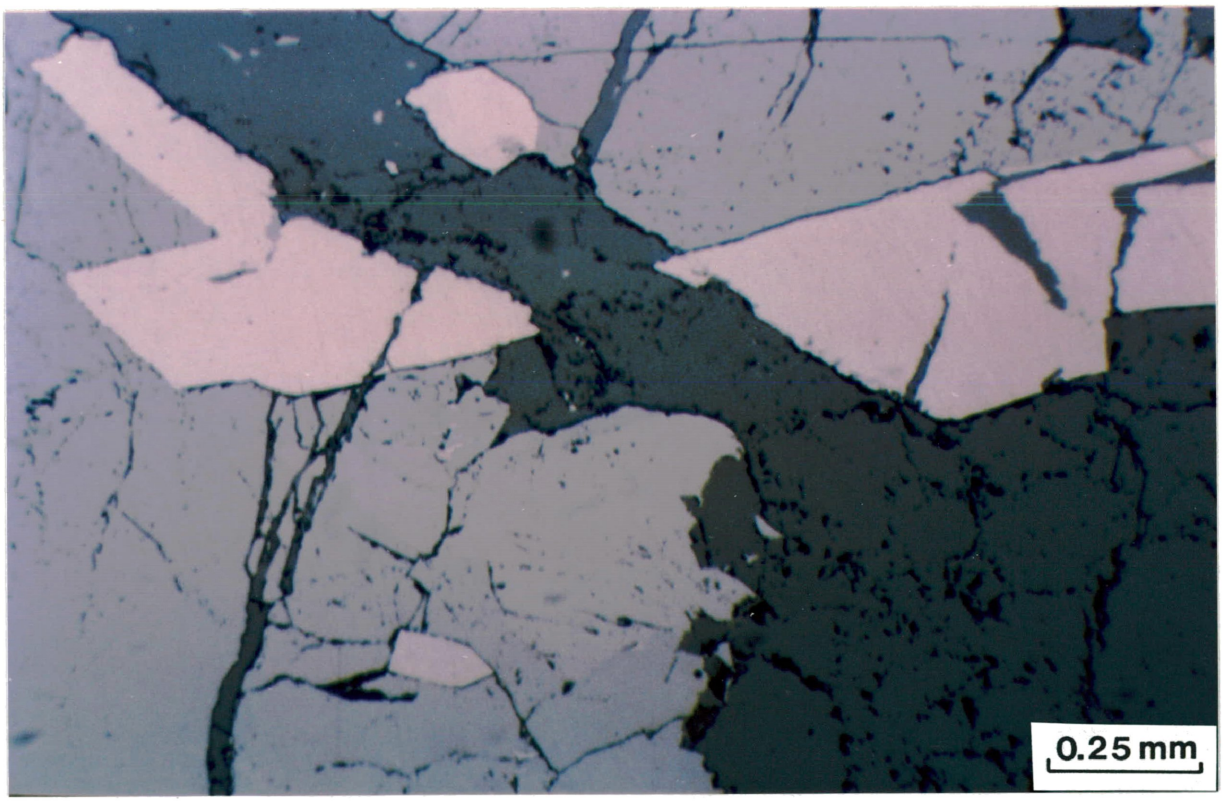

Fig. 3-7. Photomicrograph of ferrocolumbite crystal (white) in Sn oxide minerals (light grey) offset by later cleavelandite (dark grey); intermediate zone, MNW pegmatite.

all primary lithiophlite-triphylite is completely oxidized. Purpurite-heterosite is masked by a dull rusty-brown-black weathering rind which is easily scraped off to reveal the purple colour of the mineral group. This phosphate was described by Pye (1965) as the manganese end-member, purpurite but X-ray powder data suggest the material is more probably an intermediate phase in the purpurite-heterosite series. Purpurite-heterosite minerals occur in dendritic masses intergrown with cleavelandite outlining original primary lithiophilite-triphylite masses up to 1 m in length (Fig. 3-8). Alluaudite, identified by X-ray powder diffraction, occurs as a replacement of purpurite-heterosite and as separate, dull green masses in the intermediate zone. Apatite is also associated with purpurite-heterosite commonly as a thin rim on the latter mineral.

Other subordinate minerals of the intermediate zone include quartz, beryl and disseminated tourmaline.

The core zone is composed almost entirely of spodumene-quartz intergrowth (SQUI) and irregularly distributed pods of massive quartz. These two main constituents of the core zone correspond to zones seven and eleven, respectively, of pegmatites from the Black Hills, South Dakota (Cameron et al., 1949) and zones six and eight, respectively, of Norton (1983). The core zone

is exposed only in the southern segment of the MNW pegmatite and has a maximum width of 3.5 m. The spodumene component of SQUI occurs as white, coarse- to medium-grained, tabular to fine-grained, acicular, white to clear crystals occasionally stained red by hematite. It is probable that the coarse-grained spodumene component of SQUI crystallized directly as spodumene whereas fine-grained spodumene has been isomorphously recrystallized from petalite. Fine-grained SQUI from the MNW pegmatite is similar to material described from the Tanco (Černý and Ferguson, 1972) and Varuträsk (Quensel, 1957) pegmatites. Remnant petalite is rare and observed in thin section as tiny interstitial grains in very fine-grained SQUI. SQUI hosts a series of accessory minerals present in subordinate quantities. Blocky perthitic microcline is present as subhedral to euhedral, white crystals occasionally exceeding 1 m in length. Beryl is distributed sporadically as milky white, subhedral crystals rarely exceeding 30 cm in length. Amblygonite has been reported from the core zone (Pye, 1965). A small amount of molybdenite was identified along a contact between SQUI and massive quartz. Two separate masses of Sn oxide minerals with manganotantalite inclusions measuring about 10 cm in maximum dimension (Fig. 3-9) were observed intergrown with SQUI. Fine-grained to microcrystalline, yellow to brown-green muscovite is sporadically distributed in small quantities through SQUI and appears to be associated with small fractures.

Fig. 3-8. Dendritic purpurite-heterosite (brown) after lithiophilite-triphylite in cleavelandite; intermediate zone, MNW pegmatite.

Fig. 3-9. Sn oxide minerals with manganotantalite inclusions (black) in SQUI; core zone, MNW pegmatite.

Central Group

Pegmatites of this group are unzoned to poorly zoned. Zonation, where observed, is identified by the presence of a fine-grained contact zone and concentration of spodumene crystals toward the centre of a pegmatite. The pegmatites consist of coarse to very coarse-grained microcline and spodumene with medium-grained quartz and muscovite, medium- to fine-grained albite and aggregates of apatite. Subordinate medium- to fine-grained garnet, tantalite-columbite minerals, purpurite-heterosite and tourmaline are present in some pegmatites of this group. Masses of saccharoidal albite are characteristic in all pegmatites of the Central Group which were examined.

Brink Deposit - The Brink occurrence northwest of Blay Lake is the westernmost exposed pegmatite of the Central Group. The Brink pegmatite consists of a fine-grained contact zone several centimetres wide grading sharply into the medium- to coarse-grained, primary mineral phases constituting the bulk of the pegmatite. A very thin discontinuous border unit of disseminated black tourmaline crystals and corresponding bleached wall rock of leucotonalite does not exceed 1 cm in width. This border unit is similar to that observed in the MNW pegmatite. The most characteristic coarse mineral phase of the Brink pegmatite is white to light pink, perthitic microcline

as poorly formed crystals up to 2 m in length, aligned perpendicular to the contact of the pegmatite (Fig. 3-10). Individual crystals increase in width toward the centre of the pegmatite. Spodumene crystals are white to light green and up to 50 cm in length. Poorly formed spodumene crystals are commonly intergrown with groundmass quartz. Massive quartz is the most characteristic groundmass phase in the Brink pegmatite and occasionally is present in small pods and veinlets. The distribution of albite as an interstitial mineral phase is difficult to establish due to similarity in colour to perthitic microcline. Most albite occurs as bulbous replacement masses of fine-grained, saccharoidal albite (Fig. 3-11) invading groundmass minerals and perthitic microcline crystals. Thin section examination of this unit reveals a mass of polysynthetically twinned, unaltered albite crystals not exceeding 1 mm in length and rare muscovite and quartz. Muscovite in the Brink pegmatite is light yellow to light green and occurs in three varieties related to grain size of individual crystals; microcrystalline, fine-grained and medium-grained. The first two types occur as irregularly shaped podiform crystal aggregates up to 30 cm in maximum dimension commonly replacing perthitic microcline and confined to central portions of the pegmatite (Fig. 3-12). Medium-grained muscovite occurs as books of platey crystals up to 4 cm in diameter and is an interstitial groundmass phase to quartz. Medium-grained muscovite occasionally grades into

Fig. 3-10. Large microcline crystals (white) aligned perpendicular to pegmatite contact; Brink pegmatite.

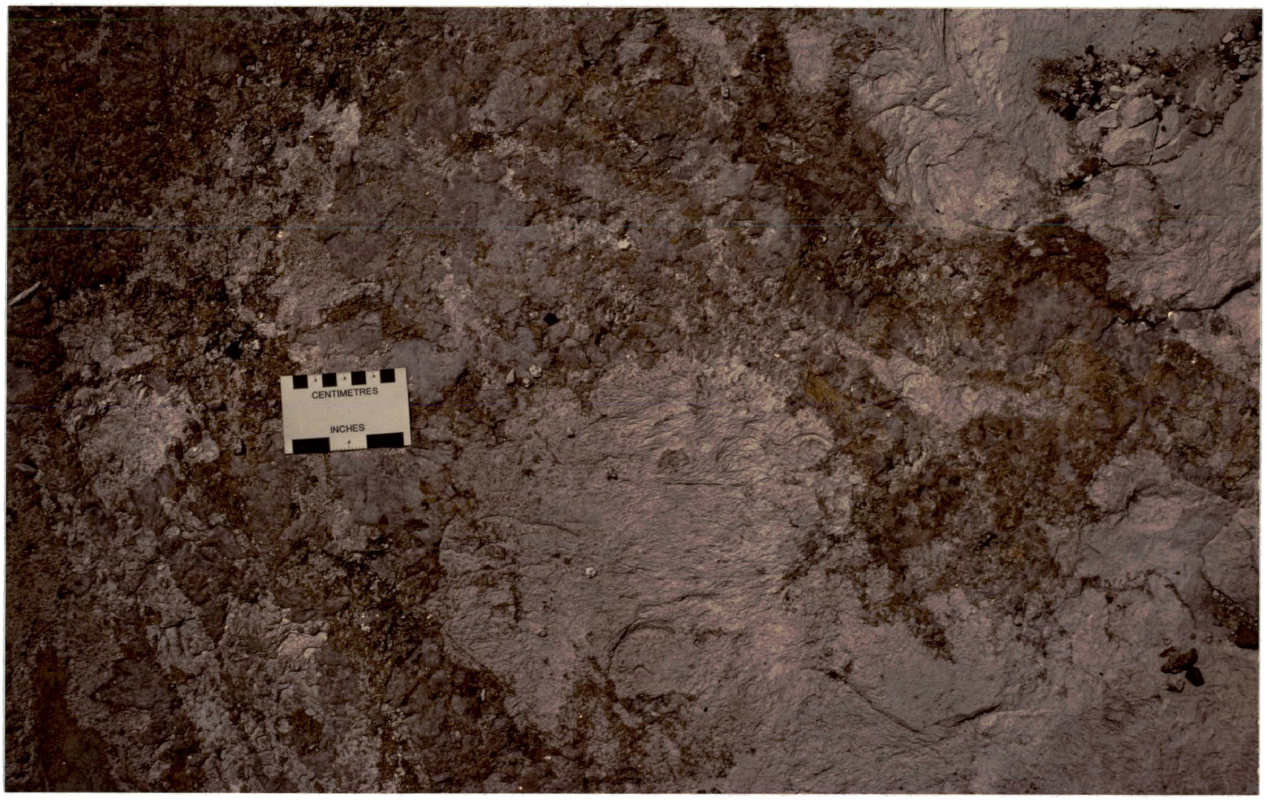

Fig. 3-11. Fine-grained saccharoidal albite masses (white) replacing primary groundmass minerals; Brink pegmatite.

podiform fine-grained muscovite. Tabular, black crystals of tantalite, up to 0.5 cm in length are present as a trace accessory interstitial mineral phase to quartz and muscovite and appears to be concentrated in the central parts of the pegmatite. Tantalite-columbite minerals occurring as tiny flakes are rare constituents in hand specimens of saccharoidal albite. Medium blue apatite is an uncommon but ubiquitous groundmass mineral in fine crystal aggregates up to 2 cm in diameter.

Southwest And Salo Deposits - The Southwest deposit occurs as small outcrops near the west bank of the Namewaminikan River about 3000 m east of Blay Lake and includes several individual pegmatites. The Salo occurrence is located about 30 m north of the Camp 95 Road beside a small beaver pond. Of these two deposits, the Southwest is strikingly similar to the Brink deposit with respect to mineralogy. The major difference between the Brink and Southwest deposits is the lack of alignment of perthitic microcline and spodumene in the later. Tantalite-columbite minerals were identified in the Southwest deposits. The mode of occurrence of tantalite-columbite minerals is similar to that of the Brink pegmatite.

Small differences were noted in the Salo pegmatite with respect to the Brink and Southwest deposits. The microcline crystals commonly contain numerous poikilitic

inclusions of quartz. Muscovite books are silvery-yellow to light green and a few small grains of purpurite-heterosite, similar to the material from the MNW pegmatite, were noted during outcrop examination.

Point, Niemi And Island Deposits - These occurrences outcrop as small, isolated exposures on or near Georgia Lake. They differ slightly from previously described pegmatites of the Central Group in that the muscovite is silvery-yellow and the spodumene content, as observed on surface exposure, is lower except for the Island occurrence where prismatic crystals up to 30 cm in length are common (Fig. 3-13). All three pegmatites have traces of interstitial red garnet associated with the groundmass. Small crystals of tourmaline up to 1 mm in length were identified in the Island deposit. Pye (1965) reported the presence of beryl in the Island occurrence. The Point deposit is the only rare-element pegmatite where graphically intergrown perthitic microcline and quartz in masses up to 30 cm were observed.

Northern Group

Pegmatites of the Northern Group have characteristic medium- to very coarse-grained perthitic microcline and spodumene crystals in a fine-grained matrix of quartz, muscovite and albite with trace amounts of apatite and garnet. The pegmatites are unzoned to poorly zoned. A

Fig. 3-12. Podiform green microcrystalline muscovite (above and left of scale bar) and fine-grained green muscovite (below scale bar) replacing perthitic microcline; Brink pegmatite.

Fig. 3-13. Large spodumene crystals (light green) in a groundmass of quartz (light grey), albite (white) and muscovite (black); Island pegmatite.

common feature to most pegmatites of this group, except in several pegmatites near Parole Lake, is the presence of aplitic stringers, bands and pods (Figs. 3-14, 3-15) within and parallel to the pegmatite contacts. They are occasionally lined with muscovite (Milne, 1962; Pye, 1965). The aplitic units are of variable dimensions and composed of albite, muscovite, quartz and traces of red garnet. Inclusions of rounded spodumene grains up to several centimetres are common in aplitic stringers from the Nama Creek deposits.

Partial to complete alteration of spodumene (Fig. 3-16) is a common feature in most pegmatites of the Georgia Lake pegmatite field but appears to be especially prevalent in the Northern Group pegmatites. The alteration is discussed by Milne (1962) and Pye (1965). The most common form of alteration is the conversion of spodumene to a dark green to black aggregate of mica commonly refered to as rotten spodumene (Cameron et al., 1949).

Small textural and mineralogical irregularities occur in the Northern Group pegmatites and are related to the spatial position of the pegmatites within the Northern Group.

Giles And Camp Deposits - The Giles pegmatite located in two outcrops and several trenches on Treasure Island on Lake Jean is composed of white microcline crystals up to

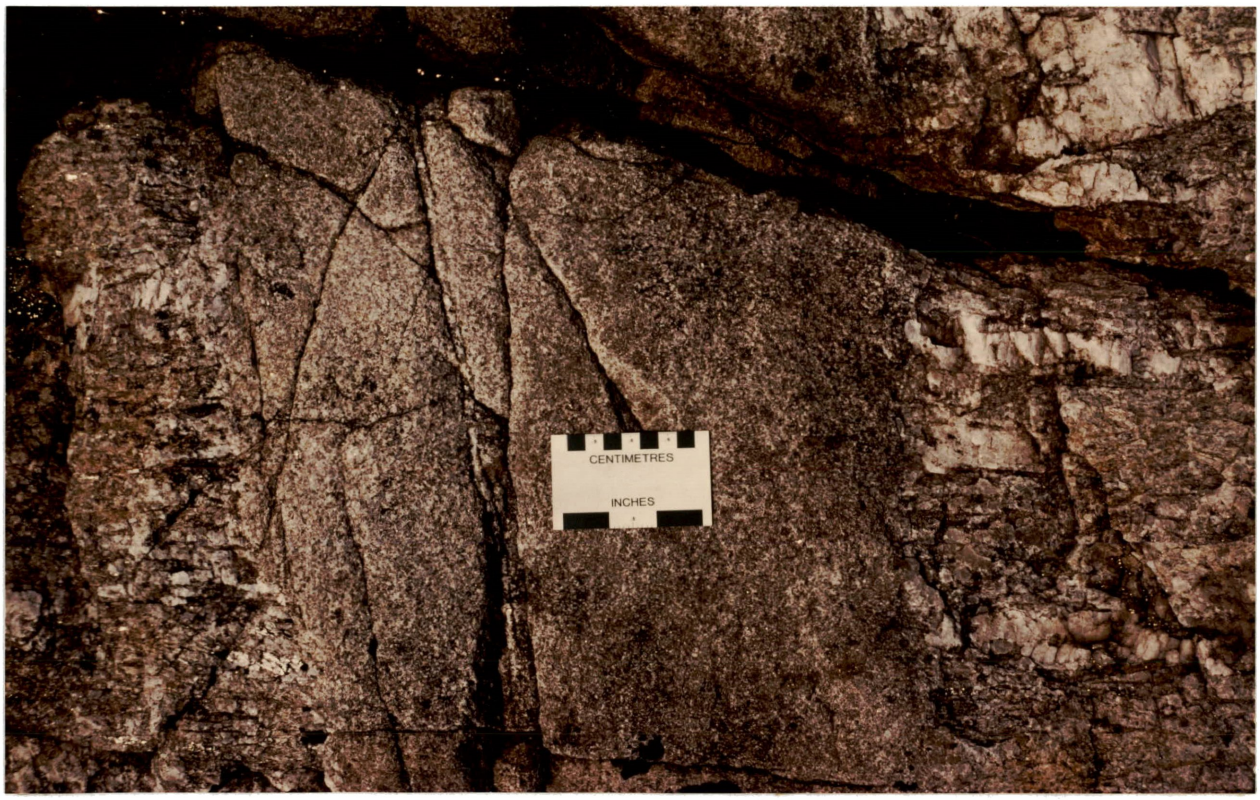

Fig. 3-14. Large aplite band (perpendicular to length of scale bar) in pegmatite; Giles pegmatite.

Fig. 3-15. Small aplite vein (above and parallel to length of scale bar) with rounded spodumene inclusions; Nama Creek North pegmatite.

30 cm in length and thin, bladed to acicular, light green spodumene crystals up to 10 cm in length, both of which are aligned perpendicular to the contact of the pegmatite. The groundmass material is mainly quartz, albite and subordinate muscovite.

The Camp pegmatite at the northwest corner of Lake Jean occurs across two small outcrops. This pegmatite is nearly identical to the Giles pegmatite except that a distinct zone of muscovite enrichment borders the pegmatites southwest contact and extends up to 4 cm into the metasedimentary wall rock and 10 cm into the pegmatite.

Nama Creek Deposits - The Nama Creek deposits include a series of five or six pegmatites northeast of Downey Lake, only two of which, the North and South pegmatites, show substantial spodumene enrichment (Fig. 3-17). Maximum measured lengths of microcline and spodumene crystals are 75 cm and 20 cm, respectively. Tension gashes, filled with quartz and some muscovite, cross-cut both the North and South pegmatites.

McVittie And Powerline Deposits - The McVittie pegmatite is exposed over seven outcrops at the north end of Dive Lake. The northern exposures are similar to the Giles and Camp deposits except for the somewhat coarser grain size of spodumene in the McVittie pegmatite. Traces of

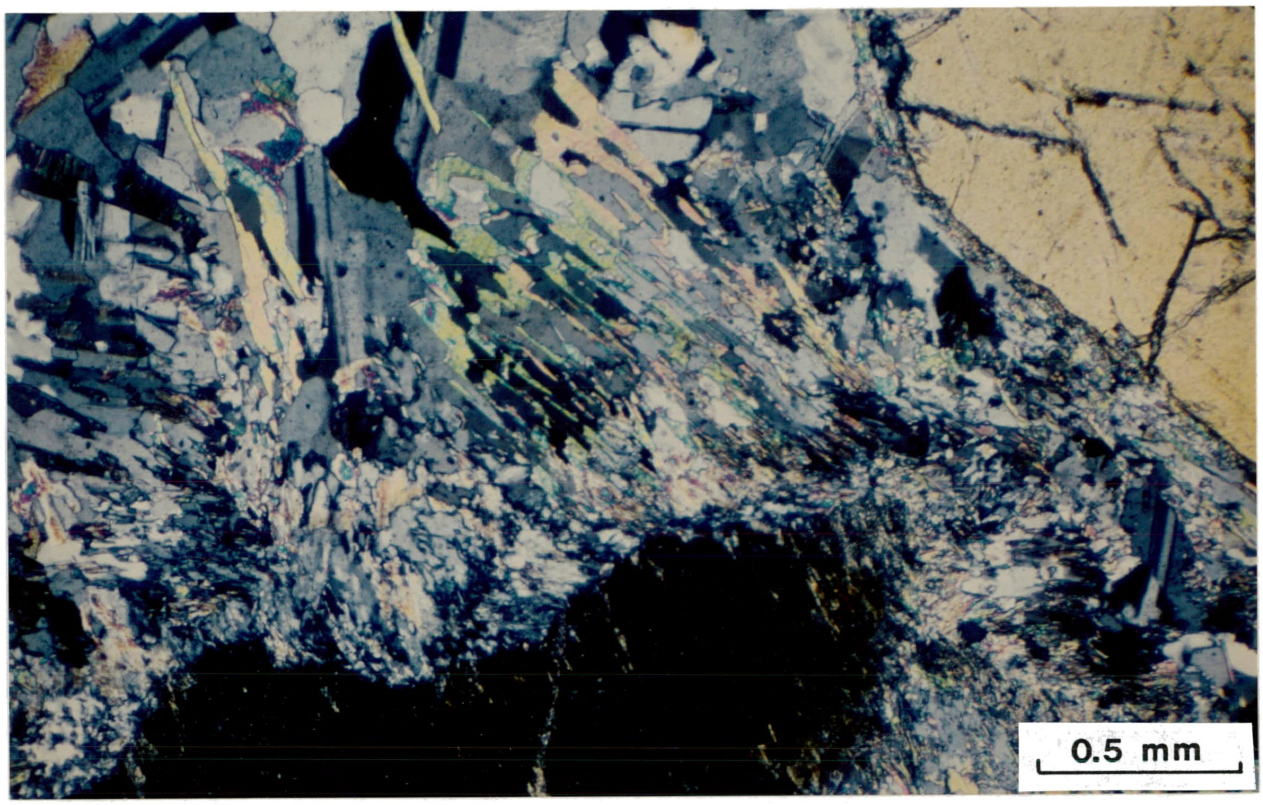

Fig. 3-16. Photomicrograph showing partial alteration of a spodumene crystal (bottom of photograph-grain at extinction) to white mica; sample from the Powerline pegmatite (cross-polarized light).

Fig. 3-17. Prismatic crystals of spodumene aligned perpendicular to pegmatite contact in a fine-grained groundmass of quartz, albite and muscovite; Nama Creek North pegmatite.

fluorite and purpurite-heterosite have been identified in hand specimens from the northern segment of the pegmatite. Toward the southern end of the pegmatite, the grain size of spodumene and microcline diminishes. At the southernmost exposure of the McVittie pegmatite, no spodumene is present and small grains of microcline up to 2 cm are incorporated into a fine, aplitic matrix.

The Powerline pegmatite is very similar, with respect to texture and mineralogy, to the southernmost segment of the McVittie pegmatite.

Mineralogical Studies

Perthitic Microcline

An attempt has been made to determine order/disorder relationships indicated by Al/Si distribution in K-rich feldspar from Georgia Lake rare-element pegmatites. Milne (1962) determined that samples of perthitic microcline from pegmatites of the Georgia Lake area contain as much 15.7% exsolved albite. Microscopic examination during the present study showed that the amount of albite-rich stringers and veinlets is highly variable in feldspar from individual pegmatites. The strongly perthitic nature of the feldspar introduces possible strain effects (Wright and Stewart, 1968). Most specimens of macro- to micro-perthitic microcline also contain poikilitic inclusions

of albite up to 3 mm in length.

X-ray powder diffractometer patters were determined for 20 K-rich feldspars from all pegmatites under study. Spectra were collected in the 20 range 19 to 60° at a scan rate of 1°2 θ/min using CuKα radiation and stored on computer disk for later retrieval. Spectra were corrected to the (111) reflection of fluorite (ASTM File # 4-864) used as an internal standard for each powder pattern. All spectra obtained showed some degree of interference from albite reflections. Broadened peaks and depressed intensities were considered to be effects produced by the perthitic nature of the feldspars and interference from albite inclusions. The spectra were indexed according to the powder pattern of maximum microcline (Borg and Smith, 1969) based on eight selected reflections of maximum microcline: $(\bar{2}01)$, (002), (131), $(1\bar{3}1)$, $(\bar{1}\bar{3}2)$, $(\bar{1}32)$, (060) and $(\bar{2}04)$. These eight reflections of maximum microcline may be discriminated from albite reflections on the same diffractometer tracing if the percent included albite introduced by inclusions and albite-rich stringers in the sample is low. Five of twenty feldspar spectra were rejected at this point because of difficulties in indexing broad, fuzzy, low intensity peaks.

Least-squares cell refinement, using the program of E. J. Gabe (personal communication, 1983), was performed

Molecular % orthoclase (n_{or}) in the Georgia Lake pegmatitic potassium feldspars is in the range 84 to 98% (Table 3-2) as determined by the equation of Kroll and Ribbe (1983), which makes use of cell volume (Appendix 2). Estimation of the molecular % orthoclase from the a cell edge (Orville, 1967) indicates the possibility of slight strain effects in the feldspars, since the determinations are commonly several % more orthoclase then values derived by the Kroll and Ribbe (1983) method.

Occupation of the T-site in alkali feldspar is by Si and Al. Four T-site orientations of molecular tetrahedra, $T_1 0$, $T_1 m$, $T_2 0$ and $T_2 m$ are characteristic of a stoichiometric triclinic unit cell of alkali feldspar. Complete ordering in alkali feldspar is achieved when 100% of the Al atoms in the crystal structure occupy the $T_1 0$ tetrahedral site (Ribbe, 1983) and is represented by the maximum microcline structural state of the K-rich phase of alkali feldspar. Preferential migration of Al into the $T_1 0$ site corresponds to conditions of low temperature crystallization of igneous rocks (Brown and Bailey, 1964) characteristic of granitic pegmatites. For example, some pegmatites are exemplary of this state (Shmakin, 1979) although irregularities from the maximum microcline structural state are noted in granitic pegmatites (Černý et al., 1984; Karnin, 1980).

b-c and α^* - γ^* plots (Stewart and Wright, 1974) are

for 15 indexed maximum microcline spectra. Of the remaining 15 samples, 5 more were rejected because of high standard errors associated mainly with cell angles of the triclinic unit cell. All samples rejected correspond to those with higher percentages of exsolved albite. Unit cell parameters of the ten remaining samples of perthitic microcline are summarized in Table 3-1. Corresponding d-spacings for each sample are tabulated in Appendix 3.

Structural state of feldspar reflects the aluminosilicate framework on an atomic scale based on the stoichiometric formula MT_4O_8 for alkali feldspar. The M-site is occupied by K and Na and minor trace elements. Orville (1967) has shown that unit cell edge *a* and cell volume are highly dependent on the proportion of K to Na in the M-site. An estimation of the amount of orthoclase molecule is only possible from the *a* cell-edge if the feldspar is strain free (Stewart and Wright, 1974). Although strain phenomena are associated with perthitic feldspars, they are most pronounced in cryptoperthitic feldspars, to a lesser extent in microperthites and are commonly absent in macroperthites. Also monoclinic potassium feldspars show more strain than triclinic phases (Stewart and Wright, 1974). Use of the strain indicator of Stewart and Wright (1974) suggests that perthitic potassium feldspars of the Georgia Lake pegmatites are strain free to slightly strained.

Table 3-1: Unit cell parameters of perthitic microcline from rare-element pegmatites

Pegmatite Sample Location	a(Å)	b(Å)	C(Å)	α	β	γ	α^*	γ^*	V(Å^3)
MNW, Wall Zone North	8.563 ±0.006	12.963 ± 0.002	7.217 ±0.003	90.57 ±0.02	116.04 ±0.04	87.96 ±0.04	90.31	91.93	719.2
MNW, Wall Zone South	8.570 ±0.014	12.963 ± 0.004	7.223 ±0.007	90.65 ±0.06	115.92 ±0.09	87.76 ±0.08	90.18	92.11	720.7
MNW, Core Zone	8.575 ±0.008	12.962 ± 0.002	7.212 ±0.004	90.39 ±0.003	116.10 ±0.05	88.04 ±0.05	90.53	92.03	718.7
Brink*	8.557 ±0.002	12.960 ± 0.001	7.217 ±0.001	90.39 ±0.01	116.10 ±0.01	88.25 ±0.01	90.39	91.70	718.9
Point	8.541 ±0.009	12.962 ± 0.003	7.216 ±0.005	90.65 ±0.04	116.04 ±0.06	87.76 ±0.06	90.29	92.11	716.9
Island	8.581 ±0.017	12.967 ± 0.005	7.219 ±0.009	90.57 ±0.07	115.97 ±0.11	87.85 ±0.10	90.41	92.16	721.8
Camp	8.559 ±0.003	12.963 ± 0.001	7.217 ±0.001	90.57 ±0.01	115.96 ±0.02	87.75 ±0.02	90.45	92.27	719.6
McVittie	8.560 ±0.009	12.962 ± 0.003	7.216 ±0.004	90.65 ±0.04	115.94 ±0.06	87.65 ±0.05	90.39	92.22	719.7
Powerline	8.568 ±0.006	12.965 ± 0.002	7.224 ±0.003	90.56 ±0.02	115.93 ±0.04	87.85 ±0.04	90.35	92.04	720.7
Nama Creek North	8.564 ±0.007	12.962 ± 0.002	7.223 ±0.004	90.56 ±0.03	115.94 ±0.05	87.85 ±0.04	90.35	92.04	719.7

* Sample obtained near the east contact of pegmatite
Crystal System: Triclinic
Space Group: $C\bar{1}$

Molecular percentage orthoclase (n_{or}) in the Georgia Lake pegmatitic potassium feldspars is in the range 84 to 98% (Table 3-2) as determined by the equation of Kroll and Ribbe (1983), which makes use of cell volume (Appendix 2). Estimation of the molecular percentage orthoclase from the a cell edge (Orville, 1967) indicates the possibility of slight strain effects in the feldspars, since the determinations are commonly several percent more orthoclase then values derived by the Kroll and Ribbe (1983) method.

Occupation of the T-site in alkali feldspar is by Si and Al. Four T-site orientations of molecular tetrahedra, T1O, T_1m, T_2O and T_2m are characteristic of a stoichiometric triclinic unit cell of alkali feldspar. Complete ordering in alkali feldspar is achieved when 100% of the Al atoms in the crystal structure occupy the T_1O tetrahedral site (Ribbe, 1983) and is represented by the maximum microcline structural state of the K-rich phase of alkali feldspar. Preferential migration of Al into the T_1O site corresponds to conditions of low temperature crystallization of igneous rocks (Brown and Bailey, 1964) characteristic of granitic pegmatites. For example, some pegmatites are exemplary of this state (Shmakin, 1979) although irregularities from the maximum microcline structural state are noted in granitic pegmatites (Cerny et al., 1984; Karnin, 1980).

b-c and α^* - γ^* plots (Stewart and Wright, 1974) are

Table 3-2: Orthoclase content (n_{or}), triclinicity, Δ, and distributions of Al in T-sites in perthitic microcline.

Pegmatite Sample Location	n_{or}[1]	n_{or}[2]	Δ[3]	$(t_{1o}+t_{1m})$	$(t_{1o}-t_{1m})$	t_{1o}	t_{1m}	t_2
MNW, Wall Zone - North	0.90	0.95	0.86	0.99	0.83	0.91	0.08	0.01
MNW, Wall Zone - South	0.94	0.96	0.92	0.99	0.97	0.98	0.01	0.01
MNW, Core Zone	0.89	0.96	0.92	0.92	0.84	0.88	0.04	0.08
Brink*	0.90	0.92	0.79	0.99	0.71	0.85	0.14	0.01
Point	0.84	0.90	0.92	0.99	0.95	0.97	0.02	0.01
Island	0.98	0.97	0.92	0.96	0.94	0.95	0.01	0.04
Camp	0.91	0.93	0.98	0.99	0.99	0.99	0.00	0.01
McVittie	0.92	0.93	0.98	0.99	0.97	0.98	0.01	0.01
Powerline	0.94	0.96	0.92	0.99	0.85	0.92	0.07	0.01
Nama Creek North	0.92	0.95	0.92	0.99	0.85	0.92	0.07	0.01

1 n_{or} - determined from equation of Kroll and Ribbe (1983)

2 n_{or} - estimated from a cell dimension (Orville, 1967)

3 Δ - triclinicity indicator (Goldsmith and Laves, 1954)

* - sample obtained near east contact of pegmatite

commonly used to represent the structural state of alkali feldspar, where the four corners of each diagram represent conditions of maximum order/disorder. The plots are based on observations by Orville (1967) and previous workers that unit cell parameters $\underline{b}$, $\underline{c}$, $\underline{\alpha}$, $\underline{\gamma}$, $\underline{\alpha}^*$ and $\underline{\gamma}^*$ are sensitive indicators of Al/Si distribution in the unit cell of alkali feldspar. The results obtained from perthitic feldspars of the Georgia Lake pegmatites are plotted on detailed portions of a $\underline{b}$-$\underline{c}$ (Fig. 3-18) and $\underline{\alpha}^*$ - $\underline{\gamma}^*$ diagram (Fig. 3-19) for alkali feldspars. On the $\underline{b}$-$\underline{c}$ plot, a tight clustering of data points is centered on the maximum microcline corner. Only one sample, from the core zone of the MNW pegmatite, deviates slightly from the maximum microcline corner. A similar distribution of samples is observed on the $\underline{\alpha}^*$ - $\underline{\gamma}^*$ plot.

The triclinic indicator Δ (Goldsmith and Laves, 1954) is used to estimate the order/disorder of a potassium feldspar where an increase in order is related to a decrease in structural symmetry. Results show triclinicities commonly in the range 0.9 to 1.0 for potassium feldspars from rare-element pegmatites of the Georgia Lake area (Table 3-2). The triclinicity of feldspar obtained near the contact of the Brink pegmatite is somewhat lower than the rest and may be representative of a small decrease in order toward the contact of the pegmatite.

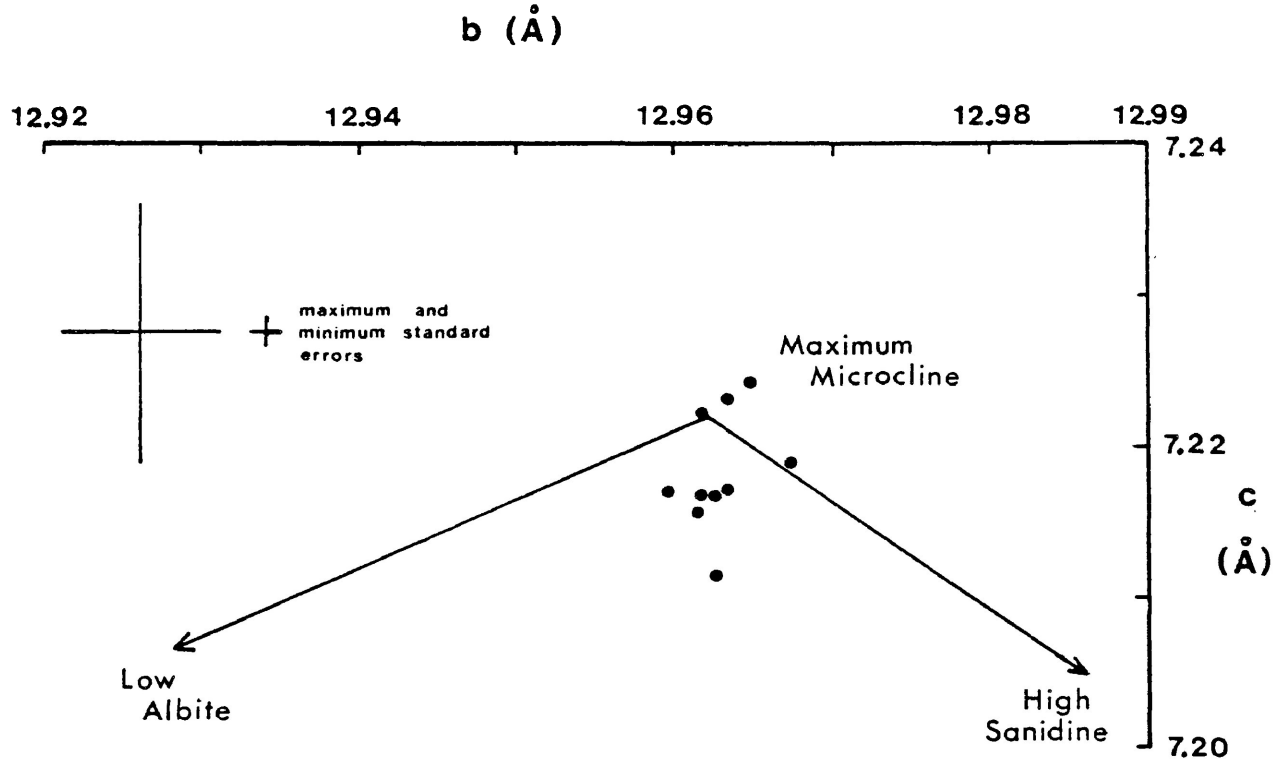

Fig. 3-18. b-c plot for alkali feldspars detailing the maximum microcline corner. Distribution of ten samples of perthitic microcline is indicated with dots (from Stewart and Wright, 1974).

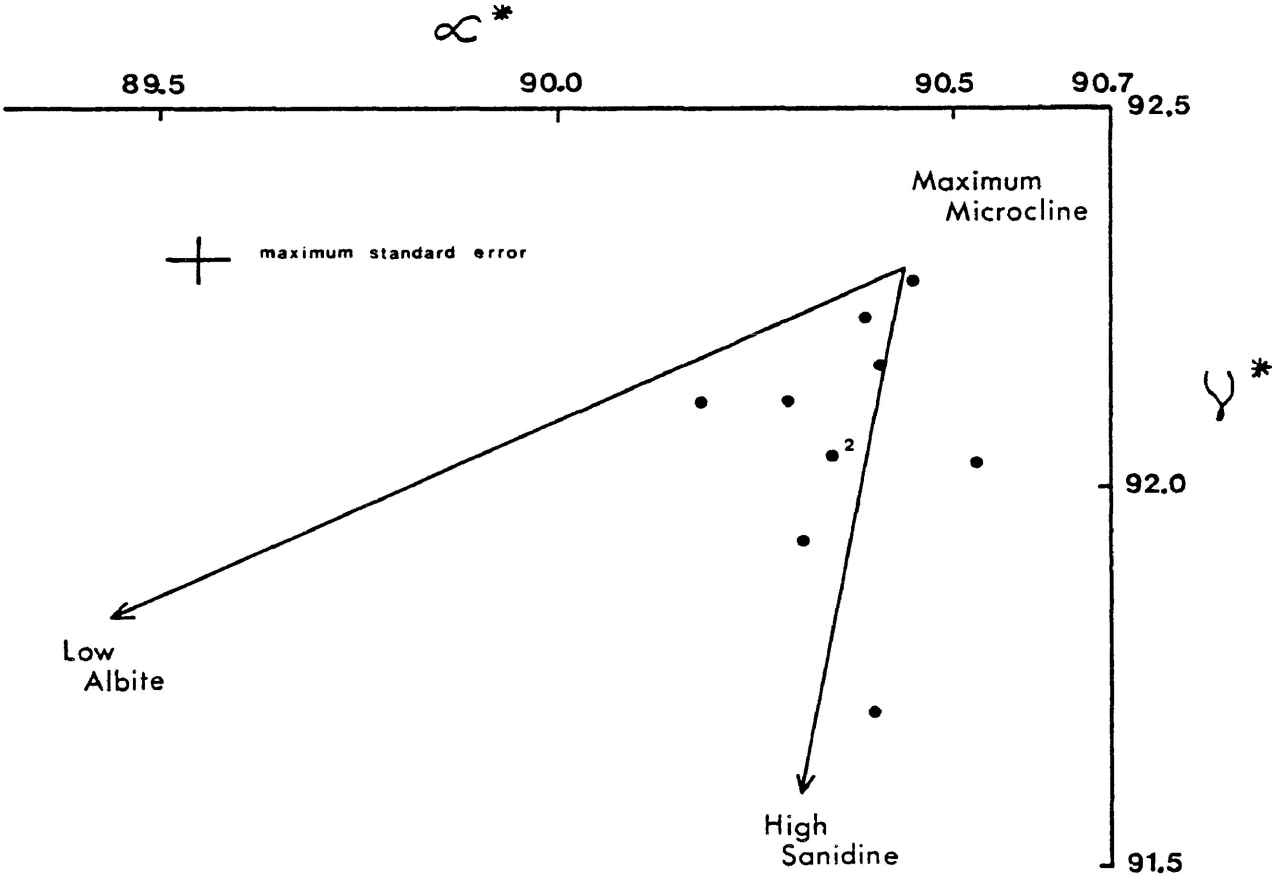

Fig. 3-19. $\underline{\alpha}^*$-$\underline{\gamma}^*$ plot for alkali feldspars detailing the maximum microcline corner. Distribution of ten samples of perthitic microcline is indicated with dots (from Stewart and Wright, 1974).

Distribution of Al in T-sites is determined by the equations (Appendix 2) of Kroll and Ribbe (1983) where t_1o, t_1m, t_2 denote the probabilities of finding Al in T_1o, T_1m and T_2 (unsubdivided) in a triclinic unit cell of alkali feldspar. The sum of the probabilities is equal to one. The probabilities are determined from refined cell parameters. Obtained results indicate a high concentration of Al in the T_1o site (Table 3-2) representing highly ordered structural states of perthitic microcline from the Georgia Lake rare-element pegmatites. There is a general parallelism between T_1o site occupancy and triclinicity. Lowest T_1o occupancy by Al corresponds to lowest triclinicity obtained from a sample from the Brink pegmatite.

Tantalite-Columbite Minerals

Tantalum-niobium minerals of the Georgia Lake rare-element pegmatites are disordered to partly ordered phases of the tantalite-columbite series. Order/disorder relationships in the tantalite-columbite solid solution series were first described by Nickel et al. (1963). End members of the series include fully ordered tantalite-columbite and fully disordered tantalite-columbite (pseudo-ixiolite) with a complete series of transitional phases. The degree of ordering is indicated by the intensities of the (020) and (110) reflections. Nickel

et al., (1963) reported intensities of 12 for (020) and 4 for (110) based on a maximum intensity of 100 for the (131) reflection of ordered tantalite-columbite. Low-angle relections indicative of superstructure are not present in fully disordered phases. Complete ordering of tantalite-columbite minerals occurs when cations Fe and Mn become separated from Ta and Nb in the crystal structure (general formula AB_2O_6 for an ordered phase). The basic unit cell of the orthorhombic tantalite-columbite series is based on the disordered phase which is identical to ixiolite. Ordering of the unit cell promotes superstructuring along the a cell-edge accompanied by a small decrease along the c cell-edge (Komkov, 1970). The a-c diagram of Černý and Turnock (1971) as recently modified by Černý and Ercit (1985) serves to graphically represent this relationship. The b cell-edge is insensitive to ordering/disordering. It was observed by Nickel et al., (1963) that disordered tantalite-columbite can be distinguished from ixiolite by heating the mineral. Heating promotes ordering by conversion of ixiolite to monoclinic wodginite and disordered tantalite-columbite to an ordered tantalite-columbite with superstructure. Powder diffractometer patterns of the ordered phases are readily distinguishable.

In the Georgia Lake area, columbite has been described from three rare-element pegmatites (Pye, 1965) although

no mineralogical or geochemical work was attempted. A small amount of columbite is also known to be present in rare-element pegmatites near Pine Portage, immediately west of the Georgia Lake area. During the present study, columbite was observed in one other deposit (Southwest) and is suspected in the Salo and Nama Creek South pegmatites in trace quantities.

Lattice parameter refinements are presented for three samples of tantalite-columbite minerals of the Georgia Lake area (Table 3-3). Sample T1 is a tantalite from the Brink pegmatite. It is a groundmass constituent intergrown with quartz and light green, medium-grained muscovite. Samples T4 and T6 are columbites from the MNW and Southwest deposits, respectively. T4 occurs as a tabular intergrowth with Sn oxide minerals and cleavelandite. T6 is from a mass of fine-grained saccharoidal albite and is present as tiny black flakes.

X-ray film patterns were obtained for samples T1, T4 and T6 with a 57.3 mm Gandolfi single-crystal camera using FeKα radiation and an exposure time of 24 hours each. In addition, powder diffractometer patterns using FeKα radiation and a scan speed of 1° 2θ/min. were run concurrently for samples T1 and T4 for the purpose of observing low-angle reflections. Insufficient material was obtained from T6 to run a powder diffractometer pattern.

Table 3-3: Unit cell parameters of tantalite-columbite minerals from the Georgia Lake Area rare-element pegmatites.

Crystal System: Orthorhombic
Space Group: Pbcn

Sample Number	Sample Location	Mineral Name*	a (Å)	b (Å)	c(Å)	V(Å^3)
T1	Brink	partly disordered manganotantalite	14.3058 ±0.0045	5.7553 ±0.0019	5.1014 ±0.0016	420.4
T4	MNW intermediate zone	disordered ferrocolumbite	4.7373 ±0.0057	5.7258 ±0.0043	5.1394 ±0.0049	139.6
T6	Southwest	disordered columbite	4.7537 ±0.0030	5.7167 ±0.0055	5.1382 ±0.0052	139.6

* mineral name partially dervied from sample geochemistry

The advantage of the Gandolfi film method is the ability to distinguish reflections of a much higher order than is possible by the powder diffraction method. The disadvantages of the Gandolfi film method include the inability to observe low-angle reflections and to quantitatively determine reflection intensities. Unit cell refinement is by the least-squares method (E. J. Gabe, personal communication, 1983) based on reflections measured from Gandolfi films. Film reflections were indexed to complete listings of lattice planes of tantalite-columbite and "pseudo-ixiolite" generated by the computer program CRYSTALINDEX (J. T. Szymański, personal communication, 1983). This program requires the input of ideal cell parameters, space group and systematic extinctions. The unit cell constants for tantalite-columbite and "pseudo-ixolite" were obtained from Foord (1982). The refined cell parameters of samples T1, T4 and T6 are based on the input of 43, 29 and 26 indexed reflections, respectively, into the least-squares cell refinement program. The indexed reflections and corresponding d-spacings on which cell refinement is based are summarized in Appendix 4.

Sample T1 is indexed to an ordered tantalite-columbite pattern. Relative intensities of the obtained peak reflections for (020) and (110) are equivalent to 7 and 4, respectively. Sample T1 plots as a partly disordered tantalite-columbite on the a-c diagram (Fig. 3-20).

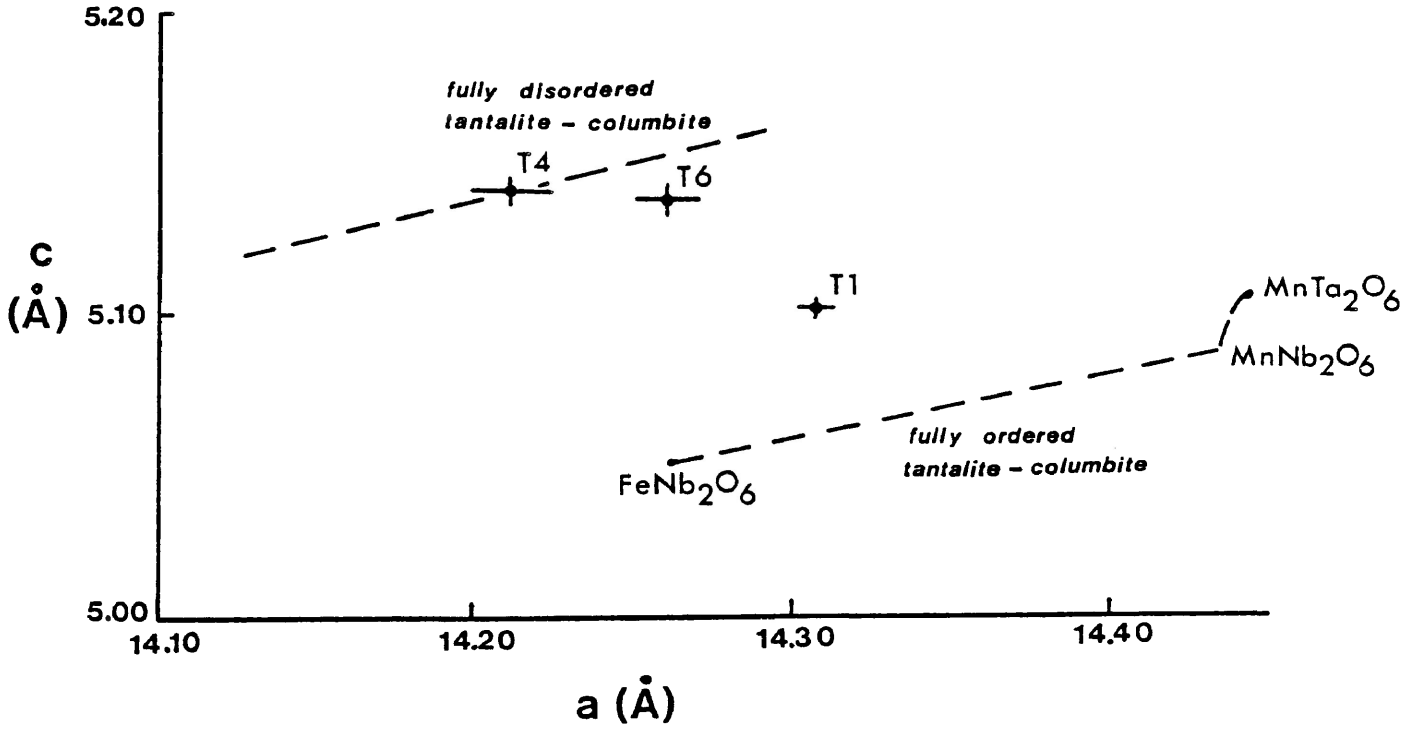

Fig. 3-20. Unit cell-edges a and c of tantalite-columbite minerals from three rare-element pegmatites plotted on a revised unit cell-edge a-c diagram. a cell-edge of disordered phases multiplied 3X (from Černý and Ercit, 1985).

Sample T4 was observed to have no low-angle reflections present. Pieces of sample T4 up to 0.5 cm in length were separated to be used in a heating experiment to determine the identity of the disordered phase by a structural inversion to a high-temperature form. The specimens were heated at 800°C for 16 hours (conditions from Černý and Turnock, 1971) in a muffle furnace provided by the Department of Chemistry, Lakehead University. Charcoal was added to the heating chamber to supress the effects of oxidation. A powder diffractometer pattern was obtained for the heated specimen. The effect of heating produced a strong (020) reflection with a relative intensity of 19. On the a-c diagram (Fig. 3-20), sample T4 (unheated) plots near the boundary of the disordered phase representative of a fully disordered structural state.

Indexing of sample T6 to a disordered phase was on the basis of distinguishable high-order reflections of the disordered unit cell and on sample geochemistry. The development of low-angle reflections for this sample was not investigated.

Staringite

Sn oxide minerals from the MNW pegmatite, originally described as cassiterite (Milne, 1962), have been observed to be structurally more closely related to staringite.

X-ray precession film patterns were obtained for two crystals of staringite; one from the core zone and one from the intermediate zone (S. A. Kissin, personal communication, 1985). Precession patterns were taken with Zr filtered MoKα radiation and exposed for 20 hours. The patterns for each crystal are identical and show the development of superstructure along the c cell edge (Fig. 3-21). X-ray film patterns were obtained for two crystals with a 57.3 mm Gandolfi single-crystal camera using FeKα radiation and an exposure time of 24 hours each and indexed to staringite. The refined cell parameters of staringite (Table 3-4) are based on the input of 35 and 32 reflections for samples from the core and intermediate zones respectively into a least-squares cell refinement program (E. J. Gabe, personal communication, 1983). The indexed film patterns are given in Appendix 5.

Geochemistry

General Statement

The geochemistry of perthitic microcline and muscovite from rare-element pegmatites was investigated for the purpose of observing regional fractionation trends and internal variation of elemental abundance within pegmatites. These two minerals were chosen since they are ubiquitous in all rare-element pegmatites of the area and are common reservoirs for elements that are sensitive indicators of the processess

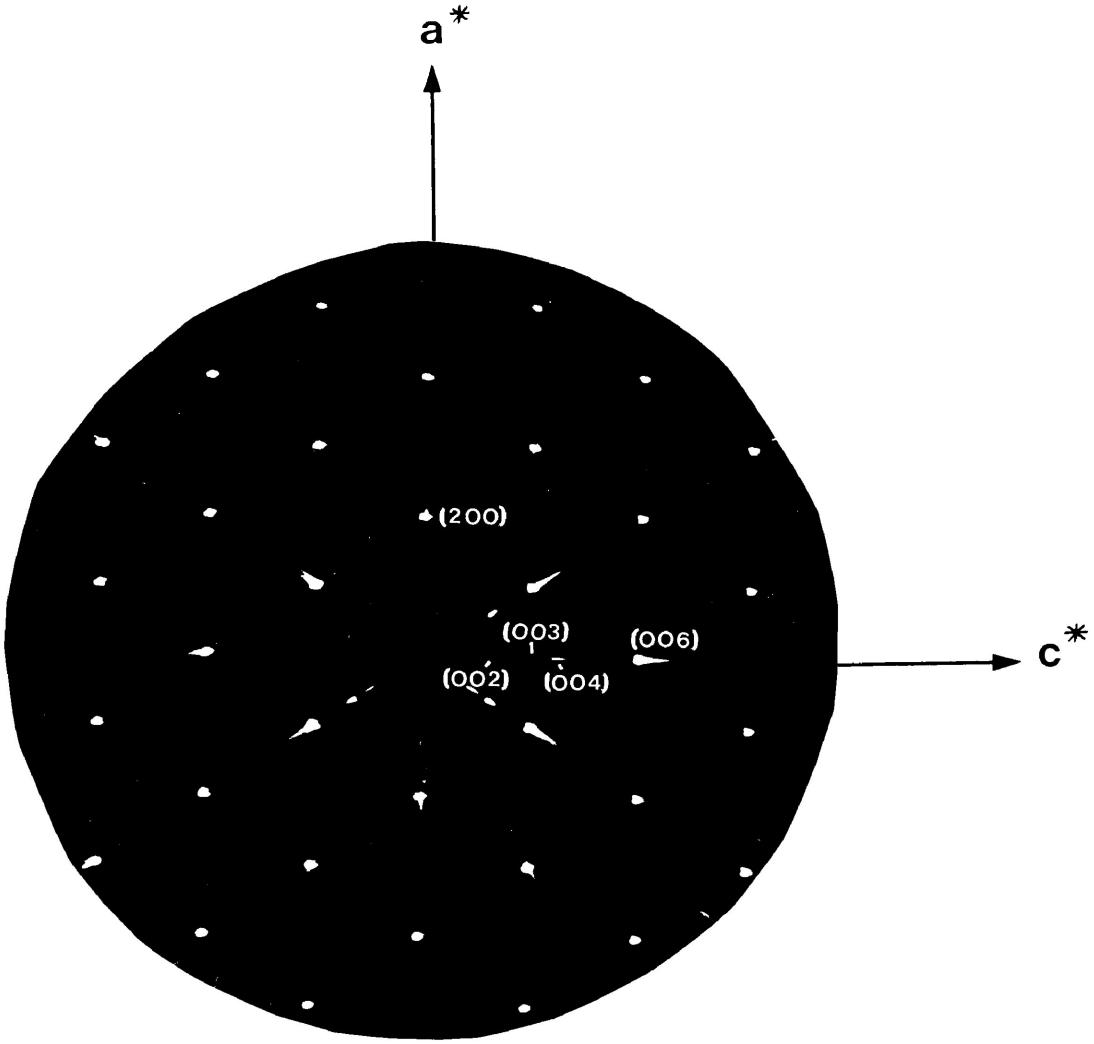

Fig. 3-21. X-ray precession pattern of (h0l)* of staringite from the core zone of the MNW pegmatite showing the development of superstructure. Indices are based on a tirutile cell ($\underline{A}=\underline{a}$, $\underline{C}=3\underline{c}$). The reflections (002) and (004), among others, are not permitted in the cassiterite space group.

Table 3-4: Unit cell parameters of staringite from the MNW pegmatite.

Crystal System: tetragonal
Space Group: $P4_2/mnm$

Sample Number	Location	a (Å)	c (Å)	V(Å^3)
S7	Core	4.7395	9.5213	213.9
	Zone	±0.0016	±0.0093	
S9	Intermediate	4.7394	9.5241	213.9
	Zone	±0.0014	±0.0095	

of fractionation. This approach to the study of fractionation trends was necessitated as opposed to regional whole rock analysis of bulk pegmatite compositions because of the coarse-grained and inhomogeneous nature of many of the pegmatites. Whole rock analysis of bulk samples may not be characteristic of the pegmatite, in general. This is especially true of the MNW pegmatite where a representative sampling of the pegmatite, as a whole, is very difficult to obtain due to pronounced development of zones. The major element content may be determined by analyzing bulk samples from each zone and readjusting the average major element content on the basis of volume % of each zone, but this approach is tedious and subject to error.

Effort was made to obtain samples of microcline and muscovite originating from the centres of pegmatites for consistency of elemental distribution, except where internal geochemical variations were to be investigated. Microcline specimens obtained from all pegmatites were of the white, blocky, perthitic type with virtually no variation in appearance in all pegmatites. Muscovite, as opposed to microcline, is highly variable within and among pegmatite groups as to origin and texture. Muscovite may be of primary or secondary origin. In some pegmatites, the origin of the muscovite is difficult to establish. With respect to Northern Group pegmatites, muscovite occurring as an

alteration of spodumene resembles primary groundmass muscovite. In the Camp pegmatite, groundmass muscovite occurs in trace quantities. Only the material from the muscovite enrichment zone at the southwest contact of the pegmatite could be sampled for muscovite. For these reasons, it is assumed that data for perthitic microcline is more representative of regional fractionation trends.

In addition to perthitic microcline and muscovite, data is presented for tantalite-columbite and Sn oxide minerals from rare-element pegmatites.

Sample Preparation

Suites of samples were obtained from each pegmatite. From these suites, samples were selected for muscovite and microcline on the basis of sample freshness and location within pegmatite. The very coarse-grained nature of perthitic microcline in many pegmatites permitted separation of mineral specimens in the field. Separation of muscovite books from the host rock was also possible in Southern and Central Group pegmatites.

Samples for microcline were crushed to a grain size of 5 mm or less. The crushed samples were hand sorted for material free of alteration or visible inclusions. Perthitic microcline samples commonly contained poikilitic

inclusions of albite that were not possible to separate. Hand sorted specimens were ground in an agate mortar mill and hand finished with mortar and pestle. About 20 g of very fine powder of each specimen was produced.

Specimens for muscovite from the Northern Group pegmatites were crushed to a grain size of 5 mm or less and hand sorted for muscovite flakes. The fine-grained nature of the groundmass muscovite introduced the possibility of partial contamination from white mica alteration of spodumene, although specimens with visible micaceous alteration of spodumene were avoided. Specimens, in which insufficient material was obtained by hand sorting (about 5 g), required heavy liquid separation with tetrabromoethane. The fine muscovite flakes of each specimen were hand crushed by mortar and pestle to a very fine powder.

Monominerallic specimens of book muscovite from Southern and Central Group pegmatites required hand separation of individual flakes. Specimens with mineral inclusions (tourmaline crystals are common in book muscovite from the MNW pegmatite) were rejected. Individual flakes of muscovite were trimmed into thin strips. Trimming of muscovite reduced the amount of time required to crush muscovite to a fine powder. Powdering of the muscovite trimmings was accomplished by hand with a mortar and pestle. Approximately 5 g of fine powder was produced for each

sample.

Two samples of microcrystalline muscovite from the MNW and Brink pegmatites were powdered in an agate mortar mill.

The fine powders provided starting materials for geochemical analysis by methods other than electron microprobe.

Polished sections of coarse material from each sample were produced for electron microprobe analysis. Microcline crystals and rock samples containing muscovite were set in Bakelite rings or on glass discs, cut and ground to 30 μm thickness and machine polished with 1 μm grit. The preparation of coarse-grained muscovite samples proved to be more problematical. Originally, books of muscovite were set in Bakelite rings with book edges perpendicular to the polishing surface. The samples were set in epoxy under vacuum. Surfaces were hand ground and machine polished. This method of sample preparation for electron microprobe was unsuccessful as polishing oil was incorporated between mica flakes and seeped out onto the polished surface during the carbon coating process. The polishing oil was impossible to remove. The more successful method of muscovite preparation involved placing thinly cut samples of book muscovite onto glass discs with thin edges

perpendicular to the polishing surface. Samples were set in epoxy under vacuum, hand ground and machine polished. Despite being set under vacuum, several samples retained air pockets between mica flakes and required hand polishing with 1 μm grit ona glass plate.

Samples of tantalite-columbite and Sn oxide minerals were set on glass discs and in Bakelite rings. Sample surfaces were ground and machine polished.

Methodology

Geochemical analysis of pegmatitic minerals incorporated the use of five separate analytical methods. SiO_2, Al_2O_3 and K_2O in feldspars and muscovites and TiO_2, FeO and MgO in muscovites were determined by electron microprobe. Rb and Cs in feldspars and muscovites and Sc, Ta and Co in muscovites were determined by instrumental neutron activation analysis. X-ray fluorescence spectrometry was used for analysis of Sr, Ba and Zr in feldspars and muscovites and Nb in muscovites. Li and Na_2O in muscovites were determined by atomic absorption. H_2O content in muscovites was obtained by a carbon-hydroden-nitrogen analyzer. Sn in selected muscovite samples was determined by the Geoscience Laboratories, Ontario Geological Survey by atomic absorption. All electron microprobe analysis of tantalite-columbite and Sn oxide minerals was performed by R. Chapman of the

University of Manitoba.

Electron Microprobe - Analysis of perthitic microcline and muscovite was performed at the University of Toronto in August and December, 1984 on the ARL and ETEC electron microprobes, respectively. Operating conditions during both investigations were: accelerating voltage 20 kV; beam current 100 mA; beam diameter ca 1 μm; fixed counting time of 100 seconds. Spectrometers in both microprobes were operated in the energy dispersive mode. Data was processed through the computer program PESTRIP.

Prior to analysis, polished sections were carbon coated in a high vacuum carbon coating chamber. Proper electrical contact along sample surfaces was ensured by applying a drop of carbon paste to the rim of the sample. The procedure to analyze samples required initial beam filament saturation, calibration of the energy spectrum on fluorescent willemite, calibration of beam current emission on a grain of cobalt followed by standardization of elements to be analyzed. Hohemfels sanidine (PS-2/8) and kaersutite (PS-2/12) were used to standardize for Si, Al, Na, K and Fe, Ti, Mg, respectively in all determinations. Frequent recalibration of standards was required on both electron microprobes.

The ARL microprobe was operated during a period of high beam current drift. As a result of sample difficulties

and beam current drift, much of the data determined by the ARL microprobe was subsequently rejected. The ETEC microprobe was operated under more favourable conditions.

An attempt was made to determine the geochemistry of tantalite-columbite and Sn oxide minerals on the ARL microprobe using the pure metals Ta, Nb, Mn, Fe, Ti and Sn as standards. The resulting total weights as oxides for each sample were consistently too high (common range 101 to 104 wt %). High totals for these minerals using pure metals as standards is a common problem (Grice et al., 1972). The data were rejected in favour of results obtained from P. Černý and R. Chapman who kindly volunteered to analyze tantalite-columbite and Sn oxide minerals using synthetic oxide standards.

Instrumental Neutron Activation Analysis (INAA) - Data for feldspars and muscovites were determined by three separate INAA experiments. In the first experiment, 12 samples of muscovite were irradiated along with three standards, SDC-1, PCC-1 and a synthetic standard of CsCl containing 189.46 ppm Cs. Elements determined in the first experiment include Cs, Rb, Ta, Sc and Co. In the second experiment, Cs and Rb were determined in 12 feldspar samples using G-2 and BCR-1 as standards. In the third experiment, eight feldspars and five muscovites were analyzed for Cs

and Rb using G-2 and BCR-1 as standards. In addition, Sc and Ta were determined in the five muscovite samples.

INAA, involving no chemical preparation, is the method commonly used for routine analysis of Cs, Ta, Sc and Co (Gibson and Jagam, 1980). Rb was found to be satisfactorily analyzed by this method because of the very high concentrations of the element in analyzed mineral samples.

Analytical procedure for all three experiments was identical. Approximately 100 mg of sample or standard was weighed on a Fisher Gram-matic balance to 0.01 mg in a specially constructed aluminum foil container. The container was folded, set in a second aluminum container and the sample number was marked on the outside. All samples in aluminum containers were packaged and sent to McMaster University, Hamilton, Ontario for irradiation. After irradiation, samples were allowed to decay for about four weeks before being transfered from aluminum containers to clear plastic vials.

Post-irradiation analysis is accomplished by INAA. Detection of γ-rays is by a hyperpure germanium crystal (APTEC/NRD). The crystal converts nuclear radiation into an electrical signal which is fed through a Tennelec TC 22 spectroscopic amplifier to a Norland IT-5400 multichannel (4096 channel) analyzer. After counting of a sample is complete, information stored in the multichannel analyzer

is displayed on a monitor attached to an Apple IIe computer, which is connected to the multichannel analyzer. This is accomplished by depressing the I/O button in the mode "all" to display live/dead time followed by "regions" to display count rate data for channels requested. After energy peaks are set for specific elements and corrected, net areas for each region are calculated and displayed on the monitor. A hardcopy of live/dead time, counting regions and net areas for an analyzed sample was obtained through a Teletype 43 printer connected to the Apple IIe computer.

Counting periods for elements Rb, Cs, Ta and Sc were in the range 1500 to 5000 seconds in all experiments. In the first experiment, Co along with Sc was counted for 20,000 seconds for each sample. This long counting period for Co was required because of a low peak to background count ratio resulting in poor counting statistics. All standards were counted for 10,000 seconds each. Data processing was accomplished through computer program NAA in the APL language for all elements except Rb. Rb concentrations were hand calculated. Concentrations of Ta, Sc and Co were determined by APL function TASCO, which also requests raw data for Eu and Hf. Concentrations for Cs were determined by APL function CESIUM.

Atomic Absorption - The instrument in use at Lakehead

University for atomic absorption is a Perkin-Elmer Model 2380 atomic absorption spectophotometer. The method requires the dissolution of all samples.

Approximately 0.5 g of each sample was weighed in a teflon beaker to 0.01 mg. Duplicates of each sample were obtained to check analytical precision. The dissolution procedure of samples is outlined in detail by Mitchell et al., (1980). Calibration standards for Li and Na were produced by dilution of standards known concentration to the range of sample concentration. Concentrations in samples were determined from curves produced for the calibration standards based on elemental absorbance.

X-ray Fluorescence And Carbon-Hydrogen-Nitrogen Analyzer - The methods of analysis by XRF and CHN were summarized in Part Two.

Error Analysis

Accuracy estimates are determined as % error of an obtained standard concentration from its true value. Accuracy of INAA data is summarized in Table 3-5. For each element, the method required running one reference standard against another. In the first experiment, accuracy of Rb and Ta is not known since only one suitable standard (SDC-1) was available for reference. Accuracy of INAA

Table 3-5: Accuracy estimates of INAA data as % error from true value.

Experiment	Elements Determined	Standards	% Error
1	Rb	SDC-1	NA
	Cs	SDC-1, Synthetic CsCl	1.66
	Ta	SDC-1	NA
	Sc	SDC-1, PCC-1	3.69
	Co	SDC-1, PCC-1	10.92
2	Rb	G-2, BCR-1	5.09
	Cs	G-2, BCR-1	5.00
3	Rb	G-2, BCR-1	3.56
	Cs	G-2, BCR-1	7.16
	Ta	G-2, BCR-1	16.40
	Sc	G-2, BCR-1	0.60

NA - not available

data is highly dependent on concentration of element in the reference standard. Decreased accuracy in relation to other elements is especially pronounced in Ta from experiment three where concentration of Ta in G-2 and BCR-1 is below 1 ppm (Abbey, 1983). In contrast, the use of high standard concentrations of Cs in the first experiment and Sc in the third experiment resulted in high accuracies.

Accuracy of electron microprobe data was not determined because of frequent restandardization. A comparison of obtained structural formula for feldspar and muscovite samples to stoichiometric formula (Deer et al., 1966) suggests the microprobe data to be of good accuracy.

Reference standard used for atomic absorption was SY-2. Percent error of derived Li concentration in SY-2 with respect to true value is 1.14% based on two determinations of Li in SY-2 with a standard deviation of 5.26% at the 2σ level of confidence. An accuracy estimate for Na_2O in muscovite by atomic absorption was not obtained.

The accuracy of X-ray fluorescence data was summarized in Part Two.

Data precision is summarized in Table 3-6. Precision estimates for SiO_2, Al_2O_3, FeO and K_2O determined by electron

Table 3-6: Precision estimates of feldspar and muscovite data at the 2σ level of confidence.

Oxide/Element	Maximum % 2σ	Minimum % 2σ	Average % 2σ
SiO_2	3.22	0.70	1.30
Al_2O_3	1.96	0.44	1.16
FeO*	12.96	3.06	8.90
Na_2O	24.40	0.00	8.42
K_2O	4.08	0.30	1.94
Li	28.18	0.12	6.72
Rb	3.85	1.43	2.63
Cs	2.30	0.40	0.99
Sr	15.38	2.66	8.86
Ba	17.43	1.46	6.87
Sc	10.43	1.46	4.69
Zr	66.49	20.99	34.39
Nb	8.19	2.43	3.76
Ta	3.52	0.55	1.10
Co	29.38	14.34	17.13

* total iron as FeO

microprobe and Li and Na_2O determined by atomic absorption were derived as a % standard deviation from a mean of duplicate analyses at the 2σ level of confidence. Precision estimates for Sr, Ba, Zr and Nb determined by X-ray fluorescence and Rb, Cs, Sc, Ta and Co determined by INAA are derived from counting statistics by the method of Bertin (1967) and presented at the 2σ level of confidence. Greater precision of data is correlatable with high elemental concentrations in a sample. Elemental concentrations in samples near the lower limit of detection yield poor precision as the result of low peak to background count rates. This is especially pronounced with Zr and Co data. Data for Sc which provided poor precision was rejected. Precision of MgO and TiO_2 was not determined. Calculated detection limits of MgO and TiO_2 at the 2σ level of confidence are 0.16 and 0.24 wt %. Obtained results for MgO and TiO_2 are at or near the detection limits and as such, the precision of MgO and TiO_2 in muscovites is considered poor.

Data quality estimates for H_2O and Sn in muscovites was not obtained.

Precision of tantalite-columbite and Sn oxide minerals determined by electron microprobe is summarized in Tables 3-7 and 3-8. A standard deviation at the 2σ level of confidence was obtained for each element. The standard

Table 3-7: Precision of tantalite-columbite mineral data determined by electron microprobe at the 2σ level of confidence.

Element	Maximum % 2σ	Minimum % 2σ	Average % 2σ
Ta	3.08	1.52	2.08
Nb	3.50	1.33	1.80
Ti	16.67	4.25	10.19
Sn	30.00	6.20	18.21
Fe	6.99	2.37	3.80
Mn	5.66	2.38	3.20
Sc	28.57	25.00	26.19

Table 3-8: Precision of Sn oxide mineral data determined by electron microprobe at the 2σ level of confidence.

Element	Maximum % 2σ	Minimum % 2σ	Average % 2σ
Ta	10.83	4.83	8.36
Nb	20.00	6.87	11.79
Ti	-----	-----	28.00
Sn	1.17	1.16	1.16
Fe	12.50	7.56	10.10
Mn	-----	-----	33.33

deviation was converted to % standard deviation for each element.

Results

Perthitic Microcline - Analytical results summarizing the geochemistry of perthitic microcline from the Georgia Lake rare-element pegmatites are presented (Tables 3-9 to 3-12). Selected variation diagrams (Figs. 3-23 to 3-34) display interelemental relationships among the perthitic microcline samples on a regional scale. The geochemical variations among three perthitic microcline samples from different parts of the MNW zoned pegmatite (Fig. 3-22), identified with triangles on all variation diagrams, are compared to the geochemistry of perthitic microcline from poorly zoned to unzoned pegmatites of the Georgia Lake area. Although the geochemistry of six microcline samples from the Brink pegmatite was determined, only sample F17 is included in the variation diagrams. The sample originates from a small trench approximately 30 m north of a larger trench from which samples F13A to F13E were obtained. Samples from the Central and Northern Groups are identified with circles and squares on all diagrams, respectively. In addition, samples from the Brink, Island and MNW core zone are identified by the initials, B, I and C, respectively.

Table 3-9: Sample locations of analyzed perthitic microcline specimens.

Group	Pegmatite	Sample Numbers
Southern (▲)	MNW - wall zone - north	F71
	MNW - wall zone - south	F76
	MNW - core zone (c)	F72
Central (●)	Brink (B)	F13A-F13E, F17
	Southwest	F100
	Salo	F88
	Niemi	F102
	Point	F114
	Island (I)	F120
Northern (■)	Nama Creek North	F48
	Nama Creek South	F54
	McVittie	F24
	Powerline	F5
	Camp	F33
	Giles	F132

Table 3-10: Chemical analysis of perthitic microcline from the MNW pegmatite

Sample	F71	F76	F72
wt %			
SiO_2	63.94	65.28	63.60
Al_2O_3	18.85	18.96	18.43
K_2O	16.04	16.21	15.32
Total	98.83	100.45	97.35
Cations 0=32			
Si	11.934	11.976	12.001
Al	4.147	4.100	4.101
K	3.819	3.795	3.689
Cation Sum	19.900	19.871	19.791
ppm			
Rb	1886	2792	6707
Cs	287	537	1015
Sr	114	94	92
Ba	891	455	416
Zr	23	≤ 7	17
ratios			
K/Rb	70.63	48.21	18.97
K/Cs	464.1	250.7	125.3
K/Ba	149.5	295.8	305.8
K/Sr	1168	1432	1383
Rb/Sr	16.54	29.70	72.90
Rb/Ba	2.12	6.14	16.12
Ba/Sr	7.82	4.84	4.52

Table 3-11: Chemical analysis of perthitic microcline from the Central Group pegmatites.

Sample	F13A	F13B	F13C	F13D	F13E	F17	F100	F88	F102	F114	F120
wt %											
SiO_2	64.79	65.20	65.31	65.64	64.67	65.65	64.88	63.67	64.61	64.93	65.18
Al_2O_3	18.56	19.08	18.83	18.98	18.81	18.51	18.87	18.71	18.57	18.59	18.31
K_2O	16.02	15.59	15.43	15.58	15.38	15.09	15.58	16.04	16.03	15.80	16.12
Total	99.37	99.87	99.57	100.20	98.86	99.25	99.33	98.42	99.21	99.32	99.61
Cations 0=32											
Si	12.011	11.985	12.028	12.017	12.002	12.097	11.996	11.939	12.000	12.022	12.055
Al	4.055	4.133	4.305	4.097	4.115	4.021	4.113	4.135	4.066	4.058	3.992
K	3.788	3.655	3.625	3.640	3.643	3.547	3.675	3.836	3.797	3.732	3.803
Cation Sum	19.854	19.773	19.958	19.754	19.760	19.665	19.784	19.910	19.863	19.812	19.850
ppm											
Rb	6920	7232	7697	8395	7491	8969	9149	5527	1717	2138	1590
Cs	695	711	855	1042	899	1120	1090	374	106	54	34
Sr	133	116	150	134	126	140	118	93	218	224	260
Ba	452	525	442	420	447	428	415	419	486	729	1097
Zr	10	9	≤ 7	≤ 7	≤ 7	≤ 7	≤ 7	8	19	17	16
ratios											
K/Rb	19.22	17.89	16.64	15.40	17.05	13.97	14.13	24.10	77.52	61.36	84.15
K/Cs	191.4	182.0	149.8	124.1	142.1	111.9	118.6	356.2	1256	2430	3935
K/Ba	294.3	246.5	289.8	307.9	285.7	292.8	311.6	317.9	273.9	180.0	122.0
K/Sr	1000	1116	854.0	964.9	1014	895.0	1096	1432	610.6	585.7	514.6
Rb/Sr	52.03	62.34	51.31	62.65	59.45	64.06	77.53	59.43	7.88	9.54	6.12
Rb/Ba	15.31	13.78	17.41	19.99	16.76	20.96	22.05	13.19	3.53	2.93	1.45
Ba/Sr	3.40	4.53	2.95	3.13	3.55	3.06	3.52	4.51	2.23	3.25	4.22

Table 3-12: Chemical analysis of perthitic microcline from the Northern Group pegmatites

Sample	F48	F54	F24	F5	F33	F132
wt %						
SiO_2	65.81	nd	65.19	65.28	66.20	65.57
Al_2O_3	18.53	nd	18.42	18.48	18.79	18.46
K_2O	15.95	nd	15.88	15.79	16.14	16.05
Total	100.29	nd	99.49	99.55	101.13	100.08
Cations O=32						
Si	12.064	--	12.052	12.053	12.041	12.056
Al	4.004	--	4.014	4.022	4.028	4.002
K	3.731	--	3.745	3.719	3.745	3.765
cation sum	19.799	--	19.811	19.794	19.814	19.823
ppm						
Rb	3077	3397	3670	5152	3485	2864
Cs	103	117	149	382	144	104
Sr	78	71	77	75	75	60
Ba	421	410	469	437	475	419
Zr	20	16	18	21	20	22
ratios						
K/Rb	43.03	--	35.91	25.45	38.45	46.51
K/Cs	1285	--	884.6	343.2	930.6	1281
K/Ba	314.5	--	281.0	300.0	282.1	317.9
K/Sr	1697	--	1712	1748	1787	2220
Rb/Sr	39.45	47.85	47.66	68.69	46.47	47.73
Rb/Ba	7.31	8.29	7.83	11.79	7.34	6.84
Ba/Sr	5.40	5.77	6.09	5.83	6.33	6.98

nd: not determined

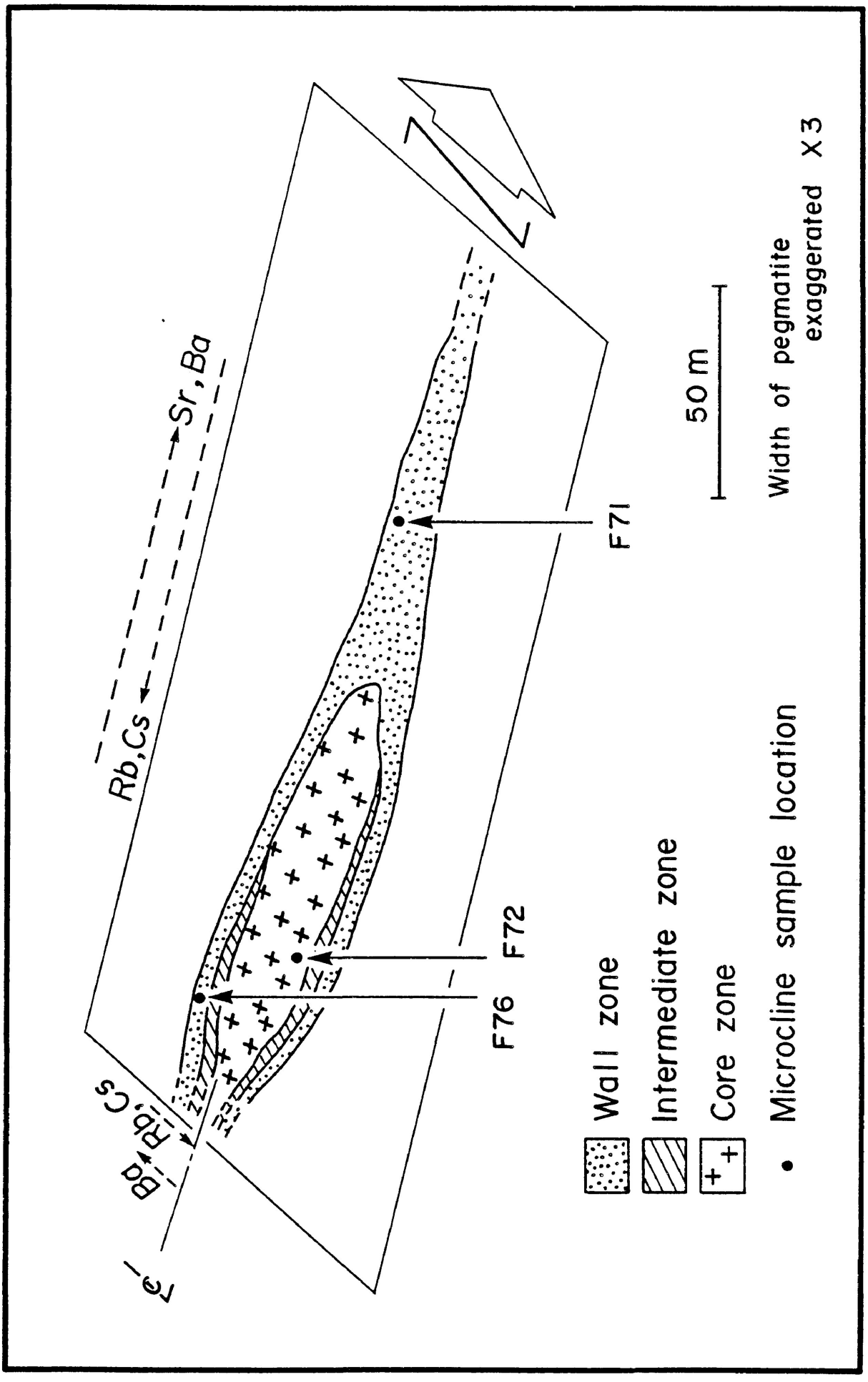

Fig. 3-22. Oblique schematic view of the MNW pegmatite showing the distribution of microcline samples. Stippled arrows indicate the direction of increase of trace element (Rb, Cs, Sr, Ba) content in perthitic microcline.

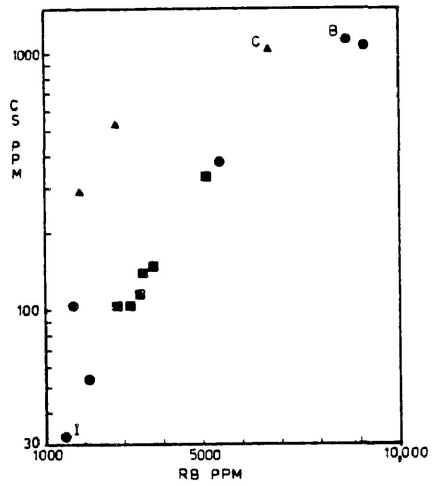

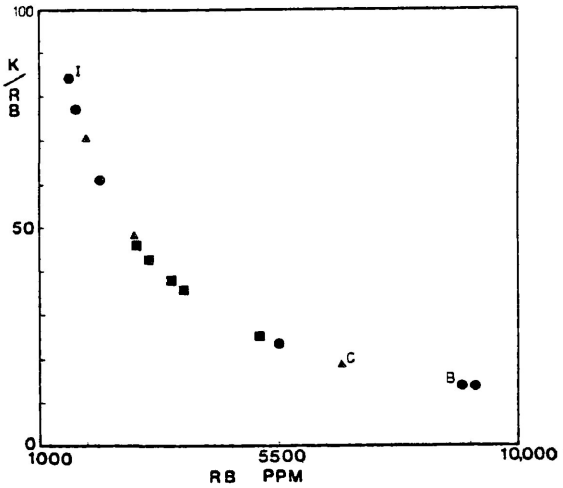

Fig. 3-23 (left). Cs versus Rb for perthitic microcline.

Fig. 3-24 (right). K/Rb versus Rb for perthitic microcline.

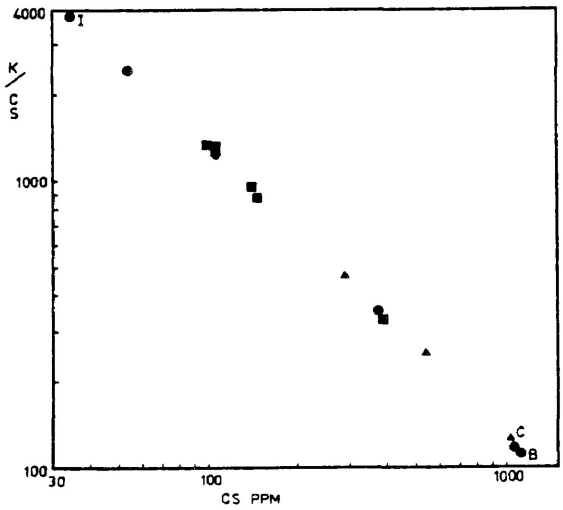

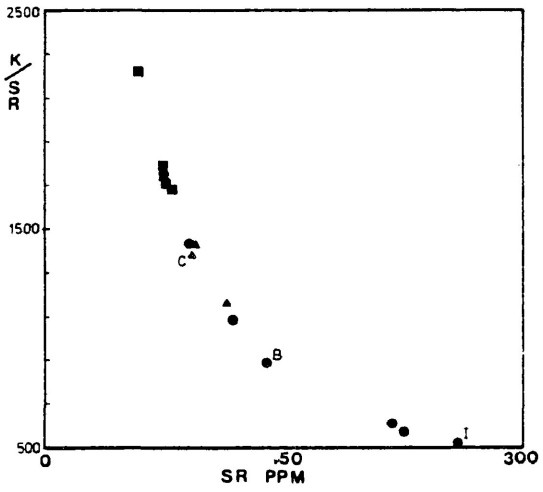

Fig. 3-25 (left). K/Cs versus Cs for perthitic microcline.

Fig. 3-26 (right). K/Sr versus Sr for perthitic microcline.

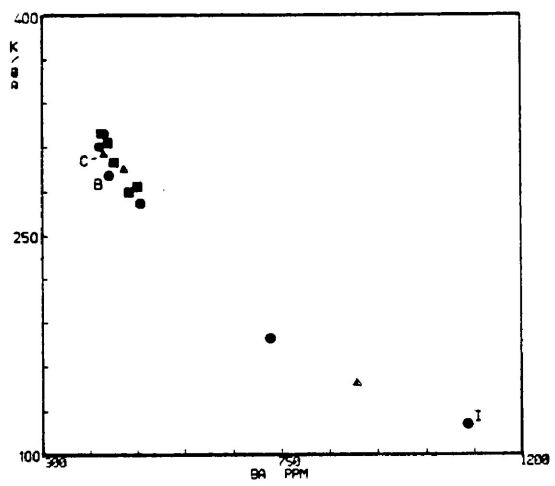

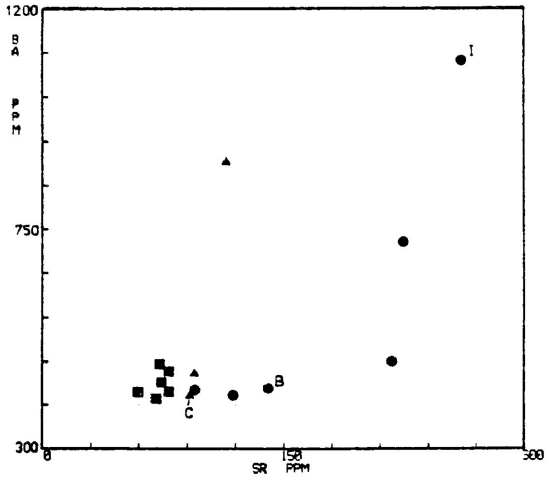

Fig. 3-27 (left). K/Ba versus Ba for perthitic microcline.

Fig. 3-28 (right). Ba versus Sr for perthitic microcline.

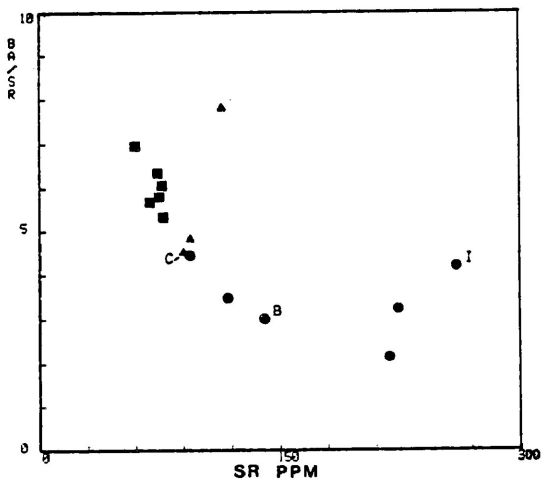

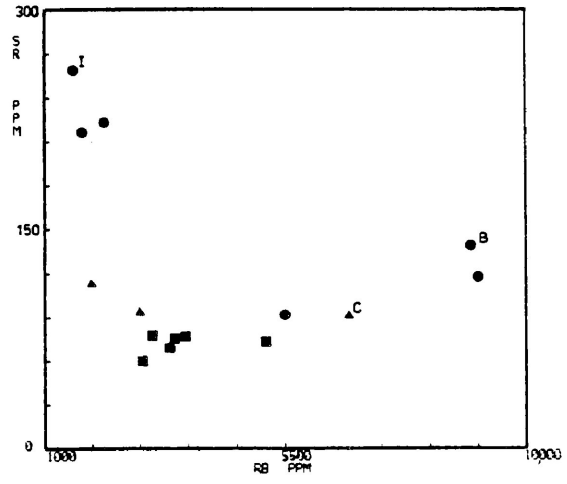

Fig. 3-29 (left). Ba/Sr versus Sr for perthitic microcline.

Fig. 3-30 (right). Sr versus Rb for perthitic microcline.

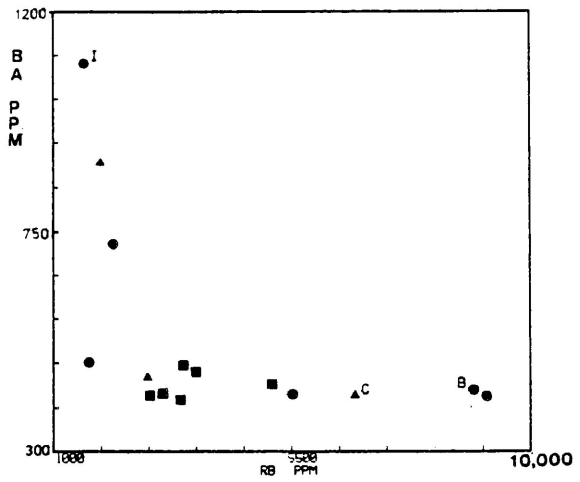

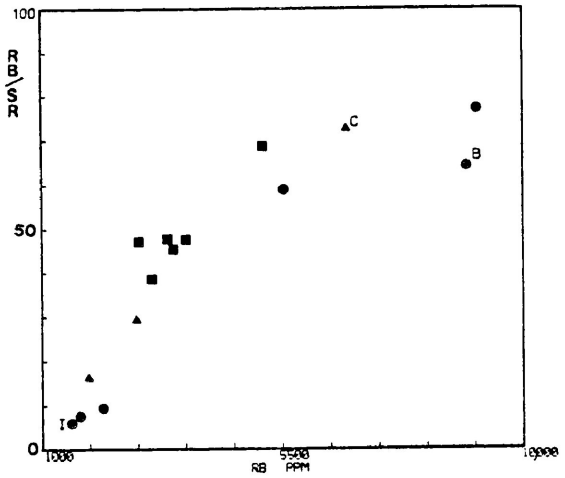

Fig. 3-31 (left). Ba versus Rb for perthitic microcline.

Fig. 3-32 (right). Rb/Sr versus Rb for perthitic microcline.

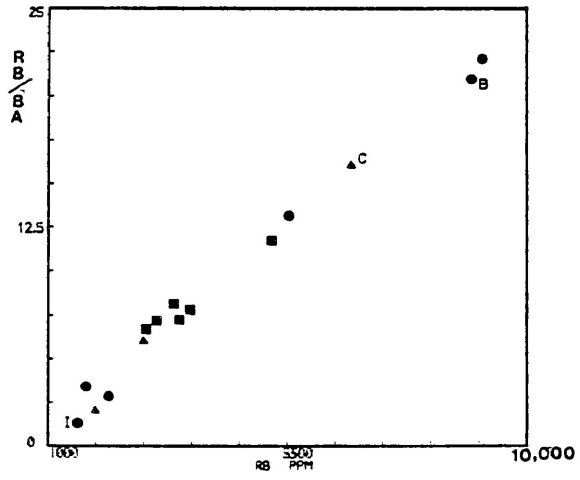

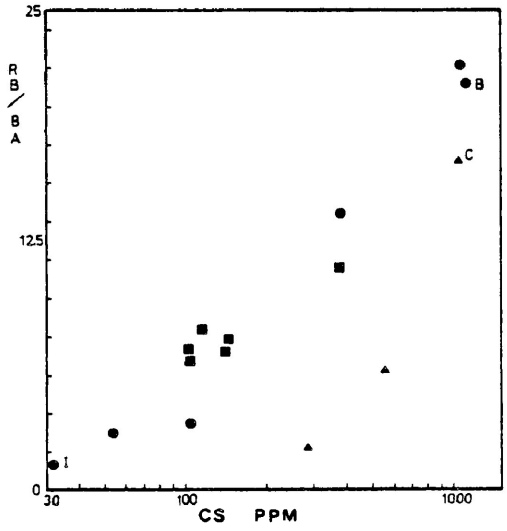

Fig. 3-33 (left). Rb/Ba versus Rb for perthitic microcline.

Fig. 3-34 (right). Rb/Ba versus Cs for perthitic microcline.

All data as oxides was determined on the ETEC microprobe. Na_2O in microcline was noted in the analysis of several samples to be in the range 0.5 to 1 wt % although replicate analyses of these samples yielded sporadic values. Although the calculated lower limit of detection of Na_2O for the ETEC microprobe is 0.26 wt % at the 2σ level of confidence, it was observed that the lower limit of detection of Na_2O at the time of operation to be at least 1 wt % Na_2O. Accumulation of dust on the beam filament resulting from a high atmospheric humidity level at the time of operation may be an explanation for the unusually high lower limit of detection of Na_2O. Perhaps for the same reason, satisfactory analyses of albite lamellae could not be obtained.

Concentration of Rb in perthitic microcline from rare-element pegmatites is in the range of 0.15 to 1 wt % (Fig. 3-23). This range is observed across the Central Group pegmatites with a gradual increase in Rb concentration from east to west. Of the Northern Group pegmatites, greatest Rb concentration (0.5 wt %) is noted in the Powerline pegmatite. A unidirectional increase in Rb across Northern Group pegmatites, as noted for the Central Group pegmatites, is not apparent. In the MNW pegmatite, Rb increases in perthitic microcline from north to south in the wall zone and toward the core zone.

Behaviour of Cs parallels Rb, but it is present in smaller concentrations than Rb. Cs increases at a greater

rate in relation to Rb in the MNW and Central Group pegmatites. A strong positive correlation exists between Rb and Cs (Fig. 3-23). It is notable that samples from the MNW pegmatite are enriched in Cs in relation to Rb with respect to pegmatites of the Central and Northern Group. Linear relationships are observed between K/Rb against Rb (Fig. 3-24) and K/Cs against Cs (Fig. 3-25) where samples F17 and F120 from the Central Group pegmatites mark the extremities in Rb and Cs concentration in perthitic microcline of the sampled pegmatites. The distribution of K/Rb against Rb and K/Cs against Cs in Northern Group pegmatites is not as variable as in the Central Group.

The variation in Sr concentration in perthitic microcline is greatest in the Central Group pegmatites. Sr decreases in the Central Group pegmatites. Sr decreases from east to west across the group although the decrease is insignificant in relation to the corresponding increase in Rb and Cs. Northern Group pegmatites show very little variation of Sr in perthitic microcline. Concentration of Sr is lower and K/Sr ratio (Fig. 3-26) greater in all samples from the Northern Group with respect to the Central Group. In the MNW pegmatite, Sr concentration in microcline decreases slightly from north to south in the wall zone, although Sr decrease to the core zone from the wall zone is insignificant.

The behaviour of Ba parallels Sr (Fig. 3-27). Ba

decreases from 0.11 to 0.04 wt % from east to west across the Central Group pegmatites. Ba concentration in perthitic microcline across the Northern Group pegmatites remains constant at 0.04 to 0.05 wt %. In samples from the wall zone of the MNW pegmatite, Ba concentration decreases from 0.09 to 0.046 wt % from north to south and to 0.042 wt % in the core zone. A plot of Ba against Sr (Fig. 3-28) shows a clustering of data points for most samples. The exception to this trend is sample F71 from the northern part of the MNW pegmatite and samples F102, F114 and F120 representing easternmost rare-element pegmatites of the Central Group. These samples can also be distinguished in Fig. 3-29 of Ba/Sr against Sr.

The variation in concentration of Sr and Ba in relation to Rb, on a regional scale, is small (Figs. 3-30, 3-31). Similar distributions can be expected for Sr and Ba against Cs. Linear positive correlations are noted in samples across the Georgia Lake pegmatite field for Rb/Sr and Rb/Ba against Rb (Figs. 3-32, 3-33). The greatest variability in Rb/Sr and Rb/Ba is in the Central Group pegmatites in relation to the other two rare-element pegmatite groups. A similar relationship occurs between Rb/Ba and Cs (Fig. 3-34) except that samples from the MNW pegmatite are skewed toward Cs in relation to the linear trend of the Central and Northern Group pegmatites.

Zr occurs in low concentrations in perthitic microcline although greater affinity for the Northern Group pegmatites and easternmost pegmatites of the Central Group is noted. Distribution of Zr in perthitic microcline from the MNW pegmatite is erratic.

Cross-section Of Brink Pegmatite - Perthitic microcline was sampled along a trench that cross-cuts the Brink pegmatite from the east to west contact. Five samples were obtained at roughly even spacing along the trench. Samples were subsequently analyzed and are identified as F13A to F13E (Table 3-11). The purpose of the experiment was to observe geochemical variations across a poorly zoned rare-element pegmatite of the Georgia Lake pegmatite field. The Brink pegmatite was the only such pegmatite which could be sampled for perthitic microcline from wall to wall.

Rb and Cs show the most pronounced variation in concentration across the Brink pegmatite. Rb varies by about 1500 ppm, Cs by 350 ppm, Sr by 35 ppm and Ba by 105 ppm. These observations are in keeping with elemental variations on a regional scale. The behaviour of Cs in perthitic microcline closely parallels that of Rb (Figs. 3-35, 3-36). Both Rb and Cs are in lowest concentration near the eastern contact of the Brink pegmatite. Abundance of Rb and Cs steadily increases to west of the centre of the pegmatite and then decreases toward the western contact.

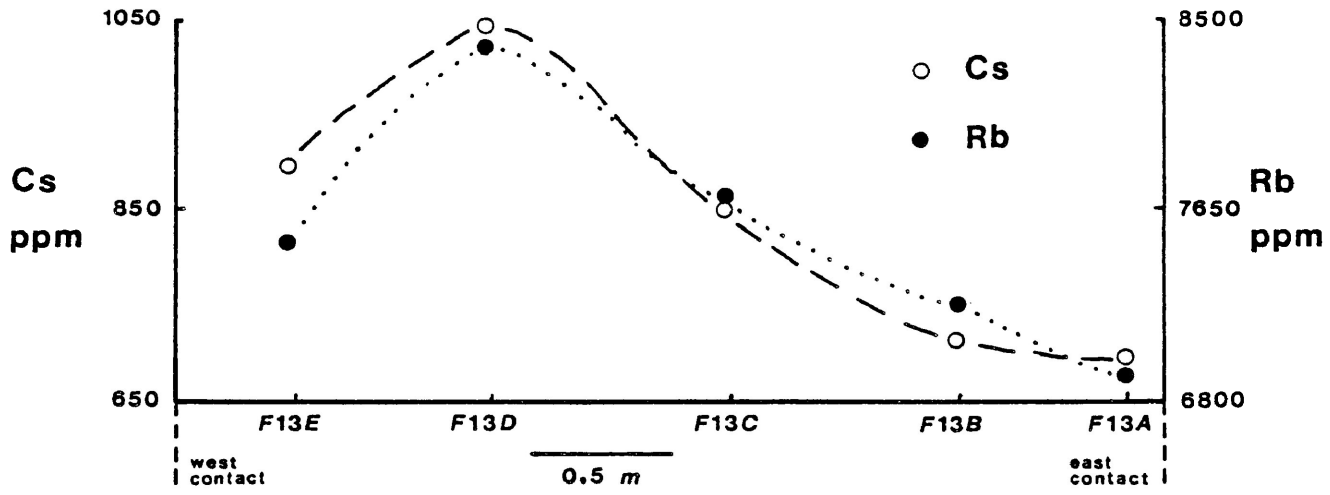

Fig. 3-35. Distribution of Cs and Rb in perthitic microcline across the Brink pegmatite.

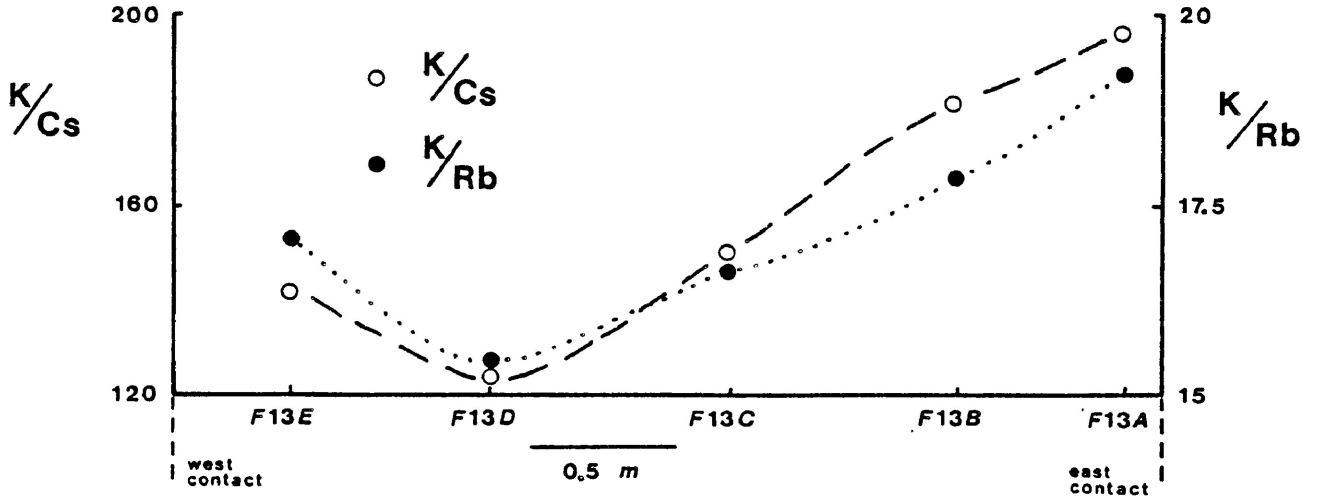

Fig. 3-36. Distribution of K/Cs and K/Rb in perthitic microcline across the Brink pegmatite.

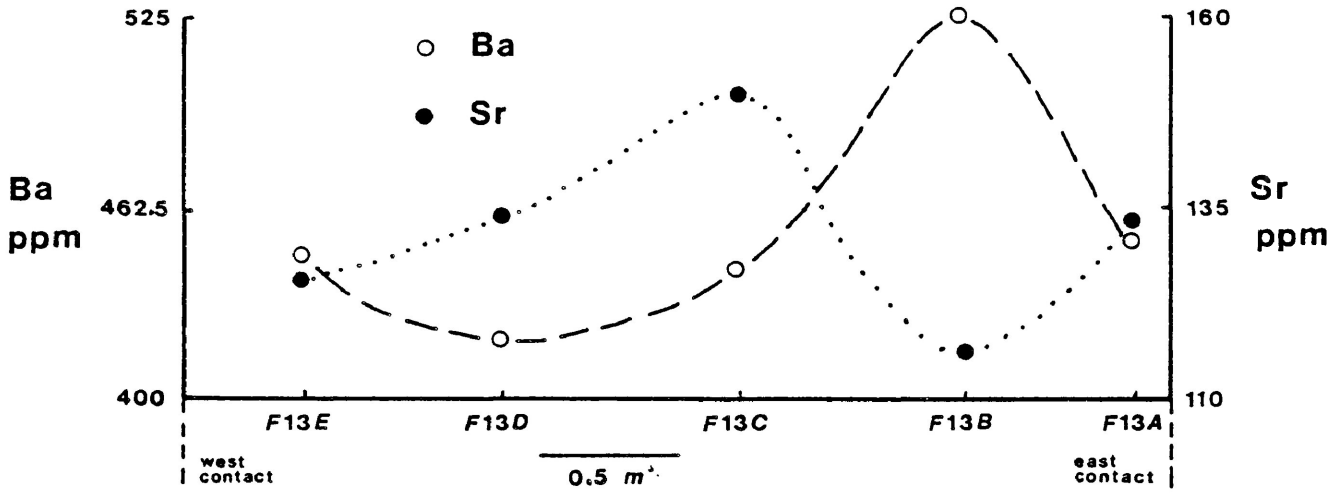

Fig. 3-37. Distribution of Ba and Sr in perthitic microcline across the Brink pegmatite.

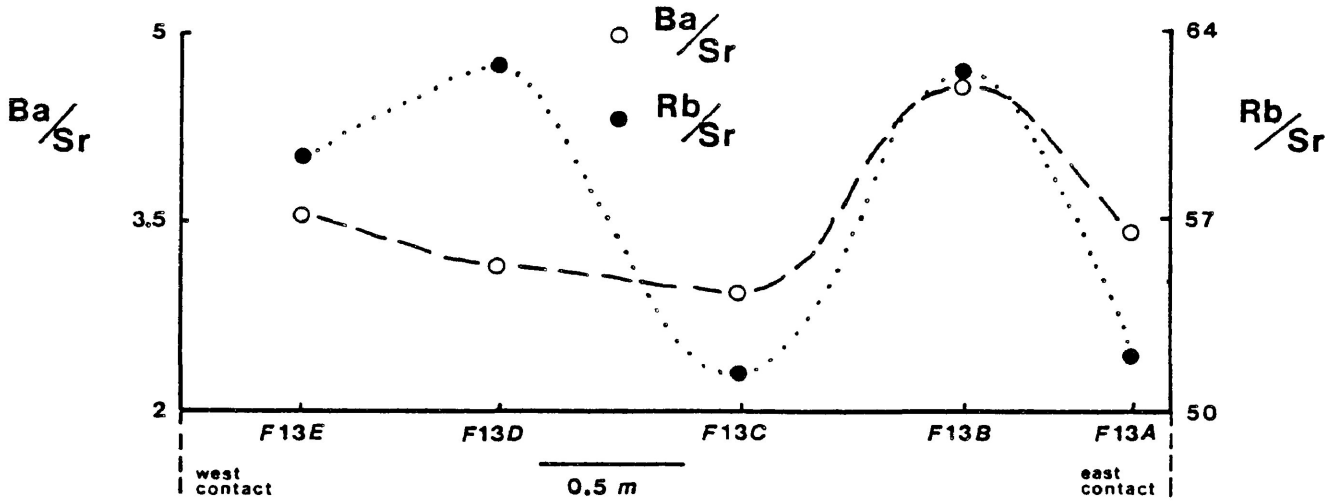

Fig. 3-38. Distribution of Ba/Sr and Rb/Sr in perthitic microcline across the Brink pegmatite.

The distribution of Sr and Ba, in perthitic microcline, is somewhat more erratic (Fig. 3-37) than Rb and Cs although minimal Ba corresponds to maximal Rb and Cs in sample F13D. The distribution of the Ba/Sr ratio (Fig. 3-38) roughly parallels that of Ba. The Rb/Sr ratio (Fig. 3-38) is at a minimum in perthitic microcline from the centre of the pegmatite and near the contacts. There is no pronounced correlation between Sr and Ba as observed for Rb and Cs.

Muscovite - Geochemical analyses of muscovite samples from rare-element pegmatites of the Georgia Lake area are presented (Tables 3-13 to 3-16). Trends in geochemistry are summarized in selected variation diagrams (Figs. 3-39 to 3-62). The data for muscovite is intended to complement data for perthitic microcline to observe elemental partitioning between the two mineral species and confirm regional fractionation trends. Four samples of book muscovite from the MNW pegmatite, identified with triangles on all variation diagrams, illustrate geochemical variations within the MNW pegmatite in relation to regional elemental distributions. Samples from the Central and Northern Group pegmatites are identified with circles and squares, respectively, on all variation diagrams. In addition, samples from the Brink and Island occurrences are noted with initials B and I, respectively, on all plots and microcrystalline secondary muscovites from the Brink and MNW pegmatites are identified by the initial S.

Table 3-13: Sample locations of analyzed muscovite specimens.

Group	Pegmatite	Sample Number	Sample Description
Southern (▲)	MNW - wall zone - west	M74	book muscovite
	MNW-intermediate zone-west	M63	book muscovite
	MNW-intermediate zone-east	M79	book muscovite
	MNW - wall zone - east	M80	book muscovite
	MNW-core zone (s)	M73	microcrystalline
Central (●)	Brink (S)	M10	microcrystalline
	Brink (B)	M12	book muscovite (green)
	Southwest	M95	book muscovite (green)
	Salo	M87	book muscovite
	Niemi	M103	book muscovite
	Point	M116	book muscovite
	Island (I)	M117	book muscovite
Northern (■)	Nama Creek North	M49	fine-grained
	Nama Creek South	M50	fine-grained
	McVittie	M29	fine-grained
	Powerline	M6	fine-grained
	Camp	M32	fine-grained
	Giles	M131	fine-grained

Table 3-14: Chemical analysis of muscovite from the MNW pegmatite

Sample	M74	M63	M79	M80	M73
wt %					
SiO_2	45.68	46.50	43.42	45.45	44.97
TiO_2	0.26	0.25	--	0.25	--
Al_2O_3	33.56	33.78	34.91	33.26	36.14
FeO*	2.54	2.21	1.80	2.32	0.70
MgO	0.96	1.06	0.42	0.79	0.36
Na_2O	0.79	0.79	0.64	0.82	0.46
K_2O	10.22	9.83	9.91	9.76	10.59
H_2O	5.31	5.76	6.93	5.13	4.41
Total	99.32	100.18	98.03	97.78	97.63
Cations 0=24					
Si	6.103	6.106	5.765	6.151	6.103
Ti	0.026	0.024	—	0.025	—
Al	5.284	5.228	5.465	5.306	5.780
Fe^{+2}	0.284	0.243	0.200	0.263	0.079
Mg	0.191	0.208	0.083	0.159	0.073
Na	0.204	0.200	0.164	0.215	0.121
K	1.742	1.647	1.679	1.685	1.833
H	4.733	5.045	6.139	4.632	3.992
cation sum	18.567	18.701	19.494	18.436	17.981
ppm					
Li	1399	1561	1060	1764	1570
Rb	2440	2557	3602	2578	4753
Cs	176	227	378	432	2053
Sr	48	52	61	49	70
Ba	508	457	387	453	398
Sc	12	11	1	10	2
Zr	23	20	14	17	11
Nb	213	213	177	229	46
Ta	56	65	61	77	141
Co	3	2	nd	nd	≤0.5
Sn	390	570	618	427	300
ratios					
K/Rb	34.75	31.91	22.85	31.42	18.49
K/Cs	481.8	359.5	217.7	187.5	42.82
K/Ba	166.9	178.6	212.7	178.8	220.9
K/Sr	1767	1569	1349	1653	1256
Rb/Sr	50.83	49.17	59.05	52.61	67.90
Rb/Ba	4.80	5.60	9.31	5.69	11.94
Mg/Li	4.15	4.10	2.36	2.72	1.40
Ba/Sr	10.58	8.79	6.34	9.24	5.69
Ta/Nb	0.26	0.31	0.34	0.34	3.07

* : all iron as FeO
nd : not determined
-- : not detected by EMP

Table 3-15: Chemical analysis of muscovite from the Central Group pegmatites

Sample	M10	M12	M95	M87	M103	M116	M117
wt %							
SiO_2	45.37	45.26	47.31	46.52	44.11	45.61	46.30
TiO_2	--	--	--	--	--	--	--
Al_2O_3	36.46	35.72	37.87	37.04	35.31	34.84	34.66
FeO*	0.63	0.63	0.17	0.54	1.96	1.84	2.12
MgO	0.44	0.37	0.36	--	0.57	0.46	1.10
Na_2O	0.74	0.73	0.65	0.77	0.74	0.79	0.71
K_2O	10.31	9.82	9.45	9.59	10.21	9.86	10.45
H_2O	4.41	5.22	4.77	4.68	4.86	6.03	5.13
Total	98.36	97.75	100.58	99.14	97.76	99.23	100.47
Cations 0=24							
Si	6.104	6.064	6.144	6.153	5.996	5.995	6.114
Ti	—	—	—	—	—	—	—
Al	5.782	5.640	5.796	5.775	5.657	5.421	5.394
Fe^{+2}	0.071	0.071	0.019	0.060	0.223	0.203	0.234
Mg	0.088	0.074	0.069	—	0.115	0.090	0.217
Na	0.192	0.190	0.164	0.191	0.194	0.201	0.182
K	1.770	1.679	1.565	1.621	1.771	1.661	1.760
H	3.958	4.666	4.132	4.130	4.407	5.310	4.519
cation sum	17.965	18.384	17.889	17.930	18.363	18.881	18.420
ppm							
Li	261	291	238	273	618	758	1326
Rb	7864	8034	7871	4794	2808	2376	1888
Cs	1181	925	479	263	104	99	49
Sr	99	99	94	75	51	56	53
Ba	422	391	401	384	447	442	600
Sc	$\leq$0.1	$\leq$0.1	$\leq$0.1	$\leq$0.1	3	2	11
Zr	$\leq$7	$\leq$7	$\leq$7	10	17	19	21
Nb	59	114	92	155	145	151	184
Ta	103	61	77	44	54	63	46
Co	$\leq$0.5	$\leq$0.5	$\leq$0.5	nd	nd	3	2
Sn	405	480	280	nd	nd	nd	324
ratios							
K/Rb	10.89	10.14	9.96	16.60	30.20	34.47	45.97
K/Cs	72.48	88.11	163.7	302.7	815.4	827.3	1771.0
K/Ba	202.8	208.4	195.5	207.3	189.7	185.3	144.7
K/Sr	864.7	823.2	834.0	1061.0	1663.0	1463.0	1638.0
Rb/Sr	79.43	81.15	83.73	63.92	55.06	42.43	35.62
Rb/Ba	18.64	20.55	19.63	12.48	6.28	5.38	3.15
Mg/Li	10.34	7.56	9.24	—	5.50	3.69	4.98
Ba/Sr	4.26	3.95	4.27	5.12	8.76	7.89	11.32
Ta/Nb	1.75	0.54	0.84	0.28	0.37	0.42	0.25

* : all iron as FeO
nd: not determined
--: not detected by EMP

Table 3-16: Chemical analysis of muscovite from the Northern Group pegmatites

Sample	M49	M50	M29	M6	M32	M131
wt %						
SiO_2	44.55	46.25	47.87	46.03	46.98	45.78
TiO_2	--	--	--	--	--	--
Al_2O_3	34.81	34.59	36.01	33.91	35.81	34.84
FeO*	1.26	2.79	1.31	3.09	1.20	2.77
MgO	0.35	--	--	0.33	0.36	0.45
Na_2O	0.83	0.78	0.65	nd	1.15	0.86
K_2O	10.29	10.43	9.53	10.15	9.65	10.40
H_2O	5.04	4.86	4.86	nd	4.68	4.77
Total	97.13	99.70	100.23	93.51	99.83	99.65
Cations 0=24						
Si	6.062	6.180	6.264	—	6.206	6.120
Ti	—	—	—	—	—	—
Al	5.582	5.447	5.554	—	5.575	5.490
Fe^{+2}	0.143	0.312	0.143	—	0.133	0.310
Mg	0.071	—	—	—	0.071	0.090
Na	0.219	0.202	0.165	—	0.295	0.223
K	1.785	1.778	1.591	—	1.625	1.774
H	4.575	4.333	4.242	—	4.124	4.254
cation sum	18.437	18.252	17.959	—	18.029	18.261
ppm						
Li	459	683	1034	nd	244	553
Rb	2929	5273	3479	nd	2920	3110
Cs	189	247	288	nd	189	135
Sr	61	60	62	97	72	60
Ba	395	398	494	415	434	516
Sc	0.8	≤0.1	1	nd	0.8	0.6
Zr	20	17	22	18	23	35
Nb	98	144	95	88	94	180
Ta	89	83	108	nd	90	50
Co	1	nd	2	nd	2	0.7
Sn	nd	nd	nd	nd	nd	nd
ratios						
K/Rb	29.16	16.42	22.74	—	27.43	27.75
K/Cs	451.9	350.6	274.7	—	423.8	639.3
K/Ba	216.2	217.6	160.1	203.1	184.6	167.3
K/Sr	1400	1443	1276	869.1	1113	1438
Rb/Sr	48.02	87.88	56.11	—	40.56	51.83
Rb/Ba	7.42	13.25	7.04	—	6.73	6.03
Mg/Li	4.58	—	—	—	9.02	2.53
Ba/Sr	6.48	6.63	7.97	4.28	6.03	8.60
Ta/Nb	0.91	0.58	1.14	—	0.96	0.28

* : all iron as FeO
nd: not determined
--: not detected by EMP

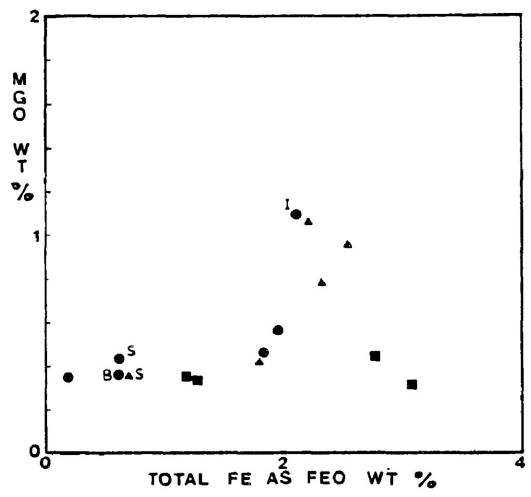

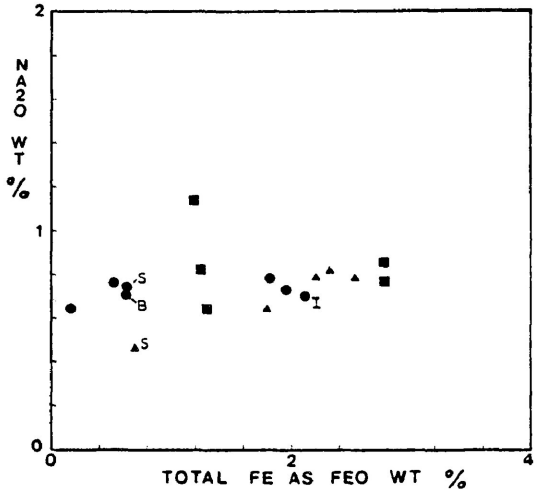

Fig. 3-39 (left). MgO versus Total iron as FeO for muscovite.

Fig. 3-40 (right). Na_2O versus Total iron as FeO for muscovite.

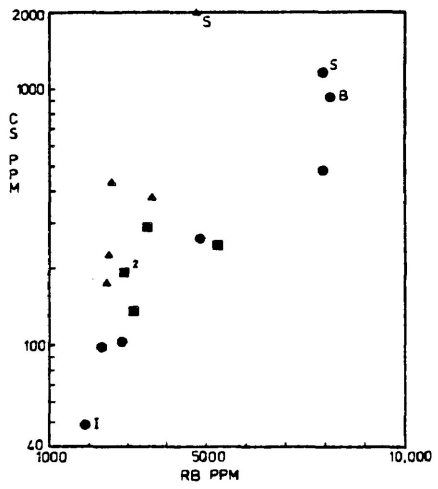

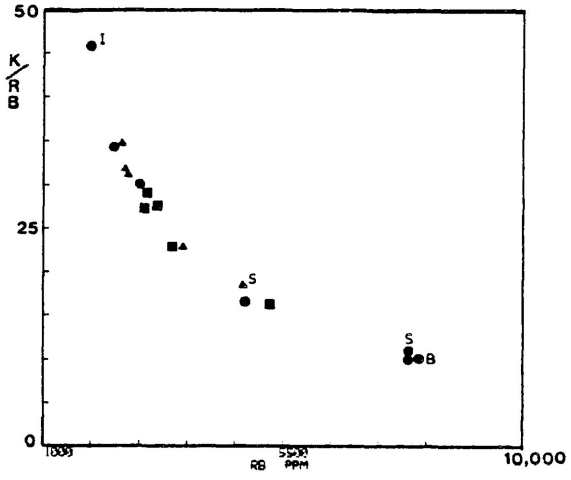

Fig. 3-41 (left). Cs versus Rb for muscovite.

Fig. 3-42 (right). K/Rb versus Rb for muscovite.

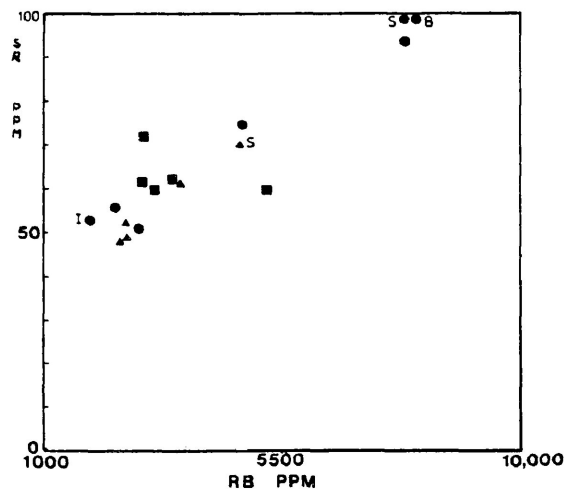

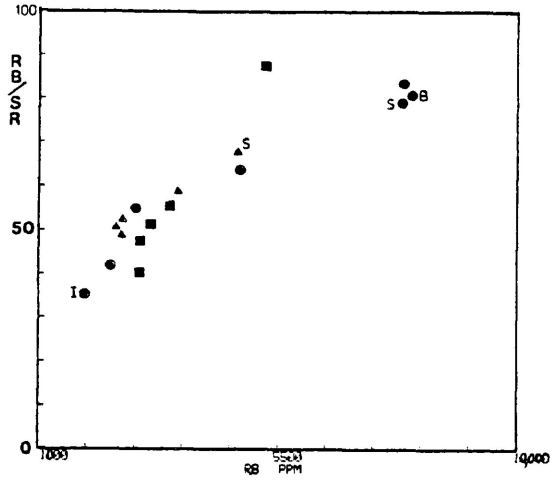

Fig. 3-43 (left). Sr versus Rb for muscovite.

Fig. 3-44 (right). Rb/Sr versus Rb for muscovite.

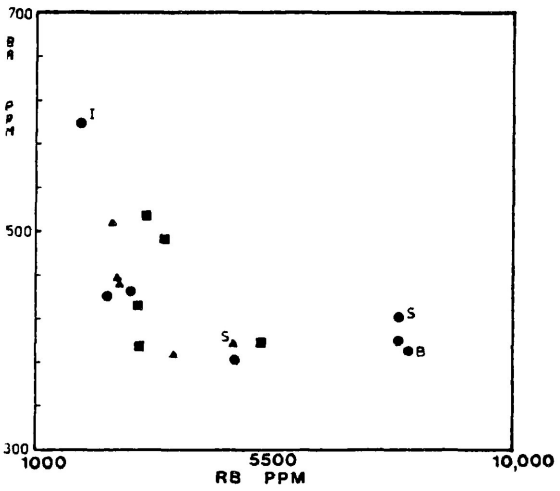

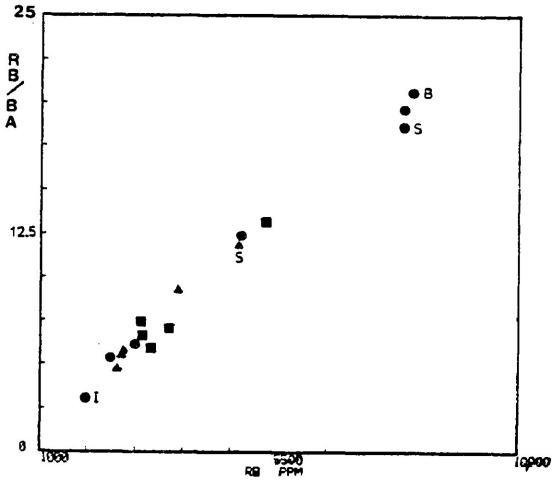

Fig. 3-45 (left). Ba versus Rb for muscovite.

Fig. 3-46 (right). Rb/Ba versus Rb for muscovite.

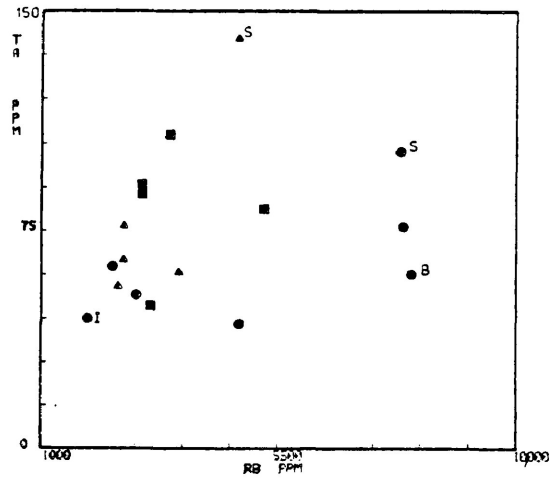

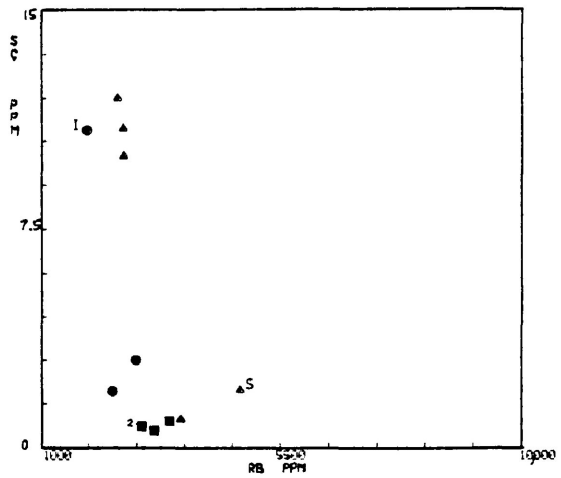

Fig. 3-47 (left). Ta versus Rb for muscovite.

Fig. 3-48 (right). Sc versus Rb for muscovite.

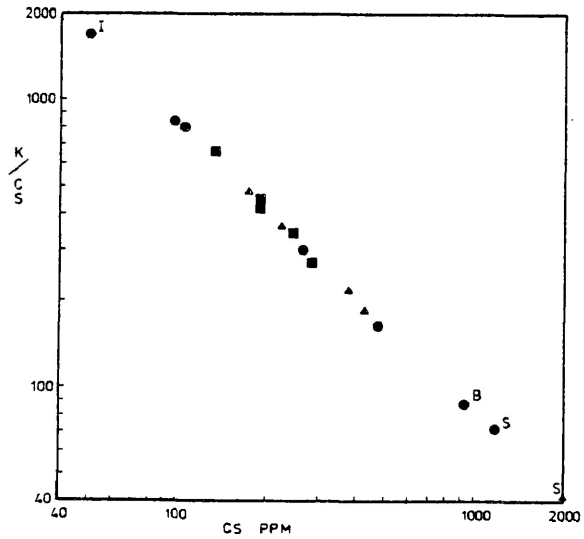

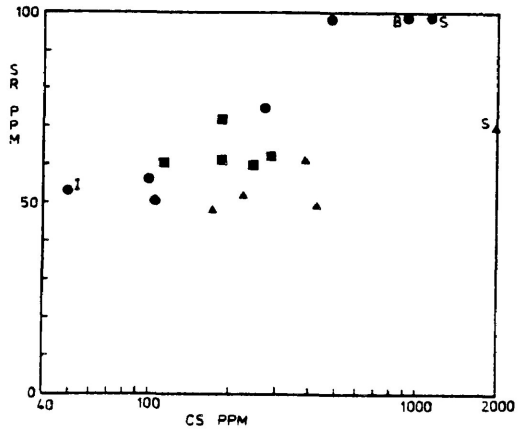

Fig. 3-49 (left). K/Cs versus Cs for muscovite.

Fig. 3-50 (right). Sr versus Cs for muscovite.

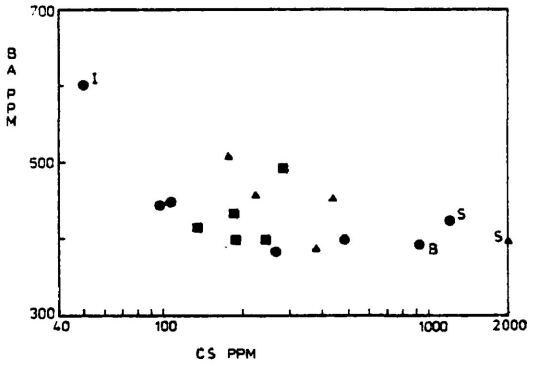

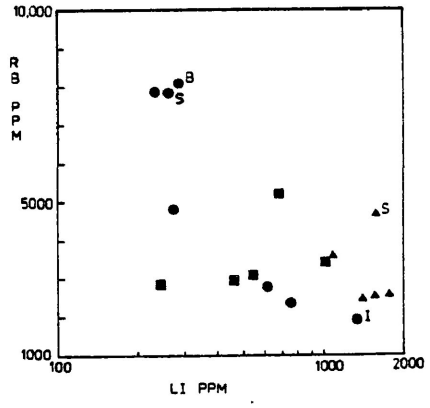

Fig. 3-51 (left). Ba versus Cs for muscovite.

Fig. 3-52 (right). Rb versus Li for muscovite.

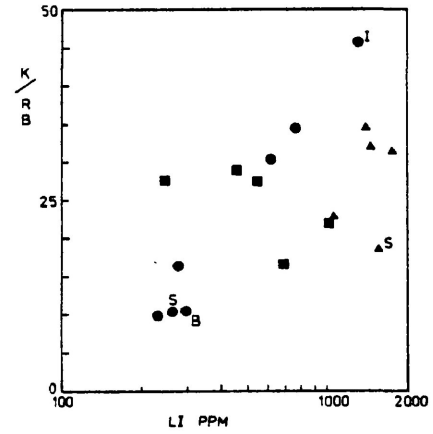

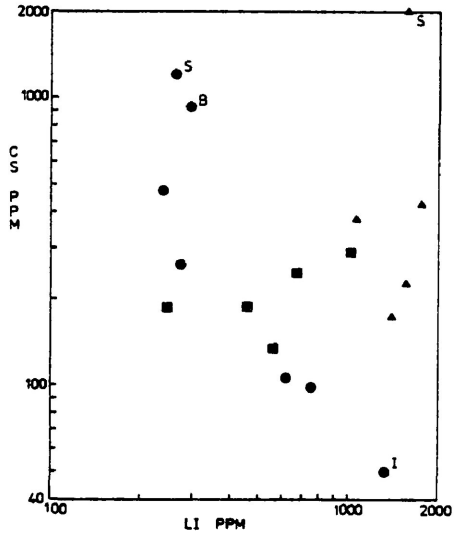

Fig. 3-53 (left). K/Rb versus Li for muscovite.

Fig. 3-54 (right). Cs versus Li for muscovite.

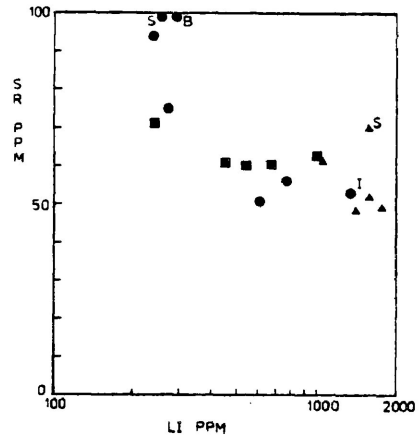

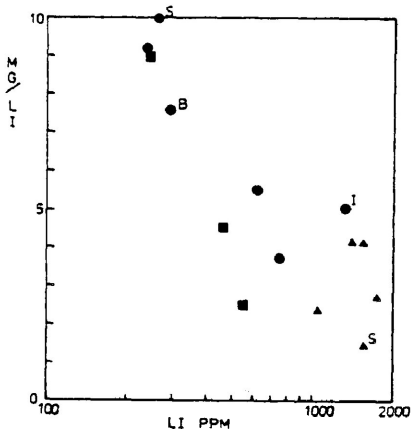

Fig. 3-55 (left). Sr versus Li for muscovite.

Fig. 3-56 (right). Mg/Li versus Li for muscovite.

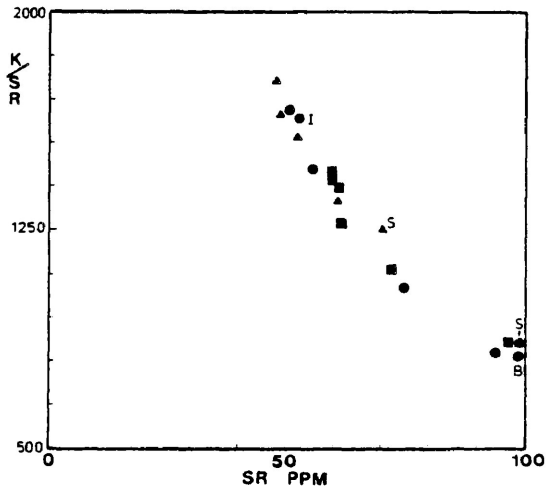

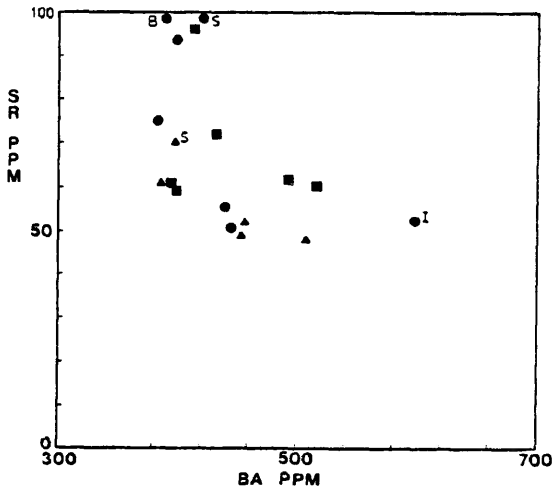

Fig. 3-57 (left). K/Sr versus Sr for muscovite.

Fig. 3-58 (right). Sr versus Ba for muscovite.

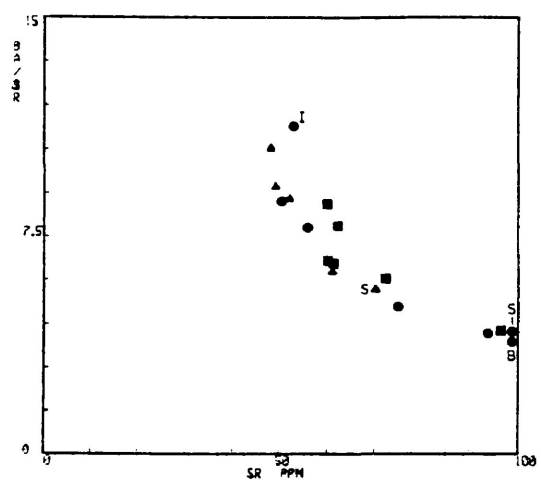

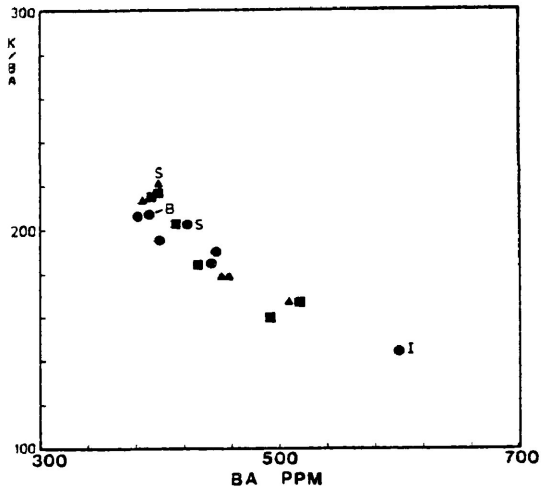

Fig. 3-59 (left). Ba/Sr versus Sr for muscovite.

Fig. 3-60 (right). K/Ba versus Ba for muscovite.

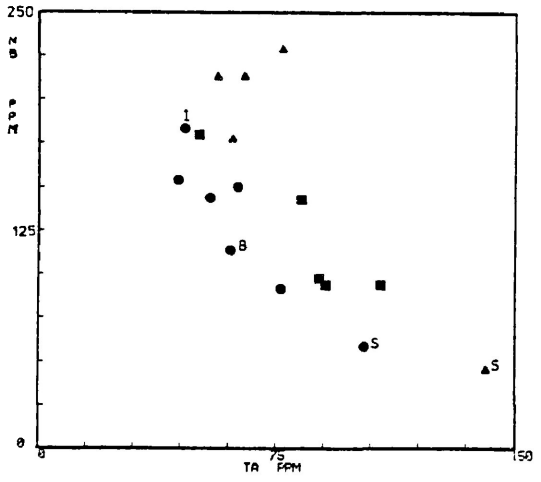

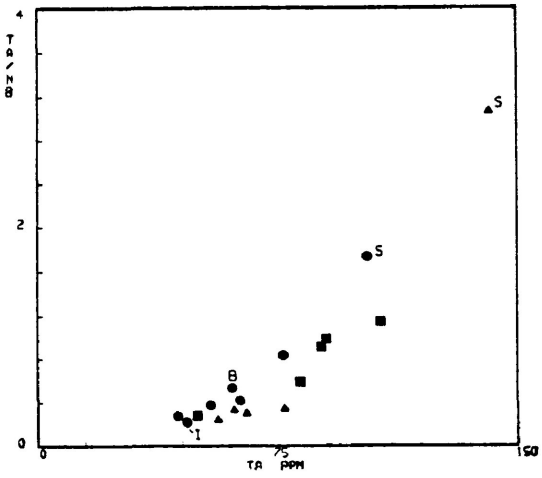

Fig. 3-61 (left). Nb versus Ta for muscovite.

Fig. 3-62 (right). Ta/Nb versus Ta for muscovite.

A comparison of major element data for muscovite shows very low variability. On the other hand, minor and trace element data is variable within and among pegmatite groups. Eight major element oxides and eleven trace elements were analyzed in pegmatitic muscovite. In addition to data presented, it is assumed that a small percentage of F is present in the muscovite structure accounting for slightly depressed oxide averages in several samples.

Among the oxides, only FeO and MgO display a crude positive correlation (Fig. 3-39). This is most pronounced in the Central Group pegmatites, where FeO and MgO decrease in a westward direction across the pegmatite group. TiO_2 was detected only in book muscovite from the MNW pegmatite. Na_2O is, in general, constant in muscovite (Fig. 3-40). The exceptions to this rule include microcrystalline muscovite from the core of the MNW pegmatite (sample F73), where Na_2O is low, and fine-grained muscovite from the muscovite-enriched contact zone of the Camp pegmatite (sample F32), where Na_2O is high.

Much of the minor and trace element data for muscovite is directly correlatable with geochemical distributions in perthitic microcline. Among the pegmatite groups, the greatest variation in Rb and Cs (Figs. 3-41, 3-42 and 3-49) is observable in the Central Group. Wt % Rb in muscovite varies from 0.2 to 0.8 in an east to west direction across

Central Group pegmatites. Similarly, Cs varies from 0.005 to 0.09 wt % along the same trend. Cs concentration is greatest in microcrystalline muscovite and is especially enriched in sample F73 from the core of the MNW pegmatite, in which Cs concentration is 0.2 wt %. It is notable that greenish varieties of muscovite are enriched in Cs (0.05 wt % or greater) relative to other varieties of muscovite.

Sr in muscovite shows a strong positive correlation with respect to Rb (Figs. 3-43, 3-44) and a positive correlation with respect to Cs (Fig. 3-50). K/Sr decreases linearly in an east to west direction across the Central Group pegmatites (Fig. 3-57). A similar, less pronounced decrease of K/Sr against Sr is observed for Northern Group pegmatites except with the absence of a distinct east to west trend.

Concentration of Ba in muscovite is in the range of co-existing perthitic microcline and does not show the large variation in concentration as with Rb and Cs. A crude negative correlation of Ba against Rb, Cs and Sr is notable in Figs. 3-45, 3-51 and 3-58, respectively. The low variation of Ba concentration in muscovite is exemplified by a strong positive correlation of Rb/Ba against Rb (Fig. 3-46).

Concentration of Li in sampled muscovites varies from 0.02 to 0.18 wt %. In relation to Central and Northern

Group pegmatites, muscovite from the MNW pegmatite shows greatest enrichment in Li. A decrease of Li in muscovite occurs in the Central Group pegmatites in a general east to west direction. The decrease is not as pronounced as a corresponding increase in Rb, Cs and Sr resulting in a crude negative correlation with respect to Rb (Fig. 3-52), Cs (Fig. 3-54) and Sr (Fig. 3-55). Similarly, a decrease in the Mg/Li ratio is observed with increasing Li (Fig. 3-56). A positive linear correlation of Li against K/Rb (Fig. 3-53) occurs over Central Group pegmatites only. This relation is random in the MNW pegmatite and Northern Group pegmatites. It is notable that among the microcrystalline muscovites, Li concentration is highly variable but is in the range of book muscovite from the same pegmatite.

Sc occurs in muscovite in concentrations greater than 1 ppm only in the MNW pegmatite and easternmost pegmatites of the Central Group (Fig. 3-48). Sc does not show any apparent trend among Northern Group pegmatites.

As in perthitic microcline, Zr appears to be slightly enriched in muscovite samples from Northern Group pegmatites in the range 17 to 35 ppm and most deficient in westernmost pegmatites of the Central Group.

Concentration of Co in muscovite is at or near the

determined detectability limit of Co of 0.5 ppm.

Both Ta and Nb concentrations in muscovite are in the range 44 to 229 ppm. Among the elements determined, Ta and Nb are correlatable only with each other. A decrease of Nb in muscovite corresponds directly to an increase in Ta concentration (Fig. 3-61). No apparent distribution of Ta with respect to other elements is noted; for example, Ta against Rb (Fig. 3-47). The microcrystalline muscovites of the MNW and Brink pegmatites are noticeably enriched in Ta with respect to Nb in relation to other analyzed muscovite samples as illustrated by the Ta/Nb ratio (Fig. 3-62).

Sn in muscovite was determined in only 9 of 18 samples. No data is available for Sn in muscovite from Northern Group pegmatites. Sn in muscovite from the MNW and Central Group pemgatites is in the range 280 to 618 ppm. Greatest concentration of Sn in muscovite (> 500 ppm) occurs in the intermediate zone of the MNW pegmatite. In the Central Group pegmatites, Sn does not show any apparent trend.

Cross-section Of MNW Pegmatite - Four samples of book muscovite (Tables 3-13, 3-14) were obtained from the MNW pegmatite (Fig. 3-3) in order to observe the geochemistry of muscovite across the zones of this pegmatite. Plots for selected elements and corresponding ratios are obtained

along a cross-section across the surface of the MNW pegmatite (Figs. 3-63 to 3-70). Geochemistry of microcrystalline muscovite (sample M73) from the core zone is omitted in the cross-sections. Book muscovite, similar to that of the wall and intermediate zones, is not present in the core zone.

Elemental distributions in muscovite across wall and intermediate zones show considerable variability. Greater variations in concentration of most elements are noted for the east side of the pegmatite. In addition, elemental distributions are not correlatable on either side of the core zone, in all cases. FeO and MgO are enriched in the west relative to the east side of the pegmatite (Fig. 3-63), although FeO and MgO from the wall zone of the east side of the pegmatite approach similar concentrations noted for the west side of the pegmatite. Na_2O and Li are nearly parallel in relative elemental distribution across the pegmatite (Fig. 3-64). Rb and Cs, noted to be positively correlatable on a regional scale, do not show a similar distribution in muscovite across the MNW pegmatite (Figs. 3-65, 3-66). Rb increases toward the centre of the pegmatite, although at a greater rate along the east side of the pegmatite. Cs concentration in muscovite increases linearly across the pegmatite from the west to east. On the east side of the core zone, Sr distribution does not correlate with Ba although on the west side of the pegmatite,

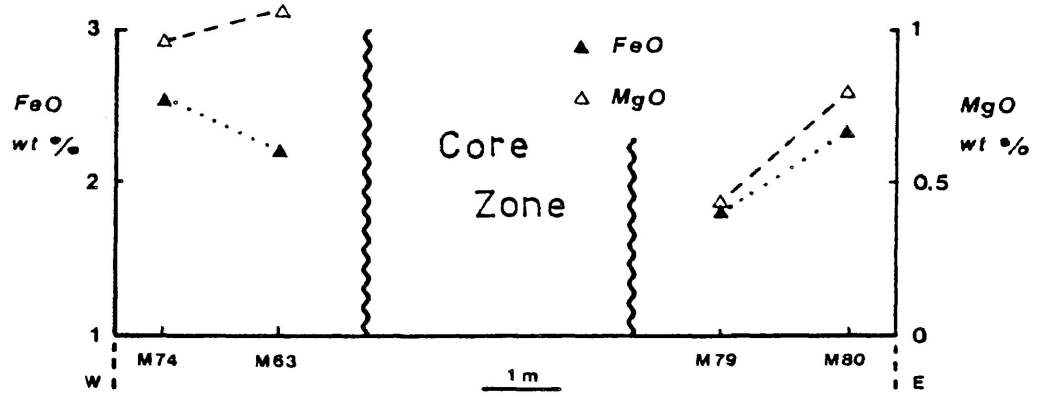

Fig. 3-63. Distribution of total iron as FeO and MgO in muscovite across the MNW pegmatite.

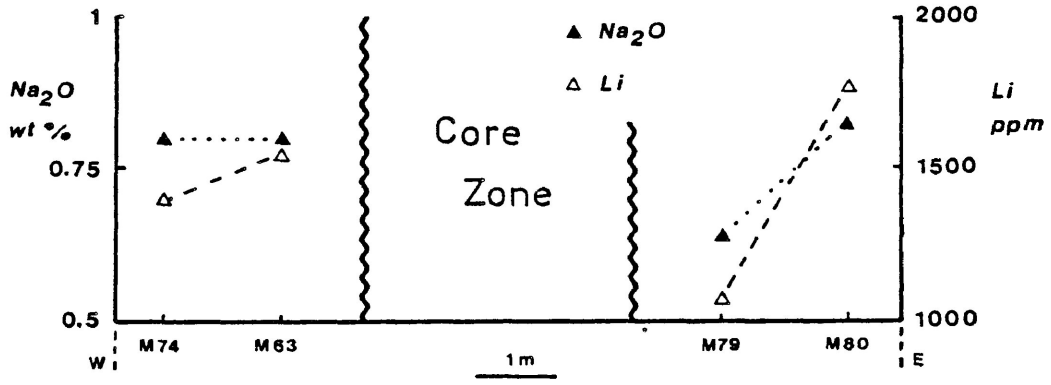

Fig. 3-64. Distribution of Na_2O and Li in muscovite across the MNW pegmatite.

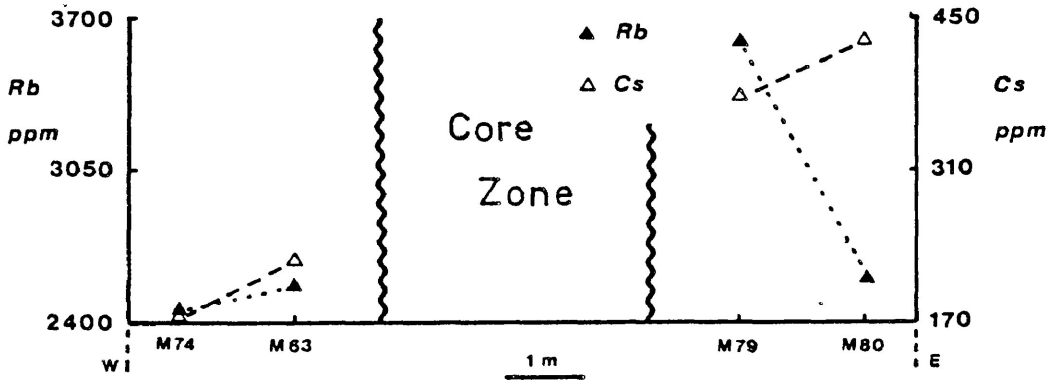

Fig. 3-65. Distribution of Rb and Cs in muscovite across the MNW pegmatite.

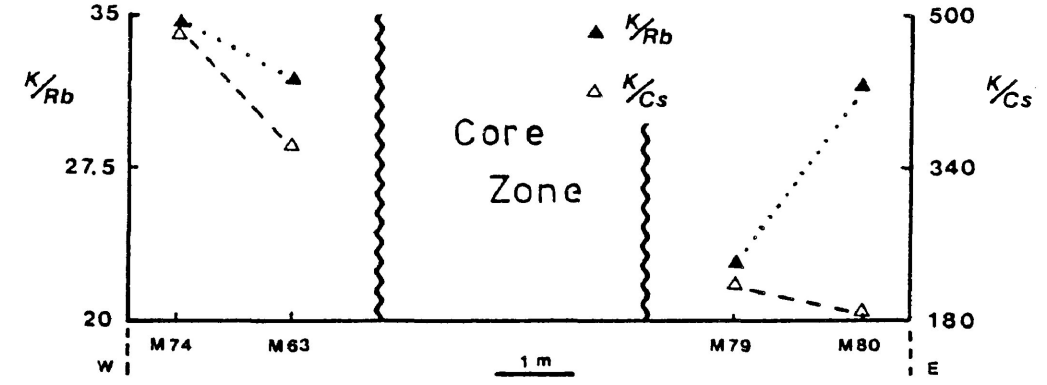

Fig. 3-66. Distribution of K/Rb and K/Cs in muscovite across the MNW pegmatite.

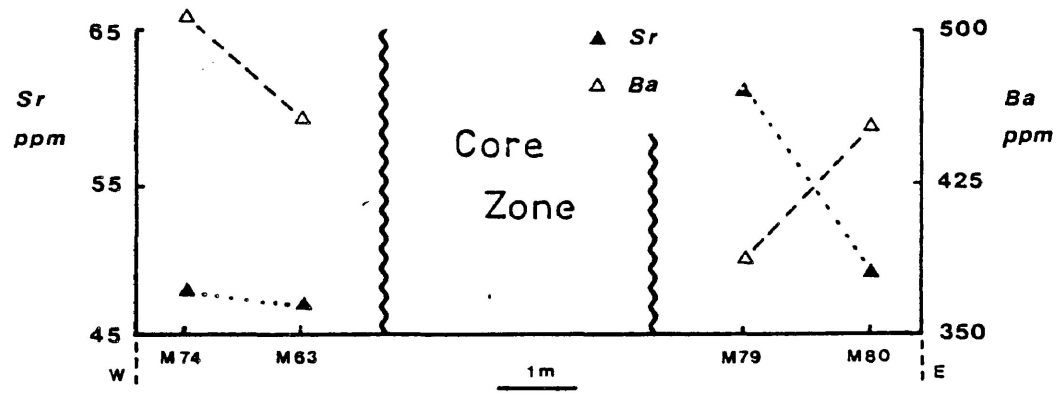

Fig. 3-67. Distribution of Sr and Ba in muscovite across the MNW pegmatite.

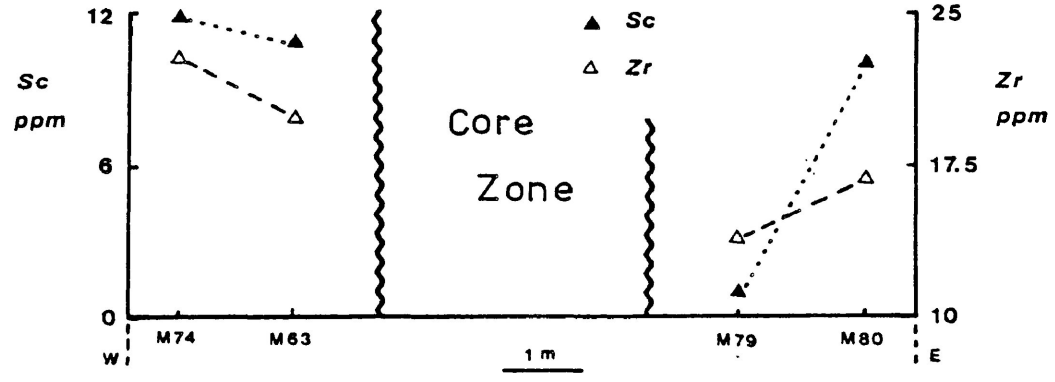

Fig. 3-68. Distribution of Sc and Zr in muscovite across the MNW pegmatite.

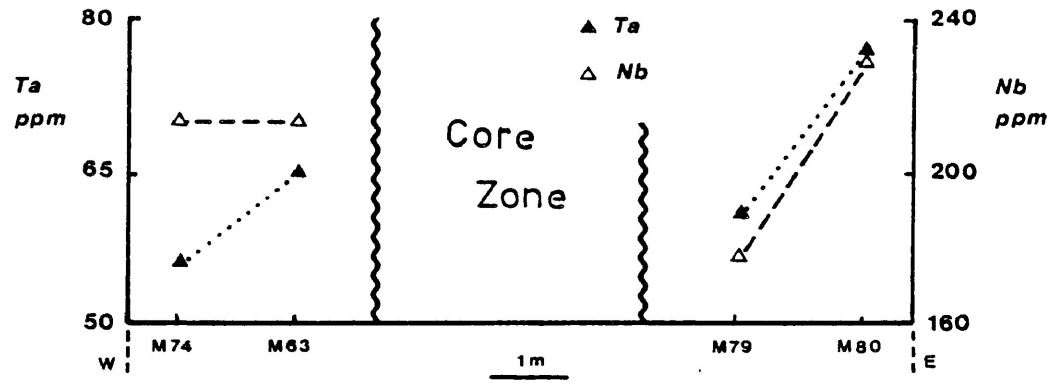

Fig. 3-69. Distribution of Ta and Nb in muscovite across the MNW pegmatite.

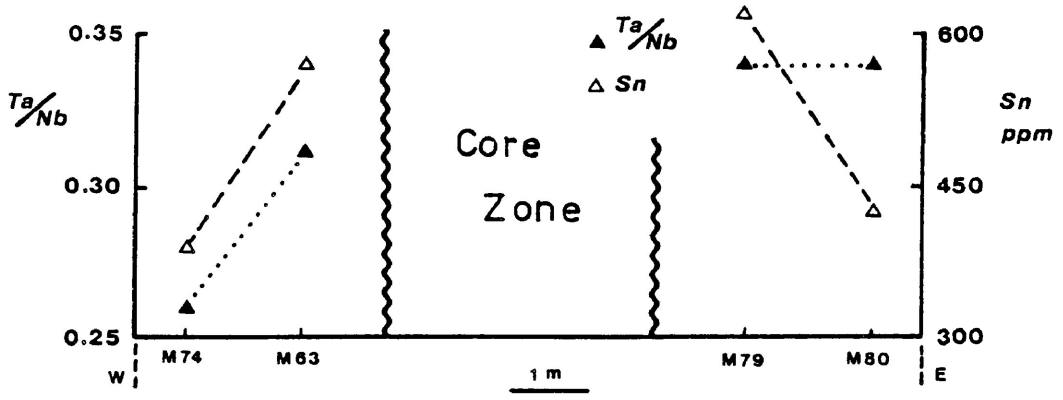

Fig. 3-70. Distribution of Ta/Nb and Sn in muscovite across the MNW pegmatite.

Sr and Ba both decrease toward the core (Fig. 3-67). Sc and Zr, although present in very low concentrations, decrease toward the core of the pegmatite (Fig. 3-68). Distribution of Ta east of the core zone parallels that of Nb (Figs. 3-69, 3-70) with a decrease in concentration toward the core zone. On the west side of the core zone, Ta decreases toward the contact of the pegmatite while the Nb concentration remains constant. In relation to the other elements, Sn shows the most uniform distribution in zones on either side of the pegmatite core with an apparent increase in muscovite toward the core of the pegmatite (Fig. 3-70).

Tantalite-Columbite Minerals - Tantalite-columbite minerals were analyzed from three rare-element pegmatites (Tables 3-17, 3-18). Sample T1, as noted previously, originates from the groundmass of the Brink pegmatite and is intergrown with quartz and green muscovite. Samples T2, T3, T4 and T5 are from the MNW pegmatite. Sample T6 consists of three grains from the Southwest deposit. Figs. 3-71 and 3-72 demonstrate differences in geochemistry of tantalite-columbite minerals in the Georgia Lake rare-element pegmatites.

Interstitial tantalite (sample T1) from the Brink pegmatite was found to contain several intergrown phase of tantalite and rare columbite. Compositions range from

Table 3-17: Electron microprobe traverse across sample Tl, tantalite from the Brink pegmatite

Probe Location	Tl-1(L)	Tl-2(L)	Tl-3(L)	Tl-4(L)	Tl-5(L)	Tl-6(L)	Tl-7(L)	Tl-8
Ta_2O_5 (wt %)	53.85	60.62	61.35	64.18	64.33	56.18	73.90	43.93
Nb_2O_5	29.55	23.37	22.12	19.07	19.26	27.09	10.63	38.98
TiO_2	---	0.40	0.26	0.43	---	0.42	---	0.31
SnO_2	0.39	0.36	0.52	0.26	---	0.68	---	0.13
FeO*	3.81	8.82	7.00	6.73	6.67	7.90	4.99	3.50
MnO	12.86	6.68	8.41	8.50	8.66	8.35	9.78	13.93
Sc_2O_3	0.05	---	---	---	---	---	---	0.12
Total	**100.53**	**100.25**	**99.65**	**99.17**	**98.93**	**100.61**	**99.31**	**100.91**

Probe Location	Tl-1(D)	Tl-2(D)	Tl-3(D)	Tl-4(D)	Tl-5(D)	Tl-6(D)	Tl-6-1(D)	Tl-7(D)
Ta_2O_5 (wt %)	44.62	49.20	43.05	40.28	42.68	60.43	33.62	51.68
Nb_2O_5	38.72	34.30	39.96	43.12	39.78	22.47	47.58	31.58
TiO_2	0.19	0.42	---	---	0.10	0.36	0.54	---
SnO_2	---	---	---	---	0.20	0.44	---	---
FeO*	3.62	11.53	3.70	4.13	12.05	7.07	12.12	3.36
MnO	13.48	4.91	13.55	13.30	4.95	8.77	6.00	13.21
Sc_2O_3	---	---	---	---	---	---	---	---
Total	**100.64**	**100.35**	**100.27**	**100.82**	**97.75**	**99.55**	**99.86**	**99.83**

Tl-1 to Tl-5: Grain 1
Tl-6 to Tl-8: Grain 2
(L) : light backscattered image
(D) : dark backscattered image
* : all iron as FeO

Table 3-18: Electron microprobe analysis of tantalite-columbite minerals from the MNW and Southwest deposits.

Sample	T2	T3A	T3B	T4-1	T4-2	T4-3	T4-4
Ta_2O_5(wt%)	59.59	46.84	46.70	20.24	20.39	20.21	19.63
Nb_2O_5	22.87	30.43	31.65	59.88	59.39	59.12	59.60
TiO_2	0.50	3.54	3.01	0.82	1.02	1.15	1.23
SnO_2	1.69	3.48	1.79	0.37	0.53	---	0.39
FeO*	4.60	13.90	12.42	14.48	14.45	14.25	14.13
MnO	10.60	2.06	3.43	5.09	5.09	4.93	4.95
Sc_2O_3	---	---	---	---	---	---	---
Total	99.86	100.24	99.01	100.90	100.88	99.65	99.93

Sample	T5-1	T5-2	T5-3	T6A	T6B	T6C
Ta_2O_5(wt%)	20.15	19.66	20.50	25.40	23.88	22.81
Nb_2O_5	58.87	59.44	59.63	55.82	57.21	57.50
TiO_2	1.53	1.48	1.09	0.38	0.28	---
SnO_2	0.49	0.44	0.58	---	0.53	---
FeO*	14.24	14.43	14.19	9.74	10.30	8.83
MnO	4.96	4.57	4.54	8.81	9.09	9.72
Sc_2O_3	---	---	---	---	---	0.11
Total	100.25	100.03	100.52	100.14	101.29	98.96

T2: core zone, MNW pegmatite
T3A,B: intermediate zone, MNW pegmatite, inclusions in Sn oxide minerals
T4-1 to T4-2: EMP traverse across sample T4; intermediate zone, MNW pegmatite
T5-1 to T5-3: EMP traverse across sample T5; intermediate zone, MNW pegmatite
T6A,B,C: Southwest pegmatite
*: all iron as FeO

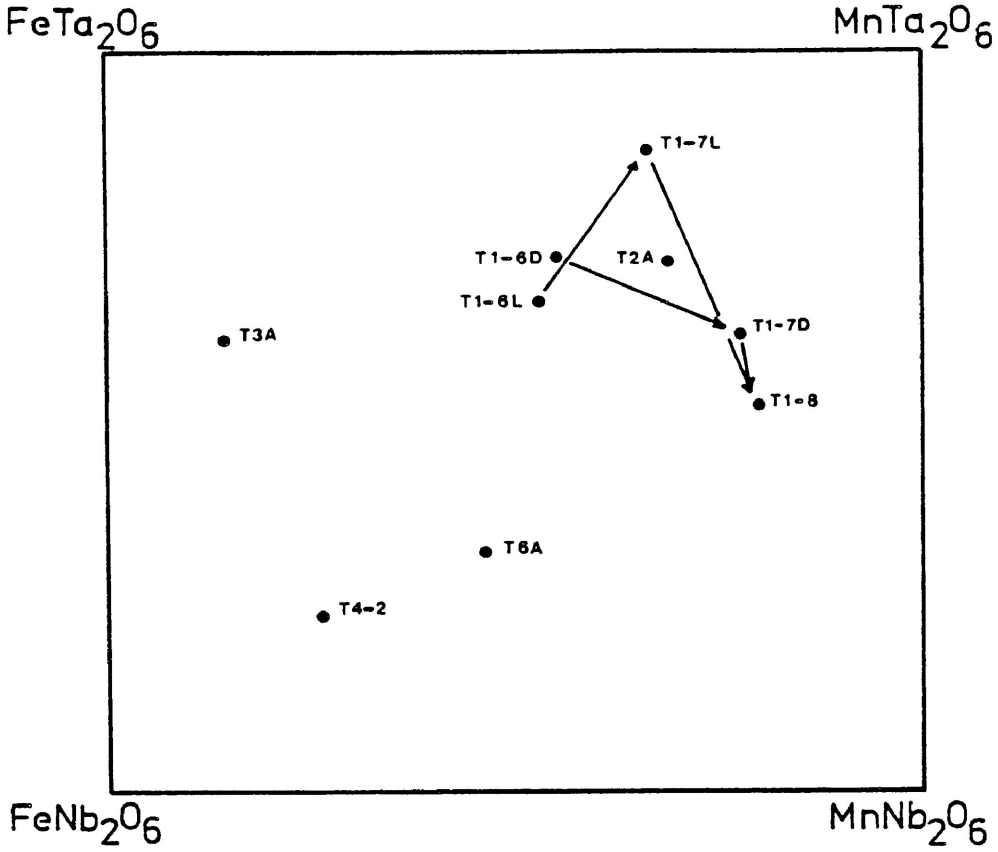

Fig. 3-71. Composition tetrahedron for tantalite-columbite minerals. Arrows indicate an electron microprobe traverse across a single inhomogeneous tantalite grain of sample T1 from the Brink pegmatite (from Černý, 1975).

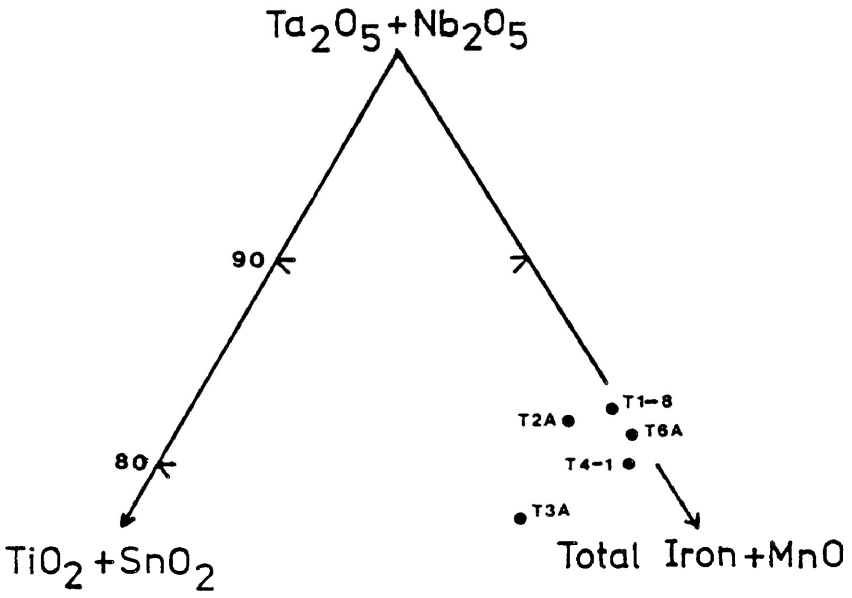

Fig. 3-72. Tantalite-columbite minerals plotted in the $(Ta_2O_5+Nb_2O_5)$-(Total iron+MnO)-(TiO_2+SnO_2) triangle (from Černý, 1975).

mangano- to ferrotantalite with subordinate inclusions of ferrocolumbite. The dominant phase is manganotantalite. Sample T1 consists of two grains (Figs. 3-73, 3-74) occurring in close proximity from within the same hand sample. Backscattered electron imaging reveals Grains 1 and 2 to consist of a fine to coarse intergrowth of tantalite phases. The phases are distinguished by light (Phase L) and dark (Phase D) backscattered electron images. Grain 2 of sample T1, in addition, includes a third phase of ferrocolumbite (microprobe location T1-6-1D) and contains an area of homogeneous manganotantalite. Tantalite phases from inhomogenous portions of Grains 1 and 2 are crudely zoned with respect to Ta_2O_5, Nb_2O_5, MnO and FeO (Figs. 3-75 to 3-78). Zonation in tantalite-columbite is attributed to a slow rate of cooling and possible incomplete miscibility of the isomorphous tantalite-columbite series (Barsanov et al., 1971; Knorring and Condliffe, 1984). From the geochemistry of tantalite phases in Grains 1 (Figs. 3-75, 3-76) and 2 (Figs. 3-77, 3-78), it is observed that an increase in Ta_2O_5 corresponds directly to a decrease in Nb_2O_5. Similarly, an increase in MnO along a grain results in a proportional decrease in FeO. In Grain 1, tantalite Phase L is enriched in Ta_2O_5 relative to tantalite Phase D. Conversely, tantalite Phase L is deficient in Nb_2O_5 relative to tantalite Phase D. Both Ta_2O_5 and Nb_2O_5 in both phases vary by 1 wt % (Fig. 3-75). MnO and FeO vary more irregularly across Grain 1 (Fig. 3-76) with respect

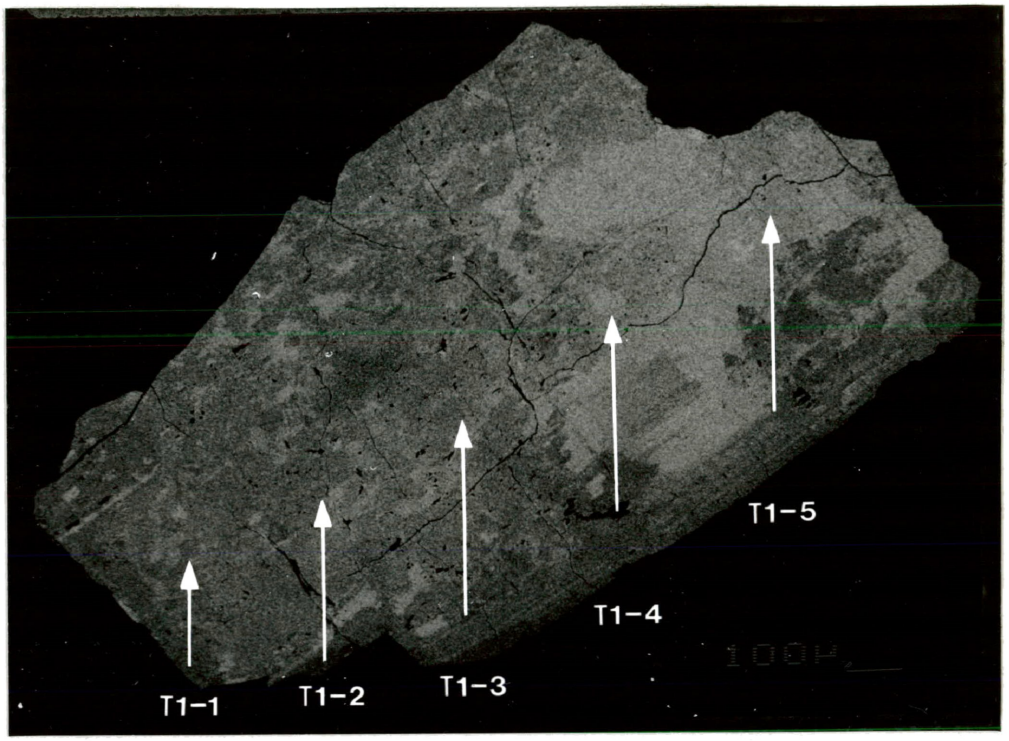

Fig. 3-73. Backscattered electron image of sample TI, Grain I, tantalite from the Brink pegmatite. Positions along the grain analyzed by electron microprobe are indicated by arrows.

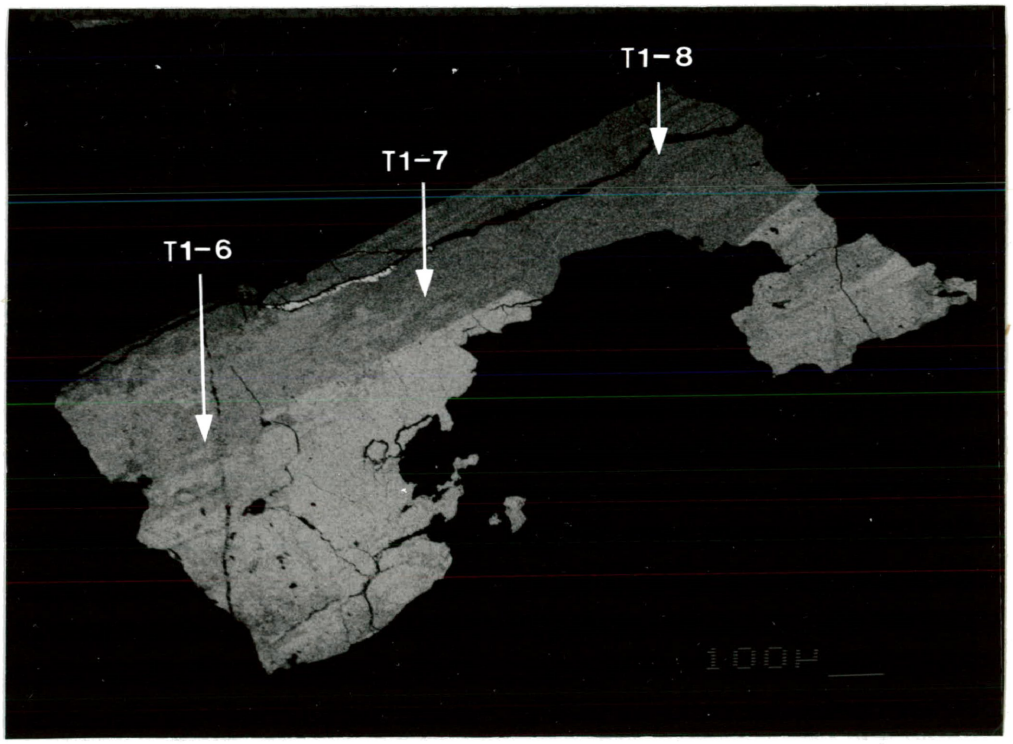

Fig. 3-74. Backscattered electron image of sample TI, Grain 2, tantalite from the Brink pegmatite. Positions along the grain analyzed by electron microprobe are indicated by arrows.

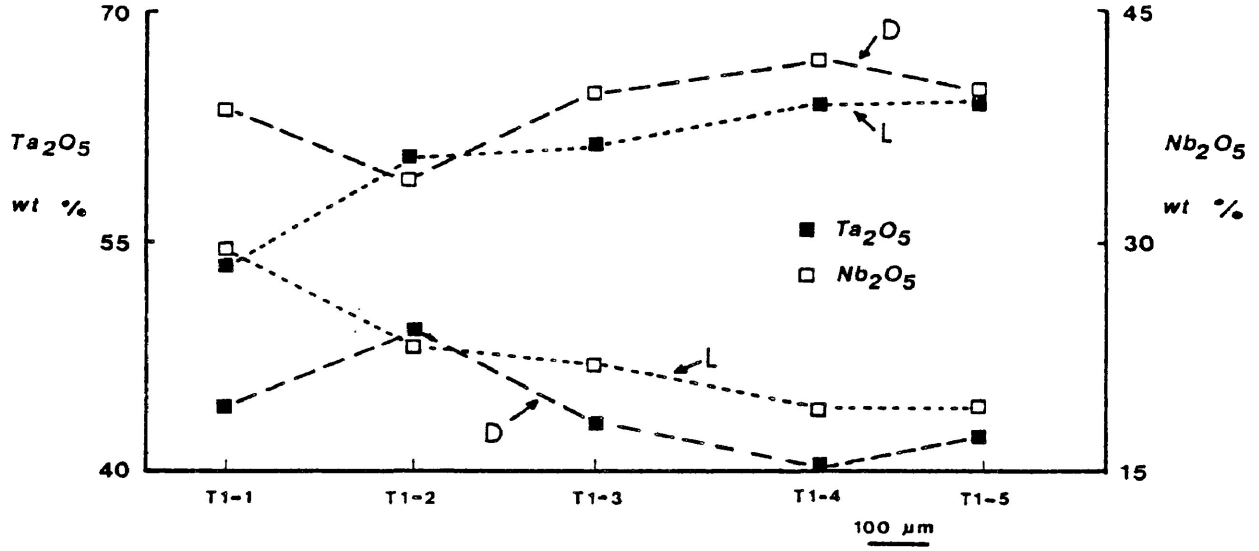

Fig. 3-75. Distribution of Ta_2O_5 and Nb_2O_5 across Grain I of sample TI. L - Phase L; D - Phase D.

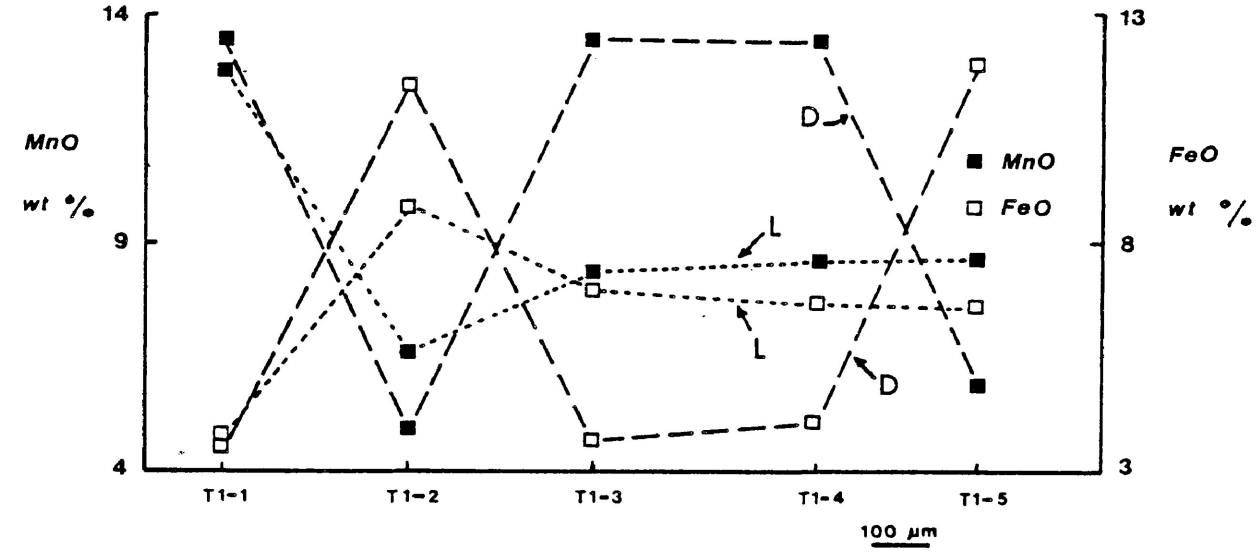

Fig. 3-76. Distribution of MnO and FeO across Grain I of sample TI. L - Phase L; D - Phase D.

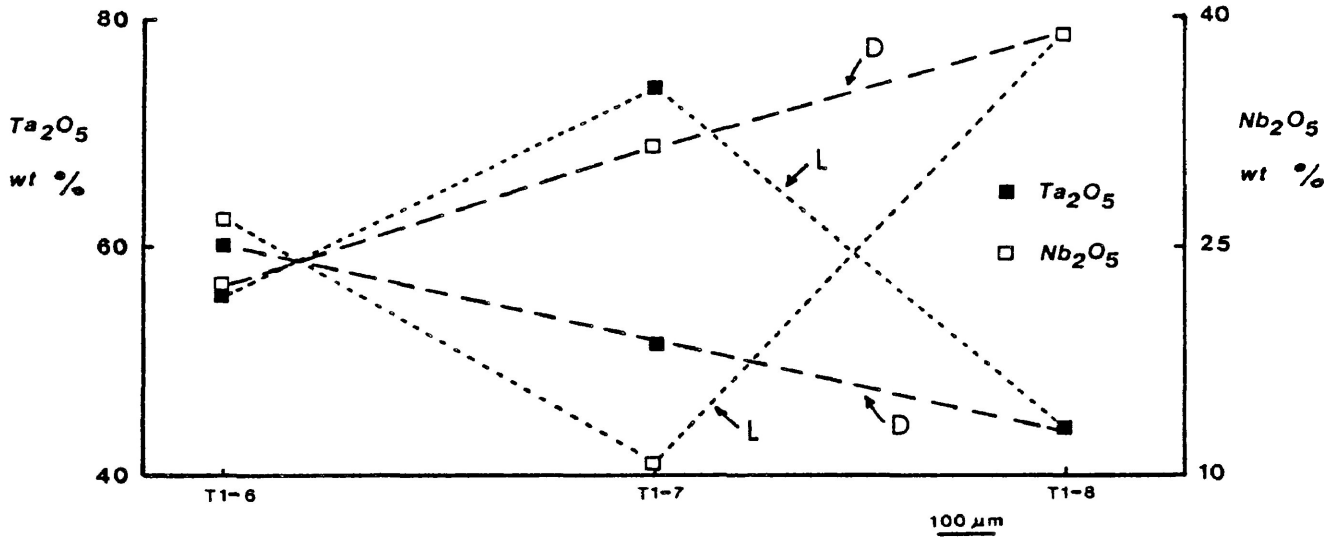

Fig. 3-77. Distribution of Ta_2O_5 and Nb_2O_5 across Grain 2 of sample T1. L - Phase L; D - Phase D.

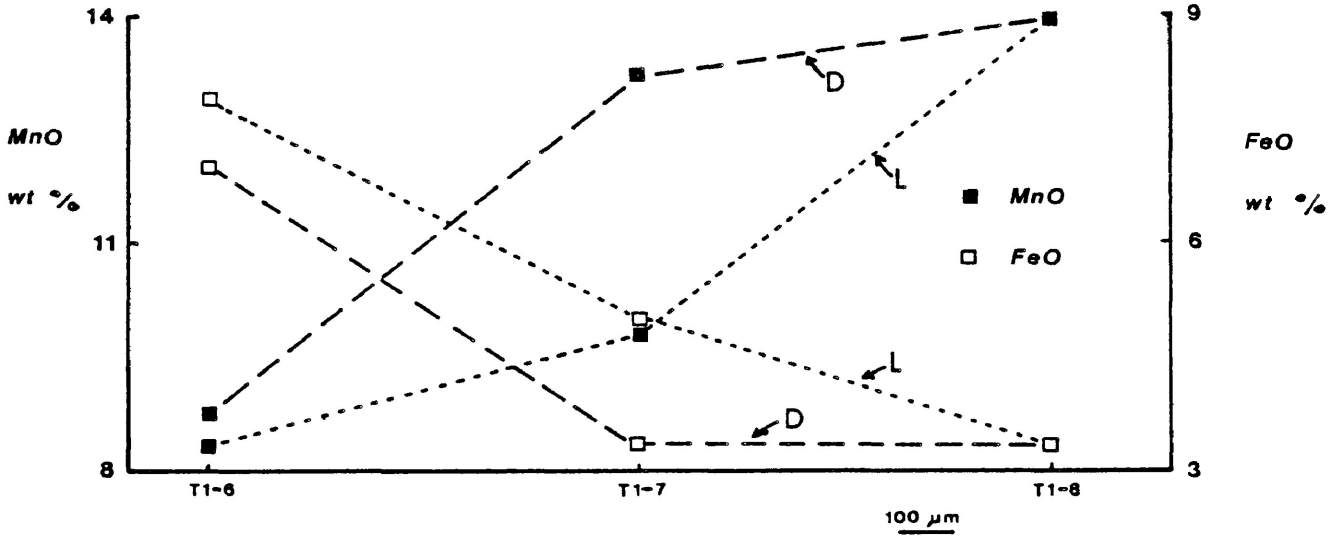

Fig. 3-78. Distribution of MnO and FeO across Grain 2 of sample T1. L - Phase L; D - Phase D.

to Ta_2O_5 and Nb_2O_5. Three points along Grain 2 were analyzed by an electron microprobe traverse. At one end of Grain 2, one homogeneous phase is present which is deficient in Ta_2O_5 and enriched in Nb_2O_5 with respect to the two separated phases of tantalite, which occupy a portion of the grain. Distribution of Ta_2O_5 and Nb_2O_5 in tantalite phases of Grain 2 is represented in Fig. 3-77. Similarly, variation in MnO and FeO in tantalite phases across Grain 2 is illustrated in Fig. 3-78.

Most tantalite-columbite minerals from the MNW pegmatite occur as inclusions in Sn oxide minerals (samples T2, T3). As an exception in the intermediate zone, tabular ferrocolumbite crystals are also distributed between plates of cleavelandite (samples T4, T5). Manganotantalite (sample T2) is confined to the core zone. Compositions in the intermediate zone range from ferrotantalite to ferrocolumbite. Ferrotantalite (sample T3) is enriched in TiO_2 and SnO_2 relative to ferrocolumbite. Electron microprobe analysis along the edge (sample T4-1 to T4-4) and along the face (sample T5-1 to T5-3) of a tabular crystal of ferrocolumbite reveal no inhomogeneity as encountered in tabular crystals of tantalite from the Brink pegmatite.

Columbite from the Southwest deposit, identified as samples T6A to T6C (Table 3-18) occurs as tiny platey inclusions in saccharoidal albite, as noted previously.

Analytical results indicate no substantial variation in geochemistry of these columbite crystals.

Sn Oxide Minerals - Sn oxide minerals in the Georgia Lake rare-element pegmatites are known only from the MNW pegmatite. Electron microprobe analyses of Sn oxide minerals are summarized in Table 3-19. Sample S7A,B originates from the core zone of the MNW pegmatite and contains inclusions of manganotantalite. Samples S8A,B and S9 originate from the intermediate zone and contain inclusions of ferrotantalite-ferrocolumbite.

The characteristic Sn oxide mineral is staringite although the structure is modulated as witnessed by poorly developed superstructure (Fig. 3-21). Although wt % Ta_2O_5 is somewhat less than is commonly attributed for staringite (Burke et al., 1969; Khvostova et al., 1974), it is higher in some samples than is commonly encountered in cassiterite (Foord, 1982; Moore and Howie, 1979). Modulation of the structure may result from the cell structures attempt to accomodate a moderately high Ta_2O_5 content. Presumably, a moderately high Ta_2O_5 content can be accomodated in a high-temperature form of cassiterite which is structurally disordered. Cooling leads to attempts to order, although the ordering is modulated as the result of incipient formation of superstructure of the unit cell (S. A. Kissin, personal communication, 1985). The presence of ordered

Table 3-19: Electron microprobe analysis of Sn oxide minerals from the MNW pegmatite.

Sample	S7A	S7B	S8A	S8B	S9
Ta_2O_5(wt %)	2.49	8.34	1.91	2.15	4.15
Nb_2O_5	------	1.52	------	0.29	1.87
TiO_2	------	------	------	------	0.42
SnO_2	98.39	89.42	97.78	97.16	91.90
FeO*	0.41	1.50	0.55	0.69	1.53
MnO	-----	------	------	------	0.12
Total	101.28	100.78	100.25	100.29	100.30

S7A,B: core zone

S8A,B, S9: intermediate zone

*: all iron as FeO

cassiterite in the MNW pegmatite cannot be discounted since the Ta_2O_5 content in some analyzed samples is low.

Fractionation Trends

Variations in the geochemistry of perthitic microcline and muscovite are used to study trends in fractionation on a regional scale and within specific rare-element pegmatites (e.g., Breaks, 1980; Černý et al., 1981; Černý et al., 1984; Shearer et al., 1983, 1985; Trueman and Černý, 1982). Fractionation is determined mainly by the enrichment of specific elements and indicates the degree of geochemical evolution of an igneous body. Granitic pegmatites of the rare-element type represent plutonic bodies with high degrees of fractionation (Černý, 1982). Thus, enrichment of elements with greater affinity for the melt phase is observed in rare-element pegmatites. Rare-element pegmatites are commonly enriched in Li, Rb, Cs, Nb, Ta and Sn and depleted in Fe, Mg, Sr, Ba, Sc, Zr and Co relative to less fractionated rocks (Ginsburg, 1960; Vlasov, 1966). This normal behaviour of elements was also observed in granitoid instrusions of the Georgia Lake area (Part 2) but is much more highly pronounced in the rare-element pegmatites. Although the relative geochemical evolution of pegmatites may be deduced by the enrichment or depletion of specific elements in perthitic microcline and muscovite, it is notable that the behaviour of elements among the two minerals is not always parallel and therefore not in all cases

representative of the distribution of elements in whole rock. For example, Sr is not captured in muscovite to the extent that it is in feldspar during the pegmatite process (Vlasov, 1966). In Georgia Lake rare-element pegmatites, Sr becomes depleted in perthitic microcline with progressive fractionation whereas Sr becomes enriched in muscovite with fractionation. Also, Li in muscovite from more geochemically fractionated pegmatites of the Central Group (eg., Brink, Southwest) is depleted relative to less fractionated pegmatites (eg., Island, Point).

Of the alkalis that become enriched in K-minerals of late pegmatitic stages, Rb is most nearly related to K in terms of ionic radius and easily substitutes for K. This substitution is so favourable that Rb does not form minerals of its own but is camouflaged in K-feldspar and muscovite (Heier and Adams, 1964). The common range of Rb concentration in K-feldspar and muscovite in granitic pegmatites varies from 0.01 to 1-2 wt % (Aleksandrov and Laricheva, 1983). In perthitic feldspars and muscovites from rare-element pegmatites of the Georgia Lake area, Rb concentration is variable but does not exceed 1 wt %. Rb and the K/Rb ratio are the best indicators of fractionation in K-feldspar and muscovite because of the strong coherence and simple relationships among the elements K and Rb.

The behaviour of Cs parallels that of Rb in K-feldspar

and muscovite, where Cs substitutes for K. Cs is incorporated into K minerals to an appreciable amount only in the very latest stages of pegmatite crystallization (Heier and Adams, 1964). Because of the larger size of the Cs ion with respect to K, Cs becomes preferentially enriched in the mica structure as opposed to K-feldspar (Heier, 1962). Smith (1983) suggested that most data for Cs in feldspars is of low accuracy and that pegmatitic feldspar is prone to error from mica impurities. In sampled perthitic feldspars from Georgia Lake rare-element pegmatites, muscovite impurities are negligible. With respect to Rb, Cs distributions are commonly more erratic (Černý, 1975) in their variation. Results obtained from Georgia Lake rare-element pegmatites are in keeping with this observation.

Li geochemistry differs from the other alkali elements in that Li will substitute for Mg, Fe^{+2}, Al^{+3} and Ti^{+4} (Goldschmidt, 1954). Li in K-feldspars commonly does not exceed several tens ppm (Smith, 1983), and Li is preferentially enriched in muscovite. In muscovites from the Georgia Lake rare-element pegmatites, Li concentration is low (<2000 ppm). The lowest Li concentrations in muscovite coincide with high Rb and Cs concentrations. Muscovites from spodumene-bearing pegmatites are commonly depleted in Li relative to muscovites from other types of pegmatites (Gordiyenko, 1971). This observation may

be explained by the preferential concentration of Li into a separate mineral phase (spodumene) with differentiation as opposed to incorporation into the muscovite structure.

In muscovite, Ta^{+5} and Nb^{+5} substitute for Ti^{+4} and Al^{+3} (Parker and Fleischer, 1968) whereas Sn^{+4} substitutes for Fe^{+2} and Fe^{+3} (Taylor, 1979) as isomorphous impurities. Ringwood (1955) has shown that these elements form complexes and have a tendency to accumulate in residual magmas until a sufficient concentration is reached to precipitate separate phases although Ta, Nb and Sn ions will also be incorporated in coexisting muscovite. From muscovites of the rare-element pegmatites of the Georgia Lake area, the concentration of Ta, Nb and Sn is erratic with respect to Rb and Cs.

On a regional scale across the Georgia Lake pegmatite field, there is no single fractionation trend along which the differentiation of all rare-element pegmatites proceeded. Instead, one fractionation trend that relates only the Central Group pegmatites can be established. This trend is determined by an increase in Rb, Rb/Ba and Cs and corresponding decrease in K/Rb, K/Cs in perthitic microcline and muscovite in a general east to west or a northeast to southwest direction across the Central Group. The Brink and Southwest deposits represent the most highly fractionated pegmatites while the Island, Point and Niemi pegmatites are least fractionated. The geochemistry of the Salo pegmatite suggests that it is intermediate in geochemical

evolution. Similar mineralogy and textural features among these pegmatites and strong geochemical fractionation across the Central Group suggest a common origin for this group of pegmatites with a source area to the east of Georgia Lake. In addition, it is potentially conceivable that the MNW zoned pegmatite is a highly differentiated pegmatite related to the same trend along which the Central Group pegmatites were emplaced.

On the basis of obtained geochemical data, no major trend in igneous fractionation can be established across Northern Group pegmatites. Although the exposed area covered by the Northern Group pegmatites is larger than that of the Central Group, elemental variations are small with respect to those of the Central Group pegmatites. Differentiation of Northern Group pegmatites is approximately intermediate with respect to the extremes observed in Central Group pegmatites as indicated by perthitic microcline and muscovite geochemistry. Localized trends in the Northern Group are observed. Rb and Cs increase in perthitic microcline and muscovite from the Nama Creek North to South pegmatites, in perthitic microcline from the McVittie to Powerline pegmatites and from the Giles to Camp pegmatites. It is possible these localized trends are not significant, as they may be attributed to geochemical variations within pegmatites.

Internal pegmatite fractionation is most highly pronounced in the zoned MNW pegmatite of the Southern Group. In perthitic microcline, Rb and Cs become enriched from a north to south direction in the wall zone. This observation is coupled with a decrease in Sr and Ba along the same trend. Increased fractionation from the wall zone to the core zone is established by an increase in Rb and Cs and decrease in Ba toward the core zone (Fig. 3-22). The fractionation trends in the MNW pegmatite outline a primary crystallization sequence from north to south and from the wall zone to the core zone. These observations are in keeping with the convention that primary sequential crystallization of zoned pegmatites progresses from the wall zone inward to the core zone (Cameron et al., 1949). Progressive inward fractionation is also established by the decrease in the Fe/Mn and Nb/Ta ratios (Černý et al., 1981) from the intermediate to the core zones in the tantalite-columbite minerals.

The geochemical distinction between a poorly zoned and a well zoned pegmatite can be made on the basis of a lesser degree of internal differentiation from outer to inner sections of the former. This observation is upheld by a smaller variation in Rb, Cs, K/Rb, K/Cs, Rb/Sr and Rb/Ba in perthitic microcline across the Brink pegmatite (poorly zoned) as opposed to the internal variations in the MNW pegmatite.

Petrogenesis

Regional Context

Rare-element pegmatites of the Georgia Lake area are of magmatic derivation and crystallized from low viscosity hydrous silicate fluids passively emplaced into pre-existing dilation zones. Pye (1965) provided possible evidence for this mode of origin. The most notable evidence of passive emplacement is the sharp contacts of the pegmatites, where observed, with host rocks. No offset was observed on a quartz vein which the Brink pegmatite cross-cuts. Milne (1962) observed that if the Brink pegmatite could be removed, the walls would collapse to fit exactly.

Two possible hypotheses concerning the derivation of pegmatitic fluids are anatexis of high-grade metamorphic rock and igneous fractionation from granitic intrusions (Černý, 1982). The later hypothesis is the most widely accepted mode of origin of fluids crystallizing rare-element pegmatites. The Georgia Lake area provides an excellent opportunity to test these hypotheses because of the close proximity of highly fractionated leucogranites to the pegmatite field.

Important to the study of petrogenesis of rare-element pegmatites is regional zonation. In many pegmatite fields, a regional zonation is observed in which a specific suite

of rare minerals characterize a particular zone of pegmatites located at a certain distance from a fluid source granitoid. In the Ross Lake area of the Northwest Territories, Hutchinson (1955) observed that pegmatites are spatially zoned in relation to the Redout Lake granite and genetically related to the granite. Nedumov (1964) pointed out similar relationships of mineral zonation of rare-element pegmatite fields of Africa and Siberia. With increasing distance from related granitic intrusions, Mulligan (1962) observed the following zones:

(1) Barren granite pegmatites with accessory beryl and rare Li-minerals;

(2) Complex generally well zoned pegmatites containing both beryl and Li-minerals;

(3) Pegmatites with Li-minerals and little or no beryl.

All three of these zones are represented in the Georgia Lake area at progressive distances north from the Glacier Lake Pluton. Regional zonation implies progressive geochemical evolution and specialization of pegmatites at greater distances from the fluid source. Geochemical evidence derived during the present study suggests that application of a regional zonation model to the Georgia Lake pegmatite field, as a whole, is unrealistic; i.e. it is clear that the northernmost Nama Creek pegmatites are not the most highly fractionated pegmatites of the pegmatite field. There is no clear fractionation trend,

as pointed out earlier, in perthitic microcline or muscovite which would suggest unidirectional fractionation across the pegmatite field. It is also highly improbable that a sufficiently high thermal gradient would have been maintained in the country rock to allow migration of hydrous silicate fluids in fractures for many kilometres across the pegmatite field before the magmatic component was totally exhausted. Instead, it is suggested that emplacement of pegmatites is more localized and is related to specific source fluid areas.

On the basis of geochemical evidence obtained and localized regional zonation, rare-element pegmatites were derived from three or possibly four source fluid areas accounting for the Central Group, Northern Group, Southern Group (MNW pegmatite) and Cosgrave Lake beryl occurrences. Although the mode of pegmatitic fluid derivation for all pegmatites may not be identical, it is probable that all pegmatites of the Georgia Lake area were emplaced during the same tectonic event, i.e. anatexis of metasediments with subsequent emplacement of pegmatites and two-mica leucogranites.

It is suggested that Central Group pegmatites were derived from a common source to the east of the group. This is determined, as previously discussed, by an increase in Rb, Cs and Rb/Ba and a corresponding decrease in K/Rb

and K/Cs in an east to west direction across the rare-element pegmatites of this group. The most highly fractionated pegmatites of this group are spodumene-bearing with minor tantalite-columbite. The least fractionated spodumene-bearing pegmatite of the Central Group was reported to contain some beryl (Pye, 1965). Between Georgia and Barbara Lakes a pegmatite outcrops which is beryl-bearing (F. Breaks; written communication, 1984). On Barbara Lake, numerous barren pegmatites outcrop. Thus, a regional zonation of pegmatites is established across the Central Group; from east to west - barren pegmatites, beryl-bearing, beryl- and spodumene-bearing and spodumene-bearing with accessory rare minerals.

The beryl-bearing pegmatites near Cosgrave Lake may represent another related episode of rare-element pegmatite intrusion to the Central Group although from a separate undetermined source fluid area. Geochemistry of these pegmatites was not investigated, thus the direction of pegmatite fractionation through these occurrences cannot be established, although a northward fractionation trend from the Glacier Lake Pluton cannot be discounted.

The origin of the MNW pegmatite is difficult to determine since this pegmatite is unique in the Georgia Lake pegmatite field with respect to strongly developed zoning and high degree of internal geochemical

differentiation. As noted previously, the MNW pegmatite may be related to the intrusion of the Central Group, emplaced at a distance and at a higher crustal level from other pegmatites of the Central Group. This interpretation is suggested by the unique presence of spodumene-quartz intergrowth pseudomorphs after petalite and the greater influence of aqueous fluids on the MNW pegmatite resulting in large scale replacement of primary crystallized minerals. Contrary to this explanation is that the MNW pegmatite was derived from fluids generated during the emplacement of the MNW Stock which hosts the zoned pegmatite (Breaks, 1980). According to the criteria of Ayres and Černý (1982), the MNW Stock is a possible parental granitoid to rare-element pegmatites.

The derivation of Northern Group pegmatites is difficult to interpret in relation to fractionation from a granitic intrusion. The lack of a distinct trend in fractionation across the Northern Group and small elemental variations with respect to Central Group pegmatites coupled with no variation in regional zonation suggest that the source fluids of the Northern Group pegmatites were of a different derivation from Central Group pegmatites. Anatexis of high-grade metamorphic rocks may be responsible for Northern Group pegmatites. The Northern Group pegmatites may be representative of an early anatectic phase of the melting process of pelitic metasediments which accounts for the

intrusion of two-mica leucogranites to the south and east of the pegmatite field. The implication is that Northern Group pegmatites and two-mica leucogranites were derived from a Li-rich source. Norton (1973) suggested a hypothesis of potential melting of metasediments in the formation of Li-rich rare-element pegmatites independent of granitic magma. The problematic points of this hypothesis, as discussed by Černý (1982), include the availability of Li-rich sediments in a geological framework and the high degree of parital melting required to release substantial Li into an anatectic melt. If the direct anatexis mechanism is viable, then there is no reason why both mechanisms of pegmatite derivation may not have operated in the Georgia Lake area during the major episode of granitic and pegmatitic intrusion.

Internal Evolution

Crystallization of granitic pegmatite is based on the model of Jahns and Burnham (1969). Although the model is dated, it has not been modified to any significant extent since its publication. The Jahns-Burnham model is derived to a large extent from previously proposed models of pegmatite crystallization by other authors. The model assumes the emplacement of a low-viscosity pegmatitic magma (Burnham, 1964) into an essentially closed system. The appearance of a separate supercritical aqueous fluid

(Burnham and Jahns, 1961) during some stage in the crystallization of the pegmatite is the critical factor in the development of pegmatitic textures and introduction of replacement effects. The supercritical aqueous phase is interpreted (Jahns and Burnham, 1969) to be introduced into the system of a crystallizing pegmatite from a water saturated silicate melt. Upon water saturation, a free aqueous phase would separate immiscibly from the silicate melt and accumulate along crystal-melt interfaces as thin films.

In summary, the crystallization sequence of granitic pegmatite is in three major stages:

(1) Crystallization Of A Volatile-rich Silicate Melt - Minerals crystallized during this stage are anhydrous with or without accessory OH-bearing phases. Products of this stage are rocks with normal phaneritic textures.

(2) Simultaneous Crystallization From A Silicate Melt And An Exsolved Supercritical Aqueous Fluid - This stage is responsible for the crystallization of the greatest proportion of primary minerals in a pegmatite. The appearance of characteristic very coarse-grained crystals and primary crystallization of wall and

intermediate zones in zoned pegmatites is attributed to this stage. Replacement of crystallized phases is initiated in this stage.

(3) Crystallization In The Presence Of A Supercritical Aqueous Fluid Without A Silicate Melt - Products of this stage include crystallization of quartz cores and progressive metasomatic replacement of crystallized minerals.

Late pegmatitic phases result from hydrothermal effects attributed to circulation of subcritical volatile fluids through fractures in the pegmatite. Products of this phase include quartz-rich fracture fillings and late-stage alteration or corrosion of crystallized mineral phases.

The supergene stage is the degenerative phase in the evolution of a pegmatite and results from weathering of surficial outcrop exposures.

All the stages of pegmatite evolution are demonstrated in rare-element pegmatites of the Georgia Lake area, although the influence of each stage appears to be variable with respect to a given pegmatite group. Crystallization directly from a hydrous silicate melt without the presence of a separate supercritical aqueous phase is volumetrically insignificant in all pegmatites of the Georgia Lake area.

This stage of crystallization is restricted to thin, discontinuous contact zones of a few centimetres width and is difficult to observe in most pegmatites.

Simultaneous crystallization in the presence of both a silicate melt and a supercritical aqueous fluid is the mechanism responsible for the bulk of the Central and Northern Group pegmatites. This process is exemplafied by the preferential inward growth of coarse perthitic microcline (Fig. 3-10) and spodumene (Fig. 3-17) in a fine- to medium-grained groundmass of albite, quartz and muscovite. Jahns and Tuttle (1963) explained that phases crystallized from an aqueous fluid are much coarser than those crystallized from a melt. Preferential extraction of K into the aqueous phase over Na acccunts for the dominance of microcline as a coarse-grained phase over albite. The common perthitic nature of microcline is achieved via the aqueous fluid phase, which acts as a potent flux at high pressures (Jahns and Tuttle, 1963), causing the albite in solid solution with microcline to unmix. All observed microcline samples from Georgia Lake pegmatites are perthitic.

In the rare-element pegmatites of the Georgia Lake area, discontinuous aplitic stringers and layers parallel to pegmatite contacts are restricted to Northern Group pegmatites. These aplites cross-cut microcline and spodumene

crystals and in some instances, engulf pre-crystallized spodumene (Fig. 3-15). Several pegmatites (McVittie, Powerline) contain segments which are predominantly aplitic in texture. The derivation of the aplites is considered to be a result of a pressure quench produced from a drop in temperature through loss of volatiles (Černý, 1975; Jahns and Tuttle, 1963) reverting to conditions of magmatic crystallization. The confinement of aplitic layers to the Northern Group pegmatites suggests that Northern Group pegmatites may have been subject to some form of tectonic activity producing internal fractures in pegmatites during a late stage of primary crystallization. This activity could have resulted from mass emplacement of granitoids in the area and would imply that Northern Group pegmatites predate other rare-element pegmatites of the area.

Development of a petalite-spodumene-quartz core in the MNW pegmatite and the small discontinuous quartz pods in the central portions of the Brink pegmatite is ascribed to crystallization in the presence of a supercritical aqueous fluid phase in the absence of a silicate melt. Luth and Tuttle (1969) demonstrated that the composition of the aqueous fluid phase is skewed toward quartz in the haplogranite system. Stewart (1978) determined that if the composition of the aqueous fluid remains constant by buffering in the presence of quartz and petalite, the precipitating solid would be silica-rich.

Metasomatic replacement of crystallized minerals by internally derived alkali-rich supercritical fluids (Jahns, 1955) is variably developed in rare-element pegmatites of the Georgia Lake area. The effects of metasomatic replacement are most pronounced in the MNW pegmatite, moderately developed in the Central Group and uncommon in the Northern Group pegmatites. In the MNW pegmatite, the most significant form of replacement is the large development of cleavelandite as radiating fans forming an albitization front enveloping the core zone. Breaks (1980) made this observation although cleavelandite of the MNW pegmatite was originally ascribed to a primary origin (Milne, 1962). The concordant nature of cleavelandite to the zonal structure of the pegmatite makes it difficult to recognize as a replacement phase. The texture of cleavelandite from the MNW pegmatite appears similar to that of the Varusträsk pegmatite in Sweden where cleavelandite is seen to replace quartz (Quensel, 1957). The proposal by London and Burt (1982a) that cleavelandite complexes are the result of reaction of residual fluids with solidified quartz and spodumene seems fitting for the MNW pegmatite (Fig. 3-5). Muscovite accompanies cleavelandite in the MNW pegmatite and probably crystallized at the expense of perthitic microcline, which is not present along the albitization front in the intermediate zone. In outcrop, cleavelandite is observed to replace oxidized lithiophilite-triphylite masses (Fig. 3-8), Sn oxide minerals

and ferrocolumbite (Fig. 3-7). A second type of albitization in the form of saccharoidal albite with disseminated tourmaline is restricted to the wall zone of the MNW pegmatite. Saccharoidal albite forms discordant stringers and masses at the expense of wall zone quartz and perthitic microcline. Other subordinate forms of metasomatic replacement in the MNW pegmatite include tourmalinization along the pegmatite contact, K metasomatism of core zone spodumene-quartz intergrowth to very fine-grained or microcrystalline muscovite and Na followed by Ca metasomatism of oxidized lithiophilite-triphylite by recrystallization to alluaudite and apatite, respectively. The absence of lepidolite replacement in the MNW pegmatite, or the Georgia Lake pegmatite field in general, can be ascribed to low F activity in aqueous fluids at the subsolidus stage of pegmatite crystallization (Černý and Burt, 1984; Hawthorne and Černý, 1982; Munoz, 1971).

Metasomatic replacement of Central Group pegmatites is dominated by albitization in the form of discordant masses of very fine-grained saccharoidal albite (Fig. 3-11). Subordinate replacement effects include tourmalinization along pegmatite contacts and replacement of perthitic microcline by fine-grained to microcrystalline muscovite (Fig. 3-12). Unlike the MNW pegmatite, most metasomatic replacement products are confined to central parts of Central Group pegmatites.

In comparison to the MNW pegmatite and Central Group pegmatites, Northern Group pegmatites are, in general, free of metasomatic replacement products. This effect could be attributed to a loss of supercritical fluids from pegmatites before large scale replacement was initiated.

Post pegmatitic alteration effects in Georgia Lake rare-element pegmatites are volumetrically insignificant and include alkali leaching (Li) from lithiophilite-triphylite to purpurite-heterosite (Moore, 1982; Shigley and Brown, 1985) and alteration of spodumene to a dark green-black mass of muscovite (Pye, 1965, 1968).

Petrogenetic Significance Of Spodumene

It is possible to make inferences about the temperature and pressure at time of pegmatite emplacement based on the nature of the spodumene(s) present in a pegmatite. Heinrich (1975, 1976) identified three paragenetic types of pegmatitic spodumene:

(1) Phenocrystic spodumene is commonly greenish with a high Fe_2O_3 (0.6 to 0.9 wt %) content. This type of spodumene is characteristic of unzoned or poorly zoned pegmatites.

(2) Zonal spodumene is white with a low Fe_2O_3 (0.01

- 0.03 wt %) content and occurs in intermediate zones and cores of zoned pegmatites.

(3) Secondary spodumene is white and commonly fine-grained with a very low Fe_2O_3 (0.007 - 0.03 wt %) content. This variety of spodumene is produced by the isochemical breakdown of petalite to yield spodumene and quartz.

All stable spodumene found in nature is of the type, α - spodumene (Munoz, 1969). In rare-element pegmatites of the Georgia Lake area, Type (1) spodumene is confined to the Northern and Central Groups whereas Type (3) occurs in the core zone of the MNW pegmatite. Some of the spodumene from the MNW core zone may be Type (2); i.e. coarse white spodumene as laths up to several tens of centimetres in length intergrown with some quartz.

London and Burt (1982b) indicated that spodumene-bearing pegmatite crystallizes in the temperature range of 300 to 650°C based on fluid inclusion studies by other authors. Appleman and Stewart (1968) observed that substitution of Fe^{+3} for Al^{+3} in spodumene greatly increases the temperature of stability of spodumene. Norton (1981) noted that a decrease in Fe content of spodumene corresponds to a change from magmatic crystallization to crystallization from a supercritical aqueous fluid. This observation implies

a resultant change in physico-chemical conditions of spodumene crystallization along a thermal gradient. Based on these observations it is possible to infer that Type (1) spodumene (Heinrich, 1976) crystallizes at a higher temperature than Type (2), thus, Northern and Central Group pegmatites of the Georgia Lake area may have crystallized at a higher temperature than the MNW pegmatites.

The mineral petalite is stable only at temperatures below 680°C at any pressure (Stewart, 1963). Stability of petalite has been determined in the range 2 to 4 kbars (Rossovskiy and Matrosov, 1974), although London (1981) showed that petalite may be stable to lower pressures.

The stability relationships between spodumene and petalite (Fig. 3-79) have been most recently investigated by London (1984). It is inferred from London's investigation that stability of spodumene or petalite is more a function of pressure than temperature. Of rare-element pegmatites from the Georgia Lake area, Northern and Central Group pegmatites may have crystallized at higher temperatures than the MNW pegmatite, as noted previously, within a pressure range of 4 kbars or greater. In the MNW pegmatite, Fe-poor spodumene is present along with pseudomorphic masses of fine-grained spodumene-quartz intergrowth after petalite. The spodumene, spodumene-quartz assemblage in the core of the MNW pegmatite suggests that crystallization of the

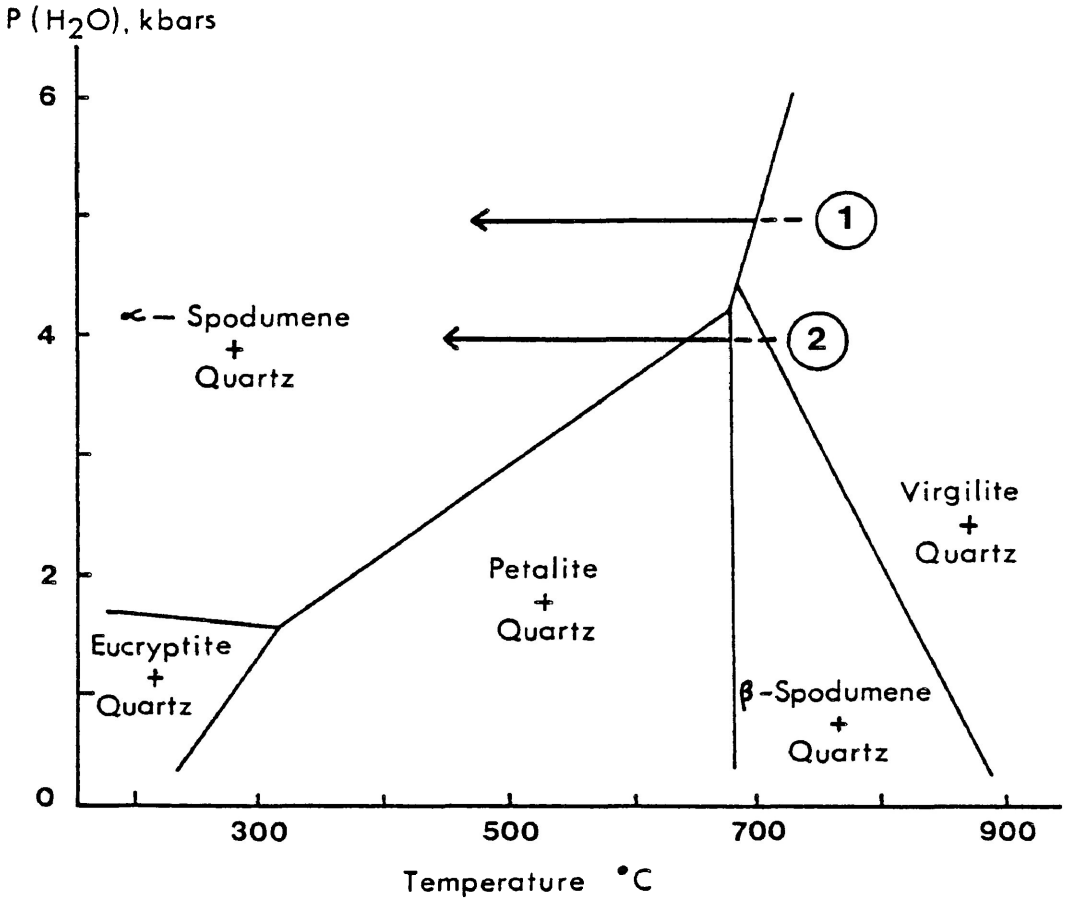

Fig. 3-79. Stability relations in the system $LiAlSiO_4$-SiO_2-H_2O (from London, 1984).
1 - Possible crystallization path of a pegmatite from either the Northern or Central Groups.
2 - Possible crystallization path of the MNW pegmatite.

core was near the petalite- α -spodumene join probably near the upper pressure stability limit of petalite of about 4 kbars. The inference from the spodumene-petalite stability diagram is that Northern and Central Group pegmatites were emplaced at a deeper crustal level than the zoned MNW pegmatite.

Economic Considerations

Spodumene-bearing pegmatites of the Georgia Lake area contain the largest known concentration of lithium in the Quetico Subprovince. These pegmatites have been known for their lithium potential for over 30 years but have never been exploited. In relation to the entire western Superior Province, Georgia Lake rare-element pegmatites account for about 25% of known lithium reserves based on tonnage of lithium. Table 3-20 compares reserves of lithium in pegmatites from the western Superior Province. The listed reserves of lithium are subeconomic, at present market conditions, in light of low demand for lithium, high pegmatitic lithium reserves elsewhere in North America and other geological settings from which lithium can be obtained.

During the present study, it was discovered that tantalite-columbite minerals are more extensively distributed in Georgia Lake pegmatites then had previously been reported.

Table 3-20: Published grade-tonnage data of lithium for Archean pegmatites of the western Superior Province (from Williams and Trueman, 1978).

Subprovince	# Of Deposits	Name	Tonnes	%Li,	Tonnes Li
Gods Lake	3		NA	NA	
Berens River	0				
Uchi	1		NA	NA	
English River	17	Buck/Coe	725,760	2.13	7,285
		Irgon	1,091,815	1.5	7,622
		Eagle	544,320	1.4	3,547
		Spot	3,583,440	1.28	21,347
		Tanco	6,649,550	2.77	85,650
Wabigoon	22	Lucy	226,800	1.75	1,847
Quetico	36	*Brink	1,108,122	1.63	8,387
		*Jean Lake	1,532,260	1.3	9,271
		*McVittie	236,779	1.03	1,135
		*Nama Creek	3,894,004	1.06	19,210
		*Jackpot	1,814,400	1.09	9,204
		*Vegan	680,400	1.38	4,370
		Lac la Croix	1,383,480	1.27	8,177
Wawa	0				
TOTAL	79		23,244,306		194,470

* Georgia Lake rare-element pegmatite occurrence

NA - not available

Although traces of tantalite-columbite minerals are dispersed with interstitial minerals (Brink, Southwest) and spodumene-quartz intergrowth (MNW), most of these minerals are associated with secondary albitization. This association is especially prominent in the MNW pegmatite, where the bulk of tantalite-columbite minerals, occurring as inclusions in Sn oxide minerals and as separate tabular crystals, are concentrated along the albitization front marked by fans of cleavelandite. The vertical extent of the albitization front is not known. Based on surface examination, the tantalite-columbite minerals of the MNW pegmatite are potentially ore grade.

Breaks (1980) discussed the MNW pegmatite as a prospect with ceramic potential since spodumene of the core zone is the low Fe type. In addition, the MNW pegmatite can be regarded as a potential pollucite prospect indicated by high Cs concentration (0.2 wt %) of microcrystalline muscovite associated with core zone spodumene-quartz intergrowth. Propsects associated with the core zone would be of low tonnage and probably subeconomic since the core zone is known to pinch out at a maximum depth of about 30 m (Milne, 1962).

Geochemical prospecting methods in the Georgia Lake area may reveal rare-element pegmatites of greater economic potential. All known rare-element pegmatites were discovered

by outcrop examination or by diamond drilling below known occurrences. It is notable that all studied rare-element pegmatites of the area except MNW occur where surface relief is low. The potential for discovery of unexposed rare-element pegmatites is great.

Fractionation trends in rare-element pegmatites of the Georgia Lake area can be used to delineate an area with promise for highly differentiated pegmatites. The fractionation trend across Central Group pegmatites indicates that highly fractionated pegmatites are associated with the western or southwestern portion of this pegmatite group. A thorough geochemical survey of the region between Blay and Cosgrave Lakes may reveal more highly differentiated pegmatites of the Central Group or possibly spodumene pegmatites associated with the Cosgrave Lake beryl occurrences. Delineation of promising areas for pegmatite prospecting among the Northern Group pegmatites cannot be established because of a lack of distinct fractionation trends through the group.

Geochemical analysis of perthitic microcline from the MNW pegmatite revealed this pegmatite to be internally highly fractionated in a north to south direction along strike and toward the core of the pegmatite. A similar analysis of numerous simple pegmatites occurring within and near the MNW Stock, based on internal pegmatite

fractionation, may delineate other zoned differentiated pegmatites similar to the MNW pegmatite.

Trueman and Černý (1982) endorse geochemical detection of dispersion haloes in exploration for unexposed pegmatites. Dispersion haloes result from the diffusion of elements, particularly alkali elements, into pegmatitic exocontacts during the process of pegmatite consolidation. In relation to Georgia Lake rare-element pegmatites, Li is the most sensitive indicator element of such a dispersion halo. Li is enriched in a sample of granite (BG4) obtained 2 m from the MNW pegmatite relative to a similar sample (BG5) obtained about 1 km away. Other elements determined in samples BG4 and BG5 do not show substantial variation in concentration. Granitoid sample BG23, obtained from an area north of Lake Jean where stringers of spodumene pegmatite are numerous, is anomalously enriched in Li (0.09 wt %) and high in Rb (0.04 wt %) relative to other analyzed granitoid samples from the Georgia Lake area.

PART FOUR CONCLUSIONS

Two-mica leucogranites, allied to the S-type granitoids, flank the rare-element pegmatite field to the south and east as a large plutonic body with minor satellitic intrusions. Two-mica leucogranites are fine- to coarse-grained granitoids with ubiquitous biotite and muscovite and subordinate garnet. Geochemically, the two-mica leucogranites are the most highly fractionated granitoids of the area and are presumed to be derived as partial melts of pelitic metasediments. Other quantitatively less important granitoids of the Georgia Lake area include the Kilgour lake Group granitoids and tonalitic sills. The granitoids of the Kilgour Lake Group are centered on a small body of gabbro-metagabbro. Felsic granitoids of the group are compositionally granodiorites and tonalites with porphyritic phases flanking the southern segment of the group. The Kilgour Lake Group granitoids, allied to I-type granitoids, are characterized by ubiquitous hornblende and sphene and are geochemically less fractionated in relation to two-mica leucogranites. The Kilgour Lake Group granitoids are presumed to be derived by fractional crytallization of a mantle or lower crustal melt; an event which preceded emplacement of two-mica leucogranites. The tonalitic sills are widespread throughout the pegmatite field, although quantitatively subordinate and geochemically less fractionated with respect to two-mica leucogranites. The tonalitic sills may represent an early partial melting

event of sodic metagreywacke.

Spodumene-bearing, rare-element pegmatites of the Georgia Lake area are divided into three groups, Southern, Central and Northern Group pegmatites. The MNW pegmatite is the only representative of the Southern Group and is characterized by internal zoning, highly developed replacement textures, strong internal fractionation, as determined by perthitic microcline geochemistry and by the unique presence of spodumene-quartz intergrowth after petalite in the Georgia Lake pegmatite field. Central Group pegmatites are unzoned to poorly zoned with moderately to poorly developed replacement textures and are linked by a distinct fractionation trend through this group, as determined by perthitic microcline and muscovite geochemistry. Northern Group pegmatites have a groundmass which is finer-grained than Central Group pegmatites. Internally contained aplitic bands and stringers in most pegmatites and the lack of a distinct regional fractionation trend are characteristic of the Northern Group.

Two modes of source fluid derivation may have operated during the emplacement of the rare-element pegmatites. Central Group pegmatites were derived by the process of igneous fractionation from a granitic source in the vicinity of Barbara Lake and emplaced as low viscosity volatile-rich melts in a direction away from the probable fluid source

area. This is indicated by a fractionation trend defined most clearly by the concentration of Rb and Cs in perthitic microcline and muscovite across the group. The MNW pegmatite of the Southern Group may represent a highly differentiated pegmatite related to the intrusion of Central Group pegmatites, or it is derived from the MNW Stock which hosts the pegmatite. Derivation of Northern Group pegmatites may have resulted from direct anatexis of Li-rich pelitic metasediments.

Perthitic microcline from rare-element pegmatites has the maximum microcline structural state. This implies low temperatures of primary igneous crystallization for the Georgia Lake rare-element pegmatites.

A Sn oxide mineral occurring commonly in the MNW pegmatite, previously described as cassiterite, has been determined to be a mineral more closely associated to staringite based on the development of superstructure within the crystal structure and the somewhat higher Ta_2O_5 content then is commonly noted in cassiterite.

Tantalite-columbite minerals in rare-element pegmatites were found to be more extensively distributed than had previously been reported. Tantalite-columbite minerals occur as interstitial groundmass minerals and in saccharoidal albite in Central Group pegmatites. In the MNW pegmatite,

tantalite-columbite minerals occur as inclusions in Sn oxide minerals and as tabular crystals along the albitization front in the intermediate zone.

REFERENCES

Abbey, S.
1983: Studies in "Standard Samples" of Silicate Rocks and Minerals. Geol. Surv. of Canada, Paper 83-15, 114 p.

Aleksandrov, I. V. and Laricheva, O. O.
1983: Rubidium distribution in the muscovites and potash feldspars from granite pegmatites. Geochem. Int. 20, 58-66.

Appleman, D. E. and Stewart, D. B.
1968: Crystal chemistry of spodumene type pyroxenes. Geol. Soc. Amer. Spec. Pap. 101, 5-6, abstr.

Arth, J. G.
1979: Some, trace elements in trondhjemites-their implications to magma genesis and paleotectonic setting. In: Trondhjemites, Dacites and Related Rocks (F. Barker, ed.). Elsevier, Amsterdam, 123-132.

Ayres, L. D.
1978: Metamorphism in the Superior Province of northwestern Ontario and its relationship to crystal development. In: Metamorphism in the Canadian Shield (J. A. Fraser and W. W. Heywood, eds.). Geol. Surv. of Canada, Paper 78-10, 25-36.

Ayres, L. D. and Černý, P.
1982: Metallogeny of granitoid rocks in the Canadian Shield, Can. Mineral. 20, 439-536.

Barsanov, G. P., Yeremin, N. I. and Sergeyeva, N. Y.
1971: Columbite-tantalite zoning as revealed by electron-probe microanalysis. Dokl. Acad. Sci. USSR, Earth Science Section 201, 174-176.

Bertin, E. P.
1967: Practical Aspects of Chemical Analysis by X-ray Secondary-Emission (Fluorscence) Spectrometry. Radio Corporation of America, Harrison, N. J., 81 p.

Borg, I. Y. and Smith, D. K.
1969: Calculated X-ray Powder Patterns for Silicate Minerals. Geol. Soc. Amer. Memoir 122, 896 p.

REFERENCES
Continued

Breaks, F. W.
1980: Lithophile mineralization in northwestern Ontario: rare-element granitoid pegmatites. In: Summary of Field Work 1980 (V. G. Milne, O. L. White, R. B. Barlow, J. A. Robertson and A. C. Colvine, eds.). Ont. Geol. Sur. Misc. Paper 96, 5-9.

Breaks, F. W. and Bond, W. D.
1977: Manifestations of recent reconnaissance investigations in the English River subprovince, northern Ontario. In: Geotraverse Conference Proceedings 1977, University of Toronto, 170-211.

Breaks, F. W., Bond, W. D. and Stone, D.
1978: Preliminary Geological Synthesis of the English River Subprovince, Northwestern Ontario and its Bearing Upon Mineral Exploration. Ont. Geol. Surv. Misc. Paper 72, 55 p.

Brown, B. E. and Bailey, S. W.
1964: The structure of maximum microcline. Acta Cryst. 17, 1391-1400.

Burke, E. A. J., Kieft, C., Feluis, R. O. and Adusumilli, M.S.
1969: Staringite, a new Sn-Ta mineral from north-eastern Brazil. Mineral. Mag. 37, 447-452.

Burnham, C. W.
1964: Viscosity of a water-rich pegmatite melt at high pressures. Geol. Soc. Amer. Spec. Paper 76, 26, abstr.

Burnham, C. W. and Jahns, R. H.
1961: Experimental studies of pegmatite genesis - The composition of pegmatite fluids. Geol. Soc. Amer. Spec. Paper 68, 143-144, abstr.

Cameron, E. N., Jahns, R. H., McNair, A. H. and Page, L. R.
1949: Internal structure of granitic pegmatites. Econ. Geol. Monograph 2, 115 p.

Cawthorn, R. G., Strong, D. F. and Brown, P. A.
1976: Origin of corundum-normative intrusive and extrusive magmas. Nature 259, 102-104.

REFERENCES
Continued

Černý, P.
1975: Granitic pegmatites and their minerals: selected examples of recent progress. Fortschr. Miner. 52, 225-250.

Černý, P.
1982: Petrogenesis of granitic pegmatites. In: Short Course in Granitic Pegmatites in Science and Industry (P. Černý, ed.), Mineral. Assoc. of Can. Short Course Handbook 8, 405-461.

Černý, P. and Burt, D. M.
1984: Paragenesis, crystallochemical characteristics, and geochemical evolution of micas in granite pegmatites. In: Micas (S. W. Bailey, ed.), Mineral. Soc. of Amer., Reviews in Mineralogy 13, 257-297.

Černý, P. and Ercit, T. S.
1985: Some recent advances in the mineralogy and geochemistry of Nb and Ta in rare-element granitic pegmatites. Bull. Mineral. 108, in press.

Černý, P. and Ferguson, R. B.
1972: The Tanco pegmatite at Bernic Lake, Manitoba. IV. Petalite and spodumene relations. Can. Mineral. 11, 660-678.

Černý, P., and Smith, J. V., Mason, R. A. and Delaney, J. S.
1984: Geochemistry and petrology of feldspar crystallization in the Věžná pegmatite, Czechoslovakia. Can. Mineral. 22, 631-651.

Černý, P. and Trueman, D. L.
1978: Distribution and petrogenesis of lithium pegmatites in the western Superior province of the Canadian Shield. Energy 3, 365-377.

Černý, P., Trueman, D. L., Ziehlke, D. V., Goad, B. E. and Paul, B. J.
1981: The Cat Lake-Winnipeg River and the Wekusko Lake Pegmatite Fields, Manitoba. Manitoba Dept. of Energy and Mines, Min. Res. Div., Econ. Geol. Rept. ER80-1, 234 p.

REFERENCES
Continued

Černý, P. and Turnock, A. C.
1971: Niobium-tantalum minerals from granitic pegmatites at Greer Lake, southeastern Manitoba. Can. Mineral. 10, 755-772.

Chappell, B. W.
1978: Granitoids from the Moonbi District, New England Batholith, eastern Australia. J. Geol. Soc. Aust. 25, 267-283.

Chappell, B. W. and White, A. J. R.
1974: Two contrasting granite types. Pacific Geol. 8, 173-174.

Clarke, D. B.
1981: The mineralogy of peraluminous granites: a review. Can. Mineral. 19, 3-17.

Collins, W. J., Beams, S. D., White, A. R. and Chappell, B. W.
1982: Nature and origin of A-type granites with particular reference to southeastern Australia. Contrib. Mineral. Petrol. 80, 189-200.

De Albuquerque, C. A. R.
1977: Geochemistry of the tonalitic and granitic rocks of the Nova Scotia southern plutons. Geochim. Cosmochim. Acta 41, 1-13.

Deer, W. A., Howie, R. A. and Zussman, J.
1966: An Introduction to the Rock-Forming Minerals. Longman, London, 528 p.

Didier, J., Duthou, J. L. and Lameyre, J.
1982: Mantle and crustal granites: genetic classification of orogenic granites and the nature of their enclaves. J. Volcanol. Geotherm. Res. 14, 125-132.

El Bouseily, A. M. and El Sokkary, A. A.
1975: The relation between Rb, Ba and Sr in granitic rocks. Chem. Geol. 16, 207-219.

Ermanovics, I. F., McRitchie, W. D. and Houston, W. N.
1979: Petrochemistry and tectonic setting of plutonic rocks of the Superior Province in Manitoba. In: Trondhjemites, Dacites and Related Rocks (F. Barker, ed.). Elsevier, Amsterdam, 323-362.

REFERENCES
Continued

Foord, E. E.
1982: Minerals of tin, titanium, niobium and tantalum in granitic pegmatites. In: Short Course in Granitic Pegmatites in Science and Industry (P. Černý, ed.), Mineral. Assoc. of Can. Short Course Handbook 8, 187-238.

Gibson, I. L. and Jagam, P.
1980: Instrumental neutron activation analysis of rocks and minerals. In: Short Course in Neutron Activation Analysis in the Geosciences (G. K. Muecke, ed.) Mineral Assoc. of Can. Short Coarse Handbook 5, 109-131.

Ginsburg, A. I.
1960: Specific geochemical features of the pegmatite process. Int. Geol. Congress, 21st sess. Norden, Rept. Pt. 17, 111-121.

Glikson, A. Y.
1971: Primitive Archean element distribution patterns: chemical evidence and geotectonic significance. Earth Planet. Sci. Lett. 12, 309-320.

Goldschmidt, V. A.
1958: Geochemistry (A. Muir, ed.). Oxford, London, 730 p.

Goldsmith, J. R. and Laves, F.
1954: The microcline-sanidine stability relations. Geochim. Cosmochim. Acta 5, 1-19.

Gordiyenko, V. V.
1971: Concentration of Li, Rb and Cs in potash feldspar and muscovite as criteria for assessing the rare metal mineralization in granite pegmatites. Int. Geol. Rev. 13, 134-142.

Grice, J. D., Černý, P. and Ferguson, R. B.
1972: The Tanco pegmatite at Bernic Lake, Manitoba. II. Wodginite, tantalite and related minerals. Can. Mineral. 11, 609-642.

Harvey, P. K., Taylor, D. M. Hendry, R. D. and Bancroft, F.
1973: An accurate fusion method for the analysis of rocks and chemically related materials by X-ray fluorescence spectrometry. X-ray Spect. 2, 33-44.

REFERENCES
Continued

Hawthorne, F. C. and Černý, P.
1982: The mica group. In: Short Course in Granitic Pegmatites in Science and Industry (P. Černý, ed.). Mineral. Assoc. of Can. Short Course Handbook 8, 63-98.

Heier, K. S.
1962: Trace elements in feldspars - a review. Norsk. Geol. Tiddskr. 42, 415-454.

Heier, K. S. and Adams, J. A.
1964: The geochemistry of the alkali metals. Phys. Chem. Earth 5, 253-381.

Heinrich, E. W.
1975: Economic geology and mineralogy of petalite and spodumene pegmatites. Indian Jour. Earth Sci. 2, 18-29.

Heinrich, E. W.
1976: A comparison of three major lithium pegmatites: Varuträsk, Bikita and Bernic Lake. In: Lithium Resources and Requirements by the Year 2000 (J. D. Vine, ed.). U. S. Geol. Surv. Prof. Paper 1005, 50-54.

Hine, R. Williams, I. S., Chappell, B. W. and White, A. J. R.
1978: Contrasts between I- and S- type granitoids of the Kosciusko batholith. J. Geol. Soc. Aust. 25, 219-234.

Hutchinson, R. W.
1955: Regional Zonation of Pegmatites Near Ross Lake, District of Mackenzie, Northwest Territories. Geol. Surv. of Canada, Bull. 34, 50 p.

Jahns, R. H.
1955: The study of pegmatites. Econ. Geol., 50th Anniv. Vol. 1, 1025-1130.

Jahns, R. H. and Burnham, C. W.
1969: Experimental studies of pegmatite genesis. I. A model for the derivation and crystallization of granitic pegmatites. Econ. Geol. 64, 843-864.

REFERENCES
Continued

Jahns, R. H. and Tuttle, O. F.
1963: Layered pegmatite aplite intrusives. Mineral. Soc. Amer. Spec. Paper 1, 78-92.

Jenkins, R, H, and DeVries, B.
1970: Worked Examples in X-ray Spectrometry. Springer Verlag, New York, 129 p.

Karnin, W. D.
1980: Petrographic and geochemical investigations on the Tsaobismund pegmatite dyke, South West Africa/Namibia. Neues Jahrb. Mineral. Monatsh. 5, 193-205.

Khvostova, V. A., Slesarchuk, V.S. and Laputina, I. P.
1974: First find of staringite in the Soviet Union. Tr. Mineral. Muz. Akad. Nauk SSSR 23, 226-228, in Russian.

Kilinc, I. A.
1972: Experimental study of partial melting of crustal rocks and formation of migmatites. Int. Geol. Congress, 24th sess. Montreal, Section 2, 109-113.

Kleeman, A. W.
1965: The origin of granitic magmas. J. Geol. Soc. Aust. 12, 35-52.

Knorring, O. v. and Condliffe, E.
1984: On the occurrence of niobium-tantalum and other rare-element minerals in the Meldon aplite, Devonshire. Mineral. Mag. 48, 443-448.

Komkov, A. I.
1970: Relationship between X-ray constants of columbite and composition. Dokl. Acad. Sci. USSR, Earth Science Section 195, 117-119.

Kroll, H. and Ribbe, P. H.
1983: Lattice parameters, composition and Al, Si order in alkali feldspars. In: Feldspar Mineralogy, 2nd ed. (P. H. Ribbe, ed.). Mineral. Soc. of Amer., Reviews in Mineralogy 2, 57-99.

Lasmanis, R.
1978: Lithium resources in the Yellowknife area. Northwest Territories, Canada. Energy 3, 399-407.

REFERENCES
Continued

London, D.
1981: Preliminary experimental results in the system $LiAlSiO_4$-SiO_2-H_2O. Carnegie Inst. Wash. Year Book 80, 341-345.

London, D.
1984: Experimental phase equilibria in the system $LiAlSiO_4$-SiO_2-H_2O: a petrogenetic grid for lithium-rich pegmatites. Amer. Mineral. 69, 995-1004.

London, D. and Burt, D. M.
1982a: Alteration of spodumene, montebrasite and lithiophilite of the White Picacho District, Arizona. Amer. Mineral. 67, 97-113.

London, D. and Burt, D. M.
1982b: Lithium aluminosilicate occurrences in pegmatites and the aluminosilicate phase diagram. Amer. Mineral. 67, 483-493.

Loiselle, N. C. and Wones, D. R.
1979: Characteristics and origin of anorogeneic granites. Geol. Soc. Amer., Abstr. with Prog. 11, 468.

Luth, W. C., Jahns, R. H. and Tuttle, O. F.
1964: The granite system at pressures of 4 to 10 kilobars. J. Geophys. Res. 69, 759-773.

Luth, W. C. and Tuttle, O. F.
1969: The hydrous vapour phase in equilibrium with granite and granite magmas. In: Igneous and Metamorphic Geology (L. H. Larsen, M. Prinz and V. Mason, eds.). Geol. Soc. Amer. Memoir 115, 513-548.

McCrank, G. F. D., Misiura, J. D. and Brown, P. A.
1981: Plutonic Rocks in Ontario. Geol. Surv. of Canada, Paper 80-23, 171 p.

Mehnert, K. R.
1971: Migmatites and the Origin of Granitic Rocks. Elsevier, Amsterdam, 405 p.

Milne, V. G.
1962: The Petrography and Alteration of Some Spodumene Pegmatites near Beardmore, Ontario. unpublished Ph.D. thesis, Univ. Toronto, Toronto, Ont. 242 p.

REFERENCES
Continued

Mitchell, R. H., Poulsen, H. and Jensen, E.
1980: Analysis of Silicate Rocks: Major Elements, Rb, Sr, Y, Zr, Nb and Ba by Wet Chemical and X-ray Fluorescence Methods. Geochemistry Laboratory Publication 1, Lakehead University, Thunder Bay, Ont. 51 p.

Moore, F. and Howie, R. A.
1979: Geochemistry of some Cornubian cassiterites. Mineral. Deposita 14, 103-107.

Moore, P. B.
1973: Pegmatite phosphates: descriptive mineralogy and crystal chemistry. Mineral. Record 4, 103-130.

Moore, P. B.
1982: Pegmatite minerals of P(V) and B(III). In: Short Course in Granitic Pegmatites in Science and Industry (P. Černý, ed.). Mineral. Assoc. of Can. Short Course Handbook 8, 267-291.

Mulligan, R.
1962: Origin of the lithium and beryllium-bearing pegmatites. Can. Inst. Min. Met. Trans. 65, 423-426.

Mulligan, R.
1965: Geology of Canadian Lithium Deposits. Geol. Surv. of Canada, Econ. Geol. Rept. 21, 131 p.

Mulligan, R.
1973: Lithium distribution in Canadian granitoid rocks. Can. J. Earth Sci. 10, 316-323.

Mulligan, R.
1980: Lithophile Element Content of Some Canadian Granitoid Rocks. Geol. Surv. of Canada, Open File, Rept. 666, 30 p.

Munoz, J. L.
1969: Stability relations of $LiAlSi_2O_6$ at high pressures. Mineral. Soc. Amer. Spec. Paper 2, 203-209.

Munoz, J. L.
1971: Hydrothermal stability relations of synthetic lepidolite. Amer. Mineral. 56, 2069-2087.

REFERENCES
Continued

Nedumov, I. B.
1964: The process of differentiation of pegmatitic melt and the role of tectonics in the formation of rare-element pegmatites. Int. Geol. Congress, 22nd sess. New Delhi, Rept. Pt. 6, 116-139.

Nickel, E. H. , Rowland, J. F. and McAdam, R. C.
1963: Ixiolite, a columbite substructure. Amer. Mineral. 48, 961-979.

Norrish, K. and Chappell, B. W.
1967: X-ray fluorescence spectrography. In: Physical Methods in Determinative Mineralogy (J. Zussman, ed.). Academic Press, London, 161-214.

Norrish, K. and Hutton, J. T.
1969: An accurate X-ray spectrographic method for the analysis of a wide range of geological samples. Geochim. Cosmochim. Acta 33, 431-453.

Norton, J. J.
1973: Lithium, cesium and rubidium- the rare alkali metals. In: United States Mineral Resources (D.A. Brobst and W. P. Pratt, eds.). U. S. Geol. Surv. Prof. Paper 820, 365-378.

Norton, J. J.
1981: Iron content of spodumene in different mineral assemblages of pegmatites, Black Hills, South Dakota. Geol. Soc. Amer., Rocky Mt. Sect. 34th Ann. Meeting, Rapid City, Abstr. Prog., 221.

Norton, J. J.
1983: Sequence of mineral assemblages in differentiated granitic pegmatites. Econ. Geol. 78, 854-874.

Orville, P. M.
1967: Unit cell parameters of the microcline -low albite and the sanidine - high albite solid solution series. Amer. Mineral. 52, 55-86.

Parker, R. L. and Fleischer, M.
1968: Geochemistry of Niobium and Tantalum. U. S. Geol. Surv. Prof. Paper 612, 43 p.

Pitcher, W. S.
1979a: The nature, ascent and emplacement of granitic magmas. J. Geol. Soc. London 136, 627-662.

REFERENCES
Continued

Pitcher, W. S.
1979b: Comments on the geological environments of granites. In: Origin of Granitic Batholiths - Geochemical Evidence (M. P. Atherton and J. Tarney, eds.). Shiva Publishing, Kent, 1-8.

Pye, E. G.
1965: Geology and Lithium Deposits of the Georgia Lake Area. Ont. Dept. of Mines, Geol. Rept. 31, 113 p.

Pye, E. G.
1968: Geology of the Cresent Lake Area. Ont. Dept. of Mines, Geol. Rept. 55, 72 p.

Quensel, P.
1957: The paragenesis of the Varuträsk pegmatite including a review of its mineral assemblage. Ark. Min. Geol. 2, 9-126.

Ribbe, P. H.
1983: Chemistry, structure and nomenclature of feldspars. In: Feldspar Mineralogy, 2nd ed. (P.H. Ribbe ed.). Mineral. Soc. of Amer., Reviews in Mineralogy 2, 1-19.

Ringwood, A. E.
1955: The principles governing trace-element behaviour during magmatic crystallization. Part II. The role of complex formation. Geochim. Cosmochim. Acta 7, 242-254.

Rossovskiy, L. N. and Matrosov, I. I.
1974: Pseudomorphs of quartz and spodumene after petalite and their importance to the pegmatite forming process. Dokl. Acad. Sci. USSR, Earth Science Section 216, 1135-1137.

Shearer, C. K., Papike, J. J. and Laul, J. C.
1983: Compositional variations in coexisting muscovite and potassium feldspar within three compositionally distinct pegmatites from the Custer pegmatite district, South Dakota. Geol. Soc. America, Abstr. with Prog. 15, 435.

Shearer, C. K., Papike, J. J. and Laul, J. C.
1985: Chemistry of potassium feldspars from three zoned pegmatites, Black Hills, South Dakota: Implications concerning pegmatite evolution. Geochim. Cosmochim. Acta 49, 663-673.

REFERENCES
Continued

Shigley, J. E. and Brown, G. E.
1985: Occurrence and alteration of phosphate minerals at the Stewart Pegmatite, Pala District, San Diego County, California. Amer. Mineral. 70, 395-408.

Shmakin, B. M.
1979: Composition and structural state of K-feldspars from some U.S. pegmatites. Amer. Mineral. 64, 49-56.

Smith, I. E. M. and Williams, J. G.
1980: Geochemical variety among Archean granitoids in northwestern Ontario. In: The Continental Crust and its Mineral Deposits (D. W. Strangway, ed.). Geol. Assoc. of Can. Spec. Paper 20, 181-192.

Smith, J. V.
1983: Some chemical properties of feldspars. In: Feldspar Mineralogy, 2nd ed. (P. H. Ribbe, ed.). Mineral. Soc. of Amer., Reviews in Mineralogy 2, 281-296.

Stewart, D. B.
1963: Petrogenesis and mineral assemblages of lithium - rich pegmatites. Geol. Soc. Amer. Spec. Paper 76, abstr.

Stewart, D. B.
1978: Petrogenesis of lithium-rich pegmatites. Amer. Mineral. 63, 970-980.

Stewart, D. B. and Wright, T. L.
1974: Al/Si order and symmetry of natural alkali feldspars, and the relationship of strained cell parameters to bulk composition. Bull. Soc. fr. Mineral. Cristallogr. 97, 356-377.

Stockwell, C. H., McGlynn, J. C., Emslie, R. F., Sanford, B. V., Norris, A. W., Donaldson, J. A., Fahrig, W. F. and Currie, K. L.
1970: Geology of the Canadian Shield. In: Geology and Economic Minerals of Canada (R. J. W. Douglas, ed.). Geol. Surv. of Canada, Econ. Geol. Rept. 1, 43-150.

Streckeisen, A. L.
1976: To each plutonic rock its proper name. Earth Sci. Rev. 12, 1-33.

REFERENCES
Continued

Taylor, R. G.
1979: Geology of Tin Deposits. Elsevier, Amsterdam, 543 p.

Trueman, D. L. and Černý, P.
1982: Exploration for rare-element granitic pegmatites. In: Short Course in Granitic Pegmatites in Science and Industry (P. Černý, ed.). Mineral Assoc. of Can. Short Course Handbook 8, 463-493.

Tuttle, O. F. and Bowen, N. L.
1958: Origin of Granite in the Light of Experimental Studies in the System $NaAlSi_3O_8$-$KAlSi_3O_8$-SiO_2-H_2O. Geol. Soc. Amer. Memoir 74, 153 p.

Vlasov, K. A.
1966: Geochemistry and Mineralogy of Rare Elements and Genetic Types of Their Deposits. Israel Program for Scientific Translations, Jerusalem.

White, A. J. R.
1979: Sources of granite magmas. Geol. Soc. America, Abstr. with Prog. 11, 539.

White, A. J. R. and Chappell, B. W.
1977: Ultrametamorphism and granitoid genesis. Tectonophysics 43, 7-22.

Williams, C. T. and Trueman, D. L.
1978: An estimation of lithium resources and potentials of northwestern Ontario, Manitoba and Saskatchewan, Canada. Energy 3, 409-413.

Windley, B. F.
1976: New tectonic models for the evolution of Archean continents. In: The Early History of the Earth (B. F. Windley, ed.). John Wiley and Sons, London, 105-111.

Windley, B. F.
1977: The Evolving Continents. John Wiley and Sons, Chichester, 285 p.

Wright, T. L. and Stewart, D. B.
1968: X-ray and optical study of alkali feldspar: I. Determination of composition and structural state from refined unit cell parameters and 2V. Amer. Mineral. 53, 38-87.

REFERENCES
Continued

Zwart, H. J.
1967: The duality of orogenic belts. Geol. Mijnbouw 46, 283-309.

APPENDIX I

Analytical parameters for elemental determinations by X - ray fluorescence spectrometry.

Oxide/Element	Crystal	Mode	Collimator	Peak 2θ	Bckgnd	Z	LL	WD	T_P	T_B
SiO_2	PET	FC	C	108.95°	+2°	2	150	250	100	10
TiO_2	LIF	FC	F	86.24	+1.8	3	180	250	10	1
Al_2O_3	PET	FC	C	144.56	-1.5	1	225	200	100	10
Fe_2O_3	LIF	FC	F	57.62	-1.0	3	300	220	40	4
MnO	LIF	FC	F	63.03	+2.0	3	250	250	100	10
MgO	ADP	FC	C	136.35	+1,-0.6	1	250	350	100	100
CaO	LIF	FC	F	113.16	+1.6	3	180	250	10	1
Na_2O	RbAP	FC	C	53.91	-1.7	1	250	200	100	10
K_2O	PET	FC	C	50.49	+1.5	3	200	200	10	1
P_2O_5	PET	FC	F	59.15	+2.0	2	150	300	100	10
Rb	LIF	SC	F	26.65	+0.8,-0.7	5	160	300	10	10
Sr	LIF	SC	F	25.22	+0.8,-0.8	5	160	300	10	10
Ba	LIF	FC	F	87.05	+0.9,-0.3	2	250	300	20	20
Zn	LIF	SC	F	47.71	-1.0	4	250	200	10	10
Zr	LIF	SC	F	22.58	+0.7,-0.8	5	160	300	10	10
Nb	LIF	SC	F	21.46	+0.3,-0.4	5	160	300	10	10

Bckgnd = Background ($2\theta \pm$ peak angle)
Z, LL, WD = Potentiometer settings
T_P = Peak counting time (seconds)
T_B = Background counting time (seconds)

APPENDIX 2

Equations for the determination of cell volume, reciprocal cell angles, α^* and γ^*, molecular % Or and distribution of Al in T - sites for maximum microcline from refined cell parameters.

(1) Cell volume - triclinic

$$V = abc\sqrt{1 - \cos^2\alpha - \cos^2\beta - \cos^2\gamma + 2\cos\alpha\cos\beta\cos\gamma}$$

(2) Reciprocal cell angle α^*

$$\cos\alpha^* = \frac{\cos\beta\cos\gamma - \cos\alpha}{\sin\beta\sin\gamma}$$

(3) Reciprocal cell angle γ^*

$$\cos\gamma^* = \frac{\cos\alpha\cos\beta - \cos\gamma}{\sin\alpha\sin\beta}$$

(4)+ Molecular % orthoclase

$$n_{Or} = -1227.8023 + 5.35958V - 7.81518 \cdot 10^{-3}V^2 + 3.80771 \cdot 10^{-6}V^3$$

(V = volume: triclinic)

(5)+ Equations to derive Al content in T - sites

$$(t_1o + t_1m) = \frac{b - 0.7138 - 1.7505 \cdot c}{-7.7245 + 1.0150 \cdot c}$$

$$(t_1o - t_1m) = \frac{\alpha^* + 89.118 - 1.9902\gamma^*}{-24.691 + 0.2229\gamma^*}$$

+ from Kroll and Ribbe (1983)

APPENDIX 3

X - ray powder patterns for maximum microcline from MNW, Brink, Point, Island, Camp, McVittie, Powerline and Nama Creek North pegmatites.

Perthitic microcline from the MNW pegmatite, wall zone, north end of pegmatite

H	K	L	2-TH(OBS)	2-TH(CALC)	DE	2-TH	WAVELENGTH	D(OBS)	D(CALC)
-2	0	1	21.060	21.049	0.011		1.54065	4.2152	4.2174
0	0	2	27.510	27.490	0.020		1.54065	3.2398	3.2421
1	-3	1	29.510	29.518	-0.008		1.54065	3.0246	3.0238
1	-3	1	30.210	30.218	-0.008		1.54065	2.9561	2.9553
-1	-3	2	32.160	32.161	-0.001		1.54065	2.7812	2.7811
-1	3	2	32.460	32.461	-0.001		1.54065	2.7561	2.7561
0	6	0	41.810	41.807	0.003		1.54065	2.1589	2.1590
-2	0	4	50.560	50.562	-0.002		1.54065	1.8039	1.8038

Perthitic microcline from the MNW pegmatite, wall zone, south end of pegmatite

H	K	L	2-TH(OBS)	2-TH(CALC)	DE	2-TH	WAVELENGTH	D(OBS)	D(CALC)
-2	0	1	21.050	21.042	0.008		1.54065	4.2172	4.2187
0	0	2	27.450	27.436	0.014		1.54065	3.2467	3.2483
1	-3	1	29.450	29.456	-0.006		1.54065	3.0306	3.0301
1	-3	1	30.200	30.205	-0.005		1.54065	2.9571	2.9565
-1	-3	2	32.150	32.119	0.031		1.54065	2.7820	2.7847
-1	3	2	32.500	32.469	0.031		1.54065	2.7526	2.7554
0	6	0	41.800	41.810	-0.010		1.54065	2.1594	2.1588
-2	0	4	50.500	50.513	-0.013		1.54065	1.8059	1.8054

Perthitic microcline from the MNW pegmatite, core zone

H	K	L	2-TH(OBS)	2-TH(CALC)	DE	2-TH	WAVELENGTH	D(OBS)	D(CALC)
-2	0	1	21.010	21.019	-0.009		1.54065	4.2251	4.2233
0	0	2	27.510	27.526	-0.016		1.54065	3.2398	3.2380
1	-3	1	29.510	29.504	0.006		1.54065	3.0246	3.0252
1	-3	1	30.260	30.254	0.006		1.54065	2.9513	2.9519
-1	-3	2	32.210	32.225	-0.015		1.54065	2.7770	2.7757
-1	3	2	32.410	32.425	-0.015		1.54065	2.7603	2.7590
0	6	0	41.810	41.806	0.004		1.54065	2.1589	2.1590
-2	0	4	50.610	50.603	0.007		1.54065	1.8022	1.8024

Perthitic microcline from the Brink pegmatite

H	K	L	2-TH(OBS)	2-TH(CALC)	DE	2-TH	WAVELENGTH	D(OBS)	D(CALC)
-2	0	1	21.060	21.057	0.003		1.54065	4.2152	4.2159
0	0	2	27.510	27.504	0.006		1.54065	3.2398	3.2405
1	-3	1	29.560	29.562	-0.002		1.54065	3.0196	3.0194
1	-3	1	30.210	30.212	-0.002		1.54065	2.9561	2.9559
-1	-3	2	32.210	32.211	-0.001		1.54065	2.7770	2.7769
-1	3	2	32.410	32.411	-0.001		1.54065	2.7603	2.7602
0	6	0	41.810	41.809	0.001		1.54065	2.1589	2.1589
-2	0	4	50.560	50.561	-0.001		1.54065	1.8039	1.8038

Perthitic microcline from the Point pegmatite

H	K	L	2-TH(OBS)	2-TH(CALC)	DE	2-TH	WAVELENGTH	D(OBS)	D(CALC)
-2	0	1	21.110	21.101	0.009		1.54065	4.2053	4.2071
0	0	2	27.510	27.494	0.016		1.54065	3.2398	3.2416
1	3	1	29.510	29.517	-0.007		1.54065	3.0246	3.0239
1	-3	1	30.260	30.266	-0.006		1.54065	2.9513	2.9507
-1	-3	2	32.160	32.141	0.019		1.54065	2.7812	2.7828
-1	3	2	32.510	32.491	0.019		1.54065	2.7520	2.7536
-0	6	0	41.810	41.815	-0.005		1.54065	2.1589	2.1586
-2	0	4	50.560	50.569	-0.009		1.54065	1.8039	1.8036

Perthitic microcline from the Island pegmatite

H	K	L	2-TH(OBS)	2-TH(CALC)	DE	2-TH	WAVELENGTH	D(OBS)	D(CALC)
-2	0	1	21.010	21.013	-0.003		1.54065	4.2251	4.2244
0	0	2	27.460	27.466	-0.006		1.54065	3.2456	3.2449
1	3	1	29.460	29.458	0.002		1.54065	3.0296	3.0299
1	-3	1	30.210	30.208	0.002		1.54065	2.9561	2.9563
-1	-3	2	32.110	32.151	-0.041		1.54065	2.7854	2.7819
-1	3	2	32.410	32.451	-0.041		1.54065	2.7603	2.7569
-0	6	0	41.810	41.795	0.015		1.54065	2.1589	2.1596
-2	0	4	50.560	50.545	0.015		1.54065	1.8039	1.8044

Perthitic microcline from the Camp pegmatite

H	K	L	2-TH(OBS)	2-TH(CALC)	DE	2-TH	WAVELENGTH	D(OBS)	D(CALC)
-2	0	1	21.060	21.066	-0.006		1.54065	4.2152	4.2141
0	0	2	27.460	27.470	-0.010		1.54065	3.2456	3.2444
1	3	1	29.460	29.456	0.004		1.54065	3.0296	3.0300
1	-3	1	30.260	30.256	0.004		1.54065	2.9513	2.9517
-1	-3	2	32.160	32.161	-0.001		1.54065	2.7812	2.7811
-1	3	2	32.460	32.461	-0.001		1.54065	2.7561	2.7561
-0	6	0	41.810	41.811	-0.001		1.54065	2.1589	2.1588
-2	0	4	50.560	50.558	0.002		1.54065	1.8039	1.8039

Perthitic microcline from the McVittie pegmatite

H	K	L	2-TH(OBS)	2-TH(CALC)	DE	2-TH	WAVELENGTH	D(OBS)	D(CALC)
-2	0	1	21.060	21.066	-0.006		1.54065	4.2152	4.2141
0	0	2	27.460	27.470	-0.010		1.54065	3.2456	3.2444
1	3	1	29.460	29.456	0.004		1.54065	3.0296	3.0300
1	-3	1	30.260	30.256	0.004		1.54065	2.9513	2.9517
-1	-3	2	32.160	32.141	0.019		1.54065	2.7812	2.7828
-1	3	2	32.510	32.491	0.019		1.54065	2.7520	2.7536
-0	6	0	41.810	41.819	-0.009		1.54065	2.1589	2.1584
-2	0	4	50.560	50.565	-0.005		1.54065	1.8039	1.8037

Perthitic microcline from the Powerline pegmatite

H	K	L	2-TH(OBS)	2-TH(CALC)	DE	2-TH	WAVELENGTH	D(OBS)	D(CALC)
-2	0	1	21.050	21.042	0.008		1.54065	4.2172	4.2187
0	0	2	27.450	27.437	0.014		1.54065	3.2467	3.2483
1	-3	1	29.450	29.456	-0.006		1.54065	3.0306	3.0301
1	-3	1	30.200	30.205	-0.005		1.54065	2.9571	2.9565
-1	-3	2	32.150	32.139	0.011		1.54065	2.7820	2.7829
-1	3	2	32.450	32.439	0.011		1.54065	2.7570	2.7579
0	6	0	41.800	41.802	-0.002		1.54065	2.1594	2.1592
-2	0	4	50.500	50.506	-0.006		1.54065	1.8059	1.8057

Perthitic microcline from the Nama Creek North pegmatite

H	K	L	2-TH(OBS)	2-TH(CALC)	DE	2-TH	WAVELENGTH	D(OBS)	D(CALC)
-2	0	1	21.060	21.051	0.009		1.54065	4.2152	4.2169
0	0	2	27.460	27.445	0.015		1.54065	3.2456	3.2474
1	-3	1	29.460	29.466	-0.006		1.54065	3.0296	3.0290
1	-3	1	30.210	30.216	-0.006		1.54065	2.9561	2.9555
-1	-3	2	32.160	32.146	0.014		1.54065	2.7812	2.7823
-1	3	2	32.460	32.446	0.014		1.54065	2.7561	2.7573
0	6	0	41.810	41.813	-0.003		1.54065	2.1589	2.1587
-2	0	4	50.510	50.517	-0.007		1.54065	1.8055	1.8053

APPENDIX 4

X - ray powder patterns for tantalite - columbite minerals from the Brink, MNW and Southwest pegmatites.

Sample TI - tantalite from the Brink pegmatite (ordered)

H	K	L	2-TH(OBS)	2-TH(CALC)	DE	2-TH	WAVELENGTH	D(OBS)	D(CALC)
3	1	0	24.429	24.238	0.191		1.54178	3.6436	3.6720
3	1	1	30.086	29.982	0.104		1.54178	2.9702	2.9802
0	2	0	31.138	31.077	0.061		1.54178	2.8722	2.8777
5	0	1	35.943	35.988	-0.045		1.54178	2.4985	2.4955
2	0	2	37.445	37.431	0.014		1.54178	2.4016	2.4025
3	2	1	40.849	40.665	0.184		1.54178	2.2090	2.2186
3	1	2	43.152	43.183	-0.031		1.54178	2.0963	2.0949
0	2	2	47.457	47.640	-0.183		1.54178	1.9157	1.9088
6	2	0	49.660	49.654	0.006		1.54178	1.8358	1.8360
3	3	0	51.312	51.333	-0.021		1.54178	1.7805	1.7798
6	0	2	52.563	52.537	0.026		1.54178	1.7410	1.7418
6	2	1	53.164	53.006	0.158		1.54178	1.7227	1.7275
3	1	3	60.022	59.946	0.076		1.54178	1.5413	1.5430
6	2	2	62.325	62.308	0.017		1.54178	1.4897	1.4901
9	1	1	63.226	63.382	-0.156		1.54178	1.4707	1.4674
3	3	2	63.777	63.761	0.016		1.54178	1.4593	1.4596
6	0	3	67.782	67.673	0.109		1.54178	1.3825	1.3844
9	1	2	71.736	71.879	-0.143		1.54178	1.3157	1.3134
5	4	1	76.492	76.407	0.085		1.54178	1.2453	1.2465
9	3	0	78.144	78.074	0.070		1.54178	1.2231	1.2240
6	4	1	80.347	80.145	0.202		1.54178	1.1950	1.1975
2	5	0	85.353	85.427	-0.074		1.54178	1.1372	1.1364
13	0	0	88.957	88.938	0.019		1.54178	1.1003	1.1004
2	4	3	90.259	90.480	-0.221		1.54178	1.0877	1.0857
11	2	2	91.680	91.657	0.023		1.54178	1.0746	1.0748
8	3	3	96.066	96.065	0.001		1.54178	1.0368	1.0368
10	2	3	97.868	97.777	0.091		1.54178	1.0225	1.0232
2	0	5	99.470	99.498	-0.028		1.54178	1.0103	1.0100
5	3	4	101.472	101.470	0.002		1.54178	0.9957	0.9957
9	5	0	111.468	111.559	-0.091		1.54178	0.9328	0.9323
4	4	4	113.320	113.439	-0.119		1.54178	0.9228	0.9221
9	5	1	114.772	114.401	0.371		1.54178	0.9152	0.9171
11	4	2	117.325	117.355	-0.030		1.54178	0.9026	0.9024
5	6	1	118.927	118.856	0.071		1.54178	0.8950	0.8954
10	5	1	121.430	121.565	-0.135		1.54178	0.8838	0.8833
4	3	5	124.033	123.892	0.141		1.54178	0.8730	0.8735
14	3	2	129.840	130.082	-0.242		1.54178	0.8511	0.8503
1	1	6	133.444	133.303	0.141		1.54178	0.8392	0.8396
3	6	3	138.951	139.030	-0.079		1.54178	0.8231	0.8229
11	5	2	141.454	141.484	-0.030		1.54178	0.8167	0.8166
12	4	3	145.108	145.228	-0.120		1.54178	0.8081	0.8078
10	2	5	149.814	150.003	-0.189		1.54178	0.7984	0.7981
18	1	0	156.822	156.564	0.258		1.54178	0.7869	0.7873

Sample T4 - columbite from the MNW pegmatite, intermediate zone (disordered)

H	K	L	2-TH(OBS)	2-TH(CALC)	DE	2-TH	WAVELENGTH	D(OBS)	D(CALC)
1	1	0	24.493	24.386	0.107		1.54178	3.6343	3.6500
1	1	1	30.203	30.027	0.176		1.54178	2.9589	2.9759
0	2	0	31.405	31.241	0.164		1.54178	2.8484	2.8629
1	2	0	36.013	36.676	-0.663		1.54178	2.4938	2.4502
2	0	0	38.317	37.986	0.331		1.54178	2.3490	2.3687
1	2	1	40.922	40.797	0.125		1.54178	2.2053	2.2117
1	1	2	43.276	43.047	0.229		1.54178	2.0906	2.1012
0	2	2	48.085	47.546	0.539		1.54178	1.8922	1.9123
2	2	0	50.138	49.973	0.165		1.54178	1.8194	1.8250
1	3	0	51.891	51.628	0.263		1.54178	1.7620	1.7703
2	0	2	52.893	52.543	0.350		1.54178	1.7309	1.7416
2	2	1	53.644	53.262	0.382		1.54178	1.7085	1.7198
1	1	3	60.106	59.615	0.491		1.54178	1.5393	1.5508
1	3	2	64.063	63.847	0.216		1.54178	1.4535	1.4579
2	0	3	67.920	67.469	0.451		1.54178	1.3800	1.3881
1	0	4	76.435	76.875	-0.440		1.54178	1.2461	1.2400
2	4	1	80.642	80.612	0.030		1.54178	1.1914	1.1917
4	2	1	91.962	92.142	-0.180		1.54178	1.0720	1.0704
2	5	0	96.269	96.785	-0.516		1.54178	1.0351	1.0310
3	3	3	102.080	101.999	0.081		1.54178	0.9914	0.9920
2	1	5	111.797	111.903	-0.106		1.54178	0.9310	0.9304
1	6	1	114.001	113.769	0.232		1.54178	0.9192	0.9204
4	4	0	115.103	115.303	-0.200		1.54178	0.9135	0.9125
0	6	2	119.410	119.017	0.393		1.54178	0.8928	0.8946
1	6	2	122.415	122.550	-0.135		1.54178	0.8796	0.8791
5	3	0	130.713	130.563	0.150		1.54178	0.8481	0.8487
2	6	2	134.019	134.180	-0.161		1.54178	0.8374	0.8369
2	5	4	146.641	146.942	-0.301		1.54178	0.8047	0.8041
2	1	6	150.148	150.229	-0.081		1.54178	0.7978	0.7977

Sample T6 - columbite from the Southwest pegmatite (disordered)

H	K	L	2-TH(OBS)	2-TH(CALC)	DE	2-TH	WAVELENGTH	D(OBS)	D(CALC)
1	1	0	24.418	24.351	0.067		1.54178	3.6452	3.6551
1	1	1	30.033	30.001	0.032		1.54178	2.9753	2.9784
0	2	0	31.504	31.293	0.211		1.54178	2.8396	2.8583
0	0	2	35.315	34.923	0.392		1.54178	2.5415	2.5691
1	2	0	36.017	36.585	-0.568		1.54178	2.4935	2.4496
2	0	0	37.621	37.850	-0.229		1.54178	2.3908	2.3769
1	2	1	40.730	40.807	-0.077		1.54178	2.2152	2.2112
1	1	2	43.437	43.033	0.404		1.54178	2.0832	2.1018
0	2	2	47.649	47.589	0.060		1.54178	1.9064	1.9107
1	3	0	51.644	51.678	-0.034		1.54178	1.7698	1.7687
2	2	1	52.897	53.193	-0.296		1.54178	1.7308	1.7219
1	1	3	59.967	59.611	0.356		1.54178	1.5425	1.5509
3	1	1	63.677	63.560	0.117		1.54178	1.4613	1.4637
3	2	0	67.788	67.594	0.194		1.54178	1.3824	1.3859
1	0	4	76.630	76.873	-0.243		1.54178	1.2434	1.2401
2	4	1	80.741	80.637	0.104		1.54178	1.1901	1.1914
1	2	4	85.254	85.318	-0.064		1.54178	1.1383	1.1376
2	0	4	86.256	86.025	0.231		1.54178	1.1276	1.1301
4	2	0	89.064	89.255	-0.191		1.54178	1.0992	1.0974
3	4	1	95.783	95.755	0.028		1.54178	1.0391	1.0393
3	3	3	101.599	101.379	0.280		1.54178	0.9948	0.9928
3	1	4	103.203	103.298	-0.095		1.54178	0.9836	0.9830
5	1	1	113.465	113.345	0.120		1.54178	0.9220	0.9226
0	6	2	119.348	119.298	0.050		1.54178	0.8931	0.8933
5	3	2	145.504	145.313	0.191		1.54178	0.8072	0.8076
5	2	3	149.816	149.942	-0.126		1.54178	0.7984	0.7982

APPENDIX 5

X - ray powder patterns for staringite from the MNW pegmatite.

Staringite from the MNW pegmatite, core zone

H	K	L	2-TH(OBS)	2-TH(CALC)	DE	2-TH	WAVELENGTH	D(OBS)	D(CALC)
1	1	0	26.722	26.597	0.125		1.54178	3.3359	3.3513
1	0	3	34.429	33.994	0.435		1.54178	2.6048	2.6371
2	0	0	37.982	37.968	0.014		1.54178	2.3689	2.3697
1	1	3	38.582	39.088	-0.506		1.54178	2.3334	2.3044
2	1	3	52.344	51.870	0.474		1.54178	1.7478	1.7626
2	2	0	54.696	54.781	-0.085		1.54178	1.6781	1.6757
1	1	5 *	55.496	55.500	-0.004		1.54178	1.6557	1.6557
0	0	6	58.249	58.128	0.121		1.54178	1.5839	1.5869
3	1	0	62.102	61.909	0.193		1.54178	1.4945	1.4988
1	1	6	65.405	65.027	0.378		1.54178	1.4268	1.4342
3	0	3	66.505	66.059	0.446		1.54178	1.4059	1.4143
2	0	6	72.010	71.556	0.454		1.54178	1.3114	1.3186
3	2	3	78.966	78.805	0.161		1.54178	1.2124	1.2144
4	0	0	81.268	81.176	0.092		1.54178	1.1838	1.1849
2	2	6	84.070	83.989	0.081		1.54178	1.1513	1.1522
3	3	0	87.473	87.273	0.200		1.54178	1.1151	1.1171
1	4	3	90.475	91.003	-0.528		1.54178	1.0857	1.0808
4	2	0	93.478	93.339	0.139		1.54178	1.0586	1.0598
1	0	9	96.380	96.596	-0.216		1.54178	1.0343	1.0325
3	2	7 *	109.291	109.285	0.006		1.54178	0.9452	0.9452
5	1	0	111.993	112.069	-0.076		1.54178	0.9299	0.9295
3	3	6	115.296	115.113	0.183		1.54178	0.9125	0.9135
5	0	3	116.297	116.155	0.142		1.54178	0.9076	0.9083
4	2	6	122.302	122.021	0.282		1.54178	0.8801	0.8813
5	2	3	130.609	130.727	-0.118		1.54178	0.8485	0.8481
4	4	0	133.661	133.883	-0.222		1.54178	0.8385	0.8378
1	5	5 *	134.362	134.707	-0.345		1.54178	0.8363	0.8353
3	2	9	138.215	138.574	-0.359		1.54178	0.8251	0.8242
5	3	0	143.169	143.036	0.133		1.54178	0.8125	0.8128
4	4	3	143.670	144.212	-0.542		1.54178	0.8113	0.8101
5	1	6	147.573	147.962	-0.389		1.54178	0.8028	0.8020
3	5	2 *	148.524	148.371	0.153		1.54178	0.8009	0.8012
4	4	4 *	154.579	154.550	0.029		1.54178	0.7903	0.7903
6	0	0	155.480	154.802	0.678		1.54178	0.7889	0.7899
6	1	0	163.036	163.286	-0.250		1.54178	0.7794	0.7792

* reflections unique to staringite

Staringite from the MNW pegmatite, intermediate zone

H	K	L	2-TH(OBS)	2-TH(CALC)	DE	2-TH	WAVELENGTH	D(OBS)	D(CALC)
1	1	0	26.737	26.597	0.140		1.54178	3.3341	3.3513
1	0	3	34.147	33.987	0.160		1.54178	2.6257	2.6376
2	0	0	37.752	37.969	-0.217		1.54178	2.3828	2.3697
2	1	3	51.972	51.865	0.107		1.54178	1.7594	1.7628
2	2	0	54.826	54.781	0.045		1.54178	1.6744	1.6756
3	1	0	61.086	61.909	-0.823		1.54178	1.5169	1.4987
3	0	3	66.242	66.055	0.187		1.54178	1.4108	1.4144
3	0	6	71.533	71.540	-0.007		1.54178	1.3189	1.3188
3	2	3	78.960	78.802	0.158		1.54178	1.2125	1.2145
4	0	0	81.246	81.176	0.070		1.54178	1.1840	1.1849
2	2	6	84.150	83.973	0.177		1.54178	1.1504	1.1524
3	3	0	87.455	87.274	0.181		1.54178	1.1152	1.1171
3	1	6	89.958	90.048	-0.090		1.54178	1.0906	1.0898
4	1	3	91.260	91.000	0.260		1.54178	1.0784	1.0808
4	2	0	93.463	93.340	0.123		1.54178	1.0587	1.0598
4	0	6	108.901	108.561	0.340		1.54178	0.9475	0.9495
5	1	0	112.156	112.070	0.086		1.54178	0.9290	0.9295
3	3	6	115.260	115.096	0.164		1.54178	0.9127	0.9135
5	0	3	116.312	116.152	0.160		1.54178	0.9075	0.9083
4	3	3	116.512	116.152	0.360		1.54178	0.9065	0.9083
3	0	9	122.420	122.517	-0.097		1.54178	0.8796	0.8792
5	5	3	130.581	130.723	-0.142		1.54178	0.8486	0.8481
4	4	0	134.036	133.885	0.151		1.54178	0.8374	0.8378
3	2	9	138.292	138.521	-0.229		1.54178	0.8249	0.8243
5	3	0	142.999	143.038	-0.039		1.54178	0.8129	0.8128
4	4	3	143.850	144.207	-0.357		1.54178	0.8109	0.8101
5	1	6	147.605	147.934	-0.329		1.54178	0.8028	0.8021
5	3	2*	148.606	148.370	0.236		1.54178	0.8008	0.8012
6	0	0	154.665	154.805	-0.140		1.54178	0.7901	0.7899
5	3	3	155.566	156.486	-0.920		1.54178	0.7868	0.7874
6	0	2*	163.427	163.191	0.236		1.54178	0.7790	0.7793
1	6	1*	165.330	166.139	-0.809		1.54178	0.7723	0.7766

* reflections unique to staringite